CHEMISTRY HALL LIBRARY

*On the Ring Opening Reaction of ε-Caprolactam Derivatives**

By Hirosuke YUMOTO, Kenzaburoh IDA and Naoya OGATA

(Received October 14, 1957)

It must be considered for the condensation polymerization whether ring-monomer and -oligomers are stable or not; if └A┘ or └A–A┘ is considerably stable in comparison with –A– or –A–A–, such a large quantity of the ring-monomer or -dimer may be produced that the polymer molecule can not be found in the reaction product. δ-Aminovaleric acid or δ-valerolactam is an instance of the former case and α-amino-acid dimer or diketopiperazine is that of the latter case. Thus the ring-chain equilibrium is not only interesting in the structural chemistry but also important for the purpose of polymer manufacturing. It is the object of this paper to study experimentally the influence of side chains on ε-caprolactam polymerization.

Results

Monomethyl-ε-caprolactam. — Methyl cyclohexanone (b. p. 160~170°C) was obtained from cresol (b. p. 190~200°C) through methyl cyclohexanol (b. p. 165~175°C) by the usual method. Methyl-ε-caprolactam (b. p. 123~124°C/5mmHg) was prepared from methyl cyclohexanone with a yield of 75 % by Schmidt's method using sodium azide[1]. This monosubstituted caprolactam, which was a mixture of α, β, γ, δ and ε-derivative, was used for the polymerization experiment; the melting point of the polymer is 164~166°C. Methyl-ε-aminocaproic acid was prepared by the hydrolysis of methyl-ε-caprolactam.

About 3 g. of monomethyl-ε-caprolactams was previously polymerized, with 0.1~0.05 g. of monomethyl-ε-aminocaproic acid as the catalyst, by heating in a glass tube at 230°C for 100 hr. Then, after the tube was sealed, heating was continued at 280°C for 15 hr., at 257°C for 25 hr., at 215°C for 30 hr. or at 182°C for 30 hr. to reach the equilibrium at each temperature. The quantities of lactam-monomer and -oligomers were measured by the same procedure with that for the unsubstituted polycapramide[2]. The intrinsic viscosity of polymerized contents was also measured in the cresol solution at 25°C. The obtained results are shown in Table I.

TABLE I

ANALYTICAL VALUES OF POLY-MONOMETHYL-ε-CAPRAMIDE

($L_1°$ or $L_2°$ = mole of lactam-monomer or -oligomers in the product in the case that 1 mol. of monomer is initially used for polymerization)

Temp. of polymerization °C	$L_1°$ mol.	$L_2°$ mol.	$[\eta]^{25°C}_{cresol}$
280	0.198	0.022	0.56
257	0.164	0.023	0.57
230	0.150	0.021	0.64
205	0.129	0.021	0.69
182	0.119	0.018	0.74

The equilibrium of the reactions concerning lactam-monomer,

$$\mathrm{NH\cdot CO\cdot C_5H_9(CH_3)} + [\text{——}\mathrm{NH_3^+}] \underset{\kappa}{\overset{k}{\rightleftarrows}} [\text{——}\mathrm{NH\cdot CO\cdot C_5H_9(CH_3)\cdot NH_3^+}] \quad (1)$$

can be expressed by the following equation for the high polymeric system[2];

$$L_1° = A\kappa/k = AK \quad (2)$$

where $L_1°$ is the mole number of lactam-monomer at equilibrium, A the whole mole number of the average unit of the Brownian motion in the reaction phase, k the rate constant of ring-opening reaction, κ that of ring-closuring one and K the chain-ring equilibrium constant.

The values of A were determined by the experiment which follows. Monomethyl-ε-caprolactam was diluted with thymol at various ratios and polymerized at 230°C for 100 hr.; analytical results for products are given in Table II. The following equation can be applied to the increase of $L_1°$ with dilution as shown in the previous paper[3];

$$L_1°/(1-L_1°) = \kappa/k\{(S+L_1°)/(1-L_1°)\} + (\kappa/k)\alpha \quad (3)$$

where the mole number of the diluent per 1 mol. of the initial lactam-monomer is denoted by S and, on assuming that 1 mol. of lactam polymerizes completely into a chain molecule, the mole number

* Presented at the Annual Meeting of the Chemical Society of Japan at Kyoto, April 3, 1956.

1) T. Hoshino, Y. Iwakura and H. Iwasaki, *J. Polymer Chem. (Japan)*, **2**, 280 (1945).

2) H. Yumoto, This Bulletin, **28**, 94 (1955).

3) H. Yumoto, ibid., **28**, 101 (1955).

of the average unit of the Brownian motion by α. The data in Table II are used for Fig. 1, which satisfy the equation 3. From Fig. 1, α is estimated to be ca. 0.6 and consequently the average unit of the Brownian motion of chain macromolecules corresponds to 1.66(=1/0.6) structure units, i.e. 13.3(=8×1.66) skeleton atoms or 11.6(=7×1.66) ring-forming atoms. This value is smaller than 19 skeleton atoms for the unsubstituted one[3]; it means that the side chain such as methyl group makes the chain-molecules more kinky and activities of reaction components larger.

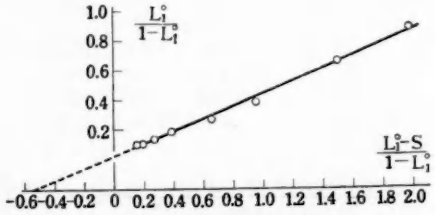

Fig. 1. The effect of dilution on the polymerization of monomethyl-ε-caprolactam.

TABLE II

ANALYTICAL VALUES OF PRODUCTS IN THE CASE THAT MONOMETHYL-ε-CAPROLACTAM IS POLYMERIZED UNDER THE DILUTION IN THYMOL AT 230°C

Initial Monomer mol.	Thymol mol.	L_1° mol.	L_2° mol.	$[\eta]^{25°C}_{cresol}$
1.00	0.846	0.349	0.027	—
〃	0.675	0.297	0.029	0.35
〃	0.507	0.229	0.027	0.39
〃	0.338	0.189	0.025	0.41
〃	0.169	0.155	0.023	0.51
〃	0.085	0.141	0.022	0.60
〃	0.043	0.132	0.021	0.65
〃	0.000	0.133	0.021	0.59

When there is no diluent,

$$A = L_1^\circ + (1 - L_1^\circ)\alpha \qquad (4)$$

The value of α for unsubstituted poly-ε-capramide is hardly changed at all with the temperature in the range from 200 to 250°C[3]. On the assumption that α is 0.6, equilibrium constants $K(=\kappa/k)$ can be found by equations 4 and 2; they were calculated as given in Table III. The relation between K and the absolute temperature T in Fig. 2 is expressed as follows:

$$\log K = 0.39 - 500/T \qquad (5)$$

Then the heat of the ring-opening reaction was estimated to be 2.3 kcal/mol., which is smaller than the value 3.5 kcal/mol. for the unsubstituted one[3].

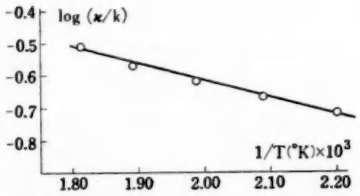

Fig. 2. The effect of temperature on the polymerization of monomethyl-ε-caprolactam.

TABLE III

EQUILIBRIUM CONSTANTS ON RING-CHAIN EQUILIBRIA AT VARIOUS TEMPERATURES FOR MONOMETHYL-ε-CAPROLACTAM

Temp. °C	L_1° mol.	A mol.	K
280	0.198	0.639	0.310
257	0.164	0.624	0.263
230	0.150	0.617	0.237
205	0.129	0.608	0.212
182	0.119	0.603	0.197

(1 mol. of lactam monomer is used for polymerization)

The relation between the intrinsic viscosities in the cresol solution ($[\eta]$) and the number average degrees of polymerization ($\bar{P}$), which were calculated from the numbers of the carboxyl end-group, is shown in Fig. 3. The following equation can be derived approximately,

$$\bar{P} = K_m[\eta]^a$$

where K_m is 214 and a is 1.67; these are

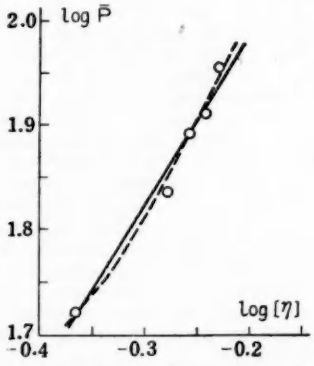

Fig. 3. The relation between the degree of polymerization of poly-monomethyl-ε-capramide and its intrinsic viscosity in cresol solution at 25°C.

TABLE IV
ANALYTICAL VALUES FOR POLY-MONOMETHYL-ε-CAPRAMIDE USING ACETIC ACID TO CONTROL THE DEGREE OF POLYMERIZATION

Acetic acid mol./1mol. of lactam monomer	-COOH mol./127 g of polymer	$-NH_2$ mol./127 g of polymer	$[\eta]^{25°C}_{cresol}$
0.0200	1.89×10^{-2}	0.27×10^{-2}	0.431
0.0100	1.44 〃	0.45 〃	0.526
0.0066	1.30 〃	0.51 〃	0.554
0.0050	1.21 〃	0.53 〃	0.569
0.0033	1.11 〃	0.60 〃	0.584

greater than the values of K_m(=127) and a(=1.44) for the unsubstituted one.[4]

N-Methyl-ε-caprolactam. — *N*-methyl-ε-caprolactam (b. p. = 124°C/123 mmHg and n_D^{25} = 1.428) was prepared from ε-caprolactam by dimethyl sulfuric acid[5], and *N*-methyl-ε-aminocaproic acid containing 2 moles of the water of crystallization (m. p. 69°C) was obtained by the acid hydrolysis of *N*-methyl-ε-caprolactam[5]. On heating *N*-methyl-ε-caprolactam at 230°C with water, water and benzoic acid, or water and ε-aminocaproic acid, no polymer molecules were obtained. *N*-methyl-ε-aminocaproic acid transformed into *N*-methyl-ε-caprolactam on heating at 230°C. *N*-methylol-ε-caprolactam, prepared from ε-caprolactam and formladehyde[5], did not polymerize, either.

These results agree with J. Prochazka's, that *N*-substituted caprolactam does not polymerize[6]. Poly-*N*-methyl-ω-hendecanamid or -undecanamid has been known[7]. Then the reason, why *N*-derivatives of ε-caprolactam can not polymerize, seems to be ascribed to their small ring size.

Dimethyl-ε-caprolactam.—The mixture of α, δ and β, ε-dimethyl ε-caprolactam (m. p. 95~98°C, b. p. 110~115°C/5 mmHg) was prepared from *p*-xylenol through *p*-dimethyl cyclohexanol (b. p. 179°C), *p*-dimethyl cyclohexanone(b.p. 80°C/25 mmHg) and its oxime (m. p. 97°C) by a process similar to that for the caprolactam manufacturing. Dimethyl-ε-aminocaproic acid (m. p. 173~175°C) was obtained by the hydrolysis of dimethyl ε-caprolactam.

Dimethyl ε-caprolactam was heated with catalysts at 230°C for five hours but did not polymerize at all. When dimethyl ε-aminocaproic acid was heated at 230°C for five hours, it only transformed into dimethyl ε-caprolactam and no polymer was obtained.

It is suggested, therefore, when two hydrogen atoms on the different carbon atoms in ε-caprolactam ring are replaced by methyl groups, the ring-chain equilibrium shifts extremely to the ring-form. Even by the use of amino acid for the starting material, it changes into lactam ring by the intramolecular condensation; the contribution of the intermolecular condensation is too small to give the polymer molecule.

Hoshino has already published in 1941[8] the experiment that menton isoxime (methyl isopropyl ε-caprolactam) does not polymerize at all.

Conclusion

The experimental results on the ring-chain equilibria for monomethyl ε-caprolactam can be analyzed through the same procedure with that for the unsubstituted one; the substitution shifts the equilibrium to the ring-form. The heat of reaction, i. e. the energy difference between the chain and the ring form for the monomethyl derivative is 2.3 kcal/mol., which is smaller than 3.5 kcal/mol. for the unsubstituted one.

For dimethyl and *N*-methyl or -methylol derivatives the equilibria shift too much in favor of the ring-form to give polymer molecules at high temperatures. When amino acids, which are prepared from these lactams by hydrolysis, are heated, they transform into lactam. The theoretical interpretation on these behaviors can be made by the intramolecular rotational isomers[9], which will be reported subsequently. The average unit of the Brownian motion of chain molecules, i. e. the segment, for the monomethyl derivative is 13.3 skeleton atoms which is smaller than 19 skeleton atoms for the unsubstituted polycapramide; the substitution makes it easier for chain molecules to be kinky.

Summary

The ring-chain equilibria,

$$-CO-R-NH- \rightleftharpoons \begin{matrix} CO-R-NH \\ | \quad\quad | \end{matrix}$$

were investigated experimentally for ε-caprolactam derivatives and their results

4) O. Fukumoto, *J. Polymer Sci.*, **22**, 263 (1956).
5) R. E. Benson and T. L. Cairns, *J. Am. Chem. Soc.*, **70**, 2115 (1948).
6) J. Procházka, *Chem. Listy.*, **37**, 202 (1943); *Chem. Abst.*, **40**, 2113 (1946).
7) G. Champetier and R. Aelion, *Bull. soc. chim. France*, 683 (1948); *Chem. Abst.*, **42**, 7099 (1948).
8) K. Hoshino, *J. Chem. Soc. Japan Pure Chem. Sec. (Nippon Kagaku Zassi)*, **63**, 1184 (1942).
9) H. Yumoto, Presented at the Symposium on the Structural Chemistry of the Chemical Society of Japan in Nagoya, October 16, 1956.

could be analyzed by the method similar to that for ε-caprolactam. For the monomethyl derivative the equilibrium shifts to the ring-form and ΔH has been estimated to be 2.3 kcal/mol. which is smaller than ΔH(=3.5 kcal/mol.) for the unsubstituted. For dimethyl and *N*-methyl or -methylol derivatives equilibria shift too much to the ring-form to give polymers at high temperatures. The average unit of the Brownian motion of polymer chain molecules, i. e. the segment, for the monomethyl derivative is 13.3 skeleton atoms which is smaller than 19 skeleton atoms for unsubstituted polycapramide; the substitution makes it easier for chain molecules to be kinky.

The authors wish to thank Drs. K. Hoshino and H. Kobayashi who instructed them and permitted the publication.

Nylon Laboratory, Research Department
Toyo Rayon Co., Ltd.
Minato-ku, Nagoya

Studies on the Antitubercular Compounds. XIII. Preparation of Some Derivatives of Benzimidazole and 2, 1, 3-Benzothiadiazole***

By Isao SEKIKAWA

(Received November 11, 1957)

In the foregoing paper[1], several kinds of 2-substituted benzimidazole compound were prepared and their antibacterial activities in vitro were examined. As a result 2-mercaptomethylbenzimidazole was found to be most effective against Mycobacterium tuberculosis.

Brown et al.[2] and Kushner et al.[3], who studied the tuberculostatic action of alkylmercapto derivatives, found that structural modification, which increased its ability to release ethylmercaptan,increased the antitubercular activity. Therefore, a series of alkylthioether was prepared for comparative studies as indicated in Table I. A compound which was formed by condensation of *o*-phenylenediamine with alkylthioglycolic acid in the presence of dilute hydrochloric acid was identical with that obtained by condensation of mercaptomethylbenzimidazole with alkyl bromide, thus confirming the fact that *S*-alkylation occurred.

Benzimidazole derivatives having substituents at the phenyl nucleus are shown in Table II. Condensation of 3,4-diaminophenetole with formic acid in the presence of dilute hydrochloric acid gave 5-ethoxybenzimidazole, which was converted into VI by the acid cleavage of ether group. VII was obtained by amination of the corresponding acid chloride. VIII was

TABLE I
2-ALKYLMERCAPTOMETHYLBENZIMIDAZOLE DERIVATIVES

No.	R	Method of prepn.	Yield (%)	m. p. (°C)	Appearance	Formula	Analysis (%) Calcd. C	Calcd. H	Found C	Found H
I	CH_3	b	90	156—157	Pale yellow needles	$C_9H_{10}N_2S$	60.64	5.60	60.37	5.96
II	C_2H_5	b	60	136—137	White needles	$C_{10}H_{12}N_2S$	62.46	6.29	62.57	6.69
III	*n*-C_3H_7	b	80	122—124	〃	$C_{11}H_{14}N_2S$	64.04	6.34	63.67	7.01
IV	*n*-C_4H_9	a	68	143—144	〃	$C_{12}H_{16}N_2S$	65.41	7.31	65.10	7.45
		b	95							

* This constitutes a part of a series entitled "Studies on the Antitubercular Compounds" by S. Kakimoto.

** A part of this study was presented at the Annual Meeting of the Chemical Society of Japan in Tokyo in April 6, 1957. Paper XII, S. Kakimoto and K. Yamamoto: *Kekkaku no Kenkyu* (Annual Report of the Research Institute for Tuberculosis, Hokkaido University), **6**, 1 (1956).

1) S. Kakimoto and I. Sekikawa, *J. Chem. Soc. Japan, Pure Chem. Sec.*, (*Nippon Kagaku Zassi*), **77**, 78 (1955).
2) H. D. Brown, M. Solotorvsky and I. H. Quastel, *J. Am. Chem. Soc.*, **76**, 3860 (1954).
3) S. Kushner, H. Dalalian and L. Bach, ibid., **77**, 1152 (1955).

TABLE II

BENZIMIDAZOLE DERIVATIVES

V	5-NO_2[4]
VI	5-OH
VII	5-$CONH_2$
VIII	5-$CONHNH_2$

TABLE III

2,1,3-BENZOTHIADIAZOLE DERIVATIVES

IX	5-NO_2[5]
X	5-OH[6]
XI	4-NO_2[7]
XII	4-$NHCOCH_3$[8]

prepared by the usual method.

2,1,3-Benzothiadiazole derivatives, which were formed by replacing the carbon atom of 2-position in benzimidazole molecule with sulfur atom, are shown in Table III. Reduction of XI with tin or stannous chloride in the presence of hydrochloric acid gave the parent *o*-phenylenediamine and sulfur. Vigorous reduction produced hydrogen sulfide[9]. Khaletskiĭ et al.[10] obtained a 4-amino compound by reduction of the nitro compound with acetic acid and iron powder. However, the present author found that the compound was very readily obtained by reducing the nitro compound with sodium chloride and iron powder in the presence of a minute amount of hexachloroplatinic acid.

Recently, Huebner et al.[11] reported a relation between chemical structure and antibacterial activity in the case of over three hundred compounds of *N,N'*-disubstituted thiourea derivatives and Konopka et al.[12] found that 4-ethoxy-4'-*iso*-butoxythiocarbanilide and 4-*n*-butoxy-4'-dimethylaminothiocarbanilide were the most effective in vivo.

A series of *N*-(Benzothiadiazolyl-4)-*N'*-(*p*-alkoxyphenyl)-thiourea, indicated in Table IV, was prepared. XIII, XIV, XV, XVI and XVII were derived from 4-aminobenzothiadiazole and phenyl-, *p*-methoxyphenyl-, *p*-ethoxyphenyl-, *p*-*n*-propoxyphenyl- and *p*-*n*-butoxyphenyl-isothiocyanate by the usual method.

Upon oxidation of 5-methylbenzothiadiazole with potassium permanganate by the usual procedure, the corresponding 5-benzothiadiazolecarboxylic acid was not obtained; an unknown acidic substance of m.p. 281°C (decomp.) was, on the other hand, formed. The investigation of the structure of this compound is now in progress.

The antitubercular activities of all derivatives described above were examined in vitro, and found less active than 2-mercaptomethyl-benzimidazole[1].

Experimental

IV. (a) A mixture of 2 g. of *o*-phenylenediamine, 3 g. of *n*-butylmercaptoacetic acid, 10 ml. of concentrated hydrochloric acid, and 10 ml. of water was refluxed for 12 hr., and the solution was concentrated under reduced pressure. The residue was dissolved in 10 ml. of water, and the solution was poured slowly into 20 ml. of cold concentrated ammonium hydroxide. The solid thus formed was recrystallized from 70% ethanol to give 3 g. (68%) of white needles m.p. 145°.

V. (b) To a solution of 0.5 g. sodium metal in 30 ml. of *n*-butanol, 3.3g. of 2-mercaptomethylbenzimidazol was added, with stirring. The mixture was cooled and 2.7 g. of *n*-butylbromide in 10 ml. of *n*-butanol was added in small portions during 10 min. The mixture was then stirred for another 15 min., and then refluxed for 5 hr. After removal of the *n*-butanol, 70 ml. of water was added and allowed to stand overnight in an ice box. The solidified product was recrystallized from 70% ethanol to give 4.3 g. (95%) of

TABLE IV

N-(BENZOTHIADIAZOLYL-4)-*N'*-SUBSTITUTED THIOUREA DERIVATIVES

No.	Substituent	Yield (%)	m. p. (°C)	Appearance	Formula	Analysis (%) Calcd. C	Calcd. H	Found C	Found H
XIII	C_6H_5–	73	154—155	Yellow needles	$C_{13}H_{10}N_4S_2$	54.52	3.52	54.40	3.93
XIV	*p*-CH_3O–C_6H_4–	65	161—162	〃	$C_{14}H_{12}ON_4S_2$	53.14	3.82	53.14	4.10
XV	*p*-C_2H_5O–C_6H_4–	70	173—174	〃	$C_{15}H_{14}ON_4S_2$	54.52	4.27	54.56	4.56
XVI	*p*-C_3H_7O–C_6H_4–	54	146—148	〃	$C_{16}H_{16}ON_4S_2$	55.79	4.68	55.83	4.83
XVII	*p*-C_4H_9O–C_6H_4–	57	139—141	〃	$C_{17}H_{18}ON_4S_2$	56.96	5.06	57.32	5.30

4) G. M. van der Want, *Rec. trav. chim.*, **67**, 45 (1948).
5) A. M. Khaletskiĭ and V. G. Pesin, *Zhur. Obshchei Khim.*, **24**, 133 (1954); *Chem. Abst.*, **49**, 3170 (1955).
6) Heineman, *Friedländer*, **11**, 1126 (1915).
7) L. S. Efros and R. N. Levit, *Zhur. Obshchei Khim.*, **23**, 1552 (1953); *Chem. Abst.*, **48**, 1209 (1956).
8) L. S. Efros and R. N. Levit, ibid **25**, 199 (1955); *Chem. Abst.*, **50**, 1783 (1954).
9) Bayer and Co., *Friedländer*, **2**, 534 (1891).
10) A. M. Khaletskiĭ and V. G. Pesin, *Zhur Obshchei Khim.*, **20**, 1914 (1950); *Chem. Abst.*, **46**, 106 (1952).
11) C. F. Huebner, J. L. Marsh, P. H. Mizzoni, R. P. Mull, D. C. Schroeder, H. A. Trovell and C. R. Scholz, *J. Am. Chem. Soc.*, **75**, 2274 (1953).
12) E. A. Konopka, P. C. Eisman, R. L. Mayer, F. Paker and S. L. Pobbins, *Amm. Rev. Tuberc.*, **70**, 130 (1954).

white needles, m.p. 143~144°C, showing no depression on admixture with the above-mentioned sample (a).

Anal. Found: C, 65.10; H, 7.45. Calcd. for $C_{12}H_{16}N_2S$: C, 65.41; H, 7.31%.

VI. A mixture of 7.5 g. of 3, 4-diaminophenetole dihydrochloride, 10 ml. of 80% formic acid, 5 ml. of concentrated hydrochloric acid, and 30 ml. of water was refluxed for 8 hr. The mixture was evaporated under a reduced pressure and the residue was poured into 30 ml. of concentrated ammonium hydroxide. The solid thus formed was recrystallized from ethanol to give 4.6 g. (85%) of 5-ethoxybenzimidazole, m.p. 118~119°C.

Anal. Found: C, 66.64; H, 6.18. Calcd. for $C_9H_{10}ON_2$: C, 66.65; H, 6.15%.

The hydrolysis was carried out by gently refluxing a mixture of 1.2 g. of 5-ethoxybenzimidazole and 4 ml. of hydriodic acid (d=1.7) for 7hr. After removal of the excess of hydriodic acid in vacuo, the residue was dissolved in 5 ml. of water and neutralized with sodium hydrogen carbonate. The product deposited was recrystallized from water to give 0.8 g. (80%) of white needles, m.p. 216~217°.

Anal. Found: C, 62.98; H, 4.84. Calcd. for $C_7H_6ON_2$: C, 62.68; H, 4.51%.

VII. Upon oxidation of 8.5g. of 5-methylbenzimidazole with 35 g. of potassium permanganate by the usual procedure, 5-benzimidazolecarboxylic acid was obtained; the crude product was dissolved in aqueous ammonia solution, and treated with active carbon. Precipitation with acetic acid gave 7 g. (70%) of white needles, m.p. 325°C (decomp.).

Anal. Found: C, 59.05; H, 3.95. Calcd. for $C_8H_6O_2N_2$: C, 59.26; H, 3.73%.

A mixture of 1.2 g. of 5-benzimidazolcarboxylic acid and 12 ml. of thionyl chloride was refluxed for 5 hr. Excessive thionyl chloride was removed and dried off in a vacuum desiccator. The residue was poured slowly, with stirring, into 15 ml. of cold concentrated ammonia water. The solid was recrystallized from water to give 0.6 g. (50%) of white prisms, m. p. 247~248°C (monohydrate).

Anal. Found: C, 53.70; H, 5.43; H_2O 10.13. Calcd. for $C_8H_7ON_3 \cdot H_2O$: C, 53.62; H, 5.62; H_2O 10.05%.

VIII. A mixture of 5 g. of 5-benzimidazolecarboxylic acid, 100 ml. of absolute ethanol, and 3 ml. of concentrated sulfuric acid was refluxed for 10 hr. After removal of the excess of ethanol in vacuo, the residue was treated with 20 ml. of water and neutralized with sodium hydrogen carbonate. A white crystalline precipitate was immediately formed. After standing for several hours at 0°C, the solid was collected and recrystallized from ethanol to give 4.1 g. (70%) of ester, m.p. 101~103°C.

A mixture of 5.3 g. of ester, 2.5 ml. of hydrazinhydrate (80%), and 10 ml. of ethanol was heated on a water bath for 10 hr. After removing the ethanol, the solidified residue was recrystallized from ethanol, affording 4 g. (82%) of acid hydrazide in the form of white needles, m.p. 240°, 248°C (decamp.).

Anal. Found: C, 54.71; H, 4.73. Calcd. for $C_8H_8ON_4$: C, 54.54; H, 4.58%.

Reduction of 4-nitrobenzothiadiazole.—To a suspension of 10 g. of 4-nitrobenzothiadiazole in 100 ml. of 10% sodium chloride solution, 0.3 ml. of 0.5% hexachloroplatinic acid solution was added and stirred in a hot water bath. When 4-nitro derivative was melted, 30 g. of iron powder was added in one portion. The mixture was heated and stirred for an additional 1 hr., cooled, and extracted with 50 ml. of benzene (twice). The benzene layer was dried and distilled. The residue was recrystallized from water to give 4 g. of yellow needles, m.p. 67—68°C[13].

The acetylation was carried out by gently refluxing a mixture of 0.7 g. of 4-amino compound, 4 ml. of acetic acid, and 0.7 ml. of acetic anhydride for 1 hr. Recrystallization from water gave 0.5 g. of white needles, m.p. 152°C[14].

XIII. A mixture of 3 g. of 4-aminobenzothiadiazole, 2.7 g. of phenylisothiocyanate, and 5 ml. of alcohol was refluxed for 1 hr. to give 4.2 g. (73%) of the desired product melting at 150°C. The crude material was recrystallized from ethanol to yield a pure substance melting at 154~155°.

Anal. Found: C, 54.40; H, 3.93. Calcd. for $C_{13}H_{10}N_4S_2$: C, 54.52; H, 3.52%.

The author wishes to express his gratitude to Professor S. Kakimoto of Hokkaido University for his kind encouragement and advice.

The Research Institute for Tuberculosis
Hokkaido University, Sapporo

13) m. p. 68°C[8]
14) m. p. 152.5°C[8]

Ultraviolet Absorption Spectra of Three Isomeric Pyridine Monocarboxylic Acids and Their N-Oxides

By Norisuke HATA

(Received October 15, 1957)

In a previous paper[1], the author has reported the effect of hydroxymethyl group on the absorption spectra of pyridine and pyridine *N*-oxide. In order to obtain the knowledge on the effect of an electron-attracting substituent, the present author measured the ultraviolet absorption spectra of three isomeric pyridine monocarboxylic acids and their *N*-oxides in various solvents, and discussed the solvent effects on their spectra and also the effect of a carboxyl group on the absorption spectra of pyridine and pyridine *N*-oxide. The results of these spectral measurements were shown to be interpreted under the assumption of the intramolecular hydrogen bond formation or the steric interaction in picolinic acid and its *N*-oxide.

Experimental

Commercial picolinic, nicotinic, and isonicotinic acid were purified by recrystallization from ethanol several times.

Picolinic acid: m. p., 135°~7°C; nicotinic acid: m. p., 232°C; isonicotinic acid: m. p., 315°C.

Picolinic[2] and isonicotinic acid *N*-oxide[3] were synthesized by the method given in all kinds of literature, and nicotinic acid *N*-oxide was synthesized by treating the nicotinic acid with aqueous hydrogen peroxide in glacial acetic acid in a similar way as for isonicotinic acid *N*-oxide, all of which were purified by recrystallisation from ethanol or methanol several times.

Picolinic acid *N*-oxide: m. p., 160°C, (from ethanol); nicotinic acid *N*-oxide: m. p., 247°~8°C, decomp., (from methanol); isonicotinic acid *N*-oxide: m. p., 260°C, (from methanol).

Solvents used in the spectral measurements were dioxane, ethanol and water which were purified according to the directions described in "Organic Solvents"[4]. The ultraviolet absorption spectra were measured with a Shimadzu Quartz Spectrophotometer Type QB-50, using a fused quartz cell of 1 cm. thickness.

1) N. Hata, This Bulletin, in press.
2) R. Adams and S. Miyano, *J. Am. Chem. Soc.*, **76**, 3168 (1954).
3) E. Chigi, *Ber.*, **75**, 1318 (1942).
4) A. Weissberger and E. S. Proskauer, "Organic Solvents" 2nd. Ed., (1955).

Results and Discussion

Figs. 1 to 6 show the absorption curves of three isomeric pyridine monocarboxylic acids and their *N*-oxides in various solvents, and the schematic spectra of these compounds are given in Fig. 7. The observed values of maximum wavelength, wave number, and molar extinction coefficient are listed in Table I.

(1) Pyridine monocarboxylic acids:— From the spectral measurements of these compounds, the following results were obtained for the absorption appearing in the region between 35000 cm^{-1} and 40000 cm^{-1}.

a) The absorption maximum of picolinic acid does not essentially shift in solvents such as dioxane, ethanol and water, but that of nicotinic or isonicotinic acid shifts to the shorter wavelength in the above order of solvents.

b) The absorption maxima of all these compounds occur in the shorter wavelength than that of benzoic acid[5].

c) The absorption at about 38900 cm^{-1} (257 mμ) of pyridine in ethanol shifts to longer wavelength by the introduction of a carboxyl group to the pyridine nucleus[8].

The 38500 cm^{-1} (260 mμ) absorption of benzene shifts to the longer wavelength by substituting a carboxyl group into the benzene nucleus. This shift is regarded as mainly due to the electron migration effect from the benzene ring to the carboxyl group[9]. Moreover, it may be

5) The absorption maximum of benzoic acid occurs in 36750 cm^{-1} (272 mμ) in dioxane or ethanol[6] and 36890 cm^{-1} (271 mμ) in water[7], where the value of absorption maximum in various solvents shows that of the greatest intensity in the fine structures of this band.
6) H. E. Ungnade and R. W. Lamb, *J. Am. Chem. Soc.*, **74**, 3789 (1952).
7) C. Moser and A. I. Kohlenberg, *J. Chem. Soc.*, **1950**, 804.
8) In this paper, the effects of a carboxyl group on the absorption spectra of pyridine and pyridine *N*-oxide are discussed in relation to the spectra of ethanol solution, since the compounds used in this experiment are insoluble in non-polar solvents.
9) About the effect of the substituent on the electronic absorption spectrum of benzene, see, for example, W. West, "Chemical Applications of Spectroscopy", Chapter V, New York, (1956).

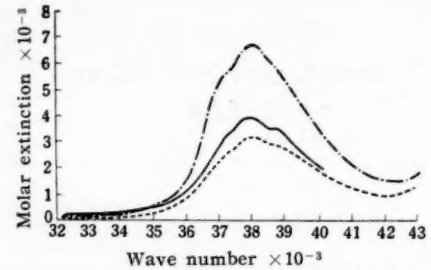

Fig. 1. Absorption curve of picolinic acid.
—— Dioxane. - - - Ethanol. -·-·- Water.

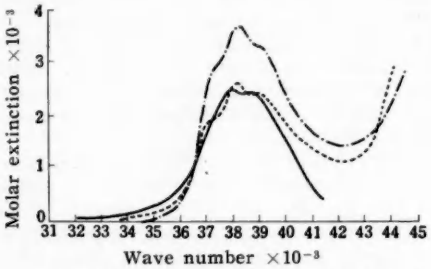

Fig. 2. Absorption curve of nicotinic acid.
—— Dioxane. - - - Ethanol. -·-·- Water.

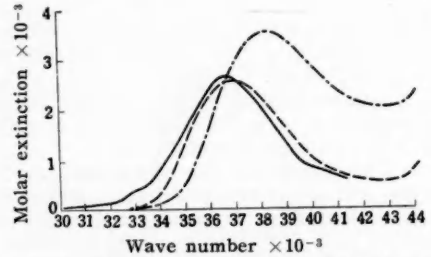

Fig. 3. Absorption curve of isonicotinic acid.
—— Dioxane. - - - Ethanol. -·-·- Water.

expected that there exists a qualitatively parallel relationship between the wavelength shift and the magnitude of the electron migration. If one of the C—H groups of benzene is replaced by a nitrogen atom, the electron migration possibly decreases to some extent compared with the case of benzoic acid, since the electron attracting power of the nitrogen atom of pyridine nucleus competes with that of the carboxyl group. Thus, pyridine monocarboxylic acid absorbs the shorter wavelength light than benzoic acid does. Here, since the competetive resonance interaction between the nitrogen atom and the carboxyl group is the greatest in nicotinic acid, its absorption spectrum appears in the region of the shorter wavelength than that of the other two acids.

It is of interest to know that the absorption maximum of pyridine shifts to longer wavelength by the introduction of a carboxyl group upon the pyridine nucleus. Particularly in the case of 2-carboxyl substitution, the absorption maximum locates at the shorter wavelength than that of 4-carboxyl substitution. These facts are remarkably different from the effect of substitution of an electron-repelling group(e.g., methyl, amino, halogen etc.). In this case, the absorption maximum of 2-substituted derivatives occurs in the longer wavelength than that of 4-substituted ones[1,10]. To explain such a displacement toward shorter wavelength of the absorption band of picolinic acid (when compared with the absorption band of isonicotinic acid), we assumed the formation of the intramolecular hydrogen bond as shown in (A) for

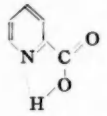

(A)

picolinic acid. This assumption leads to the conclusion that the electron migration from the pyridine ring to the carboxyl group in picolinic acid should be somewhat prevented by the increase in the electronegativity of the nitrogen atom caused by the formation of such an intramolecular hydrogen bond, from which the hindrance of resonance of this molecule may result. Consequently, the absorption spectrum of picolinic acid appears in the shorter wavelength than that of isonicotinic acid in which the intramolecular hydrogen bond does not occur.

Moreover, it seems to be accepted as an additional evidence for such an intramolecular hydrogen bond formation that the absorption maximum in dioxane solution of picolinic acid does not shift in solvents such as ethanol and water acting as a proton donor to the nitrogen atom of pyridine nucleus.

(2) Pyridine monocarboxylic acid *N*-oxides :—From the spectral measurements of these compounds, the following results are obtained for the absorption appearing in the region between 30000 and 41000 cm^{-1}.

a) The absorption maxima of these

10) H. Tsubomura, *J. Chem. Soc. Japan, Pure Chem. Sec.*, (*Nippon Kagaku Zassi*), **78**, 293 (1957).

compounds show a greater blue shift with the change of the solvents from dioxane to ethanol and water[11]. However, the extent of the shift in picolinic acid *N*-oxide is smaller than that in nicotinic or isonicotinic acid *N*-oxide.

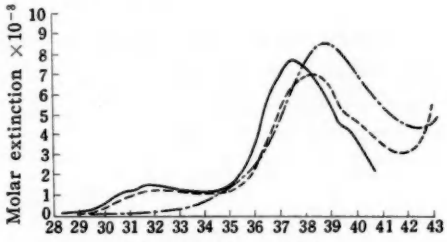

Fig. 4. Absorption curve of picolinic acid *N*-oxide.
—— Dioxane. - - - Ethanol. -·-·- Water.

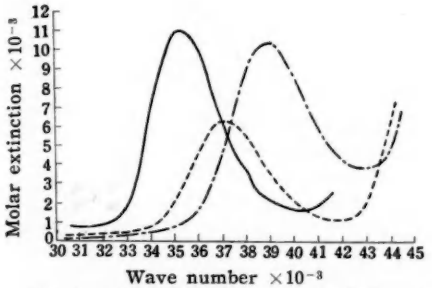

Fig. 5. Absorption curve of nicotinic acid *N*-oxide.
—— Dioxane. - - - Ethanol. -·-·- Water.

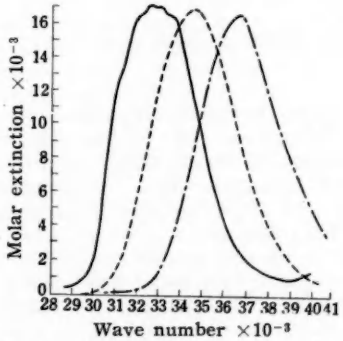

Fig. 6. Absorption curve of isonicotinic acid *N*-oxide.
—— Dioxane. - - - Ethanol. -·-·- Water.

b) The absorption spectrum of picolinic acid *N*-oxide shows considerable similarity to that of picolinic acid in the value of maximum wavelength. On the other hand, for nicotinic or isonicotinic acid *N*-oxide, the maximum wavelength is noticeably different from that of the corresponding acid.

c) The maximum wavelength of isonicotinic acid *N*-oxide in water is nearly the same value with that of isonicotinic acid in dioxane, while the maximum wavelength of picolinic acid *N*-oxide in water locates at the shorter wavelength than that of the corresponding acid in dioxane.

d) The absorption at about 37700 cm^{-1} (265 mμ) of pyridine *N*-oxide in ethanol shifts to the longer wavelength by the substitution of a carboxyl group at 3- or 4-position and to the shorter wavelength by that at 2-position.

It is infarred from the value of dipole moment[13] and the chemical reactivity[14] of pyridine *N*-oxide that the electron migration both into the pyridine ring from the N—O group, and in the opposite direction, is possible. From the studies of dipole moments of 4-substituted pyridine *N*-oxides by Katritzky et al.[15], however, it was shown that the N—O group behaves as an electron-attracting group when 4-substituent (Z) is an electron-repelling group as shown in (B). On the other hand, the N—O group shows a character acting as

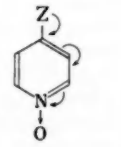

(B)
(Z=CH_3, Cl, $N(CH_3)_2$, etc.)

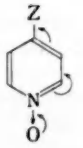

(C)
(Z=NO_2, $COOC_2H_5$ etc.)

an electron repelling group when 4-substituent (Z) is an electron attracting group as shown in (C). Therefore, if one assumes the N—O group as an electron-repelling group in pyridine monocarboxylic acid *N*-oxides, the following qualitative discussions are made for their spectra.

The absorption spectrum of pyridine monocarboxylic acid *N*-oxide is expected

11) Such a greater blue shift is probably due to the hydrogen bonding effect between the oxygen atom of N-O group and R-OH of solvent like other pyridine *N*-oxides[1,12].

12) T. Kubota, *J. Pharm. Soc. Japan* (*Yakugaku Zassi*), **74**, 831 (1954). M. Ito and N. Hata, This Bulletin, **28**, 260 (1955). N. Hata, ibid., **29**, 82 (1956).

13) E. P. Linton, *J. Am. Chem. Soc.*, **62**, 1945 (1940).

14) E. Ochiai, *J. Org. Chem.*, **18**, 534 (1953).

15) A. R. Katritzky et al., *J. Chem. Soc.*, **1957**, 1769.

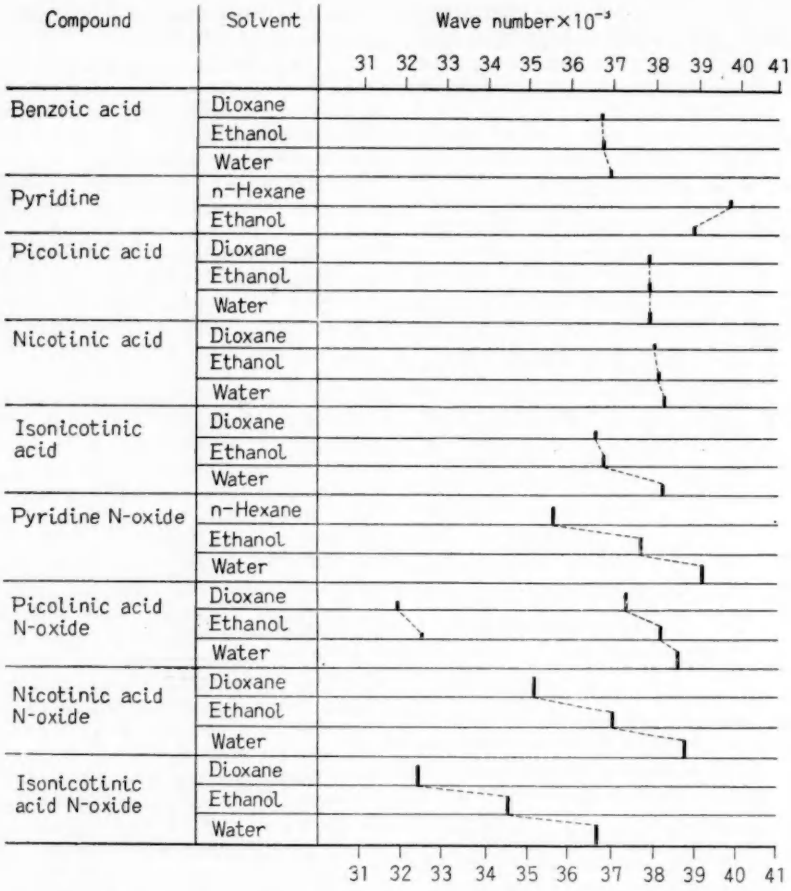

Fig. 7. Schematic spectra of three isomeric pyridine monocarboxylic acids and their *N*-oxides.

to occur in the region of the longer wavelength than that of pyridine *N*-oxide or benzoic acid, because the electron migration from the ring to the carboxyl group is facilitated by the N—O group acting as an electron-repelling group. Here, since the resonance interaction between N—O and carboxyl group is the greatest in picolinic and isonicotinic acid *N*-oxides, it is presumed that the absorption spectra of these two *N*-oxides occur in the longer wavelength than that of nicotinic acid *N*-oxide. Although nicotinic or isonicotinic acid *N*-oxide shows an effect expected above, picolinic acid *N*-oxide shows a blue-shift with a decreased intensity like other 2-substituted pyridine *N*-oxides[1,16]. To explain these facts, the author attributed the formation of the intramolecular hydrogen bond and the steric interaction in picolinic acid *N*-oxide, both of which prevented the resonance of this molecule.

Firstly, if one assumes the intramolecular hydrogen bond as shown in (D) for picolinic acid *N*-oxide, the electron migration

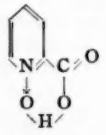

(D)

from the oxygen atom of N—O group to the pyridine ring may be somewhat pre-

16) N. Ikekawa and Y. Sato, *Pharm. Bull.*, **2**, 400 (1954).

TABLE I

WAVE LENGTHS, WAVE NUMBERS, AND MOLAR EXTINCTION COEFFICIENTS OF THREE ISOMERIC PYRIDINE MONOCARBOXYLIC ACIDS AND THEIR *N*-OXIDES

Compound	Solvent	Wave length ($m\mu$)	Wave Number (cm^{-1})	Molar extinction coefficient
Picolinic acid	Dioxane	264	37900	3980
	Ethanol	264	37900	3240
	Water	264	37900	6750
Nicotinic acid	Dioxane	263	38000	2500
		259	38600	2460
	Ethanol	262	38100	2640
		257	38900	2430
	Water	261.5	38200	3660
Isonicotinic acid	Dioxane	273	36600	2670
	Ethanol	271.5	36800	2580
	Water	261.5	38200	3520
Picolinic acid *N*-oxide	Dioxane	313	31900	1500
		268	37350	7700
	Ethanol	307.5	32500	1250
		261.5	38200	7000
	Water	259	38600	8600
Nicotinic acid *N*-oxide	Dioxane	284	35200	11000
	Ethanol	269.5	37100	6300
	Water	258	38800	10300
Isonicotinic acid *N*-oxide	Dioxane	308.5	32400	17000
	Ethanol	289	34600	16000
	Water	272	36700	16300

vented owing to the increase in its electronegativity caused by this intramolecular hydrogen bond. Therefore, the maximum wavelength of picolinic acid *N*-oxide may be close to that of picolinic acid. Such an intramolecular hydrogen bond will also decrease the effect of the solvent acting as a proton donor to the oxygen atom of N—O group on the absorption spectrum of picolinic acid *N*-oxide. The above expectations are in good agreement with the experimental results a) and b).

Secondly, it is also necessary to consider the steric or the electrostatic interaction between the N—O group and the carboxyl group. As is seen from Table I, the maximum wavelength lies in the order of 4-> 3->2-isomer and the intensity decreases remarkably in the same order. These facts are partly regarded to be due to the obstruction of the coplanarity of this molecule caused by the steric or the electrostatic interaction between N—O group and carboxyl group, just as in the spectra of ortho-substituted benzoic acids[7], by which the conjugation between the ring and the carboxyl group becomes weakened[17]. Such interactions are the greatest in picolinic acid *N*-oxide and the small electrostatic interaction may also arise from the polarities of N—O group and carboxyl group in nicotinic acid *N*-oxide. This consideration is in agreement with the spectral behavior of these compounds.

It seems probable that the experimental results c) are accounted for by the weakening of the conjugation between the ring and the carboxyl group in picolinic acid *N*-oxide, (when compared with that of corresponding acid) resulting from the steric or the electrostatic effect mentioned above. If the conjugation between the ring and the carboxyl group of pyridine monocarboxylic acid *N*-oxide were nearly identical with that of the corresponding acid, an increase in the electronegativity of the oxygen atom caused by the hydrogen bond formation between the

17) About the steric effect in the electronic absorption spectra see, for example, E. A. Braude and E. S. Waight, "Progress in Spectrochemistry. I." (edited by W. Klyne), London, p. 136, (1954).

oxygen atom of N—O group and the hydrogen atom of water should result in the fact that the wevelength of the absorption maximum observed with the *N*-oxide molecule might be similar to that of the corresponding acid.

In the case of picolinic acid *N*-oxide, in addition to the strong absorption band near 37350 cm^{-1} (268 mμ), a small one at about 31900 cm^{-1} (313 mμ) is observed in dioxane, which shows a blue shift in ethanol and apparently disappears in water. This disappearance is possibly due to the overlap with the strong absorption band at the shorter wavelength. This absorption may be regarded as due to an n–π^* transition like other pyridine *N*-oxides.

Summary

The ultraviolet absorption spectra of 2-, 3- and 4-pyridine monocarboxylic acid and their *N*-oxides were measured in various solvents. The absorption spectra of these compounds with the exception of picolinic acid show the blue shift with the change of the solvent from dioxane to ethanol and water.

The absorption band of picolinic acid occurs in the region of the shorter wavelength than that of isonicotinic acid; this fact may be caused by the formation of the intramolecular hydrogen bond, which prevents the resonance of this molecule. The absorption band of picolinic acid *N*-oxide occurs in the region of the shorter wevelength than that of nicotinic or isonicotinic acid *N*-oxide, for which the present author attributed the formation of the intramolecular hydrogen bond and the steric interaction in picolinic acid *N*-oxide.

We also observed the n–π^* absorption in picolinic acid *N*-oxide.

The author wishes to express his hearty thanks to Professor S. Imanishi of Kyushu University for his kind guidance and encouragement. Thanks are also due to Dr. E. Suenaga of Nagasaki University for his support throughout this work.

Faculty of Pharmacy, Nagasaki University, Nagasaki

Some Studies of the Inductive Effect

By Shiro MAEDA

(Received October 12, 1957)

Inductive effect has long been recognized as a useful idea in organic chemistry, particularly in relation to chemical reactivity problems. We can see the occurrence of this effect among the values of electric dipole moment of various molecules, most remarkably in some chain homologues.

In most cases, it is relatively a simple matter to take this effect qualitatively into consideration, but rather difficult quantitatively. In recent years, some developments were brought about on the latter point. Morino, Miyagawa and Oiwa[1] have established an empirical rule successfully applicable to the electric moments of various haloalkanes. Smith, Ree, Magee and Eyring[2] have developed a semi-classical theory advantageous for the application to chemical reactivity problems. Cahill and Mueller[3] have treated the effect of carboxylic group on the adjacent C-C bond quantum-mechanically.

For all these and previous studies, however, the theoretical basis of inductive effect can not yet be considered to be well established enough for quantitative applications. Now, in this paper, an approximate method will be developped to

1) Y. Morino, I. Miyagawa and J. Oiwa, *Botyu-kagaku*, **15**, 181 (1950). I. Miyagawa, *J. Chem. Soc. Japan, Pure Chem. Sec.* (*Nippon Kagaku Zassi*), **75**, 1061 (1954).

2) R. P. Smith, T. Ree, J. L. Magee and H. Eyring, *J. Am. Chem. Soc.*, **73**, 2263 (1951).

3) J.M. Cahill and C.R. Mueller, *J. Chem. Phys.*, **24** 513 (1956).

estimate the details of induced electric moment in non-conjugate systems, with some illustrative applications to haloalkane molecules.

An Approximate Expression of the Polarity of Bond

The object of the present work is the description of saturated systems such as substituted paraffin compounds. It is a conclusion of chemical experiences that the bonding electron pair of each separate bond in such a molecule can be regarded as fairly well localized. For such systems, the treatment based on bond orbital wave functions may be a fairly good approximation.

The bond orbital ϕ_i of the i-th bond A-B may be approximated by the localized molecular orbital as given by Eq. 1,

$$\phi_i(1)=a_i\chi_{Ai}(1)+b_i\chi_{Bi}(1) \tag{1}$$

where χ_{Ai} and χ_{Bi} are the valence atomic orbitals of both atoms. Each ϕ_i is subjected to the normalization condition, Eq. 2.

$$\int\phi_i^*(1)\phi_i(1)d\tau_1=a_i^2+2a_ib_iS_i+b_i^2=1 \tag{2}$$

$$S_i=\int\chi_{Ai}^*(1)\chi_{Bi}(1)d\tau_1$$

A quantity Q_i is also used as defined in Eq. 3, named "bond charge" by Mulliken[4], in the present formulation as the principal parameter.

$$Q_i=a_i^2-b_i^2=(a_i^2+a_ib_iS_i)-(b_i^2+a_ib_iS_i) \tag{3}$$

Now, when the complete localization of bond obitals were assumed, the electronic energy of a molecule may be approximately expressed by Eq. 4, the basic elucidation for which is given in appendix.

$$E=2\sum H_i+\sum_{i,j}(2-\delta_{ij})J_{ij} \tag{4}$$

$$H_i=\int\phi_i^*(1)h_1\phi_i(1)d\tau_1 \tag{5}$$

$$J_{ij}=\int\phi_i^*(1)\phi_j^*(2)(e^2/r_{12})\phi_i(1)\phi_j(2)d\tau_1d\tau_2 \tag{6}$$

In Eq. 4, H_i and J_{ij} are the bare-nuclear field orbital energy and the coulomb integral as given in Eqs. 5 and 6 respectively, where h_1 is the bare nuclear field energy Hamiltonian, r_{12} the interelectronic distance, and $\delta_{ij}=1$ or 0 for $i=j$ or $\neq j$.

With the ϕ_i given in Eq. 1, H_i can be written as Eq. 7 taking Eq. 2 into consideration.

$$H_i=(1/2)(\alpha_A^i+\alpha_B^i)+(1/2)Q_i(\alpha_A^i-\alpha_B^i)+2a_ib_i\beta_i \tag{7}$$

$$\left.\begin{aligned}\alpha_A^i&=\int\chi_{Ai}^*(1)h_1\chi_{Ai}(1)d\tau_1,\\ \alpha_B^i&=\int\chi_{Bi}^*(1)h_1\chi_{Bi}(1)d\tau_1\\ \beta_i&=\int\chi_{Ai}^*(1)h_1\chi_{Bi}(1)d\tau_1\\ &\quad-(1/2)S_i(\alpha_A^i+\alpha_B^i)\end{aligned}\right\} \tag{8}$$

Further, it is transformed to Eq. 9 by expanding $2a_ib_i$ into a power series of Q_i.

$$H_i=(1/2)(\alpha_A^i+\alpha_B^i)+(\beta_i/1+S_i)-(1/2)(\alpha_A^i-\alpha_B^i)Q_i-(1/2)\beta_iQ_i^2-(1/8)(1-S_i^2)\beta_iQ_i^4\cdots\cdots \tag{9}$$

In order to express J_{ij} by a simple function of Q_i's, we shall adopt the approximate equation (10)[4].

$$\phi_i^*\phi_i\approx(1+Q_i)\chi_{Ai}^*\chi_{Ai}+(1-Q_i)\chi_{Bi}^*\chi_{Bi} \tag{10}$$

Then Eq. 11 is obtained, where the coefficients C^{ij}'s take the form of Eq. 12.

$$J_{ij}=C_0^{ij}+C_i^{ij}Q_i+C_j^{ij}Q_j+C_{ij}^{ij}Q_iQ_j \tag{11}$$

$$\left.\begin{aligned}C_0^{ij}&=(1/4)[(ii/jj)+(ii/j'j')\\ &\quad+(i'i'/jj)+(i'i'/j'j')]\\ C_i^{ij}&=(1/4)[(ii/jj)+(ii/j'j')\\ &\quad-(i'i'/jj)-(i'i'/j'j')]\\ C_j^{ij}&=(1/4)[(ii/jj)-(ii/j'j')\\ &\quad+(i'i'/jj)-(i'i'/j'j')]\\ C_{ij}^{ij}&=(1/4)[(ii/jj)-(ii/j'j')\\ &\quad-(i'i'/jj)+(i'i'/j'j')]\end{aligned}\right\} \tag{12}$$

$$(pq/rs)=\int p^*(1)s^*(2)(e^2/r_{12})q(1)r(2)d\tau_1d\tau_2,$$

(i, i', j, j' represent χ_{Ai}, χ_{Bi}, $\chi_{A'j}$, $\chi_{B'j}$, respectively).

Consequently, the total energy E is approximately given by Eq. 13.

$$E=\sum_i\{(\alpha_A^i+\alpha_B^i)+(2\beta_i/1+S_i)+\sum_j(2-\delta_{ij})C_0^{ij}+Q_i[(\alpha_A^i-\alpha_B^i)+2\sum_j(2-\delta_{ij})C_i^{ij}]-(\beta_i-C_{ij}^{ij})Q_i^2+\sum_{j\neq i}2C_{ij}^{ij}Q_iQ_j-(1/4)(1-S_i^2)\beta_iQ_i^4\cdots\cdots\} \tag{13}$$

Now, in Eq. 13, each Q_i has to take the value so as to minimize E, according to the variation principle; that is, Eq. 14 must be fulfiled by all Q_n's.

$$\partial E/\partial Q_n=0 \tag{14}$$

This equation takes the form of an infinite series in Q's in the present formulation. But, the Q's appearing in the

4) R. S. Mulliken, *J. chim. phys.*, 46, 497, 675 (1949).

systems in which we are interested are supposed to be fairly small against unity, and the approximate equation 15 may serve the purpose, where the quadratic and successive higher terms were neglected, and $\gamma_n = -\beta_n + C_{nn}^{nn}$.

$$[(\alpha_A^n - \alpha_B^n) + \sum_i 2(2-\delta_{ni}) C_n^{ni}] + 2\gamma_n Q_n + 4 \sum_{i \neq n} C_{ni}^{ni} Q_i = 0 \quad (15)$$

If we could solve the simultaneous equations resulting from Eq. 15, approximate $Q's$ for all separate bonds might be determined. But it seems hardly possible, at present, because of the difficulty in fixing the values of necessary integrals, especially α and γ. In the present calculation, however, we do not look for the $Q_i's$ themselves, but their changes due to some change in molecular constitution.

Now, we shall consider about the changes of Q of residual C–H or C–C bonds, due to subsitution by some polar group. In such a case, a hydrocarbon molecule before the substitution is taken as the reference constitution, for which Eq. 15 is written as Eq. 16; where Q_i^0 represents the magnitude in the reference constitution.

$$[(\alpha_A^n - \alpha_B^n) + \sum_i 2(2-\delta_{ni}) C_n^{ni}] + 2\gamma_n Q_n^0 + 4 \sum_{i \neq n} C_{ni}^{ni} Q_i^0 = 0 \quad (16)$$

When m C–H bonds corresponding to 1-st to m-th in reference constitution were replaced by other kind of polar bond, e. g. $CX_1 \cdots\cdots CX_m$, then Eq. 15 is written as Eq. 17 for each C–H or C–C bond in substituted constitution;

$$[(\bar{\alpha}_A^n - \bar{\alpha}_B^n) + \sum_{i=1}^{m} 4\bar{C}_n^{ni} + \sum_{i=m+1}^{z} 2(2-\delta_{ni}) C_n^{ni}] + 2\gamma_n Q_n + 4 \sum_{i=m+1, \neq n}^{z} C_{ni}^{ni} Q_i + 4 \sum_{i=1}^{m} \bar{C}_{ni}^{ni} Q_i = 0 \quad (17)$$

(z: the final number of bonds).

where the bar above some quantities implies the change due to substituion. It is to be noted, here, that β (and consequently γ) may be taken as fairly invariable at the substitution[1]. Subtracting Eq. 16 from Eq. 17, Eq. 18 is obtained.

$$[(\bar{\alpha}_A^n - \alpha_A^n) - (\bar{\alpha}_B^n - \alpha_B^n) + 4\sum_{i=1}^{m} (\bar{C}_n^{ni} - C_n^{ni})] + 2\gamma_n (Q_n - Q_n^0) + 4\sum_{i=1}^{m} (\bar{C}_{ni}^{ni} Q_i - C_{ni}^{ni} Q_i^0) + 4\sum_{i=m+1, \neq n}^{z} C_{ni}^{ni} (Q_i - Q_i^0) = 0 \quad (18)$$

In this equation, the braced term, which represents the change of penetration energy due to the substitution (cf. Eq. 12), may well be neglected as fairly small. Thus, Eq. 18 may be simplified as follows:

$$\gamma_n (Q_n - Q_n^0) + 2\sum_{i=1}^{m} (\bar{C}_{ni}^{ni} Q_i - C_{ni}^{ni} Q_i^0) + 2\sum_{i=m+1, \neq n}^{z} C_{ni}^{ni} (Q_i - Q_i^0) = 0 \quad (19)$$

(for every unsubstituted bond, n).

On the other hand, for change of Q of the substituent bond C–X, the simplest molecule CH_3X is taken as the reference constitution. Then the similar procedure as above gives Eq. 20 finally.

$$\gamma_n (Q_n - Q_n^0) + 2\sum_{i=1, \neq n}^{z} (\bar{C}_{ni}^{ni} Q_i - C_{ni}^{ni} Q_i^0) = 0 \quad (20)$$

(for every substituted bond, n).

In the following calculation, Eqs. 19 and 20 shall be used together to calculate the approximate magnitudes of induced polarity $(Q_n - Q_n^0)$.

Some Reference to Molecular Polarizability

Now, it is helpful for the present study to treat the molecular polarizability from the same point of view as above. The polarizability along one of the principal axes y of a molecule is given by Eq. 21, where f is a homogeneous electric field parallel to y-axis.

$$\alpha_y = -(\mathrm{d}^2 E / \mathrm{d}f^2)_{f=0} \quad (21)$$

The total energy E under the field is written as Eq. 22 which includes several f-dependent terms in addition to Eq. 13.

$$E = \sum_i \{(\alpha_A^i + \alpha_B^i) + (2\beta_i/1+S_i) + \sum_j (2-\delta_{ij}) C_0^{ij} - f(y_A^i + y_B^i) + Q_i[(\alpha_A^i - \alpha_B^i) + \sum_j 2(2-\delta_{ij}) C_i^{ij} - f(y_A^i - y_B^i)] + \gamma_i Q_i^2 + \sum_{j \neq i} 2C_{ij}^{ij} Q_i Q_j - (1/4)(1-S_i^2)\beta_i Q_i^4 \cdots\} \quad (22)$$

where y_A^i and y_B^i denote the average positions of electrons as given by

$$y_A^i = \int \chi_{Ai}^*(1) y_1 \chi_{Ai}(1) \mathrm{d}\tau_1,$$

and

$$y_B^i = \int \chi_{Bi}^*(1) y_1 \chi_{Bi}(1) \mathrm{d}\tau_1 \quad (23)$$

where y_1 is the y-coordinate of electron 1. Then, Eq. 24 results from Eqs. 21 and 22.

$$\alpha_y = \sum_i \{2Q_i (y_A^i - y_B^i - 2\sum_{j \neq i} C_{ij}^{ij} \dot{Q}_j)$$

$$+\dot{Q}_i^2[-2\gamma_i+3(1-S_i^2)\beta_i Q_i^2+\cdots]$$
$$-\ddot{Q}_i[\alpha_A^i-\alpha_B^i+2\textstyle\sum_j(2-\delta_{ij})C_i^{ij}+2\gamma_i Q_i$$
$$+4\textstyle\sum_{j\neq i}C_{ij}^{ij}Q_j-(1-S_i^2)\beta_i Q_i^3+\cdots]\}_{f=0} \quad (24)$$

$$\dot{Q}=(dQ_i/df)_{f=0},\quad \ddot{Q}_i=(d^2Q_i/df^2)_{f=0} \quad (25)$$

On the other hand, all $Q's$ have to satisfy Eq. 26 which corresponds to Eq. 14 in the last section.

$$\partial E/\partial Q_i=\alpha_A^i-\alpha_B^i+\textstyle\sum_j 2(2-\delta_{ij})C_i^{ij}-f(y_A^i-y_B^i)$$
$$+2\gamma_i Q_i+\sum_{j\neq i}4C_{ij}^{ij}Q_j-(1-S_i^2)\beta_i Q_i^3+\cdots=0 \quad (26)$$

Since this equation should hold for arbitrary value of f, Eq. 27 is available also.

$$[d(\partial E/\partial Q_i)/df]_{f=0}=-(y_A^i-y_B^i)+2\gamma_i\dot{Q}_i$$
$$+\sum_{j\neq i}4C_{ij}^{ij}\dot{Q}_j-3(1-S_i^2)\beta_i(Q_i)_{f=0}^2\dot{Q}_i+\cdots=0 \quad (27)$$

Thus, Eq. 28 is obtained finally from the combination of Eqs. 24 and 27. It shows also that the approximation employed thus far is consistent with the expression of bond moment given by Eq. 29.

$$\alpha_y=\textstyle\sum_i\dot{Q}_i(y_A^i-y_B^i) \quad (28)$$

$$m_i=Q_i(y_A^i-y_B^i) \quad (29)$$

The values of γ_i, which is essential to carry out the calculation formally given in the last section, can be determined by solving Eq. 28 simultaneously with Eq. 27′,

$$(y_A^i-y_B^i)-2\gamma_i\dot{Q}_i-\sum_{j\neq i}4C_{ij}^{ij}\dot{Q}_j=0 \quad (27')$$

where the fourth and further terms in Eq. 27 have been neglected. It must be noticed here, however, that the α_y in Eq. 28 represents only longitudinal contributions of bond polarizabilities dismissing the transverse; that is, as to methane, for example, $\alpha_y=(4/3)\alpha_{L(CH)}$, where $\alpha_{L(CH)}$ is the longitudinal bond polarizability determined empirically for CH bond. We solve Eqs. 28 and 27′ with such an α_y and theoretically calculated C_{ij}^{ij} and $(y_A^i-y_B^i)$, giving γ_{CH}. Next, γ_{CC} can be determined by similar calculation for ethane molecule, where γ_{CH} obtained above be available. In this way, the values of γ_i for several bonds were evaluated presuming that they are actually definite by bond species, and given in Table I.

TABLE I

Bond A–B	C–H	C–C	C–Cl	C–Br	unit
γ_{AB}	0.396	0.309	0.368	0.388	e^2/a_0
$\alpha_L(AB)$	7.9*	18.8*	36.7*	50.4*	10^{-25} cc.
$y_A^{AB}-y_B^{AB}$	1.291	1.372	2.461	2.915	a_0**

* H. A. Stuart, "Die Struktur des freien Molekuls" pp. 449, Springer, (1952).
** Bohr radius.

Illustrative Examples

Some examples of the calculation for the systems of the simplest type will be shown. Throughout them, Q_{CH}^0 and Q_{CC}^0 have presumably been taken equal to zero, and, necessary integrals such as $C_{ij}^{ij}(i\neq j)$, y_A^i and y_B^i were computed with Slater atomic orbitals[5] assuming sp^3 tetrahedral hybridization for carbon, except C_{ij}^{ij} of non-neighbors which were approximated by point charge model.

Example I. CH_3X (cf. Fig. 1)

Fig. 1

Fig. 2

For the CH bond of this type of molecule, Eq. 19 is written as Eq. i,

$$\gamma_{CH}Q_{CH}+2(C_{CH,CX}Q_{CX}+2C_{1,2}Q_{CH})=0 \quad (i)$$

where the superscripts in C_{ij}^{ij} were dropped. On the other hand, this type is taken as the reference constitution for all other X-substituted systems in the sense stated under Eq. 19. Therefore, Q_{CX} is taken so as the electric moment to be in accord with observed value. That is, Eq. ii is adopted as the second condition,

$$M_{exp}(CH_3X)=M_{cal}(CH_3X)=m_{CX}^{\rightarrow}+m_{CH}^{\leftarrow} \quad (ii)$$

where each bond moment is given by Eqs. iii and iv.

$$m_{CH}^{\leftarrow}=(1+Q_{CH})y_C^{CH}+(1-Q_{CH})y_H^{CH} \quad (iii)$$

5) J. C. Slater, *Phys. Rev.* **36**, 57 (1930).

$$m_{CX}^{\rightarrow}=(1-Q_{CX})y_C^{CX}+(1+Q_{CX})y_X^{CX} \quad \text{(iv)}$$

Then, Q_{CH} and Q_{CX} can be determined from these equations, and induced bond moment is given by Eq. v.

$$\Delta m_{CH}=Q_{CH}(y_C^{CH}-y_H^{CH}) \quad \text{(v)}$$

Example II. C_2H_5X (cf. Fig. 2)

The staggered form is assumed in this case. Then, Eq. 19 is written down as Eqs. iv~ix for the adjacent, *trans*, and *gauche* C–H bonds as to C–X bond respectively.

$$\gamma_{CH}Q_{CH}+C_{1,CX}Q_{CX}+C_{1,2}Q_{CH}+C_{CH,CC}Q_{CC}+C_{1,g}(Q_{CHg}+Q_{CHl})+C_{1,t}Q_{CHg}=0 \quad \text{(vi)}$$

$$\gamma_{CH}Q_{CHg}+C_{g,CX}Q_{CX}+(C_{1,g}+C_{1,t})Q_{CH}-C_{CH,CC}Q_{CC}+C_{1,2}(Q_{CHg}+Q_{CHl})=0 \quad \text{(vii)}$$

$$\gamma_{CH}Q_{CHl}+C_{t,CX}Q_{CX}+2C_{1,g}Q_{CH}-C_{CH,CC}Q_{CC}+2C_{1,2}Q_{CHg}=0 \quad \text{(viii)}$$

$$\gamma_{CC}Q_{CC}+C_{CC,CH}Q_{CX}+C_{CH,CC}(2Q_{CH}-2Q_{CHg}-Q_{CHl})=0 \quad \text{(ix)}$$

On the other hand, Eq. 20 is written as Eq. x for CX bond,

$$\gamma_{CX}(Q_{CX}-Q'_{CX})+2C_{1,CX}(Q_{CH}-Q'_{CH})+C_{CC,CX}Q_{CC}-C_{1,CX}Q'_{CH}+2C_{t,CX}Q_{CHg}+C_{t,CX}Q_{CHl}=0 \quad \text{(x)}$$

where the primed quantities represent the corresponding values in reference constitution CH_3X. In this way, all Q values can be determined.

For the other type of molecules, a similar procedure can be applied.

Results and Discussion

The theory has really been applied to the inductive effect occurring in some haloalkane molecules, the results of which are given in Table II and Fig. 3. For the present time, we have dealt with chloro- and bromo derivatives for which reliable experimental data could be obtained.

Looking at the Table II, the correspondence between the calculated and the experimental electric moments may be called fairly good in spite of several shortcomings in this treatment as mentioned below. Therefore, it may be permissible to

TABLE II

Molecule	Δm_{CH}	m^*_{CX}	M_{cal}		M_{exp}	Reference
CH_3Cl	0.186 D.	1.674 D.	(1.86) D.		1.86, 1.87 D.	1) 2), 3)
CH_3Br	0.167	1.623	(1.79)		1.78, 1.79, 1.80	4), 5), 3)
CH_2Cl_2	0.299	1.148	1.671		1.57, 1.62	1), 6)
CH_2Br_2	0.252	1.044	1.496		1.43	7)
$CHCl_3$	0.377	0.797	1.174		1.01, 1.15	1), 8)
$CHBr_3$	0.313	0.700	1.013		0.90, 0.99, 1.3	8), 9), 10)
C_2H_5Cl		1.773	2.029		1.98, 2.00, 2.02, 2.03	11), 12), 2), 4)
C_2H_5Br		1.739	1.966		1.92, 1.99, 2.01	4), 12), 5)
i-C_3H_7Cl		1.853	2.131		2.15	5)
n-C_3H_7Cl $\begin{cases}t\\g\end{cases}$		1.794 1.825	2.178 1.974	2.044**	2.03, 2.04	7), 12)

* The value subtracted by the atomic dipole of carbon tetrahedral orbital.

** Mean value for the abundance ratio *gauche*/*trans*=2/1[13].

References:

1) G. A. Barclay and R. J. W. LeFevre, *J. Chem. Soc.*, **1950**, 556.
2) R. Sanger, O. Steiger and K. Gachter, *Helv. Phys. Acta*, **5**, 200 (1932).
3) R. G. Shulman, C. H. Townes and B. D. Dailey, *Phys. Rev.*, **78**, 145 (1950).
4) C. P. Smyth and K. B. Mcalpine, *J. Chem. Phys.*, **2**, 499 (1934).
5) L. G. Groves and S. Sugden, *J. Chem. Soc.*, **1937**, 158.
6) P. C. Mahanti and D. N. Sen-Gupta, *J. Indian Chem. Soc.*, **5**, 673 (1928).
7) H. A. Stuart, "Die Struktur des freien Molekuls" pp. 290, Springer (1952).
8) B. Timm and R. Mecke, *Z. Physik*, **98**, 363 (1936).
9) Y. K. Syrkin and M. E. Dyatkina, "Structure of Molecules and the Chemical Bond" Intersci. Publ., New York: (1950).
10) *Trans. Faraday Soc.*, **30**, Appendix (1934).
11) J. G. Gelatis, *J. Appl. Phys.*, **19**, 419 (1948).
12) P. C. Mahanti, *Phil. Mag.*, (7) **20**, 274 (1935).
13) C. Komaki, I. Ichishima, K. Kuratani, T. Miyazawa, T. Shimanouchi and S. Mizushima, This Bulletin, **28**, 330 (1955).

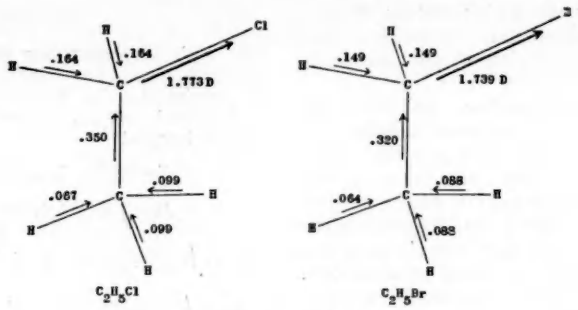

Fig. 3 (a)

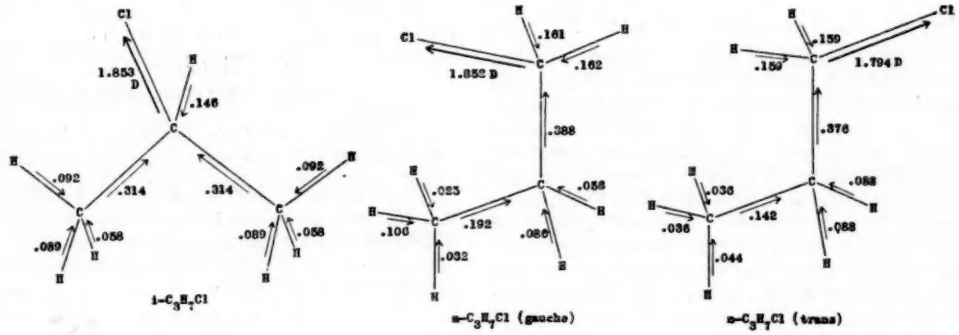

Fig. 3 (b)

discuss the detailed features of inductive effect somewhat quantitatively through the present treatment. It is also noticeable that Table II and Fig. 3 show fairly good agreement, in principal parts, with the preceding works[1,2]. In the present calculation, however, all inductive interaction terms have been included, and then, any change in the relative arrangement of bonds is reflected upon the whole results more or less, as can be observed at the difference between the *trans* and *gauche* forms of *n*-C_3H_7Cl in Fig. 3. The larger moment induced on γ-CH parallel to C-X than the β-C-H's may be understood as the marked consequence of direct effect. It must be noticed also that the *trans* form gives somewhat greater value of total moment than the *gauche* form in which actual induction is stronger than the *trans*. This means that the observed value of dipole moment can not always be taken as the measure of inductive effect without consideration about the abundance ratio of rotational isomers.

For the present calculation, we have assumed $Q^0_{CH}=0$ somewhat arbitrarily. It can readily be shown, however, that the different choice of Q^0_{CH}, which is smaller enough than Q_{CX} anyway, does not affect the results very much. Now, there may arise a question as to whether the inductive effect can be properly described with such a simple LCAO wave function as one which includes no polarization of atomic orbitals. This difficulty has essentially been avoided in the above treatment by employing the γ values determined from experimental bond polarizabilities, which are closely related phenomenally with the inductive effect. But yet, it is doubtful whether the bond polarizability data corresponding to vanishing field strength be efficient to estimate finite magnitudes of polarization. At present, little comment can be given on this problem. But the numerical results seem to permit the adoption of the data.

There still remains, however, an important problem; that is, the neglect of the possibility of transverse polarization. Considerable explanation against it might be found in the situation that the greater portion of general inductive effect is still attributable to the electronegativity change of end atoms; that is, the inductive effect

in the narrower sense, which causes mainly longitudinal polarization. However, the datails of the affair are yet an open question.

In practice of calculation, we must be concerned with the valence electronic configuration of substituent atoms. The present calculation has been carried out for $(ns)^2(np\sigma)(np\pi)^2(np\pi')^2$ configuration of halogen atoms. However, the possibility of mixing $(ns)(np\sigma)^2(np\pi)^2(np\pi')^2$ can not be ignored as has often been pointed out. After the mixing, the C-X bond moment becomes able to comprise the contribution from σ-type lone pair dipole in addition to the one from bonding pair expressed by Eq. ii, where the value of y_X^{CX} also changes with the mixing. This modification changes the formal expression of γ_{CX} and C_{Xi}'s in Eqs. 19 and 20. The formal change in γ_{CX} is not very significant, because it is determined empirically in practical calculations, as if it were a simple empirical parameter. The change in C_{Xi}'s, however, may possibly lead to markedly different results. There is no doubt that this effect might be most obvious on the neighboring bonds, and, the test-calculation has been carried out for methyl chloride and bromide. The result given in Fig. 4 shows that the effect seems not very serious.

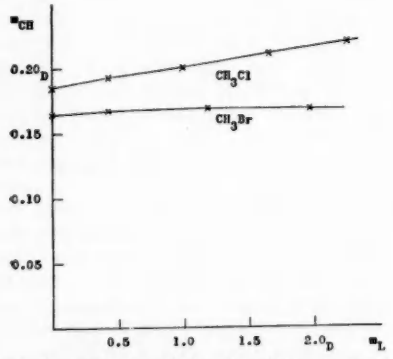

Fig. 4. The calculation has been carried out by the same procedure as in Example I, except that the lone pair dipole of X-atom, m_L, was added to M_{cal}. The bonding and lone pair orbitals of X-atom have been taken to be orthogonal with each other.

m_L can exceed the values of m_{CX} in Table II, because the latter is subtracted by the atomic dipole of carbon tetrahedral orbital.

Appendix

In SCF MO theory, the electronic energy of a molecule in closed shell state is expressed by Eq. I[4], where H_i, J_{ij}, and K_{ij} are bare nuclear field orbital energy, coulomb integral, and exchange integral

$$E=2\sum_i H_i+\sum_{i,j}(2J_{ij}-K_{ij}) \quad \text{(I)}$$

$$H_i=\int\phi_i^*(1)\,h_1\phi_i(1)\,d\tau_1 \quad \text{(II)}$$

$$J_{ij}=\int\phi_i^*(1)\phi_j^*(2)\,(e^2/r_{12})\phi_i(1)\phi_j(2)\,d\tau_1 d\tau_2 \quad \text{(III)}$$

$$K_{ij}=\int\phi_i^*(1)\phi_j^*(2)\,(e^2/r_{12})\phi_i(2)\phi_j(1)\,d\tau_1 d\tau_2 \quad \text{(IV)}$$

as given by Eqs. II$\sim$IV respectively. Now, an SCF MO ϕ_i may approximately be expressed by the linear combination of bond orbitals localized at each bond, as given by Eq. V.

$$\phi_i=\sum_r c_{ir}\phi_r \quad \text{(V)}$$

Then, we assume two approximate conditions as follows:

(1) There exists little overlapping between two different ϕ_r's, and therefore those integrals which include the product $\phi_r^*\phi_s$ $(r\neq s)$ such as S_{rs}, H_{rs}, and electronic interaction energy integrals other than coulomb type may be neglected. Then, Eq. VI may be taken as an approximate orthonormality condition.

$$\sum_r c_{ir}^* c_{jr}=\delta_{ij} \quad \text{(VI)}$$

(2) The electron density at each bond orbital and the bond order* between different bond orbitals remain constantly equal to 2 and 0 respectively, as expressed by Eq. VII.

$$\sum_i c_{ir}^* c_{is}=\delta_{rs} \quad \text{(VII)}$$

Under these assumptions, Eqs. II$\sim$IV can be written as follows:

$$H_i=\sum_r\sum_s c_{ir}^* c_{is}H_{rs}=\sum_r c_{ir}^2 H_{rr} \quad \text{(VIII)}$$

$$J_{ij}=\sum_r\sum_s\sum_t\sum_u c_{ir}^* c_{js}^* c_{it}c_{ju}(rt/su)$$
$$=\sum_r\sum_s c_{ir}^2 c_{js}^2(rr/ss) \quad \text{(IX)}$$

$$K_{ij}=\sum_r\sum_s\sum_t\sum_u c_{ir}^* c_{js}^* c_{it}c_{ju}(ru/st)$$
$$=\sum_r\sum_s c_{ir}^* c_{js}^* c_{is}c_{jr}(rr/ss) \quad \text{(X)}$$

where

$$H_{rs}=\int\phi_r^*(1)\,h_1\phi_s(1)\,d\tau_1 \quad \text{(XI)}$$

$$(rt/su)=\int\phi_r^*(1)\phi_s^*(2)\,(e^2/r_{12})\phi_t(1)\phi_u(2)\,d\tau_1 d\tau_2\,. \quad \text{(XII)}$$

Then, the total energy E can be given by Eq. XIII taking Eqs. VI and VII into consideration.

$$E=2\sum_i\sum_r c_{ir}^2 H_{rr}+\sum_i\sum_j\sum_r\sum_s(2c_{ir}^2 c_{js}^2$$
$$-c_{ir}^* c_{js}^* c_{is}c_{jr})\,(rr/ss)$$
$$=2\sum_r H_{rr}+\sum_r\sum_s(2-\delta_{rs})\,(rr/ss)\,. \quad \text{(XIII)}$$

* Similarly defined as in LCAO approximation.

The author wishes to thank Professor K. Kozima of Tokyo Institute of Technology for his valuable advice and encouragement, and Dr. S. Nagakura of Tokyo University for his helpful discussion.

Department of Chemistry, National Deffence Academy, Yokosuka

Synthesen und Konfigurationsermittlung in Rotenoid-Reihe. I. Ein Beitrag zur Synthese der Toxicarsäure

von Masateru MIYANO und Masanao MATSUI

(Eingegangen am 15 Oktober, 1957)

Die Strukturformel des auf Fische und Insekten giftig wirkenden Rotenons (I) ist gleichzeitig von Takei[1], von Butenandt[2] und von LaForge[3] aufgestellt worden. Seither von verschiedenen Arbeitsgruppen u. a. von Robertson und Mitarbb. sind viele Abbauprodukte der Rotenoide synthetisch dargestellt worden. Es bleibt heute die Aufgabe übrig, erstens die Konfigurationen des C_{12}- und C_{13}-Atoms aufzuschliessen, zweitens die natürlichen Rotenoide (Rotenon, Deguelin (II, R=H), Toxicarol (II, R=OH) usw.) zu synthetisieren.

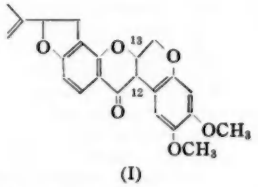

(I)

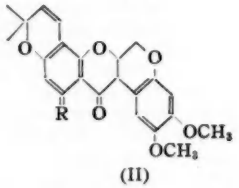

(II)

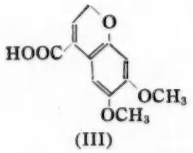

(III)

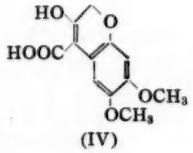

(IV)

In der vorliegenden Arbeit werden die verbesserten Synthesen der Toxicarsäure (6,7-Dimethoxy-Δ^3-chromen-4-carbonsäure) (III) berichtet.

Es entspricht die Toxicarsäure bzw. Oxynetorsäure (3-Oxy-6,7-dimethoxy-chroman-4-carbonsäure) (IV) dem halben Grundgerüst aller Rotenoide, daher scheint uns diese beiden Säuren die Schlüsselverbindungen für die gesamte Synthese von Rotenoiden zu sein. Die Toxicarsäure, welche von Butenandt[4] bei der Oxydation von *dl*-Toxicarol mit alkalischem Perhydrol und von Clark[5] auch bei der gleichen Oxydation von *dl*-Apotoxicarol(V) isoliert worden war, wurde durch sehr geschickte Reaktionsreihe von Robertson und Mitarbb[6~8]. synthetisch dargestellt. Am Anfang wollten wir diese Säure auf dem durch das Schema 1 dargestellten Wege erhalten, aber es war Essig damit, weil unter der gewöhnlichen Bedingung 6,7-Dimethoxy-chromanon (VI) die Blausäure nicht aufnimmt. Wir haben dann den anderen Weg gewählt. Ausgehend vom Robertsons Zwischenprodukt d. h. 6,7-Dimethoxy-chroman-3-keto-4-carbonsäure-äthylester (VII) durch die neuen

(1)

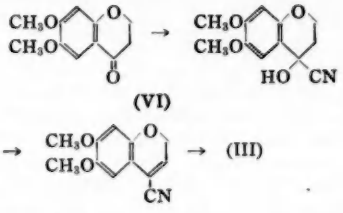

(VI)

(III)

1) S. Takei, S. Miyajima und M. Ohno, *Ber.*, **65**, 1041 (1932).
2) A. Butenandt und W. McCartney, *Ann.*, **494**, 17 (1932).
3) F. B. LaForge, *J. Am. Chem. Soc.*, **54**, 3377 (1932).
4) A. Butenandt und G. Hilgetag, *Ann.*, **495**, 172 (1932).
5) E. P. Clark, *J. Am. Chem. Soc.*, **54**, 2537 (1932).
6) A. Robertson, *J. Chem. Soc.*, **1930**, 2440.
7) A. Robertson, ebenda, **1932**, 1380.
8) A. Robertson und G. L. Rusby, ebenda, **1936**, 212.

(2) 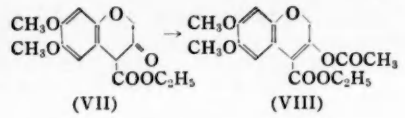

(VII) (VIII)

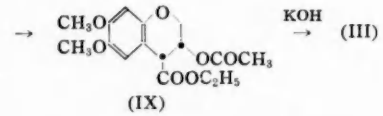

(IX)

(3) (VII) → 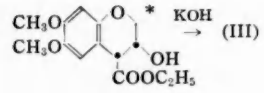

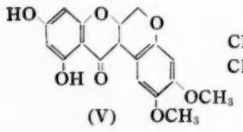

(V)

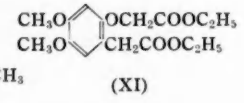

(XI)

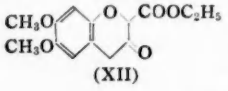

(XII)

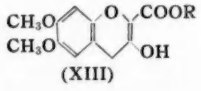

(XIII)

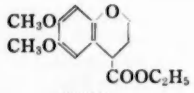

(XIV)

Reaktionen 2 und 3 haben wir die Toxicarsäure erhalten. Bei der intramolekulare Kondensation des Derrsäure-diäthylesters (XI) unter Einwirkung von Natrium hat Robertson[8] nur den 6,7-Dimethoxy-chroman-3-keto-4-carbonsäure-äthylester (VI) isoliert, dagegen haben wir neben dem letzteren den bisher noch nicht beschriebenen 6,7-Dimethoxy-chroman-3-keto-2-carbonsäure-äthylester (XII) erhalten, welcher bei der anschliessenden katalytischen Hydrierung 3-Oxy-6,7-dimethoxy-chroman-2-carbonsäure-äthylester (XIII, R=C_2H_5) liefert. Durch Versetzung vom Ketoester (VII) mit Acetanhydrid in Pyridin haben wir das entsprechende Enolacetat (VIII) dargestellt. Obwohl sich unser Enolacetat um 12~3°C niedriger Schmp. (71~2°C) als Literatur (84°C) zeigt, machen das IR- und UV-Spektrum sowie die Analysenzahlen sicher, dass unserem Enolacetat die in der Formel VIII angegebene Struktur zukommt. Bei der katalytischen Hydrierung mit Palladium-Kohle in Äthanol geht das Enolacetat in den noch nicht bekannten *dl-cis*-Acetoxynetorsäure-äthylester (3-Acetoxy-6,7-dimethoxy-chroman-4-carbonsäure-äthylester) (IX) über, der durch Behandlung mit alkoholischer Kalilauge oder Natriumcarbonat die Toxicarsäure liefert. Hingegen hat Robertson berichtet, dass sein Enolacetat (Schmp. 84°C) bei der katalytischen Hydrierung mit Platinoxyd Netorsäure-äthylester (XIV) lieferte. Auf Grund der guten Gesamtausbeute und sehr leicht verlaufenden Hydrierung scheint uns die Reaktionsfolge (2) der beste Weg zur Darstellung der Toxicarsäure zu sein. Andererseits haben wir die Robertsons Hydrierungsbedingung vom Schritt (VII) →(X) verbessert. Behandelt man den Ester (X) mit siedender alkoholischer Kalilauge, so geht es in die Toxicarsäure über. Dieser Weg ist auch das Beste zur Synthese der Toxicarsäure.

* Bestimmung dieser Konfiguration wird in der nachfolgenden Mitteilung berichtet werden.

Beschreibung der Versuche

Alle Schmpp. sind unkorrigiert.

6,7-Dimethoxy-chroman-3-keto-4-carbonsäure-äthylester (VII) und 6,7-Dimethoxy-chroman-3-keto-2-carbonsäure-äthylester (XII)—Eine Lösung von 68 g Derrsäure-diäthylester (XI) in 350 ccm Toluol und 50 ccm Xylol wird mit 8 g Natrium versetzt und 4 Stunden auf 110°C erhitzt. Nach dem Erkalten und der Zersetzung des zurückbleibenden Natriums durch Zutropfen von 40 ccm Eisessig, wird die Toluol-lösung mit Wasser gewaschen, über Natriumsulfat getrocknet und unter vermindertem Druck eingedampft. Die so erhaltenen rohen Kristalle werden in 250 ccm heissem Äthanol aufgenommen, unter Aktivkohlezusatz abfiltriert, und das Filtrat lässt sich bei Zimmertemperatur stehen. Die ausgeschiedenen Nadeln werden abgenutscht, und mit kaltem Alkohol gewaschen. Schmp. 103~5°C, Ausbeute 45 g. Beim Konzentrieren und bei der Behandlung mit Aktivkohle erhält man weitere Menge von Kristallnadeln (3 g). Obgleich diese Kristalle rein genung zu sein scheinen, sind es zwar ein Gemisch von zwei isomeren Estern. Durch zweimalige Umkristallisation aus Alkohol werden 27.5 g reinen 6,7-Dimethoxy-chroman-3-keto-4-carbonsäure-äthylester vom Schmp. 109°C isoliert.

Anal. Gef. C, 59.9; H, 5.7. Ber. für $C_{14}H_{16}O_6$: C, 60.0; H, 5.75%.

$\lambda_{max}^{Isopropanol}$ 247 mμ (ε 18800)

λ_{max} 6.01 (C=O), 6.17 (C=C) μ

6,7-Dimethoxy-chroman-3-keto-2-carbonsäure-äthylester vom Schmp. 95°C wird aus der Mutterlauge isoliert.

Anal. Gef. C, 60.0; H, 5.8. Ber. für $C_{14}H_{16}O_6$: C, 60.0; H, 5.75%.

$\lambda_{max}^{Isopropanol}$ 295 mμ (ε 5210)

λ_{max} 6.11 (C=O), 6.21 (C=C) μ

dl-cis-3-Oxy-6,7-dimethoxy-chroman-4-carbonsäure-äthylester (dl-cis-Oxynetorsäure-äthylester)* (*X*) — a) Der Ketoester (VII) (10 g) in 150ccm Essigester wird mit 4 g 10 proz. Palladium-Kohle

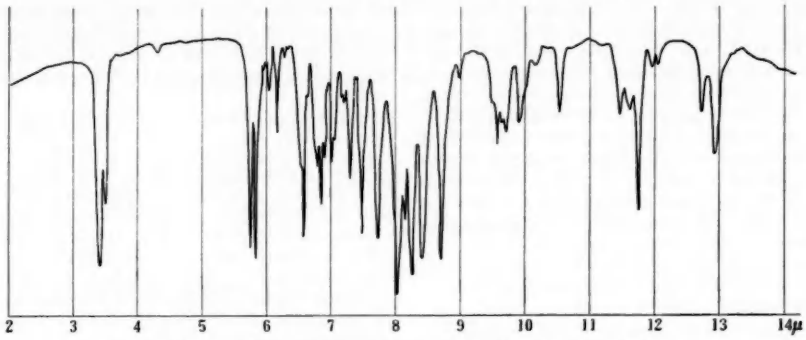

Abb. 1. IR-Spektrum des Enolacetats (XIII) in Nujol
5.75 μ(Acetat C=O), 5.84 μ(Ester C=O), 6.04 μ(konjg. C=C), 8.25 μ(Enolacetat C–C)

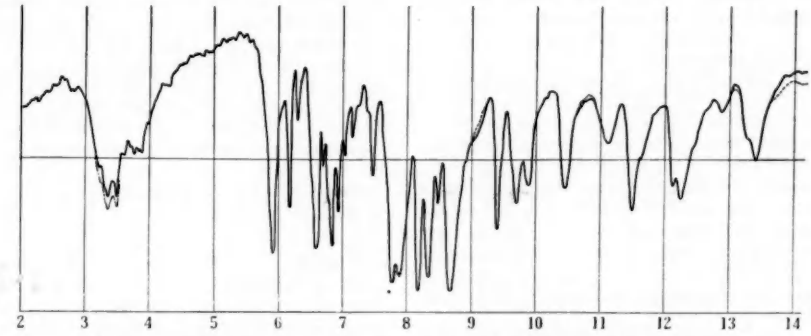

Abb. 2. IR-Spektrum der Toxicarsäure (Kaliumbromid-Presslinge)
—— Authentische Probe
------ Verseifung und Deacetylierung von Acetoxyester (s. Beschreibung der Versuche a))
----- Verseifung und Dehydratisierung von Oxynetorsäureäthylester (s. Beschreibung der Versuche b))

unter Wasserstoffström geschüttelt. Die Reaktion kommt nach Verbrauch von 1 Mol. Wasserstoff zum Stillstand. Die abfiltrierte Lösung wird in Vakuum konzentriert, mit 5 ccm Benzol aufgenommen und durch Zutropfen von 20 ccm Cyclohexan kristallisiert. Farblose Nädelchen werden abgesaugt, mit Äther gewaschen. Schmp. 108°C, Ausbeute 8.6 g.

Anal. Gef. C, 59.6; H, 6.4. Ber. für $C_{14}H_{16}O_6$: C, 59.6; H 6.5%.

Beim Eindampfen des Filtrats wird eine weitere Menge von Kristallen gewonnen (0.6 g, Schmp. 102~3°C).

b) In analoger Weise werden 10 g des Ketoesters (VII) in 50 ccm Essigster mit 1.0 g Platinoxyd unter Wasserstoffström geschüttelt. Der Oxyester (7.5 g) vom Schmp. 108°C wird erhalten.

c) Der Ketoester (VII) (5 g) nimmt 1 Mol. Wasserstoff auf beim Schütteln in 80 ccm Essigester in Gegenwart von 0.5 g Platinoxyd unter Zugabe von 1 ccm Morpholin. Die von Katalysator abgetrennte Lösung wird nach Waschen mit verd. Salzsäure, Bicarbonat-lösung und Wasser, über Natriumsulfat getrocknet, und das Lösungsmittel wird verdampft. Beim Versetzen von Äther und Cyclohexan und Stehen bei Zimmertemperatur erhält man 4.2 g von farblosen Nädelchen vom Schmp. 102~3°C. IR-Spektren der durch a), b) und c) gewonnenen drei Oxyester, die in Nujol Paste aufgenommen werden, sind ganz gleich.

***dl*-3-Oxy-6,7-dimethoxy-chroman-2-carbonsäure (*XIII*, *R*=*H*) und sein Äthylester (*XII*, *R*=C_2H_5)** —6,7-Dimethoxy-chroman-3-keto-2-carbonsäureäthylester (XII) wird in Essigester in Gegenwart von Platinoxyd reduziert. Das Hydrierungsprodukt wird vom Katalysator und Essigester befreit und gereinigt durch Umlösen aus Benzol. Schmp. 141°C.

Anal. Gef. C, 59.6; H, 6.4. Ber. für $C_{14}H_{16}O_6$: C, 59.5; H, 6.4%.

Der Oxyester wird beim 3stundigen Rückfliessen in 10 proz. alkoholischer Kalilauge zur freien Säure verseift. Schmp. 222~3°C (Umkristallisation aus Wasser).

Anal. Gef. C, 56.7; H, 5.5. Ber. für $C_{12}H_{14}O_6$: C, 5.67; H, 5.55%.

***6,7*-Dimethoxy-3-acetoxy-Δ^3-chromen-4-carbon-**

säure-äthylester (VIII)—Der Ketoester (VII) (9.0 g) wird mit 90 ccm Acetanhydrid und 45 ccm Pyridin versetzt, und die Mischung wird eine Stunde auf einem siedenden Wasserbad erhitzt, dann lässt sich bei Zimmertemperatur über Nacht stehen. Zu dieser Lösung wird 45 ccm Äthanol gegeben, und nach dem Erkalten wird das Produkt mit Äther aufgenommen. Nach Neutralwaschen der ätherischen Lösung mit verd. Salzsäure, Wasser, Bicarbonat und schliesslich mit Wasser, wird es über Natriumsulfat getrocknet und das Lösungsmittel wird verdampft. Nach der Umkristallisation aus Benzol—Cylcohexan erhält man 8.0 g des Enolacetats vom Schmp. 71～2°C (Literatur 84°C).

Anal. Gef. C, 59.6; H, 5.6. Ber. für $C_{16}H_{18}O_7$: C, 59.6; H, 5.6%.

$\lambda_{max}^{Isopropanol}$ 326 mμ (ε 4090)

Weitere Mengen (1.5 g) des Esters werden beim Eindampfen der Mutterlauge isoliert.

dl-cis-6,7-Dimethoxy-3-acetoxy-chroman-4-carbonsäure-äthylester (IX)

1.9 g des Enolacetats (VIII) werden in Äthanol mit 0.3 g 10 proz. Palladium-Kohle geschüttelt. Nach der raschen Aufnahme (2～3 Min) des Wasserstoffs (170 ccm, 1.2 Mol.) hörte die Reaktion plötzlich auf. Die alkoholische Lösung wird von Katalysator befreit und dann eingeengt. Das Rohprodukt kann ohne weitere Reinigung in die nachfolgende Reaktion übergeführt werden, nur ein Teil des Produktes wurde durch Chromatographie (vorläufig mit Säure behandelte Alumina, Benzol als Lösungsmittel) gereinigt für Elementaranalyse.

Anal. Gef. C, 59.2; H, 6.4. Ber. für $C_{16}H_{20}O_7$: C, 59.3; H, 6.2%.

$n_D^{23.5}$ 1.5250

Toxicarsäure (6,7-Dimethoxy-Δ^3-chromen-4-carbonsäure) (III) — a) Verseifung und Deacetylierung des Acetoxyesters (IX). Eine halbe Menge des rohen Acetoxyesters, der wie oben gezeigt aus den 1.9 g Enolacetaten (VIII) dargestellt wird, wird mit 15 ccm 10 proz. alkoholischer Kalilauge versetzt, und lässt sich 2 Tage bei Zimmertemperatur stehen. Zu dieser Lösung wird 50 ccm verd. Salzsäure zugegeben. Nach 2-tägigem Stehen in Eisschrank, werden die ausgeschiedenen braunen Kristallnadeln abgesaugt, mit Wasser gewaschen. So erhält man 0.7 g der fast reinen Toxicarsäure vom Schmp. 209°C (zersetz.).

Anal. Gef. C, 61.0; H, 5.1. Ber. für $C_{12}H_{12}O_5$: C, 61.0; H, 5.1.

$\lambda_{max}^{Isopropanol}$ 330 mμ (ε 4070)

Diese Säure stimmt an allen Eigenschaften mit der authentischen Toxicarsäure überein.

Die andere Hälfte des rohen Acetoxyesters wird in einer Lösung von 20 ccm 5 proz. Kaliumcarbonat und 20 ccm Äthanol gelöst. Nach 9-tägigem Stehen bei Zimmertemperatur wird die entstandene Toxicarsäure (0.6 g) analogerweise isoliert.

b) Verseifung und Dehydratisierung von Oxynetorsäure-äthylester (X)—4.0 g des *dl-cis*-Oxynetorsäure-äthylesters werden 3 Stunden in 35 ccm 10 proz. alkoholischer Kalilauge unter Rückfluss gekocht. Nach dem Erkalten werden 190 ccm Wasser und 10 ccm konz. Salzsäure zugegeben. Die ausgeschiedenen gelbbraunen Kristallnadeln werden abfiltriert, mit Wasser gewaschen. 2.7 g (80% der Theorie) des Toxicarsäure vom Schmp. 210°C (zersetz.) werden erhalten.

Anal. Gef. C, 61.0; H, 5.3. Ber. für $C_{12}H_{12}O_5$: C, 61.0; H, 5.1%.

Herren Professor Dr. R. Yamamoto und Professor Dr. Y. Sumiki danken wir herzlich für die Unterstützung und Förderung dieser Arbeit. Wir danken Herrn K. Aizawa für die Aufnahme des IR-Spektrums; Frau K. Satô, Fräulein M. Suzuki und Fräulein I. Isobe für Mikroanalysen. Herrn Dr. S. Tamura möchten wir auch an dieser Stelle für seine entgegenkommende Unterstützung danken.

Organisch-Chemisches Laboratorium,
Agrikulturlich-Chemisches
Departement, Universität
zu Tokyo, Hongo, Tokyo

Synthesen und Konfigurationsermittlung in Rotenoid-Reihe. II. Zur Synthese und Konfiguration der dl-cis- und dl-trans-Oxynetorsäure

Von Masateru MIYANO und Masanao MATSUI

(Eingegangen am 15. Oktober, 1957)

Eine Oxynetorsäure vom Schmp. 189°C neben Toxicarsäure (II) ist von Clark[1] bei der Oxydation von *dl*-Apotoxicarol (III) mit alkalischem Perhydrol isoliert worden, dazu kommt die in der Formel (I, R=H) angegebene Struktur. Ein Oxynetorsäure-äthylester (I, R=C_2H_5) ist von Robertson[2] durch die katalytische Hydrierung des zugehörigen Ketoesters (IV) dargestellt worden, aber er hat weder über die freie Säure noch seine Konfiguration beschrieben.

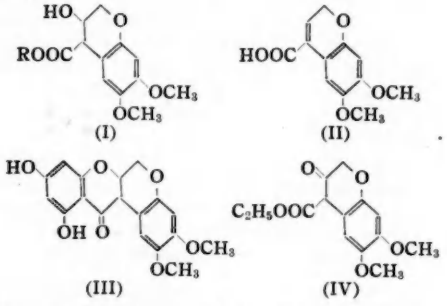

Kürzlich haben wir[3] 3-Acetoxy-6,7-dimethoxy-chroman-4-carbonsäure-äthylester (3-Acetoxynetorsäure-äthylester) (VI) durch die katalytische Hydrierung von Enolacetat (V) dargestellt. Demjenigen Ester (VI) muss die *cis*(erythro)-Konfiguration zukommen, weil bei der katalytischen Hydrierung der einfachen Doppelbindung gewöhnlich das *cis*-Addukt erhalten wird.

Wie schon von uns berichtet[3], geht der Oxynetorsäure-äthylester beim Rückfluss mit alkoholischer Kalilauge in die Toxicarsäure über. Behandelt man mit alkoholischer Kalilauge bei Zimmertemperatur, ist der Ester dagegen zu einem Stereoisomerengemisch der entsprechenden Säuren verseift worden, welches zu rund 90% aus eine Oxynetorsäure vom Schmp. 161°C und zu rund 10% aus der alternativen Oxynetorsäure vom Schmp. 156~7°C besteht. Wir dürfen diese Oxynetorsäure als Schlüsselverbindung gebrauchen, um die Konfigurationen des C_{12}- und C_{13}-Atoms des Rotenons aufzuschliessen. Diese besondere Bedeutung hat uns veranlassen dies eingehend zu untersuchen. Aus der theoretischen Überlegung kann man die entstandene Konfiguration nicht folgern. Aus der von K. von Auwers[4] und Skita[5], neuerdings von Barton[6] angegebenen Regel dürfen wir die Entstehung der *trans*(threo)-Form (X) bei der katalytischen Hydrierung von cyclischem Keton in neutraler bzw. basischer Lösung mit Platinoxyd erwarten. Wird der Ketoester (IV) durch die Enolform reduziert, dagegen soll die *cis*-Form (VII) entstehen. Infrarot-bzw. ultraviolett-Spektrum des Ketoesters bezeigen, dass derjenige Ester als Kristall oder *iso*-Propanol-lösung ganz die Enolform sei (s. Beschreibung d. Versuche). Aber in diesem Fall ist es uns unbegreiflich, dass das Enolacetat (V) ungefähr 60-malig schneller als die Enolform des Ketoesters (IV) hydriert wird, während die letztere sterisch weniger verhindert.

Um dies näher nachzuweisen, ist der Acetoxyester (VI) einerseits schonend verseift worden, damit wir *dl-cis*-Oxynetorsäure erwerben könnten. Aber, wie schon in der 1. Mitteilung erörtert, bei dieser Hydrolyse ist nur die Toxicarsäure als einziges Produkt isoliert worden. Auf der anderen Seite ist *dl*-Oxynetorsäure-äthylester (VII) mit Acetanhydrid und Pyridin versetzt worden und nach der chromatographischen Reinigung haben wir fast farbloses Öl erhalten, dessen IR-Spektrum mit demjenigen des chromatographisch gereinigten Acetoxyesters (VI) fast übereinstimmt.

Daher handelt es sich eine *dl*-Oxynetorsäure vom Schmp. 161°C um die *cis*-Form

1) E. P. Clark, *J. Am. Chem. Soc.*, **54**, 2537 (1932).
2) A. Robertson und G. L. Rusby, *J. Chem. Soc.*, **1934**, 212.
3) M. Miyano und M. Matsui, Dieses Bulletin, **31**, 267 (1958).
4) K. von Auwers, *Ann.*, **420**, 91 (1921).
5) A. Skita und W. Faust, *Ber.*, **64**, 2878 (1931).
6) D. H. R. Barton, *J. Chem. Soc.*, **1953**, 1027.

und die andere vom Schmp. 156~7°C um die *trans*-Form.

Die Oxynetorsäure vom Schmp. 161°C ist in einen Methylester vom Schmp. 74~5° und die andere Oxynetorsäure vom Schmp. 156~7°C in einen Methylester vom Schmp. 72~3°C übergegangen. Obgleich die beiden Methylester sehr ähnliche IR-Spektren aufweisen, zeigt der erste, wie der Äthylester (VII) eine starke Absorption bei 8.81 μ, während der letztere nicht.

Um die oben erwähnte Konfiguration ferner zu bestätigen, haben wir zunächst die höher schmelzende Säure mit Alkali zu isomerisieren untersucht. Wir haben die *dl-trans*-Oxynetorsäure vom Schmp. 156~7°C neben der Toxicarsäure erhalten, obwohl die Ausbeute schlecht war.

Endlich haben wir den Ketoester (IV)

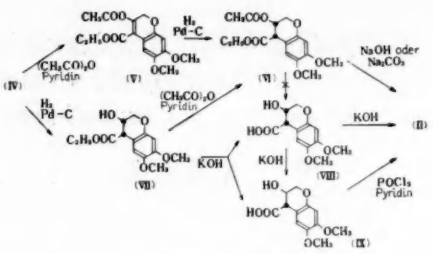

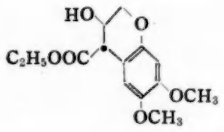

(X)

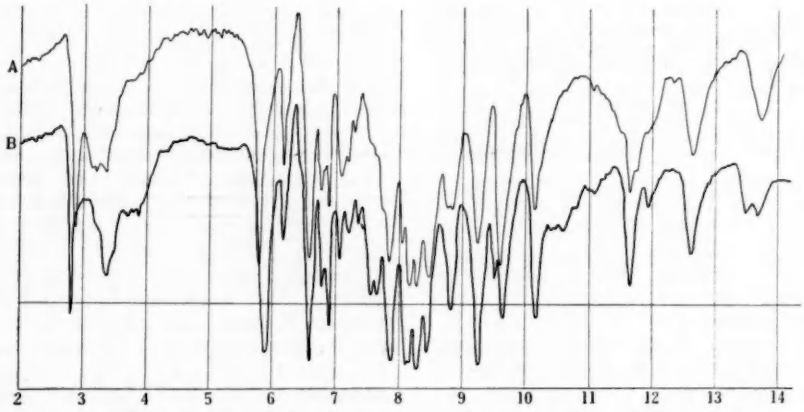

Abb. 1. IR-Spektrum der *dl-cis*-Oxynetorsäure (fest in KBr gepresst) ····· (A)
2.88 (OH), 5.79 (C=O) μ.
IR-Spektrum der *dl-trans*-Oxynetorsäure (fest in KBr gepresst) ····· (B)
2.80 (OH), 5.87 (C=O) μ.

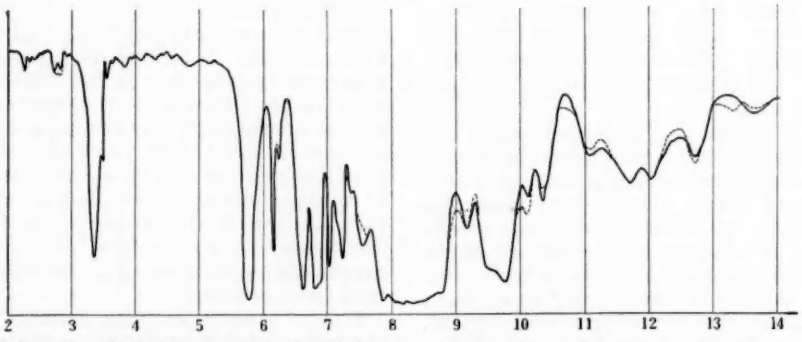

Abb. 2. IR-Spektrum des *dl-cis*-3-Acetoxy-6,7-dimethoxy-chroman-4-carbonsäure-äthylesters (flüssig).
—— Hydrierung von Enolester
------ Acetylierung von *dl-cis*-Oxynetorsäure-äthylester

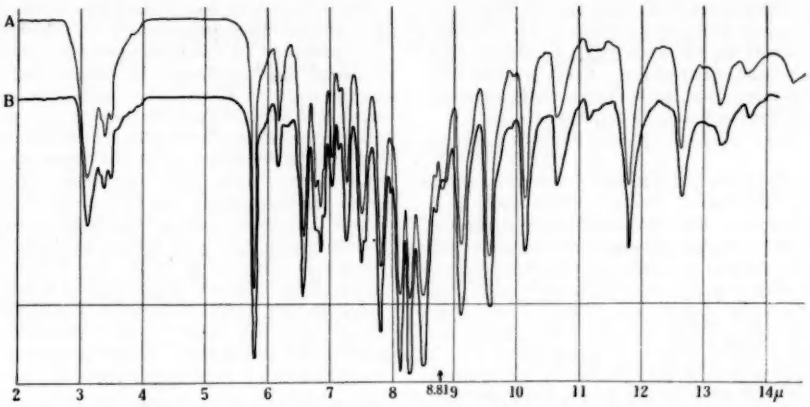

Abb. 3. IR-Spektrum des *dl-cis*-Oxynetorsäure-methylesters ..... (A)
IR-Spektrum des *dl-trans*-Oxynetorsäure-methylesters ..... (B)
(fest in KBr gepresst)

mit Natriumborohydrid reduziert, mit der Erwartung, den thermodynamisch stabileren *trans*-Ester (X) als Hauptprodukt zu erwerben. Obgleich keine reine Oxynetorsäure isoliert worden ist, wurde die Toxicarsäure nach der Dehydratisierung vom Rohprodukt mit Phosphoroxychlorid in Pyridin in geringer Ausbeute isoliert.

Unserer Erwartung zuwider, stimmt die von Clark isolierte Oxynetorsäure mit den in der vorliegenden Arbeit beschriebenen beiden Oxynetorsäuren nicht überein.

Beschreibung der Versuche

Alle Schmp. sind unkorrigiert.

dl-cis-3-Oxy-6,7-dimethoxy-chroman-4-carbonsäure (*dl-cis-Oxynetorsäure*) (*VIII*) ***und dl-trans-3-Oxy-6,7-dimethoxy-chroman-4-carbonsäure*** (*dl-trans-Oxynetorsäure*) (*IX*). — Zehn Gramme des Äthylesters (VII)[3] werden in 150 ccm 10proz. alkoholischer Kalilauge gelöst und die Lösung wird 24 Stunden bei Zimmertemperatur aufbewahrt, dann neutralisiert mit verd. Salzsäure (Congorot). Das Lösungsmittel wird abdestilliert und die zurückbleibende organische Säure in siedendem Aceton aufgenommen. Nach dem Eindampfen der Acetonlösung ist ein Rohprodukt geblieben, woraus bei der zweimaligen Umkristallisation aus 50 ccm heissem Wasser unter Aktivkohlezusatz 7.0 g der *dl-cis*-Oxynetorsäure vom Schmp. 161°C isoliert werden.

Anal. Gef.: C, 56.4; H, 5.5. Ber. für $C_{12}H_{14}O_6$: C, 56.7; H, 5.55%. λ_{max} 2.88 (OH), 5.79 (C=O) μ.

Aus der Mutterlauge, nach Konzentration und Behandlung mit Kohle erhält man 0.6 g von *dl-trans*-Oxynetorsäure vom Schmp. 156~7°C.

Anal. Gef.: C, 56.4; H, 5.5. Ber. für $C_{12}H_{14}O_6$: C, 56.7; H, 5.55%. λ_{max} 2.80 (OH), 5.87 (C=O) μ.

3-Acetoxy-6,7-dimethoxy-chroman-4-carbonsäure-äthylester (*3-Acetoxy-netorsäure-äthylester*) (*VI*).—Ein Gramm des *dl-cis*-Oxynetorsäure-äthylesters wird mit 3 ccm Acetanhydrid und 10 ccm Pyridin versetzt und 24 Stunden bei Zimmertemperatur aufbewahrt. Nach dem Eingiessen in verd. Salzsäure und Eis, wird das Produkt mit Äther extrahiert, mit Wasser, Bicarbonat, dann mit Wasser gewaschen, und über Natriumsulfat getrocknet. Beim Eindampfen des Lösungsmittels erhält man gelbliches Öl, welches hauptsächlich aus dem Acetoxyester besteht, doch mit geringer Menge der Toxicarsäure begleitet ist. Durch chromatographische Reinigung (Alumina, Benzol) erhält man den reinen Acetoxyester, dessen IR-Spektrum mit dem des in 1. Mitteilung beschriebenen *dl-cis*-Esters fast übereinstimmt (s. Abb. 2).

Anal. Gef.: C, 59.3; H, 6.2. Ber. für $C_{16}H_{20}O_7$: C, 59.3; H, 6.2%. $n_D^{23.5}$ 1.5260.

Toxicarsäure (*II*).—a) 1.0 g der *dl-cis*-Oxynetorsäure wird 3 Stunden in 10 ccm 10proz. alkoholischer Kalilauge unter Rückfluss gekocht. Nach dem Erkalten werden 50 ccm Wasser und 2.5 ccm konz. Salzsäure versetzt. Man erhält 0.83 g der Toxicarsäure vom Schmp. 206°C (zersetz.). Nach dem Umlösen aus wässerigem Aceton, Schmp. 209~210°C (zersetz.).

Anal. Gef.: C, 60.8; H, 5.3. Ber. für $C_{12}H_{12}O_5$: C, 61.0; H, 5.1%.

b) ***Natriumborohydrid Reduktion und anschliessende Dehydratisierung.***—Mit einer auf 10° gekühlten Suspension von 1.4 g Ketoester in 100 ccm Methanol wird 1 g von Natriumborohydrid versetzt. Nach 2tägigem Stehen bei Zimmertemperatur wird das Reaktionsgemisch in verd. Salzsäure eingegossen, dann in Essigester aufgenommen, mit Wasser gewaschen, und über Natriumsulfat getrocknet. Nach dem Eindampfen des Lösungsmittels versetzt man das bleibende Öl mit 30 ccm Kollidin und 1.5 ccm Phosphoroxychlorid und erhitzt die Mischung eine Stunde auf 100°C. Die so erhaltene fast farblose Lösung wird in verd. Salzsäure eingegossen, mit Essigester extrahiert. Nach dem Neutralwaschen und Eindampfen der Essigester-lösung kocht man das zurückbleibende Öl in 15 ccm alkoholischer

Kalilauge unter Rückfluss. Die bei der Wasserzugabe ausgeschiedenen Kristalle werden abfiltriert und das Filtrat wird konzentriert, und dann angesäuert mit verd. Salzsäure. Beim Stehen über Nacht scheiden die gelbbraune Kristallnadeln (ca. 6 mg) vom Schmp. 200° (zersetz.) aus.

Anal. Gef.: C, 60,2; H, 5,3. Ber. für $C_{12}H_{12}O_5$: C, 61,0; H, 5,1%.

IR-Spektrum stimmt mit dem der authentischen Probe überein.

dl-cis-3-Oxy-6,7-dimethoxy-chroman-4-carbonsäure-methylester (***dl-cis-Oxynetorsäure-methylester***).—Zu 0,5 gr der fein gepulverten *dl-cis*-Oxynetorsäure in 50 ccm Essigester gibt man Diazomethan in Äther zu. Nach 1-stundigem Stehen bei Zimmertemperatur zersetzt man überschüssiges Diazomethan mit Essigsäure, wäscht mit Bicarbonatlösung und Wasser, und trocknet über Natriumsulfat. Beim Eindampfen des Lösungsmittels und Umlösen aus Äther erhält man 0,45 gr des Methylesters vom Schmp. 74~5°.

Anal. Gef.: C, 58,2; H, 6,2. Ber. für $C_{13}H_{16}O_6$: C, 58,2; H, 6,0%.

Der Methylester (0,5 g) wird mit 10 proz. alkoholischer Kalilauge (20 ccm) versetzt und lässt sich 2 Tage beim Zimmertemperatur stehen. Nach dem Neutralisieren mit wässeriger Salzsäure und Eindampfen des Lösungsmittels unter vermindertem Druck wird die organische Substanz in heissem Aceton aufgenommen. Das Aceton wird dann abdestilliert und das zurückbleibende Produkt wird aus heissem Wasser (Aktivkohle) umkristallisiert. Schmp. und Mischschmp. 157~161°. λ_{max} 2,88(OH), 5,79(C=O) μ.

dl-trans-3-Oxy-6,7-dimethoxy-chroman-4-carbonsäure-methylester (***dl-trans-Oxynetorsäure-methylester***). — Analogerweise ergibt sich die *dl-trans*-Oxynetorsäure den Methylester vom Schmp. 72~3° (Umkristallisation aus Äther), der bei der Verseifung die *dl-trans*-Oxynetorsäure liefert.

Anal. Gef.: C, 58,4; H, 6,0. Ber. für $C_{13}H_{16}O_6$: C, 58,2; H, 6,0%.

Isomerisierung von d-lcis-Oxynetorsäure.—Ein g der *dl-cis*-Oxynetorsäure wird mit 20 ccm 10 proz. alkoholischer Kalilauge und 20 ccm Wasser versetzt und während 10 Tagen bei Zimmertemperatur aufbewahrt, und des Gemisch wird mit verd. Salzsäure angesäuert (Congorot) und unter vermindertem Druck eingedampft. Die organische Substanz wird mit siedendem Aceton extrahiert. Nach dem Vertreiben des Acetons wird der Rückstand aus 20 ccm heissem Wasser unter Aktivkohlezusatz umkristallisiert. Die sofort ausgeschiedenen gelben Kristalle der Toxicarsäure (ca. 0,1 g) wird abgesaugt und die Mutterlauge liefert *dl-cis*-Oxynetorsäure (0,6 g) beim Stehen in Kühlschrank. Die letzte Mutterlauge wird zu etwa 5 ccm eingeengt und mit Aktivkohle behandelt. Die isomerisierte *dl-trans*-Oxynetorsäure wird isoliert, ca. 0,15 g.

Herren Professor Dr. R. Yamamoto und Professor Dr. Y. Sumiki danken wir an dieser Stelle für die Unterstützung und Förderung dieser und nachfolgender Arbeiten. Herren Dr. Y. Chen, Taipei (Formosa) und Dr. W. F. Barthel, Agricultural Research Service (U. S. A.) für ihr Interesse und Überlassung von einigen Proben sind wir zu bestem Dank verpflichtet. Die Mikroanalysen wurden im analytischen Laboratorium unseres Departements ausgeführt; IR-Spektren wurden mit IR-Spektrophotometer Ôyô-Kôken, Modell DS 301 aufgenommen, wofür wir insbesondere Herrn. K. Aizawa bestens danken.

Organisch-Chemisches Laboratorium, Agrikulturlich-Chemisches Departement, Universität zu Tokyo, Hongo, Tokyo

Structural Variations of Kaolin Minerals

By Hiroshi TAKAHASHI

(Received December 12, 1957)

Kaolin minerals are made of stacking of aluminosilicate unit layers in their crystal structure. However, there are a continuous gradation in the manner of stacking from kaolinite which has a perfectly ordered sequence of layers to halloysite which has a throughly disordered sequence of layers.[1)]

In the results given by Murray, the degree of crystallinity determined by using the X-ray powder diffraction data does not agree with that based on the differential thermal analysis curve of halloysite.[2)] When one say the degree of crystallinity, however, there are two kinds of structural imperfection. One is the imperfections within the crystallographic unit layer and the other is the stacking disorder of the unit layers. As the definition of the crystallinity, both kinds of imperfection should be considered.

The purpose of this study is to determine the degree of crystallinity for all kaolin minerals through X-ray, thermal and other experimental methods, and to get some fundamental information for the relationship between structural characteristics and physico-chemical properties.

Results and Discussion

Samples.—The following kaolin minerals were investigated: Kaolinite from Mesa Alta, N.M., U.S.A., Kaolinite from Drybranch, Geor., U.S.A. The both materials are the API Standard Clay Minerals. Kibushi-clay from Shidare, Gifu, Japan which is a kaolin of fireclay type. Halloysite from Spruce Pine, N.C., U.S.A. which is the API Standard Clay Mineral and is considered to have the highest degree of crystallinity from the result of study through electron diffraction[3)]. Halloysite from Bedford, Ind., U.S.A. which is the API Standard Clay Mineral. Halloysite from Tintic, Utah, U.S.A. which is the API Standard Clay Mineral. Shichinoe-clay from Shichinoe, Aomori, Japan which is known to have a considerably low degree of crystallinity among halloysites[4)].

1) G. W. Brindley and K. Robinson, *Trans. Farad. Soc.*, **42B**, 198 (1946); S. Iwai, *Min. J.*, **1**, 233 (1955).
2) H. H. Murray, *Am. Mineral.*, **39**, 97 (1954).
3) G. Honjo and K. Mihama, *Acta Cryst.*, **7**, 511 (1954).
4) T. Sudo and H. Takahashi, "Proc. Fourth Conference on Clay and Clay Minerals", National Academy of Science-National Research Council, 1956, p. 67.

X-Ray Diffraction Studies.—From the investigation made by Brindley and Robinson, it was clarified that kaolin minerals are characterized by the stacking randomness in their structure. Their X-ray diagrams indicate the structural variations in kaolin minerals. To determine the relative degreee of crystallinity of kaolin minerals, in the present study, the criteria used by Brindley and Robinson, and some additional features found by Murray were used.

X-ray powder diffraction diagrams of kaolin minerals were obtained by X-ray diffractometer (Geigerflex). Halloysites were treated at 110°C in order to dry up the inter-layer water, this might result to have approximately the same basal spacing as in kaolinites. All specimens were ground, dried, and then sieved through 300 mesh. Experimental conditions were as follows: Filtered Cu radiation (Cu $K\alpha$: 1.5418 Å) is used at 35 kV and 15 mA, scanning speed is 1° or 1/4° 2θ per minute, time constant is 4 seconds, receiving slit is 0.2 mm or 0.1 mm, angular aperture is 1° or 1/2°.

To determine the degree of crystallinity in the X-ray diagram, the following major differences were used as criteria.

(1) Sharpness of the reflections.
(2) Number of reflections.
(3) Slight change in the basal spacing.
(4) Resolution between closely spaced reflections.
(5) Absence of certain reflections.

X-ray diffractometer traces of kaolin minerals are shown in Fig. 1. The X-ray reflections of kaolinites are sharp and distinct, and those of Spruce Pine halloysite are considerably sharp. For all other kaolin minerals, X-ray reflections are relatively broad and diffuse. These diffractometer records were made carefully by repeating the X-ray traces of specimens. It is also observable that the sharpness of reflections is dependent on particle size and orientation.

In the experiments, the specimens were prepared not to be oriented and particles of almost the same size were used, accordingly the effects of these factors might be

TABLE I

POWDER DATA OF KAOLIN MINERALS (in Å)

Brindley and Robinson			Kaolinite						Halloysite							
			Mesa Alta, N.M.		Drybranch, Geor.		Kibushi-Clay Shidare, Gifu		Spruce Pine, N.C.		Bedford, Ind		Tintic, Utah		Shichinoe, Aomori	
d	*I*	*hkl*	*d*	*I*	*d*	*I*	*d*	*I*	*d*	*I*	*d*	*I*	*d*	*I*	*d*	*I*
7.15	10+	001	7.14	VS	7.15	VS	7.20	S	7.15	VS	7.25	S	7.30	S	7.40	M
4.45	4	020	4.46	M	4.45	S	4.45	MS br	4.44	S	4.45	S	4.46	S	4.47	S
4.35	6	$1\bar{1}0$	4.35	S	4.36	M	4.33	W								
4.17	6	$11\bar{1}$	4.18	S	4.17	M										
4.12	3	$1\bar{1}\bar{1}$	4.13	W												
3.837	4	$02\bar{1}$	3.84	M	3.86	W										
3.734	2	021	3.73	W	3.74	WV										
3.566	10+	002	3.57	VS	3.58	VS	3.58	S	3.57	VS	3.63	MS	3.64	MS	3.66	M
3.365	4	111	3.37	M	3.37	W										
3.138	2	$11\bar{2}$	3.14	W												
3.091	2	$1\bar{1}2$	3.09	W												
2.748	2	022	2.75	W	2.74	W										
2.553	8	$20\bar{1}, 1\bar{3}0, 130$	2.55	MS	2.56	MS	2.56	M br	2.56	M	2.57	W br	2.57	W br	2.57	W br
							2.53	W br	2.53	W						
2.521	4	$13\bar{1}, 1\bar{1}2$	2.53	M	2.53	W										
2.486	9	$1\bar{3}1, 200, 112$	2.49	S	2.49	MS	2.50	VW br	2.49	M						
2.374	7	003	2.37	M	2.38	M	2.38	M br	2.38	M						
2.331	10	$20\bar{2}, 1\bar{3}1, 11\bar{3}$	2.33	S	2.34	S	2.34	VW br	2.33	M	(2.37	W br)	(2.37	W br)	(2.38	W br)
2.284	9	$1\bar{1}\bar{3}, 131$	2.29	MS	2.29	M			2.29	W						
2.243	1	$13\bar{2}, 040$	2.24	W	2.24	VW										
2.182	3	$13\bar{2}, 220$	2.18	W	2.18	W	2.20	VW	2.20	W						
2.127	2	$02\bar{3}, 041$	2.13	W												
2.057	1	$22\bar{2}$	2.06	W												
1.985	7	$20\bar{3}, 1\bar{3}2$	1.992	S	1.990	S	1.992	M	1.997	MS						
1.935	4	132, 221	1.941	M	1.936	M	1.90	W br								
1.892	2	$13\bar{3}$	1.902	W	1.898	W										
1.865	1	042	1.862	W												
1.835	4	$1\bar{3}\bar{3}, 202, 22\bar{3}$	1.840	M	1.840	W										
1.805	1	$11\bar{4}, 22\bar{3}$	1.810	W												
1.778	5	004	1.782	M	1.790	M	1.79	W br			1.80	W br			1.78	W br
1.704	1	$2\bar{2}2$	1.702	W												
1.682	2	$1\bar{5}0, 24\bar{1}, 31\bar{1}, 3\bar{1}\bar{1}, 222$	1.684	W	1.688	W										
1.659	8	$2\bar{1}0, 15\bar{1}, 20\bar{4}, 1\bar{5}3$	1.664	S	1.668	S	1.65	M br	1.670	MS	1.68	W br	1.68	W br	1.67	W br

Key to abbreviation: VS: very strong, S: strong, MS: medium strong, M: medium, W: weak, br: broad.

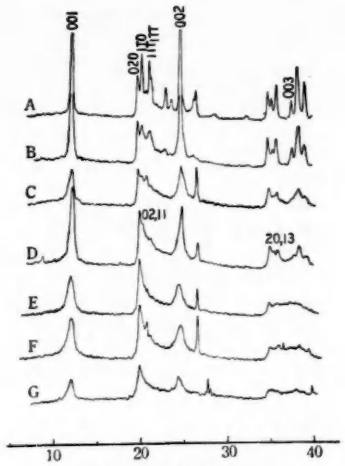

Fig. 1. X-ray diffractometer traces of kaolin minerals.
A, kaolinite, Mesa Alta, N.M., U.S.A.
B, kaolinite, Drybranch, Geor., U.S.A.
C, Kibushi-clay, Shidare, Gifu, Japan
D, halloysite, Spruce Pine, N.C., U.S.A.
E, halloysite, Bedford, Ind., U.S.A.
F, halloysite, Tintic, Utah, U.S.A.
G, halloysite, Shichinoe, Aomori, Japan

little. Among the specimens of halloysite, Spruce Pine halloysite has the largest number of reflections. The number of X-ray reflections which appear in the diagram indicates the relative degree of crystallinity.

Table I shows powder data for the kaolin minerals used in this study obtained from the X-ray diagram in Fig. 1.

The basal spacings were measured precisely. Slight changes of the basal spacings were detected for samples from Mesa Alta kaolinite to Shichinoe-clay. The basal spacing indicates a measure for the relative degree of crystallinity. The basal spacing in halloysite with lower degree of crystallinity is generally greater than that in kaolinite with higher degree of crystallinity. The slight change in the basal spacing can be attributed to the following reasons: (a) the presence of water layer between neighboring unit layers in kaolin minerals with lower degree of crystallinity, and/or (b) the disorderliness in the unit layer and looseness of the packing or stacking variations of the kaolin unit layers which should be greater in the specimens with lower degree of crystallinity.

The resolution between the closely spaced reflections in an X-ray diagram can be used as an indicator of the relative degree of crystallinity. The closely spaced reflections in an X-ray diagram of kaolinite with a considerable high degree of crystallinity are well resolved as exemplified by the reflections adjacent to the (020) and the (003) reflections of Fig. 1. These closely spaced reflections become hazy and indistinct in the diagrams of Kibushi-clay and Spruce Pine halloysite, and are completely merged in the diagrams of Bedford halloysite, Tintic halloysite and Shichinoe-clay.

The number of reflections closely related to the randomness of the stacking of kaolin unit layers. Reflections are not so many in the X-ray diagrams of kaolin minerals with lower degree of crystallinity. It is well known that the (OH) groups in the kaolin layers are arranged regular intervals along the *b*-axis, this distance being equall to $b_0/3$. This means that if one of two adjacent layers is displaced along the *b*-axis by an integral multiple of $b_0/3$, the two sheets will still be each oriented with same relationship to each other. If the displacement is not an integral multiple of $b_0/3$, then all reflections are cut out except those with a k index of $0, 3, 6, \cdots\cdots$. And if one of two adjacent layers is rotated by $n2\pi/3$, that is, random displacement is taken, all reflections indexed as (*hkl*) completely disappear. As the displacement in the kaolin layer remarkably increases and becomes irregular, the total number of reflections decreases and reflections become broad and diffuse.

As shown in Fig. 1 and Table I, Mesa Alta kaolinite has the highest degree of crystallinity and Shichinoe-clay has the lowest degree of crystallinity among the samples in this study.

Differential Thermal Analysis.—The crystallinity of kaolinite is indicated by differential thermal analysis curves..[5] Differential thermal analysis curves were made by using the same kaolin minerals as were used in the X-ray studies. The results obtained by using the differential thermal analysis curves are compared with the results of the X-ray data.

The specimens is the same as that described by Sudo et al[6]. Care was taken to place the sample into the sample block

5) R. E. Grim and W.F. Bradley, *Am, Mineral.*, **32**, 493 (1947).
6) T. Sudo et al., *J. Geol. Soc. Japan*, (*Chishitsu Gaku Zasshi*) **58**, 115 (1952).

as being packed homogeneously and keeping nearly constant weight. The mean heating rate was 12.5° per minute. It is known that the temperature of the peak of the endothermic reaction is correlated with the degree of crystallinity of kaolin minerals. However, general criteria based on differential thermal analysis curves which can be used for all kaolin minerals to determine the relative degree of crystallinity are yet to be found. In this study, the criteria used by Murray and some additional features were used to determine the relative degrees of crystallinity of the kaolin minerals.

The following measurements can be used as criteria to determine the relative degree of crystallinity:

(1) The peak temperature, the peak height and the area of the first endothermic reaction (E_{n1}) associated with the loss of the adsorbed or inter-layer water. The area is measured by a planimeter from the basal line.

(2) The peak temperature, the peak height and the area of the second endothermic reaction (E_{n2}) associated with the loss of the lattice water.

(3) The peak temperature, the peak height, the area and the breadth of the exothermic reaction (E_x) associated with the transformation to the new phase from the original mineral. The breadth is measured at the half value of the exothermic peak.

Differential thermal analysis cuves and data are shown in Fig. 2 and Table II respectively. The peak temperature of the second endothermic reaction indicates the degree of crystallinity, as the lattice water should be more tightly bonded in the kaolin with higher degree of crystallinity than the one with lower degree of crystallinity. As a large amount of energy is needed to break the bonds holding the lattice water, the peak temperature, and its peak height become higher and its area becomes larger as the degree of crystallinity becomes higher. From the data of Table II, it is clearly seen that the peak temperature, the peak height and the area of the reaction are correlated to the relative degree of crystallinity of kaolinite group based on X-ray data. This relation is also maintained in the halloysite group. However, as shown in Table II, the peak temperature, the peak height and the area of halloysite with higher degree of crystallinity are greater than those of Kibushi-clay. The

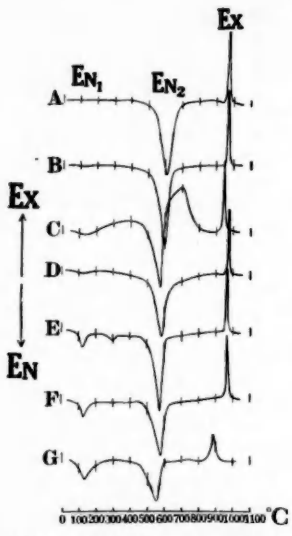

Fig. 2. Differential thermal analysis curves of kaolin minerals.
A, kaolinite, Mesa Alta, N.M., U.S.A.
B, kaolinite, Drybranch, Geor., U.S.A.
C, Kibushi-clay, Shidare, Gifu, Japan
D, halloysite, Spruce Pine, N.C, U.S.A.
E, halloysite, Bedford, Ind., U.S.A.
F, halloysite, Tintic, Utah, U.S.A.
G, halloysite, Shichinoe, Aomori, Japan

data in Table II show that in addition to those values the breadth of the exothermic reaction is also correlated to the relative degree of crystallinity. The breadth of peak of the exothermic reaction is expressed as the breadth at a half of peak height, since the expression of the breadth as the difference in temperature between the points at which the reaction begins and ends is indistinct in the measurement of those points. In Mesa Alta kaolinite and Drybranch kaolinite, the peak breadths are small, the peak temperatures are high and the heights are large. In spite of the degree of crystallinity based on X-ray data for Spruce Pine halloysite being low as compared with that of kaolinite, a higher degree of crystallinity is suggested from the character of the exothermic peak. In Kibushi-clay and halloysite excepting Spruce Pine halloysite, the degree of crystallinity is lower than that of kaolinite and Spruce Pine halloysite in the data of the final exothermic reaction. The smallness of the value of breadth of a kaolin mineral with a high degree of crystallinity confirms that the structure of the new phase

formed by exothermic reaction is correlated to the structure of original kaolin mineral, and that the more regular is the original structure, the faster is the transformation of the kaolin structure. In general, the peak temperature of the exothermic reaction of the kaolinites with a high degree of crystallinity is high, for more energy is needed in transformation to a new phase when the mother structure is stronger.

It is proved by the differential thermal analysis that Mesa Alta kaolinite, Drybranch kaolinite and Spruce Pine halloysite among the halloysite group have higher degree of crystallinity and that their crystallinity is higher than that of a kaolin of fireclay type like Kibushi-clay. Therefore, it is noteworthy that the degree of crystallinity of kaolinite determined by using a differential thermal analysis has the different meaning from that of halloysite determined by the same method.

Relationship between X-Ray and Thermal Data—The degree of crystallinity determined from the X-ray diffraction data is consistent with that from the thermal data in the series from kaolinite to kaolin of fireclay type, but not in the halloysite series.

When the inter-layer water is removed from the hydrated halloysite, it is considered that the unit layer which is structurally similar to the kaolinite layer may be the same as in a well-crystallized kaolinite. But the configuration of aluminum atoms may not be in the same manner as they are in a well-crystallized kaolinite. The possible variation in the configuration of aluminum atoms in each succesive layer is considered as a cause of broad reflections which are characteristic of the X-ray pattern of halloysite.

From the data of the X-ray diffraction, it seems that there is a continuous gradation of the structure from a kaolinite with a high degree of crystallinity to a halloysite with a low degree of crystallinity such as Shichinoe-clay. The differential thermal analysis made it clear that Spruce Pine halloysite has a high degree of crystallinity. This fact gives a valuable suggestion to the definition of the degree of crystallinity of kaolin minerals. This means that the degree of crystallinity of kaolin minerals involves two elements, that is, internal orderliness and stacking orderliness. The X-ray and thermal data suggest that X-ray reflections reveal both internal structural disorder and random stacking of the unit layers, whereas differential thermal analysis curves indicate internal structural disorder of the unit layers. Differential thermal analysis curves indicate the energy changes which a structure breaks down or a new phase forms. As shown by the thermal data, Spruce Pine halloysite has considerably perfect unit layers, however, as shown by X-ray data, the unit layers orientate with each other in a completely random manner with respect to to the *a*- and *b*-axis. In Kibushi-clay which is in a considerably low degree of crystallinity, there is a random displacement of $nb_0/3$ in different layers but not in a random orientation.

From these facts, it is considered that there are four typical variations in kaolin minerals when crystallinity is concerned.

(I) The mineral with the highest degree of crystallinity is estimated by using both X-ray and thermal method.

(II) The kaolin mineral with the lowest degree of crystallinity, estimated by using both methods.

(III) The kaolin mineral with the highest degree of crystallinity which is estimated by using X-ray method, but with the lowest degree of crystallinity by using thermal method.

(IV) The kaolin mineral with the highest degree of crystallinity estimated by using thermal method, but with lowest degree of crystallinity by using X-ray method.

These four ideal forms are related to the sizes and shapes of crystallites, physico-chemical properties and other forms.

Base Exchange Capacity.—A comparison of the relative degree of crystallinity of kaolin mineral used in this study with their base exchange capacity was made. It is well known that the base exchange capacity in kaolin mineral is attributed primarily to broken bonds[7], and possibly to negative charges of the lattice due to vacancies of alumina or silica positions in kaolin with the lower degree of crystallinity.

The base exchange capacity was determined by the titration method. The clay was treated with hydrochloric acid, to convert it into "hydrogen clay", then it was washed with water and titrated with sodium hydroxide solution. The base capacity was expressed as the number of

7) S. Speil, *J. Am. Ceram. Soc.*, **23**, 33 (1940).

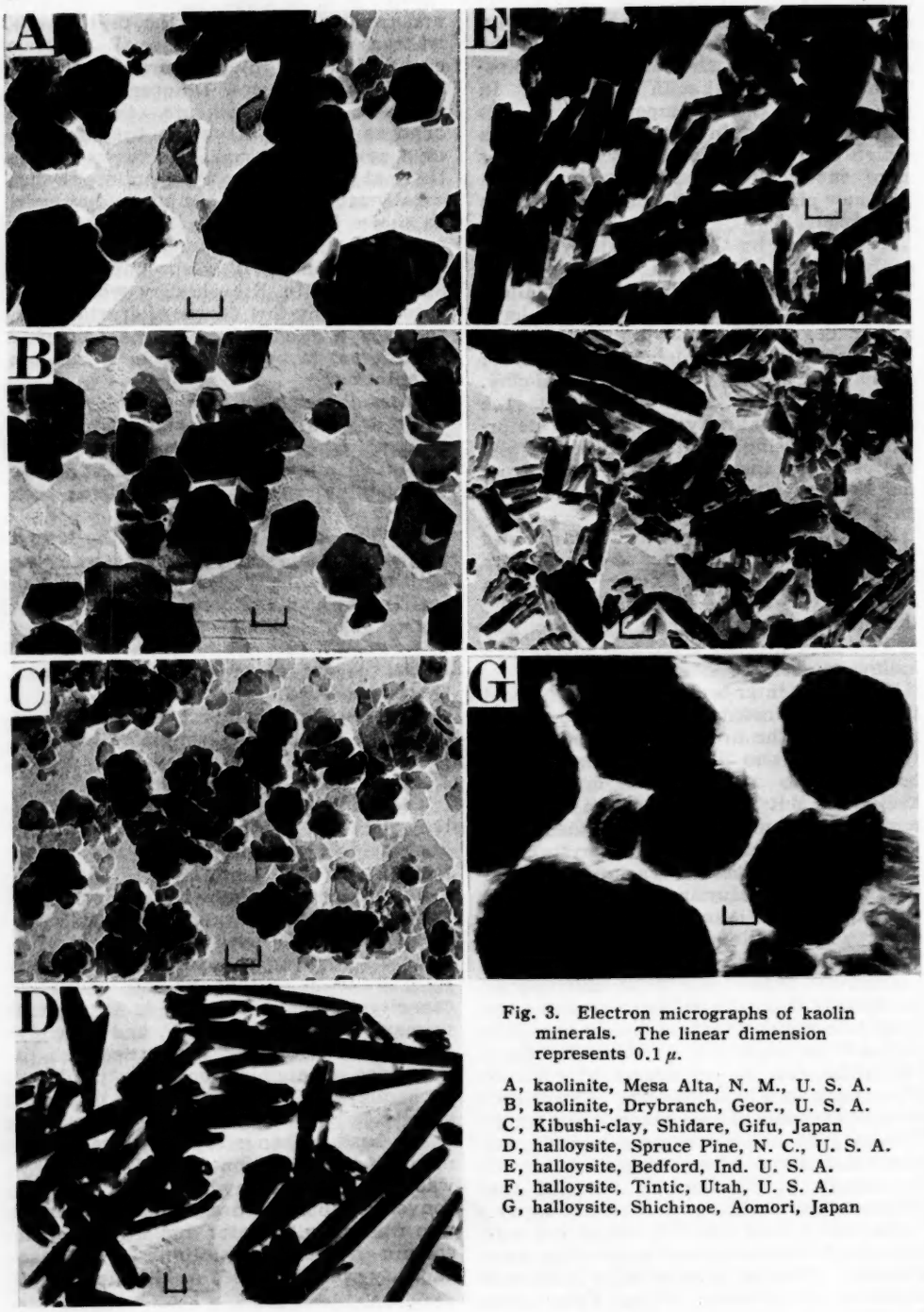

Fig. 3. Electron micrographs of kaolin minerals. The linear dimension represents 0.1 μ.

A, kaolinite, Mesa Alta, N. M., U. S. A.
B, kaolinite, Drybranch, Geor., U. S. A.
C, Kibushi-clay, Shidare, Gifu, Japan
D, halloysite, Spruce Pine, N. C., U. S. A.
E, halloysite, Bedford, Ind. U. S. A.
F, halloysite, Tintic, Utah, U. S. A.
G, halloysite, Shichinoe, Aomori, Japan

TABLE II

THERMAL DATA OF KAOLIN MINERALS

(all temp. are degrees centigrade)

Specimen	E_{n1}			E_{n2}			E_x			
	Temp.	Height	Area	Temp.	Height	Area	Temp.	Height	Area	Breadth
Kaolinite (Mesa Alta, N.M.)	—	—	—	604°	16	1080	966°	39	220	5.1°
Kaolinite (Drybranch, Geor.)	—	—	—	592	20	1280	964	41	250	4.8
Kibushi-Clay (Shidare, Gifu)	130°	1	140	574	14	740	945	13	140	10.5
Halloysite (Spruce Pine, N.C.)	125	1	70	583	17	1380	973	41	220	4.0
Halloysite (Bedford, Ind.)	125	2	110	574	16	720	970	34	170	4.5
Halloysite Tintic, Utah)	130	4	170	571	12	680	999	16	170	9.4
Halloysite (Shichinoe, Aomori)	129	6	480	550	12	660	885	7	130	23.4

TABLE III

BASE EXCHANGE CAPACITY OF KAOLIN MINERALS AT THE DRIED STATE

Specimen		Base exchange capacity (meq./100 g.)
Kaolinite	Mesa Alta, N.M., U.S.A.	1.0
	Drybranch, Geor., U.S.A.	1.4
Kibushi-clay (fireclay type)	Shidare, Gifu, Japan	7.3
Halloysite	Spruce Pine, N.C., U.S.A.	0.8
	Bedford, Ind., U.S.A.	4.0
	Tintic, Utah, U.S:A.	6.0
	Shichinoe, Aomori, Japan	12.5

TABLE IV

DENSITY OF KAOLIN MINERALS AT THE DRIED STATE

Specimen		Density (g./cc)
Kaolinite	Mesa Alta, N.M., U.S.A.	2.622
	Drybranch, Geor., U.S.A.	2.606
Kibushi-clay (fireclay type)	Shidare, Gifu, Japan	2.489
Halloysite	Spruce Pine, N.C., U.S.A.	2.561
	Bedford, Ind., U.S.A.	2.516
	Tintic, Utah, U.S.A.	2.464
	Shichinoe, Aomori, Japan	2.339

milli-equivalents of cations, per 100 g. of clay, required to bring the pH to 7.

Table III shows the base exchange capacity of kaolin samples. These results indicate that kaolin mineral with a lower degree of crystallinity has a higher base exchange capacity. Consequently, it can be concluded that the base exchange capacity is correlated to the internal randomness of structure.

Density—Another property which is considered to indicate the degree of crystallinity of kaolin minerals is their density. The density was determined with a pycnometer in carbon tetrachloride. The density of kaolin minerals used in this study are shown in Table IV. These values indicate that the density is correlated to the relative degree of crystallinity in the internal and stacking variations. The kaolinite with a higher degree of crystallinity has a larger density, and halloysite with a lower degree of crystallinity has a smaller density, with the exception of Kibushi-clay which contains organic matter as seen in the differential thermal analysis curve.

Electron Microscopic Studies.—Electron micrographs were obtained by the Hitachi HU-10A Type Electron Microscope.

Electron micrographs of kaolin minerals used in this study are shown in Fig. 3. The two kaolinites have platty particles, and the particles of Mesa Alta kaolinite has a sharp but irregular shape and the particles of Drybranch kaolinite has a hexagonal shape. The electron micrographs of halloysite samples with the exception of Shichinoe-clay have tubular particle. Bates et al. have indicated a structure that explains the tubular arrangement of halloysite.[8] That is, when the bonding forces of atoms in kaolin unit layer are very much stronger than the inter-layer forces, a particle takes tubular shape due to the characteristic of the unit layer lattice of the kaolin mineral. This means that the shape of the particle of the kaolin mineral is correlated to the disorderliness of the crystallographic unit layer and the disorderliness of the stacking of kaolin unit layer.

The X-ray data indicate that the degree of crystallinity of the Kibushi-clay is higher than that of the Spruce Pine halloysite while the thermal data indicate the opposite. This means that the kaolin layers in Kibushi-clay orient with respect to each other in relatively regular manner, but the layers themselves are less perfect than in Spruce Pine halloysite. As shown in the micrograph of Kibushi-clay, its crystal has a far finer size than the two kaolinites. The shape of Kibushi-clay is hexagonal and platty. This leads to assumption that the degree of crystallinity is the higher, the larger is the size of a crystal whose shape is platty.

Shichinoe-clay has the lowest degree of crystallinity among kaolin minerals used in this study by X-ray, thermal and other methods. As shown in a micrograph (Fig. 3-G), the shape of Shichinoe-clay is a round grain, which is well-defined and many of the grains have polyhedral outlines. The interiors of the polyhedral grains were observed in detail. It was found then that polyhedral grains are composed entirely of polyhedral crust like a cabbage. As to the shape of halloysite like the Shichinoe-clay, they were reported in previous papers.[4,9]

It is supposed that a schematic diagram for all the shapes of kaolin minerals could be drawn with respect to the degree of crystallinity in the internal randomness of the unit layer and the degree of crystallinity in the stacking randomness of kaolin layers. An ideal schematic diagram is shown in Fig. 4.

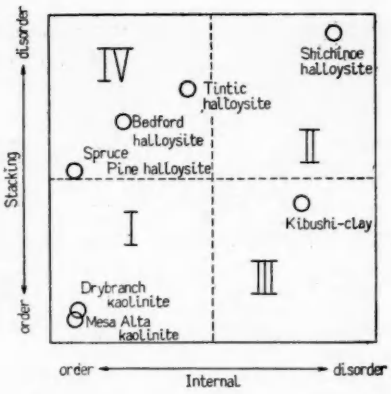

Fig. 4. A schematic diagram for the shapes of kaolin minerals with respect to two elements of the degree of crystallinity.

I : hexagonal, platty and large particle
II : fibrous, lath, cabbage like particle or rounded grain composed of fiber and lath
III : hexagonal, platty and fine particle
IV : tubular particle

All kaolin minerals are composed of kaolin unit layers, and kaolin minerals have various shapes. These facts are particularly remarkable in the hydrated halloysite clays altered from Japanese glassy tuff in the course of weathering. But the various shapes of kaolin minerals as above-mentioned can be readily understood by reference to the two elements of the randomness.

Summary

(1) The degree of crystallinity of kaolin minerals must be defined in relation to the degree of crystallinity in the internal randomness of the kaolin unit layer and that of the stacking randomness of kaolin unit layers. The X-ray diffraction data seem to reflect both internal and stacking variations.

(2) The relative degrees of crystallinity determined by the X-ray data and thermal data are consistent with each other in the series from kaolinite to fireclay. This holds also in the halloysite series. There is a continuous variation in the series from kaolinite to fireclay and also in the

8) T. F. Bates, F. A. Hildebrand and A. Swineford, *Am. Mineral.*, 35, 463 (1950).
9) H. Takahashi, *J. Electron Microscopy*, (*Denshi-Kenbikyo*), 4, 269 (1955).

halloysite series. The X-ray data indicate that some of halloysites have a low degree of crystallinity, but the thermal data show a high degree of crystallinity. This means that in most cases the displacement in the series from kaolinite to fireclay is a one-dimensional displacement with respect to the *b*-axis, while the displacement in halloysite is a rotational displacement, that is, a two-dimensional displacement.

(3) The values of the base exchange capacity of kaolinite, fireclay and halloysite are correlated to the internal disorderliness of kaolin structure.

(4) The values of density of kaolin mineral samples nearly correspond to the degrees of the crystallinity with the exception of Kibushi-clay.

(5) The variety of shapes of kaolin minerals are determined in the relation of the two elements of the internal variation and the stacking variation.

The author wishes to express his hearty thanks to Professor H. Akamatu for his continuous advice and encouragement. Thanks are due to Professor T. Sudo of the Tokyo University of Education for his valuable suggestion and discussion. The writer is also indepted to Mr. S. Sakata for the electron micrographs.

Department of Chemistry, Faculty of Science, the University of Tokyo, Hongo, Tokyo

---

The Kinetics of Displacement Reactions Involving Metal Complexes. I. Reaction between Copper(II) and Lead-Ethylenediaminetetraacetate Complexes in Aqueous Solutions

By Nobuyuki TANAKA, Kiyoko KATO and Reita TAMAMUSHI

(Received October 28, 1957)

There has been an increasing interest in the kinetics of the displacement reactions involving metal complexes of ethylenediaminetetraacetate (EDTA). Ackermann and Schwarzenbach[1] studied the kinetics of the reaction,

$$Cu^{2+}+CdY^{2-} \rightleftarrows CuY^{2-}+Cd^{2+},$$

and found that this seemingly simple reaction proceeds actually via four different paths. Bril, Bril and Krumholz[2] extended the study to the displacement reaction between lead and zinc-EDTA complexes, when they justified the "quasi-equilibrium hypothesis" which Ackermann and Schwarzenbach assumed for the reaction,

$$CdHY^{-} \rightleftarrows CdY^{2-}+H^{+} \rightleftarrows Cd^{2+}+HY^{3-}$$
$$\qquad\qquad -+2H^{+} \rightleftarrows Cd^{2+}+H_2Y^{2-}.$$

As it seemed worth while to know the reaction rate of the displacement reactions involving EDTA-complexes of other metal ions, we applied Bril et al.'s method to the reactions between copper and lead-EDTA complex,

$$Cu^{2+}+PbY^{2-} \rightleftarrows Pb^{2+}+CuY^{2-}. \qquad (1)$$

Experimental

Reagents.—The standard solution of cupric nitrate was prepared by dissolving a known amount of pure copper metal in a reagent-grade nitric acid. The solution of disodium ethylenediaminetetraacetate was standardized against the standard copper solution by the amperometric titration using a dropping mercury electrode as an indicator electrode[3]. The standard solution of lead nitrate was prepared from the commercial guaranteed grade reagent and standardized amperometrically against the standardized EDTA solution[3].

Apparatus and Procedure.—The rate of the reaction between the copper and lead-EDTA complex was followed by measuring the change of the polarographic diffusion current of the cupric ion with time. The current-time curves were obtained with a Shimadzu RP-II pen-recording polarograph using a dropping mercury electrode, which had an m value of 1.27 mg./sec. and

1) H. Ackermann and G. Schwarzenbach, *Helv. Chim. Acta*, **35**, 485 (1952).
2) K. Bril, S. Bril and P. Krumholz, *J. Phys. Chem.*, **59**, 596 (1955); **60**, 251 (1956).
3) N. Tanaka, M. Kodama, M. Sasaki and M. Sugino, *Japan Analyst (Bunseki Kagaku)*, **6**, 86 (1957).

a drop time of 3.69 sec., measured in an air-free solution of 0.1 M potassium chloride at 25°C in open-circuit.

Measurements were made in acetate buffers of pH 4.5 to 5.7 which contained 0.1 M of sodium acetate. The ionic strength was adjusted to be 0.2 with potassium nitrate. Gelatin was added as a maximum suppressor by 0.01% in concentration. The pH of the solution was measured with a Hitachi Model EHP-1 pH meter, immediately after the measurement of current-time curves, within the accuracy of 0.02 pH unit.

The reaction was initiated by adding a known amount of cupric nitrate solution into the deaerated reaction mixture with the aid of a 1 ml. syringe within one second. The solution was thoroughly stirred by bubbling nitrogen gas rapidly for 5 seconds. With this technique, reproducible current-time curves could be obtained from .15 seconds after the initiation of the reaction.

In the preliminary experiment, we observed a white salt-like compound precipitating from the solution which contained lead and EDTA ions. This compound contained lead and EDTA at the mole ratio of 2 to 1, being analyzed by the polarographic method, and was considered to be identical with that prepared by Brintzinger, Thiele and Müller[4]. Although they gave the formula $Pb_2\begin{pmatrix}(OOCCH_2)_2NCH_2\\ |\\ (OOCCH_2)_2NCH_2\end{pmatrix}$ to their compound, our experimental results suggested that the compound would have the formula Pb[PbY]. This was supported by the observations of other researchers[5,6] in which some metal-EDTA complex ions, such as CoY^- and HgY^{2-}, were found to react with excess of metal ions to form salt-like compounds, $Co[CoY]_2$, $Hg_2[HgY]$ and Hg[HgY]. The solubility product ($[Pb^{2+}]\times[PbY^{2-}]$) was measured in an acetate buffer of pH 5.0 and determined to be 3.4×10^{-5} at 15°C and 4.8×10^{-5} at 25°C*. The concentrations of lead and ethylenediaminetetraacetate in the reaction mixture were adjusted not to exceed the solubility product.

Results

The overall exchange reaction of the copper(II) and the lead-EDTA system is represented by equation (1).

$$Cu^{2+}+PbY^{2-} \rightleftarrows Pb^{2+}+CuY^{2-} \qquad (1)$$

Under the condition that lead ions and lead-EDTA complexes are present in a large excess over cupric ions, the reaction (1) can be simplified to,

$$Cu^{2+} \underset{k^-}{\overset{k^+}{\rightleftarrows}} CuY^{2-}, \qquad (2)$$

whose reaction rate is given by

$$-\frac{d[Cu^{2+}]}{dt}=k^+[Cu^{2+}]-k^-[CuY^{2-}]. \qquad (3)$$

Integrating eq. (3), we obtain,

$$\ln\{[Cu^{2+}]-[Cu^{2+}]_e\}=-(k^++k^-)t+\ln\{[Cu^{2+}]_0-[Cu^{2+}]_e\},$$

where $[Cu^{2+}]_0$ and $[Cu^{2+}]_e$ mean the initial concentration of copper ions and the concentration at equilibrium, respectively. At the equilibrium of the reaction the relation,

$$\frac{k^+}{k^-}=\frac{[CuY^{2-}]_e}{[Cu^{2+}]_e}\doteqdot K\frac{[PbY^{2-}]_0}{[Pb^{2+}]_0},$$

may be satisfied, where K represents the equilibrium constant of the reaction (1), expressed as,

$$K=\frac{[CuY^{2-}]_e[Pb^{2+}]_e}{[Cu^{2+}]_e[PbY^{2-}]_e}.$$

The values of K were determined polarographically to be 9.3 at 15°C, 12.3 at 25°C and 15.6 at 35°C in an acetate buffer of pH 5.2 at ionic strength of 0.2.

Those values were compared with the value of 5.8 which was calculated from the formation constants of PbY^{2-} and CuY^{2-} both determined by Schwarzenbach and his coworkers[7] at ionic strength 0.1 and at 20°C.

The apparent rate constants of the forward reaction (1), $k^+/[PbY^{2-}]_0$, were found independent of the initial concentration of cupric ions and that of lead-EDTA complexes, provided that the other conditions were kept the same. This is clearly shown in Table I.

TABLE I

$k^+/[PbY^{2-}]_0$ VALUES AT VARIOUS INITIAL CONCENTRATIONS (25°C, IONIC STRENGTH 0.2)

$[Cu^{2+}]_0$ M×10⁴	$[PbY^{2-}]_0$ M×10³	$[Pb^{2+}]_0$ M×10³	pH	$k^+/[PbY^{2-}]_0$ l.mole⁻¹sec.⁻¹
1.86	5.07	4.92	5.25	1.10
3.72	5.07	4.92	5.22	1.07
1.86	4.05	3.95	5.09	1.18
1.86	8.10	3.90	5.09	1.15

The apparent rate constant, $k^+/[PbY^{2-}]_0$, was obtained at varied pH's with two different concentrations of lead ions at 25°C, keeping the concentrations of other species constant. The resulting values are plotted against the hydrogen ion activity as given in Fig. 1, which clearly

4) H. Brintzinger, H. Thiele and U. Müller, *Z. anorg. allgem. Chem.*, **251**, 285 (1943).
5) G. Schwarzenbach, *Helv. Chim. Acta*, **32**, 839 (1949).
6) R. W. Schmid and C. N. Reilley, *J. Am. Chem. Soc.*, **78**, 5513 (1956).
* The details of the study will be reported elsewhere.

indicates that a linear relation exists between $k^+/[PbY^{2-}]_0$ and a_{H^+}. The same results were obtained at 15° and 35°C.

The values of $k^+/[PbY^{2-}]_0$ were also measured with different concentrations of lead at the same pH. The results obtained at 25°C are given in Fig. 2, in which the values of $k^+/[PbY^{2-}]_0$ is plotted against $1/[Pb^{2+}]_0$. Fig. 2 shows that $k^+/[PbY^{2-}]_0$ is inversely proportional to the lead concentration and that the values of $k^+/[PbY^{2-}]_0$ at $1/[Pb^{2+}]_0=0$, which were obtained by extrapolation, are dependent on the hydrogen ion activity of the solution.

Similar relations were obtained for the reverse reaction of reaction (1), which are shown in Figs. 3 and 4.

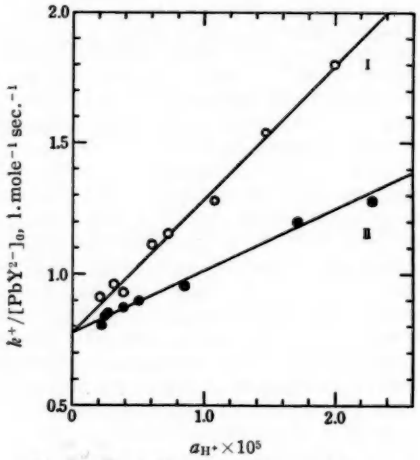

Fig. 1. $k^+/[PbY^{2-}]_0$ as a function of the hydrogen ion activity in acetate buffer-potassium nitrate solutions of ionic strength 0.2 at 25°C. Initial concentrations are: $[Cu^{2+}]_0=1.86\times10^{-4}$ M; $[PbY^{2-}]_0=4.05\times10^{-3}$ M; $[Pb^{2+}]_0=3.95\times10^{-3}$ M (curve I), 9.97×10^{-3} M (curve II).

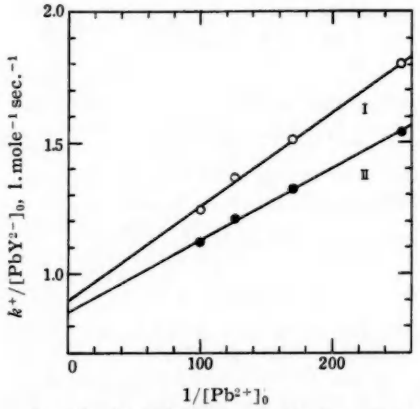

Fig. 2. $k^+/[PbY^{2-}]_0$ as a function of the reciprocal lead concentration in acetate buffer-potassium nitrate solutions of ionic strength 0.2 at 25°C. Initial concentrations are: $[Cu^{2+}]_0=1.86\times10^{-4}$ M; $[PbY^{2-}]_0=4.05\times10^{-3}$ M; pH 4.70 (curve I), 4.83 (curve II).

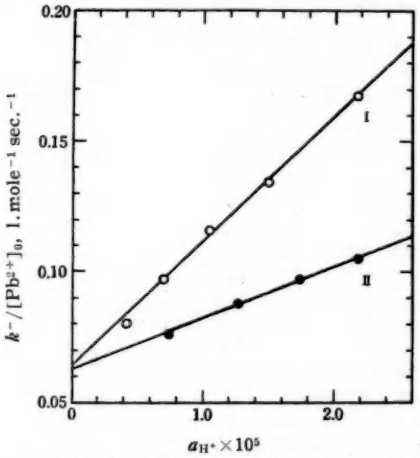

Fig. 3. $k^-/[Pb^{2+}]_0$ as a function of the hydrogen ion activity in acetate buffer-potassium nitrate solutions of ionic strength 0.2 at 25°C. Initial concentrations are: $[CuY^{2-}]_0=4.65\times10^{-4}$ M; $[PbY^{2-}]_0=4.05\times10^{-3}$ M; $[Pb^{2+}]_0=3.95\times10^{-3}$ M (curve I), 9.97×10^{-3} M (curve II).

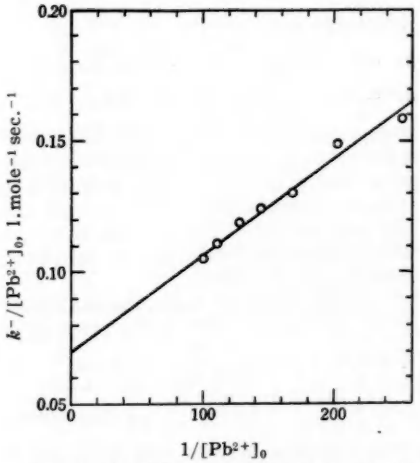

Fig. 4. $k^-/[Pb^{2+}]_0$ as a function of the reciprocal lead concentration in acetate buffer-potassium nitrate solutions of ionic strength 0.2 at 25°C. Initial concentrations are: $[CuY^{2-}]_0=4.65\times10^{-4}$ M; $[PbY^{2-}]_0=4.05\times10^{-3}$ M; pH 4.68.

Discussion

According to Bril et al.[2], who studied the forward and the reverse reaction between lead(II) and zinc-EDTA complexes and found that the overall reaction proceeds through three simultaneous reaction paths, the following mechanism was set down for the reaction (1).

$$\text{(i)}\quad Cu^{2+}+PbY^{2-} \underset{k_1^-}{\overset{k_1^+}{\rightleftarrows}} CuY^{2-}+Pb^{2+} \qquad (4)$$

$$\text{(ii)}\quad PbY^{2-}+H^+ \rightleftarrows PbHY^- \qquad (5a)$$

$$Cu^{2+}+PbHY^- \underset{k_{\text{II}}^-}{\overset{k_{\text{II}}^+}{\rightleftarrows}} CuHY^-+Pb^{2+} \qquad (5b)$$

$$CuHY^- \rightleftarrows CuY^{2-}+H^+ \qquad (5c)$$

$$\text{(iii)}\quad PbY^{2-}+H^+ \underset{k_a^-}{\overset{k_a^+}{\rightleftarrows}} Pb^{2+}+HY^{3-} \qquad (6a)$$

$$Cu^{2+}+HY^{3-} \underset{k_{\text{II}}^-}{\overset{k_{\text{II}}^+}{\rightleftarrows}} CuY^{2-}+H^+ \qquad (6b)$$

The overall reaction rate for reaction (1) is expressed by

$$-\frac{d[Cu^{2+}]}{dt}=\left\{k_1^+ +k_2^+[H^+] +k_3^+\frac{[H^+]}{[Pb^{2+}]}\right\}[Cu^{2+}][PbY^{2-}] -\left\{k_1^- +k_2^-[H^+] +k_3^-\frac{[H^+]}{[Pb^{2+}]}\right\}[Pb^{2+}][CuY^{2-}], \qquad (7)$$

and the relations,

$$k_2^+=k_{\text{II}}^+K_{PbHY}^H,\quad k_2^-=k_{\text{II}}^-K_{CuHY}^H \qquad (8)$$
$$k_3^+=k_{\text{II}}^+/(K_{PbY}K_{HY}),\quad k_3^-=k_{\text{II}}^-$$

are obtained, where K_{PbHY}^H and K_{CuHY}^H represent the equilibrium constants of the reaction (5a) and the reverse reaction of eq. (5c), respectively. K_{PbY} means the formation constant of PbY^{2-} and K_{HY}, the fourth dissociation constant of ethylenediaminetetraacetic acid.

The values obtained experimentally for $k^+/[PbY^{2-}]_0$ and $k^-/[Pb^{2+}]_0$ correspond to $\left\{k_1^+ +k_2^+[H^+]+k_3^+\frac{[H^+]}{[Pb^{2+}]}\right\}$ and $\left\{k_1^- +k_2^-[H^+]+k_3^-\frac{[H^+]}{[Pb^{2+}]}\right\}$ in eq. (7), respectively. The confirmation of this was attained in comparison of the observed relations at various pH's and at various concentrations of the lead ions as seen in Figs. 1 to 4, which consequently justified the reaction mechanism given in eqs. (4) to (6b).

The rate constants in eq. (7) were calculated from the plots of $k^+/[PbY^{2-}]_0$ (or $k^-/[Pb^{2+}]_0$) against hydrogen ion activity, which are tabulated in Table II. The activity coefficient of hydrogen ion at ionic strength of 0.2 was assumed to be 0.80.

TABLE II
RATE CONSTANTS IN EQUATION (7) OBTAINED EXPERIMENTALLY AT IONIC STRENGTH 0.2 AT VARIOUS TEMPERATURES

Temperature, °C	Rate constant, l.mole^{-1} sec.$^{-1}$					
	k_1^+	k_2^+	k_3^+	k_1^-	k_2^-	k_3^-
15	0.27	9×10^2	0.53×10^2			
25	0.78	4×10^3	1.5×10^2	0.064	2×10^2	14
35	2.2	2×10^4	3.1×10^2			

From eq. (7), the relation,

$$k_1^+/k_1^- = k_2^+/k_2^- = k_3^+/k_3^- = K \qquad (9)$$

is expected. The experimental results indicate that k_1^+/k_1^- and k_3^+/k_3^- agree with this prediction, but k_2^+/k_2^- does not. This may be due to the uncertainty which was involved in the procedure for determining the values of k_2^+ and k_2^-.

In the third process (iii), the concentration of HY^{3-} is given by

$$[HY^{3-}]=\frac{k_a^+[PbY^{2-}]+k_{\text{II}}^-[CuY^{2-}]}{k_a^-[Pb^{2+}]+k_{\text{II}}^+[Cu^{2+}]}[H^+]. \qquad (10)$$

The rate of this process, therefore, is expressed as

$$v_3=\frac{k_a^+k_{\text{II}}^+[PbY^{2-}][Cu^{2+}]-k_a^-k_{\text{II}}^-[CuY^{2-}][Pb^{2+}]}{k_a^-[Pb^{2+}]+k_{\text{II}}^+[Cu^{2+}]}\times[H^+]. \qquad (11)$$

Assuming the condition,

$$k_{\text{II}}^+[Cu^{2+}] \ll k_a^-[Pb^{2+}], \qquad (12)$$

eq. (11) can be reduced to a simpler form as given in eq. (7), *i.e.*,

$$v_3=k_3^+\frac{[Cu^{2+}][PbY^{2-}][H^+]}{[Pb^{2+}]} -k_3^-[CuY^{2-}][H^+]. \qquad (13)$$

When the condition given in eq. (12) is not fulfilled, the $k^+/[PbY^{2-}]_0$ (or $k^-/[Pb^{2+}]_0$) can not be plotted linearly against $1/[Pb^{2+}]_0$. This is not the case. The plots of $k^+/[PbY^{2-}]_0$ (or $k^-/[Pb^{2+}]_0$) *vs.* $1/[Pb^{2+}]_0$ gave straight lines and the values of $k^+/[PbY^{2-}]_0$ (or $k^-/[Pb^{2+}]_0$) at $1/[Pb^{2+}]_0=0$, obtained by extrapolation, agreed well with those calculated from the plots of $k^+/[PbY^{2-}]_0$ (or $k^-/[Pb^{2+}]_0$)

against hydrogen ion activity. These apparently confirm the fact that the condition given in eq. (12) was satisfied in the present experiments.

From the relations given in eqs. (8), the rate constants of both elementary reactions (5b) and (6b) can be calculated, provided that the values of K^{H}_{PbHY}, K_{PbY} and K_{HY} at ionic strength 0.2 and at 15°, 25° and 35°C are known. Unfortunately none of those have been reported. Schwarzenbach, Gut and Anderegg[7] determined those values at ionic strength 0.1 and at 20°C. The corrections for ionic strength were made more or less reasonably with the Debye-Hückel equation. The heat of formation of the lead-EDTA complex was reported to be −13.1 kcal./mole,[8] which was employed in the calculation of K_{PbY} at 15°, 25° and 35°C. As for K_{HY}, the values obtained by Schwarzenbach and Ackermann[9] were used after correction for temperature and ionic strength. The temperature coefficient of K_{HY} was evaluated from the values of Carini and Martell[10], who determined the fourth dissociation constant of ethylenediaminetetraacetic acid at 0°C to 30°C and at ionic strength 0.1.

Those values which were used in the calculation are given in Table III and the rate constants obtained of three elementary reactions (4), (5b) and (6b) are summarized in Table IV.

TABLE III

EQUILIBRIUM CONSTANTS AT IONIC STRENGTH 0.2 AT VARIOUS TEMPERATURES

Temperature, °C	log K_{PbY}	pK_{HY}	log K^{H}_{PbHY}
15	17.97	10.20	—
20	—	—	2.7
25	17.63	10.04	—
35	17.31	9.91	—

TABLE IV

RATE CONSTANTS FOR REACTIONS (4), (5b) AND (6b) AT IONIC STRENGTH 0.2 AT VARIOUS TEMPERATURES

Temperature, °C	Rate constant, l.mole^{-1} sec.$^{-1}$		
	k_1^+	k_{II}^+	k_{III}^+
15	0.27	2	3.2×10^9
25	0.78	8	5.8×10^9
35	2.2	40	7.8×10^9

Linear relations were found between log k^+ and $1/T$ for those three elementary reactions, which made it possible to express the rate constants in the form of the Arrhenius equation and to calculate the heat of activation and the entropy of activation. The results are given in Table V. The values for the elementary reaction (5b) are considered less accurate compared with those for the other two elementary reactions.

The authors thank the Ministry of Education for the financial support to this research.

TABLE V

RATE CONSTANTS, HEAT OF ACTIVATION AND ENTROPY OF ACTIVATION FOR REACTIONS (4), (5b) AND (6b)

Reaction	Rate constant, expressed	$\Delta H^{\neq}$ kcal./mole	$\Delta S^{\neq}$ e.u.
$Cu^{2+}+PbY^{2-}\rightarrow CuY^{2-}+Pb^{2+}$	$k_1^+=1.6\times10^{13}\exp(-18,100/RT)$	17.5	~0
$Cu^{2+}+PbHY^{-}\rightarrow CuHY^{-}+Pb^{2+}$	$k_{II}^+=4.3\times10^{20}\exp(-26,800/RT)$	26	34
$Cu^{2+}+HY^{3-}\rightarrow CuY^{2-}+H^{+}$	$k_{III}^+=2.2\times10^{15}\exp(-7,700/RT)$	7.1	9.7

7) G. Schwarzenbach, R. Gut and G. Anderegg, *Helv. Chim. Acta*, **37**, 937 (1954).
8) R. G. Charles, *J. Am. Chem. Soc.*, **76**, 5854 (1954).
9) G. Schwarzenbach and H. Ackermann, *Helv. Chim. Acta*, **30**, 1798 (1947).
10) F. F. Carini and A. E. Martell, *J. Am. Chem. Soc.*, **75**, 4810 (1953).

Department of Chemistry
Faculty of Science
Tohoku University
Katahira-cho, Sendai

Studies on Micelle Formation in Non-polar Solvent by Thermistor

By Ayao KITAHARA

(Received November 30, 1957)

It will be useful for the study of micelle formation to know the aggregation number at varying temperature. The measurement of vapor pressure depression is one of the several methods applicable to this purpose. The accuracy of the measurement has been recently increased, and the operation has become handy by the use of the thermistor which was also used for the study on micelle formation in the aqueous solution[1].

In order to obtain the aggregation number and the critical micelle concentration and to calculate the change in the thermodynamic value for micelle formation of detergents in the non-polar solvent, measurements on the vapor pressure depression and its temperature dependence were carried out using a pair of thermistors.

Experimental

Materials: Dodecylammonium benzoate, dodecylammonium butyrate and dodecylammonium caprylate were used as detergents, the preparation of which was reported already[2,3]. Cyclohexane for spectrophotometric use was employed as the solvent.

Apparatus: The vapor pressure depression was measured by making use of a couple of matched thermistors. The principle of the measurement was similar to those of McBain et al.[1], Müller et al.[4] and Davies et al.[5] Two thermistors used had resistances of 5040 and 4790 Ω at 19.9°C and the equal mean temperature coefficient of 3.7% per degree between 20° and 30°C. A Wheatstone bridge was employed for measuring the resistance change of the thermistors. Two adjacent arms were occupied by both thermistors. A fixed arm was a standard resistor of 1,000 Ω. The balancing arm consisted of a five dial resistor (R_x), variable in 0.1 Ω step. A galvanometer was a lamp-scale type having a sensitivity of 8.22×10^{-10} A per mm. The voltage which was applied potentiometrically was maintained at 0.4 V throughout the whole experiment. The cell containing both thermistors was similar to that of McBain et al.[1] and was kept in a thermostat controlled to ±0.0005°C. The well of the solvent which developed the atomosphere of the saturated vapor had been placed on the bottom of the cell.

Method: First, solvent drops were placed on both thermistors and R_x(solvent~solvent) was measured, the bridge being balanced. Next, a solvent and a solution drop were placed on each thermistor and R_x(solvent~solution) balance was also obtained. The relation between mole fraction of a solute (N) and $\Delta R_x = R_x$(solvent~solvent) $- R_x$(solvent~solution) was obtained with the cyclohexane solution of naphthalene, ranging from 0.0005 to 0.002 of N. This concentration range was chosen, because it will be safely assumed that the solutions are ideal. The result was as follows: $N = k\cdot\Delta R_x$. The values of the proportional constant k were 2.04×10^{-3} and 2.12×10^{-3} ohm^{-1} at 19.7° and 31.1°C, respectively. The measurement carried out with the cyclohexane solutions of diphenyl gave consistent values of k. ΔR_x was then measured for the detergent solutions with a method similar to that mentioned above at 19.7° and 31.1°C. The apparent mean aggregation number (Z) was calculated by the following equation 1:

$$Z = \frac{m}{k\cdot\Delta R_x}\,\frac{M_s}{1000} \qquad (1)$$

where m and M_s are the molality of the detergent and the molecular weight of the solvent, respectively; $Z = M/M_0$ (M and M_0 are the apparent mean micellar weight measured and the monomeric molecular weight of the detergent, respectively). Hence, Z has been evaluated by involving both monomer and micelle. The measurement of R_x(solvent~solvent) was always carried out before and after that of R_x(solvent~solution) throughout the whole measurement in order to ensure constancy in the thermistor conditions. ΔR_x was measured several times and the average value was adopted for the calculation of Z.

Results and Discussion

Monomer Concentration and Aggregation Number.—The values of Z calculated at 20° and 31°C are given in Table I. The fluctuation in the values of Z was not beyond ten per cent.

1) A. P. Brady, H. Huff and J. W. McBain, *J. Phys. and Colloid Chem.*, **55**, 304 (1951).
2) A. Kitahara, This Bulletin, **30**, 586 (1957).
3) A. Kitahara, ibid., **28**, 234 (1955).
4) R. H. Müller and H. J. Stolten, *Anal. Chem.*, **25**, 1103 (1953).
5) M. Davies and D. K. Thomas, *J. Phys. Chem.*, **60**, 763, 767 (1956).

TABLE I

THE VALUES OF Z, λ AND C_1

Detergent	Concentration C (millimole/l) 20°	31°	$N\times10^4$ (mole fraction)	Z 20°	31°	Kreuzer's Treatment C_1 (millimole/l) 20°	31°	λ 20°	31°	Least Square Method C_1 (millimole/l) 20°	31°	λ 20°	31°
Dodecyl-ammonium benzoate	22	22	26	3.6	2.9	4.7	5.4	—	10	2	2.3	12	6
	27	27	32	4.8	3.8	4.8	5.2						
	34	—	40	7.0	—	4.6	—						
	37	36	42	7.4	4.2	4.5	5.4						
	44	43	51	8.3	4.4	4.6	5.6						
	55	54	63	9.1	5.3	4.7	6.2						
Dodecyl-ammonium caprylate	22	22	25.4	1.8	1.6	8.8	9.5	7±1	4	10	6	6.5	2.6
	33	32	38	2.1	2.1	9.8	10.2						
	45	44	52.5	3.2	2.3	9.3	11.3						
	66	64	76	3.6	2.2	9.8	14.0						
Dodecyl-ammonium butyrate	23	23	26	2.3	1.55	6.7	10.6	9±1	6±1	8	10	8.5	6
	34	33	39.5	3.1	2.25	6.7	10.8						
	45	44	48	3.5	2.65	7.2	11.3						
	68	66	79	4.4	3.55	7.2	11.9						

TABLE II

CRITICAL MICELLE CONCENTRATION (millimole/l)

	Kreuzer's treatment 20°	30°	Solubilization mothod 20°	30°	Spectral method 20°	30°
Dodecylammonium benzoate	4.6	5.2	12±2	15±2	12±1	12±1
Dodecylammonium caprylate	8.3±0.2	9.1±0.1	16±2	16±2	—	—
Dodecylammonium butyrate	6.3±0.2	10	2±1	2±1	—	—

According to Kreuzer[5,6], the general equation 2 is obtained without making any assumption as to the nature of the associative equilibria involved.

$$\ln(1/\alpha)=(Z-1)/Z+\int_0^N\{(Z-1)/ZN\}dN \quad (2)$$

where α is the fraction of the monomer and N the total concentration of the solute in terms of mole fraction as monomer. The monomer concentration (C_1) at each concentration are obtained from the values of α which are graphically calculated from the above equation. These values of C_1 are tabulated in Table I. They are nearly independent of the concentration of detergents.

It has scarcely ever been subjected to experimental studies whether micelles should be monodisperse or not in the non-polar solvent. It was shown in ultraviolet absorption spectra of cyclohexane solutions of dodecylammonium benzoate that the extinction coefficient of the solute molecule participating in micelle formation is almost constant within a concentration range above the critical micelle concentration (*cmc*)[2]. This fact seems to be an evidence that the micelle is approximately monodisperse within this range. If the aggregation of the monomer to only one species of λ-mer is assumed*, the special relation 3 is deduced:[6,7]

$$Z=\lambda-(\lambda-1)\alpha\cdot Z \quad (3)$$

where λ is the true aggregation number evaluated by subtracting the coexisting monomer. The values of λ are graphically obtained from the plot of Z vs. $\alpha\cdot Z$. They are also shown in Table I. The λ value for dodecylammonium benzoate at 20°C was not successfully obtained because of the scattering of the plots.

The equation 3 is transformed into the following equation, using the molar concentration:

6) J. Kreuzer, *Z. physik. Chem.*, **B53**, 213 (1942).

* If a whole sequence of aggregates occurs with successive stages and the equilibrium constant at each stage is all equal, the equilibrium constant K must be described as $N(Z-1)/Z$. The values of K calculated for each concentration using this formula were not constant. Hence, such process of aggregation was not taken into consideration.

7) I. Prigogine and R. Defay, "Chemical Thermodynamics" p. 422, Longmans Green and Co., London, 1954.

$$C - \lambda C/Z + (\lambda-1)C_1 = 0$$

where C is the analytical concentration of the detergent. The values of λ and C_1 were calculated by the least square method with this equation, assuming that λ and C_1 are constant. The resulting values are given in Table I. The first value of Z was not adopted for the calculation in the case of dodecylammonium benzoate at 20°C. It is seen in Table I that these values of C_1 and λ are properly consistent with those of C_1 and λ which were calculated from the equations 2 and 3. The values of λ are comparable with those of Singleterry et al. in benzene solutions of dinonylnaphthalene sulfonate[8].

The *cmc* is obtained by plotting C_1 obtained from the equation 2 vs. C and by extrapolating to $C_1=C$. They are given in Table II and the *cmc* obtained by other methods are also shown in the table for the comparison. The agreement among these values seems to be satisfactory, when it is considered that they have been obtained by independent methods.

TABLE III
THE VALUES OF SOLUBILIZING POWER

	20°	30°
Dodecylammonium benzoate	4.7	4.0
Dodecylammonium caprylate	3.2	2.5
Dodecylammonium butyrate	20	15

It is seen from Table I that the values of λ decrease with the increase in the temperature. This corresponds qualitatively to the change of the solubilizing power with the temperature which is shown in Table III. No quantitative proportionality between them is found. The solubilizing power is defined as the moles of water solubilized per one mole of a detergent.

Calculation of Changes of Thermodynamic Values.—The *cmc* obtained from the Kreuzer's equation may be safely used for the quantitative treatment, though the C_1 obtained by the least square method is not quantitative. When the micelle is considered as the condensed phase, the following equation is deduced:[9]

$$\frac{d\ln(cmc)}{dT} = -\frac{\Delta H}{RT^2} \qquad (4)$$

where ΔH is the change of heat content associated with micelle formation at the mean temperature (25°C). ΔH was calculated from the equation 4 by the use of the *cmc* in the 2nd and 3rd columns in Table II. ΔH is independently obtained from the temperature dependence of the equilibrium constant for the λ-mer aggregation of the monomer. Thus ΔH was again calculated by the use of the λ and C_1 obtained by the least square method. These vlaues for ΔH and related ΔS are given in Table IV.

TABLE IV
THE VALUES OF ΔH AND ΔS ASSOCIATED WITH MICELLE FORMATION

	ΔH(kcal/mole)		ΔS(cal/deg/mole)	
	from *cmc*	from λ and C_1	from *cmc*	from λ and C_1
Dodecylammonium benzoate	−1.9	−5.9	−6.4	−20
Dodecylammonium caprylate	−1.7±0.5	−5.3	−5.7±1.7	−18
Dodecylammonium butyrate	−7.5±0.5	−7.5	−25±1.7	−25

The values obtained from these separate methods agree roughly with each other; hence they may be accepted as the probable values for micelle formation in the non-polar solvent. The absolute values of the heat change for micelle formation in the non-polar solvent seem to be somewhat greater than those in the aqueous solutions[9,10]. This may be due to the dipolar force or the hydrogen bonding which will participate in micelle formation of these detergents.

Summary

The apparent mean aggregation number (Z) of dodecylammonium carboxylate in cyclohexane was obtained from the vapor pressure depression measurement by the use of a pair of thermistors. The monomer concentration (C_1) was calculated from Kreuzer's equations. The C_1 was nearly independent of the concentration. The true aggregation number (λ) was obtained, assuming that the micelle is monodisperse. The *cmc* extraploated from C_1 agreed approximately with those by other methods.

The change of the heat content associated with micelle formation was calculated from the change of the *cmc* with

8) S. Kaufman and C. R. Singleterry, *J. Colloid Sci.*, **10**, 139 (1955).
9) G. Stainby and A. E. Alexander, *Trans. Faraday Soc.*, **46**, 587 (1950).
10) E. Hutchinson and L. Winslow, *J. Phys. Chem.*, **58**, 1125 (1954). E. D. Goddard and G. C. Benson, *Trans. Faraday Soc.*, **52**, 409 (1956).

the temperature and from the temperature dependence of the equilibrium constant for the λ-mer aggregation. Both agreed roughly with each other.

The author acknowledges the advice on the use of the thermistor given by Mr. Hisao Futaki in the Central Research Institute of Hitachi Manufacturing Co., and thanks Professor Hideo Akamatu for his continuing interest in this study.

Department of Chemistry, Toho University, Narashino, Chiba

Studies on the Synthesis of Metal Complexes. III. Synthesis of Ethylenediamine-carbonato, Ammine-oxalato and Ethylenediamine-oxalato Series of Cobalt(III) Complexes*

By Motoshichi MORI, Muraji SHIBATA, Eishin KYUNO and Koji HOSHIYAMA

(Received December 7, 1957)

In the preceding paper[1] of this series, a systematic method of synthesis for the ammine-carbonato series of cobalt(III) complexes was described. An important feature of the method was that it involved successive substitution of carbonate ions by ammonia groups. This method has now been extended to the synthesis of various complexes belonging to the ethylenediamine-carbonato, the ammine-oxalato and the ethylenediamine-oxalato series. All the attempts were successful; it is most interesting that a blue and a violet variety were found in every member of the present series, too. The two varieties are probably to be regarded as new complexes and also as stereoisomers.

Experimental

Synthesis.—1) *Starting material.*—Through all the procedures described below, a green cold solution of potassium tricarbonatocobaltate(III) was used as starting material. This was prepared from 20 g. of $KHCO_3$ and 10 g. of $CoCl_2 \cdot 6H_2O$—5 ml. of 30% H_2O_2 by the method described in the previous paper[1].

2) *Blue variety of potassium dicarbonatoethylenediaminecobaltate(III)*, Blue-K[Co en$(CO_3)_2$]$\cdot H_2O$.—To the green cold solution obtained in 1), was added 5 g. of ethylenediamine carbonate prepared by passing carbon dioxide into an aqueous solution of 70% ethylenediamine in the cold. The mixture was placed in an icebath until the green color of the solution changed into violetish blue within thirty minutes. When about 20 ml. absolute ethanol was added to the solution, crystals began to appear, but they were appreciably contaminated with other salts. The precipitates, therefore, were filtered off, another 50 ml. of ethanol was added to the filtrate and the solution was left for some time at nearly 0°C. The crystals were collected and purified by dissolving in as little cold water as possible and then by adding absolute ethanol. The product was washed with ethanol and ether in turn. Yield, about 4 g.

3) *Violet variety of potassium dicarbonatoethylenediaminecobaltate(III)*, Violet-K[Co en$(CO_3)_2$]$\cdot H_2O$.—After adding 5 g. of ethylenediamine carbonate to the starting material in the same manner as above, the mixture was allowed to stand at room temperature until a violet solution was obtained (about 20 min.). At the end of this period 20 ml. ethanol was added to the solution and then it was kept overnight in a refrigerator. After repeating reprecipitation three times in the same manner as in 2), the final precipitate was washed with ethanol and ether. Yield, about 6 g.

4) *Carbonato-bis (ethylenediamine) cobalt (III) chloride*, [Coen$_2CO_3$]Cl$\cdot H_2O$.—This was prepared by adding 10 ml. ethylenediamine (70%) to the green solution, heating the mixture on a water bath until the color of the solution became reddish violet, and further continuing to heat the solution in an evaporating dish. After cooling, the crude product was collected and recrystallized from water by the usual procedure. Yield, about 11 g.

5) *Tris (ethylenediamine) cobalt (III) chloride*, [Co en$_3$]Cl$_3 \cdot 3H_2O$.—Ethylenediamine (70%, 15 ml.), potassium chloride (3 g.) and active charcoal (1 g.) were introduced into the green solution,

* Presented at the Symposium on Co-ordination Compounds, Tokyo, October 27, 1956. For previous paper in this series see M. Mori, M. Shibata, E. Kyuno and H. Nakajima, This Bulletin, 29, 887 (1956).

1) M. Mori, M. Shibata, E. Kyuno and T. Adachi, This Bulletin, 29, 883 (1956).

TABLE I
THE FLOW CHART OF SYNTHESIS

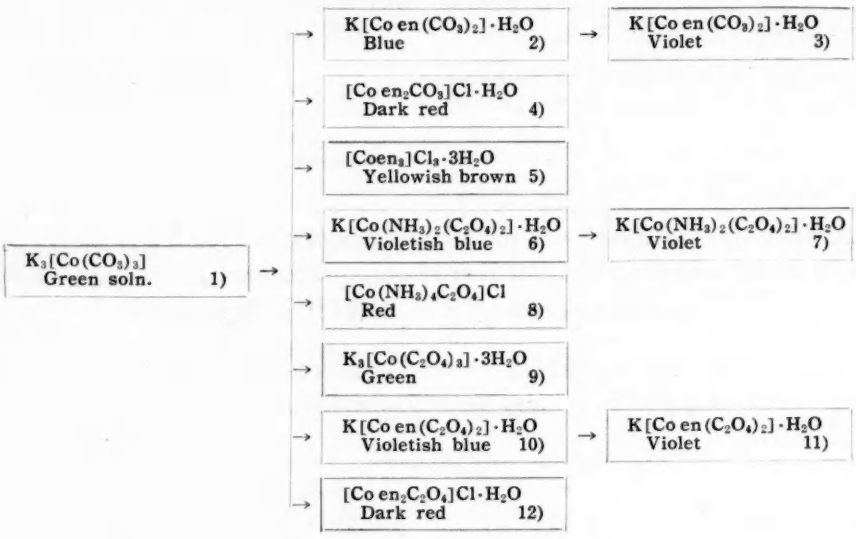

TABLE II
ANALYTICAL RESULTS (amounts in %)

	Co		N		K_2CO_3 or $K_2C_2O_4$		H_2O	
	calcd.	obsd.	calcd.	obsd.	calcd.	obsd.	calcd.	obsd.
Blue-K[Co en$(CO_3)_2$]·H_2O	19.9	19.8	9.5	9.5	23.3	24.5	6.1	5.9
Violet-K[Co en$(CO_3)_2$]·H_2O	19.9	19.6	9.5	9.4	23.3	24.6	6.1	6.2
Blue-K[Co$(NH_3)_2(C_2O_4)_2$]·H_2O	18.4	18.9	8.8	8.9	26.3	25.8	5.7	5.7
Violet-K[Co$(NH_3)_2(C_2O_4)_2$]·H_2O	18.4	18.1	8.8	8.8	26.3	26.5	5.7	5.8
Blue-K[Co en$(C_2O_4)_2$]·H_2O	16.7	16.8	7.7	7.8	23.6	23.4	5.1	5.1
Violet-K[Co en$(C_2O_4)_2$]·H_2O	16.7	16.2	7.7	7.6	23.6	25.6	5.1	5.2

and the mixture was heated on a water bath for about thirty minutes whereby the color of the solution changed into brownish yellow. After removal of the charcoal by filteration while hot, the filtrate was evaporated to about a half of the initial volume and then left to cool. The deposited crystals were washed with ethanol and dried in an oven. Yield, about 12 g.

6) *Blue variety of potassium dioxalatodiamminecobaltate (III)*, Blue-K[Co$(NH_3)_2(C_2O_4)_2$]·H_2O.—The green solution containing 10 g. of powdered ammonium oxalate was warmed on a water-bath at nearly 70°C. As soon as the solution became bluish, the vessel was dipped in an ice bath in order to stop further reaction. When the content was completely cooled, ethanol (50 ml.) was added to it and the whole was allowed to stand about an hour. The crude product was collected and reprecipitated from the cold solution by the addition of ethanol. After repeating this procedure twice, the final precipitate was washed with ethanol and ether in turn. Yield, about 7 g.

7) *Violet variety of potassium dioxalatodiamminecobaltate(III)*, Violet-K[Co$(NH_3)_2(C_2O_4)_2$]·H_2O.—The starting material, to which ammonium oxalate was added as described in the preceding paragraph, was allowed to remain on a water bath until the color turned blue and finally violet. After adding 80 ml. ethanol to the solution, it was kept overnight in a refrigerator. The violet precipitate was collected, dissolved in a small amount of cold water to remove impurities as residues, and then the complex reprecipitated by the addition of ethanol. After repetition of this procedure, the precipitate was washed with ethanol and then with ether. Yield, about 7 g.

8) *Oxalatotetramminecobalt(III) chloride*, [Co$(NH_3)_4C_2O_4$]Cl.—Powdered ammonium oxalate (5 g.) and concentrated aqueous ammonia solution (30 ml.) were added to the green solution and the mixture was warmed on a water bath at nearly 80°C with addition of ammonium chloride (in small portions, about 2 g. altogether), until the color of the mixture became pink. After cooling, about 10 ml. of ethanol was added to it

to precipitate all other salts; thereupon these were removed by filtration and another 20 ml. of ethanol was added in order to obtain the complex salt. Yield, about 6 g.

9) *Potassium trioxalatocobaltate(III)*, $K_3[Co(C_2O_4)_3]\cdot 3H_2O$.—To the cold green solution was added powdered oxalic acid (16 g.) little by little, whereby carbon dioxide was evolved and a bluish green solution was obtained. This was warmed on a water bath at nearly 60°C until no more carbon dioxide appeared. After cooling, the solution was acidified with dil. acetic acid and 50 ml. of ethanol was added to it. The product was purified as usual. Yield, about 12 g.

10) *Blue variety of potassium dioxalatoethylenediaminecobaltate(III)*, Blue-K[Co en $(C_2O_4)_2]\cdot H_2O$.—Potassium oxalate (5 g.) and ethylenediamine oxalate (5 g.) prepared by neutralizing 15 g. of ethylenediamine (70%) with 23 g. of powdered oxalic acid in the cold, were poured upon the cold green solution and the whole was left at room temperature until the color of the solution turned bluish violet, which took about half an hour. At the end of this period the solution was thoroughly cooled, and treated with a small amount of ethanol to remove foreign salts; the filtrate is further mixed with ethanol to precipitate the complex salt. The precipitate was purified from the cold solution by the addition of ethanol, and washed first with ethanol and then with ether. Yield, about 3 g.

11) *Violet variety of potassium dioxatatoethylenediaminecobaltate(III)*, Violet-K[Co en $(C_2O_4)_2]\cdot H_2O$.—This was synthesized in the same way as the blue variety, except for the mixture being heated for an hour instead of being left at room temperature. At the end of the reaction, the color of the solution changed completely to violet. Yield, about 7 g.

12) *Oxalato-bis (ethylenediamine) cobalt(III) chloride*, $[Co\,en_2(C_2O_4)]Cl\cdot H_2O$.—Oxalic acid (6 g.), potassium chloride (2 g.) and 70% ethylenediamine (16 ml.) were added to the green solution and the mixture was allowed to evaporate on a water bath until a crust was formed on the surface. After cooling, the crystals were filtered and washed with ethanol and ether in turn. Yield, about 10 g.

A flow chart of the synthesis of the above-mentioned complexes is given in Table I.

Determination of Chemical Formulae.—This was carried out for the six complexes obtained in 2), 3), 6), 7), 10) and 11), because they were thought to be new compounds. The results of thermal and chemical analysis and spectroscopic measurements were used for determining their chemical formulae in the same manner as that described in the previous paper[1]. Furthermore, coagulation values of ferric oxide sol by the complexes were measured in order to determine the valency of the complex ions. The measurements were carried out with the method used by S. Nakahara, K. Nakamoto and R. Tsuchida[2].

2) S. Nakahara, K. Nakamoto and R. Tsuchida, *J. Chem. Soc. Japan, Pure Chem. Sec.* (*Nippon Kagaku Zassi*), **74**, 488 (1953).

Results and Discussion

Analysis and Coagulation Value.—All the numerical values obtained from the chemical and the thermal analysis are given in Table II. These data seem to justify the assignment of such chemical formulae as are given in the experimental section.

Additional evidence for the validity of these formulae is afforded by the coagulation values given in Table III. Nakahara and co-workers have given 6.6 mF, 0.48 mF and 0.090 mF as the average values for uni-, bi- and tervalent complex anions respectively. In the present experiment, all of the complex species belonging to the blue variety showed coagulation values ranging from 6 mF to 7 mF, and they are consequently regarded as univalent anions. On the other hand, all the species belonging to the violet variety gave values about 3 mF, which are somewhat lower than the average value for a univalent ion, but far too high for a bivalent anion. These species may also be regarded as univalent anions provided that the deviation of their coagulation values from the average is attributed to partial liberation of the carbonate or the oxalate ion out of the complex radical by water molecules;

$$[Co\,en(CO_3)_2]^- + 2H_2O \rightleftarrows [Co\,en(H_2O)_2CO_3]^+ + CO_3^{--}$$

$$[Co(NH_3)_2(C_2O_4)_2]^- + 2H_2O \rightleftarrows [Co(NH_3)_2(H_2O)_2C_2O_4]^+ + C_2O_4^{--}$$

TABLE III

COAGULATION VALUES OF FERRIC OXIDE SOL

Blue-K$[Co(NH_3)_2(CO_3)_2]\cdot H_2O$	ca. 6 mF
Violet-K$[Co(NH_3)_2(CO_3)_2]\cdot H_2O$	ca. 3 〃
Blue-K$[Co\,en(CO_3)_2]\cdot H_2O$	ca. 6 〃
Violet-K$[Co\,en(CO_3)_2]\cdot H_2O$	ca. 3 〃
Blue-K$[Co(NH_3)_2(C_2O_4)_2]\cdot H_2O$	ca. 7 〃
Violet-K$[Co(NH_3)_2(C_2O_4)_2]\cdot H_2O$	ca. 3 〃
Blue-K$[Co\,en(C_2O_4)_2]\cdot H_2O$	ca. 7 〃
Violet-K$[Co\,en(C_2O_4)_2]\cdot H_2O$	ca. 3 〃

Absorption Spectra.—All the absorption data for newly synthesized complexes are given in Figs. 1 and 2 and Table IV together with those for previously synthesized potassium dicarbonatodiamminecobaltate(III).

Fig. 3 is a diagrammatic representation of the absorption maxima of the first band. It is seen from the figure that the frequencies for the blue variety increase in the order of NH_3-CO_3, en-CO_3, NH_3-ox and en-ox in an arithmetrical progression

TABLE IV
ABSORPTION MAXIMA AND log ε

	(10^{13} sec.$^{-1}$)					
	ν_1	log ε_1	ν_2	log ε_2	ν_3	log ε_3
Blue-K[Co$(NH_3)_2(CO_3)_2$]	52.2	2.14	76.8	2.40	126.6	4.14
Violet-K[Co$(NH_3)_2(CO_3)_2$]	55.5	1.80	80.2	2.04	128.1	4.30
Blue-K[Co en$(CO_3)_2$]	52.6	2.17	76.9	2.33	125.5	4.46
Violet-K[Co en$(CO_3)_2$]	54.9	1.94	77.3	2.31	129.8	4.29
Blue-K[Co$(NH_3)_2(C_2O_4)_2$]	53.1	2.09	79.4	2.35	129.3	4.56
Violet-K[Co$(NH_3)_2(C_2O_4)_2$]	55.3	2.08	79.3	2.58	130.4	4.06
Blue-K[Co en$(C_2O_4)_2$]	53.5	2.17	78.5	2.30	127.1	4.31
Violet-K[Co en$(C_2O_4)_2$]	54.7	1.98	77.9	2.10	129.8	3.98

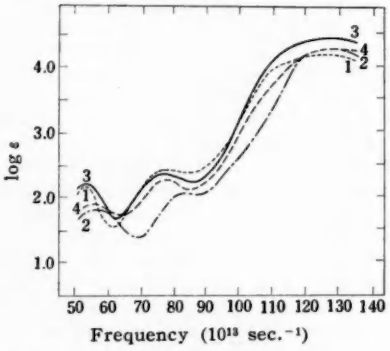

Fig. 1. Absorption spectra of:
1. Blue-K[Co$(NH_3)_2(CO_3)_2$]
2. Violet-K[Co$(NH_3)_2(CO_3)_2$]
3. Blue-K[Co en$(CO_3)_2$]
4. Violet-K[Co en$(CO_3)_2$]

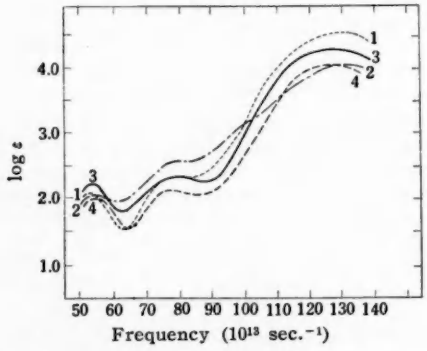

Fig. 2. Absorption spectra of:
1. Blue-K[Co$(NH_3)_2(C_2O_4)_2$]
2. Violet-K[Co$(NH_3)_2(C_2O_4)_2$]
3. Blue-K[Co en$(C_2O_4)_2$]
4. Violet-K[Co en$(C_2O_4)_2$]

(where, NH_3-CO_3 represents carbonato-diamminecobaltate(III) and so forth). These hypsochromic effects of the ligands may be explained by the familiar empirical rule that ethylenediamine is a more hypsochromic ligand than ammonia, and oxalate, than carbonate ion. On the other hand, the values for the violet variety increase in the order of en-ox, en-CO_3, NH_3-ox and NH_3-CO_3. In this case, the hypsochromic effects of the ligands are opposed to those predicted by the familiar rule.

The frequencies for the first and the second bands of the complexes belonging to each series are plotted in Figs. 4 and

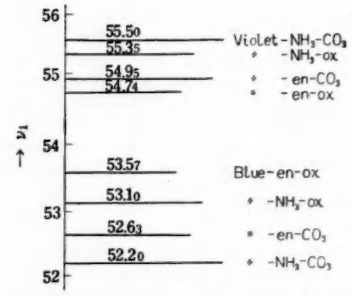

Fig. 3. Diagrammatic representation of absorption maxima.

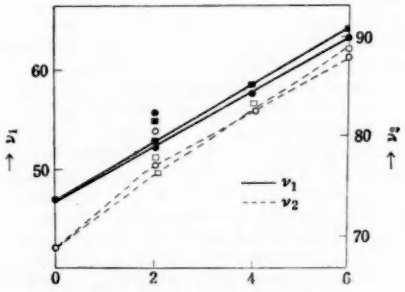

Fig. 4. Frequency position of the absorption bands of the complexes.
NH_3-CO_3 series
en-CO_3 series

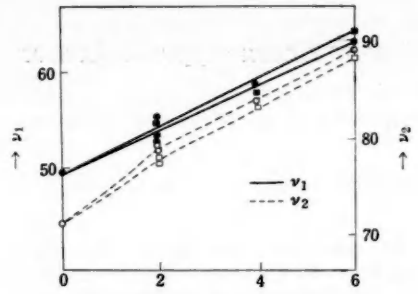

Fig. 5. Frequency position of the complexes.
NH_3-ox series
en-ox series

5, in the same manner as in the preceding paper[1], and the result shows that the same relationship exists in the present case, too.

Configuration.—In the previous paper[1] the authors assumed that the blue variety of $K[Co(NH_3)_2(CO_3)_2]\cdot H_2O$ to be the *cis* isomer and the violet one the *trans* isomer. The two varieties, blue and violet, of the complex salts obtained in the present experiment must also be regarded as stereoisomers because of 1) identity of the chemical composition, 2) equality of the valency and 3) similarity of the absorption spectra.

Assuming this to be true, the authors have attempted to find out which is *cis* and which *trans*. Y. Shimura[3] has generalized that the first band of a *trans*-isomer of a $[Co(NH_3)_4A_2]$- or a $[Co\,en_2A_2]$-type ion (A=unidentate molecule or negative ion) has shorter or longer wave lengths than that of the corresponding *cis*-isomers according as A is ahead of or behind ammonia or ethylenediamine on the spectrochemical series. If such a generalization can be extended to our $[CoX_4(NH_3)_2]$- and $[CoX_4\,en]$-type ions, the blue variety in question must be the *cis*-form and the violet variety, *trans*-form, since ethylenediamine or ammonia is ahead of the bidentate anions, carbonate and oxalate. But there is some doubt as to the legitimacy of such an extention.

There is an additional evidence; it was qualitatively observed that elution of the violet variety from the anion-exchanger column (Cl-form) was faster than that of the corresponding blue variety. The authors have already reported that the *trans*-form of $[Co(NH_3)_4X_2]^+$ or $[Co\,en_2X_2]^+$ is eluted more rapidly than the corresponding *cis*-form, and the stronger affinity of the *cis*-form to the cation exchanger may be attributed to the dipole moment resulting from the existence of acid groups in the *cis*-position[4]. Provided that the same holds in the above case, the blue variety is to be regarded as *cis*-form and the violet one, *trans*-form.

Apart from the adequacy of the above discussion on the assignment of configuration, it is natural that the diammine-type ions should exist in the *cis*- and the *trans*-form. On the other hand, it seems unreasonable to suppose the corresponding (mono) ethylenediamine-type ions exist in both forms, because it is generally agreed that an ethylenediamine is sterically incapable of spanning *trans*-positions in an octahedron. The existence of stereoisomers, however, seems invulnerable at the present stage of investigation. Consequently, further studies must be carried out to solve this problem.

Summary

Three series of cobalt(III) complexes were systematically synthesized from the green solution of potassium tricarbonatocobaltate(III) by means of successive substitution of carbonate by other groups:

i) Blue-$K[Co\,en(CO_3)_2]\cdot H_2O$,
Violet-$K[Co\,en(CO_3)_2]\cdot H_2O$,
$[Co\,en_2CO_3]Cl\cdot H_2O$, $[Co\,en_3]Cl_3\cdot 3H_2O$

ii) Blue-$K[Co(NH_3)_2(C_2O_4)_2]\cdot H_2O$,
Violet-$K[Co(NH_3)_2(C_2O_4)_2]\cdot H_2O$,
$[Co(NH_3)_4C_2O_4]Cl$,
$K_3[Co(C_2O_4)_3]\cdot 3H_2O$

iii) Blue-$K[Co\,en(C_2O_4)_2]\cdot H_2O$,
Violet-$K[Co\,en(C_2O_4)_2]\cdot H_2O$,
$[Co\,en_2(C_2O_4)]Cl\cdot H_2O$.

Of these, the blue and the violet varieties are probably to be regarded as new complexes, stereoisomeric with each other.

Department of Chemistry, Faculty of Science, Kanazawa University, Kanazawa

3) Y. Shimura, This Bulletin, **25**, 49 (1952).

4) M. Mori, M. Shibata and M. Nanasawa, ibid., **29**, 947 (1956).

Normal Vibration and Internal Rotation of Ethane-type Molecules

By Eizi HIROTA

(Received December 4, 1957)

Internal rotation is the motion in which one part of a molecule moves relatively to the other parts of the molecule.[1] In some molecules the parts are so tightly bound that their relative motion can be treated as one of the vibrational modes, but in other molecules the groups are connected loosely with each other and are able to rotate almost freely. According to the general discussion given by Born and Oppenheimer[2], the molecular vibration can approximately be treated separately from the rotation, but internal rotation does not allow such a simplified treatment; one must apply a method suitable for each case.

Many researches have been carried out on the coupling of internal rotation with overall rotation. Even in the cases where the energy of internal rotation is small or comparable in magnitude with that of overall rotation, studies have been restricted to particular types of molecules, such as symmetric[3,4] or almost symmetric top[5,6], and main interest has been concerned with the complicated rotational spectra observed by the microwave spectroscopy[7].

The other coupling scheme, the interaction of internal rotation with vibrations, is important when the energy of internal rotation becomes comparable with that of vibrations. Usually internal rotation is ignored in analyzing the normal modes, but the vibrations of low frequencies, such as deformation vibrations, do couple strongly with the internal rotation, and hence the force constants obtained by the usual procedure may sometimes be in considerable error.

At present, data are often insufficient in number to determine the general quadratic force field, and hence it is necessary to assume a particular force field, for instance, valence force field[8]. The most satisfactory field seems to be of the Urey-Bradley type[9]; the characteristic of this force field is the explicit introduction of the repulsive forces between two non-bonded atoms. Usually, however, one takes into consideration only the next nearest interaction, that is, the interaction between the next nearest atom pairs, and in this approximation the internal rotation and accordingly its coupling with the vibration are completely ignored in the analysis of the normal modes. In order to discuss the internal rotation the procedure must be extended to include the atom pairs, whose interaction hinders the internal rotation. In this paper the discussion will be restricted for simplicity to a particular case: the ethane-type molecules and as one of the most typical examples hexachloroethane will be treated in detail.

The analysis of the normal vibrations gives a basis of calculating mean square amplitudes of atom pairs (abbreviated as mean amplitudes) obtained by the recent electron diffraction experiment[10]. The mean amplitudes of some atom pairs relate closely with the internal rotation, and when one compares such observed amplitudes with those calculated on the basis of the normal coordinate analysis, an estimate can be made on the value of the potential barrier restricting the internal

1) S. Mizushima, "Structure of Molecules and Internal Rotation", Academic Press, Inc., New York, 1954.
2) M. Born and J. R. Oppenheimer, *Ann. Physik*, **84**, 457 (1927).
3) H. H. Nielsen, *Phys. Rev.* **40**, 445 (1832).
4) D. Kivelson, *J. Chem. Phys.* **22**, 1733 (1954); **23**, 2230, 2236 (1955).
5) J. S. Koehler and D. M. Dennison, *Phys. Rev.* **57**, 1006 (1940).
6) D. G. Burkhard and D. M. Dennison, ibid. **84**, 408 (1951); E. V. Ivash and D. M. Dennison, *J. Chem. Phys.* **21**, 1804 (1953); E. Bright Wilson, Jr., C. C. Lin and D. R. Lide, ibid. **23**, 136 (1955); K. T. Hecht and D. M. Dennison, ibid. **26**, 31, 48 (1957);, R. W. Kilb, C. C. Lin, and E. B. Wilson, Jr., ibid. **26**, 1695 (1957).
7) See W. Gordy, W. V. Smith and R. F. Trambarulo, "Microwave Spectroscopy", John Wiley & Sons, Inc., New York, 1953. pp 105-106; C. H. Townes and A. L. Schawlow, "Microwave Spectroscopy", McGraw Hill Book Co., Inc., New York, 1955.
8) G. Herzberg, "Molecular Spectra and Molecular Structure", Vol II, D. Van Nostrand Co., Inc., New York, 1944.
9) T. Shimanouchi, *J. Chem. Phys.* **17**, 245, 734, 848 (1949).
10) Y. Morino, K. Kuchitsu, and T. Shimanouchi, ibid. **20**, 726 (1952); Y. Morino, K. Kuchitsu, A. Takahashi, and K. Maeda, ibid. **21**, 1927 (1957); Y. Morino and E. Hirota, ibid. **23**, 737 (1955).

rotation[11]. This method of the determination of the potential barrier is very interesting and important since there are at present no other possible ways of obtaining the barrier height of ethane-type molecules, except the thermodynamic methods.

Analysis of the Normal Modes

The potential energy usually used in the analysis of the normal modes consists of terms which are functions of three kinds of coordinate: the bond lengths, the bond angles, and the distances between the next nearest atoms[12]. As stated previously, in this expression for the potential energy there are no forces restricting the rotation about the central bond ($X-X'$ axis in Fig. 1). Two types of coordinates, the distances such as Y_1-Y_2' and the

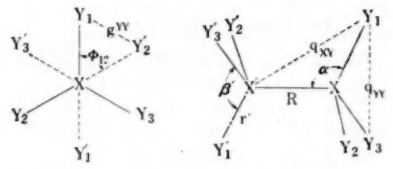

Fig. 1. Schematic diagram of X_2Y_6-type molecule

angles projected along the $X-X'$ axis such as $\phi_{12}=\angle Y_1XY_2'$, may be used to express the interaction between twe XY_3 groups, though the distances such as Y_1Y_1' are so long that the interactions associated with them can be ignored. Four new force constants being added to these coordinates, the Urey-Bradley type expression for potential energy becomes

$$\begin{aligned}2V=&2K'_{XX}R\Delta R+K_{XX}(\Delta R)^2\\&+2K'_{XY}r[\Sigma(\Delta r_i)+\Sigma(\Delta r'_i)]\\&\quad+K_{XY}[\Sigma(\Delta r_i)^2+\Sigma(\Delta r'_i)^2]\\&+2H'_{XXY}r^2[\Sigma(\Delta\alpha_i)+\Sigma(\Delta\alpha'_i)]\\&\quad+H_{XXY}r^2[\Sigma(\Delta\alpha_i)^2+\Sigma(\Delta\alpha'_i)^2]\\&+2H'_{YXY}r^2[\Sigma(\Delta\beta_{ij})+\Sigma(\Delta\beta'_{ij})]\\&\quad+H_{YXY}r^2[\Sigma(\Delta\beta_{ij})^2+\Sigma(\Delta\beta'_{ij})^2]\\&+2F'_{XY}q_{XY}[\Sigma(\Delta q_i)+\Sigma(\Delta q'_i)]\\&\quad+F_{XY}[\Sigma(\Delta q_i)^2+\Sigma(\Delta q'_i)^2]\\&+2F'_{YY}q_{YY}[\Sigma(\Delta q_{ij})+\Sigma(\Delta q'_{ij})]\\&\quad+F_{YY}[\Sigma(\Delta q_{ij})^2+\Sigma(\Delta q'_{ij})^2]\\&+2J'_{YY}g^{YY}\Sigma(\Delta g^{YY}_{ij})\\&\quad+J_{YY}\Sigma(\Delta g^{YY}_{ij})^2\\&+2\Phi'r^2\Sigma(\Delta\phi_{ij})+\Phi r^2\Sigma(\Delta\phi_{ij})^2\end{aligned}\tag{1}$$

where the last four terms are newly introduced. R denotes the equilibrium distance of $X-X'$, r that of $X-Y$ or of $X'-Y'$, q_{XY} that of $X'-Y$ or of $X-Y'$, q_{YY} that of $Y-Y$ or of $Y'-Y'$, and g^{YY} that of $Y_i-Y'_j$ with $i\neq j$. Δ indicates a small deviation from the equilibrium value. α's refer to the bond angles such as $\angle X'XY$ or $\angle XX'Y'$ and β's to $\angle YXY$ or $\angle Y'X'Y'$. As seen easily from Fig. 1 the redundant condition is given by

$$\Sigma(\Delta\phi_{ij})=0,\tag{2}$$

and the four relations

$$\Delta R:\quad K'_{XX}R+6F'_{XY}(R-r\cos\alpha)+6J'_{YY}(R-2r\cos\alpha)=0,\tag{3a}$$

$$\Delta r:\quad K'_{XY}r+F'_{XY}(r-R\cos\alpha)+2F'_{YY}r(1-\cos\beta)+2J'_{YY}[r(1/2+3/2\cos^2\alpha)-R\cos\alpha]=0,\tag{3b}$$

$$\Delta\alpha:\quad H'_{XXY}R+3H'_{YXY}r\sin\alpha\cos\alpha/\sin\beta+2J'_{YY}(R\sin\alpha-3/2\,r\sin\alpha\cos\alpha)+F'_{XY}R\sin\alpha+3F'_{YY}r\sin\alpha\cos\alpha=0,\tag{3c}$$

and

$$\Delta\phi:\quad(\kappa+\Phi')+\sqrt{3}\,H'_{YXY}\sin^2\alpha/\sin\beta+\sqrt{3}\,F'_{YY}\sin^2\alpha+\sqrt{3}/2J'_{YY}\sin^2\alpha=0\tag{3d}$$

must be fulfilled to secure the stable equilibrium. These four types of coodinates are taken to be independent; that is, two distances, $X-X'(\Delta R)$ and $X-Y(\Delta r)$, and two angles, $\angle X'XY(\Delta\alpha)$ and $\Delta\phi$. On the other hand angles $\angle YXY(\Delta\beta)$ are dependent coordinates and can be expressed in terms of $\Delta\alpha$ and $\Delta\phi$. It is a quite conspicuous difference to the usual treatment. κ is the Lagrange's multiplication factor which is used to take into consideration the redundant condition of Eq. 2.

There are eight coefficients in the linear terms, but only four of them are independent, owing to the four relations given above. These four independent coefficients and the eight force constants in the quadratic expression are the parameters available for making the calculated frequencies agree with the observed ones.

If the molecule has the staggered configuration, as is usually the case, the

11) Y. Morino and E. Hirota, ibid 28, 185 (1958).
12) See ref. 9. Recently an additional degree of freedom was introduced; that is, the bending about the middle point of the X-X bond, cf. T. Shimanouchi, *J. Chem. Phys.* **26**, 594 (1957).

molecular symmetry is D_{3d} and the normal modes are factored into five groups; three modes belong to A_{1g}, one to A_{1u}, two to A_{2u}, three pairs to E_g, and the last three ones to E_u. The symmetry coordinates are given by

$$\begin{aligned}
&S_1=1/\sqrt{6}\,[\Delta r_1+\Delta r_2+\Delta r_3+\Delta r'_1\\
&\qquad+\Delta r'_2+\Delta r'_3],\\
&S_2=\Delta R,\\
A_{1g}\quad &S_3=r/\sqrt{6}\,[\Delta\alpha_1+\Delta\alpha_2+\Delta\alpha_3+\Delta\alpha'_1 \qquad (4a)\\
&\qquad+\Delta\alpha'_2+\Delta\alpha'_3],\\
&S_{13}=r/\sqrt{6}\,[\Delta\phi_{12}+\Delta\phi_{23}+\Delta\phi_{31}\\
&\qquad+\Delta\phi_{21}+\Delta\phi_{32}+\Delta\phi_{13}],\\
A_{1u}\quad &S_4=r/\sqrt{6}\,[\Delta\phi_{12}+\Delta\phi_{23}+\Delta\phi_{31}\\
&\qquad-\Delta\phi_{21}-\Delta\phi_{32}-\Delta\phi_{13}], \qquad (4b)\\
A_{2u}\quad &\begin{cases}S_5=1/\sqrt{6}\,[\Delta r_1+\Delta r_2+\Delta r_3\\ \qquad-\Delta r'_1-\Delta r'_2-\Delta r'_3], \qquad (4c)\\ S_6=r/\sqrt{6}\,[\Delta\alpha_1+\Delta\alpha_2+\Delta\alpha_3\\ \qquad-\Delta\alpha'_1-\Delta\alpha'_2-\Delta\alpha'_3],\end{cases}\\
E_g\quad &\begin{cases}S_{7a}=1/2[\Delta r_1-\Delta r_3+\Delta r'_1-\Delta r'_3],\\ S_{7b}=1/2\sqrt{3}\,[\Delta r_1-2\Delta r_2+\Delta r_3\\ \qquad+\Delta r'_1-2\Delta r'_2+\Delta r'_3],\\ S_{8a}=r/2[\Delta\alpha_1-\Delta\alpha_3+\Delta\alpha'_1-\Delta\alpha'_3],\\ S_{8b}=r/2\sqrt{3}\,[\Delta\alpha_1-2\Delta\alpha_2+\Delta\alpha_3 \qquad (4d)\\ \qquad+\Delta\alpha'_1-2\Delta\alpha'_2+\Delta\alpha'_3],\\ S_{9a}=r/2[\Delta\phi_{12}-\Delta\phi_{23}+\Delta\phi_{21}-\Delta\phi_{32}],\\ S_{9b}=r/2\sqrt{3}\,[-\Delta\phi_{12}-\Delta\phi_{23}+2\Delta\phi_{31}\\ \qquad-\Delta\phi_{21}-\Delta\phi_{32}+2\Delta\phi_{13}],\end{cases}\\
E_u\quad &\begin{cases}S_{10a}=1/2[\Delta r_1-\Delta r_3-\Delta r'_1+\Delta r'_3],\\ S_{10b}=1/2\sqrt{3}\,[\Delta r_1-2\Delta r_2+\Delta r_3\\ \qquad-\Delta r'_1+2\Delta r'_2-\Delta r'_3],\\ S_{11a}=r/2[\Delta\alpha_1-\Delta\alpha_3+\Delta\alpha'_1-\Delta\alpha'_3],\\ S_{11b}=r/2\sqrt{3}\,[\Delta\alpha_1-2\Delta\alpha_2+\Delta\alpha_3 \qquad (4e)\\ \qquad-\Delta\alpha'_1+2\Delta\alpha'_2-\Delta\alpha'_3],\\ S_{12a}=r/2\sqrt{3}\,[\Delta\phi_{12}+\Delta\phi_{23}-2\Delta\phi_{31}\\ \qquad-\Delta\phi_{21}-\Delta\phi_{32}+2\Delta\phi_{13}],\\ S_{12b}=r/2[\Delta\phi_{12}-\Delta\phi_{23}-\Delta\phi_{21}+\Delta\phi_{32}].\end{cases}
\end{aligned}$$

S_{13} is obviously a redundant coordinate and can be ignored hereafter. S_4 corresponds to the torsional oscillation and is split by the present molecular symmetry from other symmetry coordinates. The torsional coordinate is, in general, not split from others, hence the coupling between the internal rotation and other normal modes becomes more appreciable in molecules of lower symmetry. For the ethane-type molecules the coupling is indirect: as shown in the following discussion the force constants J_{rr} and Φ introduced above enter not only in the F-matrix of A_{1u} but also in the F-matrix of other symmetries.

The unitary transformation given by Eqs. 4 factorizes also the potential energy of Eq. 1 into five parts, which are expressed by the following five F-matrices:

$$\mathrm{F}(A_{1g})=\begin{bmatrix}A+2B+2B' & & \\ \sqrt{6}\,C & A' & \\ D+2D'+2D'' & \sqrt{6}\,D_0 & L+2L'+2L''\end{bmatrix} \qquad (5a)$$

$$\mathrm{F}(A_{1u})=[N-2N'] \qquad (5b)$$

$$\mathrm{F}(A_{2u})=\begin{bmatrix}A+2B-2B' & \\ D+2D'+2D'' & L+2L'-2L''\end{bmatrix} \qquad (5c)$$

$$\mathrm{F}(E_g)=\begin{bmatrix}A-B-B' & & \\ D-D'-D'' & L-L'-L'' & \\ E-2E' & M-2M' & N-N'\end{bmatrix} \qquad (5d)$$

$$\mathrm{F}(E_u)=\begin{bmatrix}A-B+B' & & \\ D-D'+D'' & L-L'+L'' & \\ \sqrt{3}\,E & \sqrt{3}\,M & N+N'\end{bmatrix} \qquad (5e)$$

where the notations A, B, and so on are given in Fig. 2. The potential energy of the internal rotation in the present type molecule is safely assumed as $V=(V_0/2)(1-\cos 3\phi)$, which, in the high barrier approximation, can be expanded as $(9V_0/4)\phi^2$. The internal coordinate ϕ is expressed in terms of the symmetry coordinate S_4; $\phi=(1/\sqrt{6}\,r)S_4$, and the expression for the potential energy becomes $(3V_0/8r^2)S_4^2$, which is put equal to $(1/2)F_{44}S_4^2$, thus

$$\begin{aligned}
\mathrm{F}(A_{1u})&=(3/4)(V_0/r^2)\\
&=\Phi+(3/4)J_{rr}r^2\sin^4\alpha/(g^{rr})^2\\
&\quad-(1/2)J'_{rr}[\sin^2\alpha\\
&\quad+3r^2\sin^4\alpha/2(g^{rr})^2], \qquad (6)
\end{aligned}$$

$\mathrm{F}(A_{1u})$ being equal to F_{44}. It is an important relation giving V_0 in terms of the two force constants J_{rr} and Φ. It is to be noted that the two force constants, J_{rr} and Φ, important for the internal rotation enter also in the F-matrices of A_{1g}, E_g and E_u symmetries. Hence the internal rotation couples indirectly with other normal modes through J_{rr} and Φ.

The kinetic energy matrices are also factorized analogously; tedious calculation gives:

$$A = K_{XY} + F_{XY}(r - R\cos\alpha)^2/q^2_{XY} + 2F_{YY}r^2(1-\cos\beta)^2/q^2_{YY} + 2J_{YY}[r(1+3\cos^2\alpha)/2 - R\cos\alpha]^2/(g^{YY})^2 + F'_{XY}[1-(r-R\cos\alpha)^2/q^2_{XY}] + 2F'_{YY}[1-r^2(1-\cos\beta)^2/q^2_{YY}] + 2J'_{YY}\{1-[r(1+3\cos^2\alpha)/2 - R\cos\alpha]^2/(g^{YY})^2\},$$

$$B = F_{YY}r^2(1-\cos\beta)^2/q^2_{YY} - F'_{YY}[\cos\beta + r^2(1-\cos\beta)^2/q^2_{YY}],$$

$$B' = J_{YY}[r(1+3\cos^2\alpha)/2 - R\cos\alpha]^2/(g^{YY})^2 + J'_{YY}\{(-1+3\cos^2\alpha)/2 - [r(1+3\cos^2\alpha)/2 - R\cos\alpha]^2/(g^{YY})^2\},$$

$$C = F_{XY}(R - r\cos\alpha)(r - R\cos\alpha)/q^2_{XY} + 2J_{YY}[r(1+3\cos^2\alpha)/2 - R\cos\alpha] \times (R-2r\cos\alpha)/(g^{YY})^2 - F'_{XY}[\cos\alpha + (R - r\cos\alpha)(r - R\cos\alpha)/q^2_{XY}] - 2J'_{YY}\{\cos\alpha + [r(1+3\cos^2\alpha)/2 - R\cos\alpha](R-2r\cos\alpha)/(g^{YY})^2\},$$

$$A' = K_{XY} + 6F_{XY}(R - r\cos\alpha)^2/q^2_{XY} + 6J_{YY}(R-2r\cos\alpha)^2/(g^{YY})^2 + 6F'_{XY}[1-(R-r\cos\alpha)^2/q^2_{XY}] + 6J'_{YY}[1-(R-2r\cos\alpha)^2/(g^{YY})^2],$$

$$D = F_{XY}r(r - R\cos\alpha)\sin\alpha/q^2_{XY} + 3F_{YY}r^3(1-\cos\beta)\sin\alpha\cos\alpha/Rq^2_{YY} + 2J_{YY}(1/R) \times [r(1+3\cos^2\alpha)/2 - R\cos\alpha][Rr\sin\alpha - (3/2)r^2\sin\alpha\cos\alpha]/(g^{YY})^2 + F'_{XY}[\sin\alpha - r \times (r - R\cos\alpha)\sin\alpha/q^2_{XY}] + 3F'_{YY}[(r/R) - r^3(1-\cos\beta)/Rq^2_{YY}]\sin\alpha\cos\alpha + 2J'_{YY}(1/R) \times \{R\sin\alpha - (3/2)r\sin\alpha\cos\alpha - [r(1+3\cos^2\alpha)/2 - R\cos\alpha] \times [Rr\sin\alpha - (3/2)r^2\sin\alpha\cos\alpha]/(g^{YY})^2\},$$

$$D' = (3/2)F_{YY}r^3(1-\cos\beta)\sin\alpha\cos\alpha/Rq^2_{YY} + (3/2)F'_{YY} \times [(r/R) - r^3(1-\cos\beta)/Rq^2_{YY}]\sin\alpha\cos\alpha,$$

$$D'' = J_{YY}(1/R)[r(1+3\cos^2\alpha)/2 - R\cos\alpha][Rr\sin\alpha - (3/2)r^2\sin\alpha\cos\alpha]/(g^{YY})^2 - J'_{YY}(1/R)\{(3/2)r\sin\alpha\cos\alpha + [r(1+3\cos^2\alpha)/2 - R\cos\alpha] \times [Rr\sin\alpha - (3/2)r^2\sin\alpha\cos\alpha]/(g^{YY})^2,$$

$$D_0 = F_{XY}r(R - r\cos\alpha)\sin\alpha/q^2_{XY} + 2J_{YY}(1/R)[R - 2r\cos\alpha][Rr\sin\alpha - (3/2)r^2\sin\alpha\cos\alpha]/(g^{YY})^2 + F'_{XY}[r\sin\alpha/R - r(R - r\cos\alpha)\sin\alpha/q^2_{XY}] + 2J'_{YY}(1/R)\{r\sin\alpha - [R-2r\cos\alpha][Rr\sin\alpha - (3/2)r^2\sin\alpha\cos\alpha]/(g^{YY})^2\},$$

$$L = H_{XXY} + (9/2)H_{YXY}(r/R)^2\sin^2\alpha\cos^2\alpha/\sin^2\beta + F_{XY}r^2\sin^2\alpha/q^2_{XY} + (9/2)F_{YY}(r^2/R)^2 \times \sin^2\alpha\cos^2\alpha/q^2_{YY} + 2J_{YY}(1/R)^2[Rr\sin\alpha - (3/2)r^2\sin\alpha\cos\alpha]^2/(g^{YY})^2 + 2H'_{YXY}(r/R)^2(\cos\beta/\sin^3\beta)[\sin^2\beta - (9/4)\sin^2\alpha\cos^2\alpha] + F'_{XY}[r\cos\alpha/R - r^2\sin^2\alpha/q^2_{XY}] + 2F'_{YY}(r/R)^2[\cos\beta - (9/4)r^2\sin^2\alpha\cos^2\alpha/q^2_{YY}] + 2J'_{YY}(1/R^2)\{[Rr\cos\alpha - r^2(-1 + 3\cos^2\alpha)/2] - [Rr\sin\alpha - (3/2)r^2\sin\alpha\cos\alpha]^2/(g^{YY})^2\},$$

$$L' = (9/4)H_{YXY}(r/R)^2\sin^2\alpha\cos^2\alpha/\sin^2\beta + (9/4)F_{YY}(r^2/R)^2\sin^2\alpha\cos^2\alpha/q^2_{YY} + H'_{YXY}(r/R)^2(2\sin^2\beta\cos^2\alpha - 4\sin^2\beta\sin^2\alpha - 9\cos\beta\sin^2\alpha\cos^2\alpha)/4\sin^3\beta + F'_{YY}(r^2/2R^2)[\cos^2\alpha - 2\sin^2\alpha - qr^2\sin^2\alpha\cos^2\alpha/2q^2_{YY}],$$

$$L'' = J_{YY}(1/R^2)(Rr\sin\alpha - (3/2)r^2\sin\alpha\cos\alpha)^2/(g^{YY})^2 + J'_{YY}(1/R^2)\{r^2(\sin^2\alpha - (1/2)\cos^2\alpha) - (Rr\sin\alpha - (3/2)r^2\sin\alpha\cos\alpha)^2/(g^{YY})^2\},$$

$$N = \Phi + (3/2)H_{YXY}\sin^4\alpha/\sin^2\beta + (3/2)F_{YY}r^2\sin^4\alpha/q^2_{YY} + (3/4)J_{YY}r^2\sin^4\alpha/(g^{YY})^2 - H'_{YXY}(3\cos\beta\sin^4\alpha + 2\sin^2\beta\sin^2\alpha)/2\sin^3\beta - F'_{YY}\sin^2\alpha(1+3r^2\sin^2\alpha/2q^2_{YY}) - J'_{YY}[\sin^2\alpha/2 + 3r^2\sin^4\alpha/4(g^{YY})^2],$$

$$N' = (3/4)H_{YXY}\sin^4\alpha/\sin^2\beta + (3/4)F_{YY}r^2\sin^4\alpha/q^2_{YY} - H'_{YXY}(3\cos\beta\sin^4\alpha + 2\sin^2\beta\sin^2\alpha)/4\sin^3\beta - (1/2)F'_{YY}\sin^2\alpha(1+3r^2\sin^2\alpha/2q^2_{YY}),$$

$$E = (\sqrt{3}/2)F_{YY}r^2(1-\cos\beta)\sin^2\alpha/q^2_{YY} + (\sqrt{3}/2)J_{YY}r[r(1+3\cos^2\alpha)/2 - R\cos\alpha]\sin^2\alpha/(g^{YY})^2 + (\sqrt{3}/2)F'_{YY}[1-r^2(1-\cos\beta)/q^2_{YY}]\sin^2\alpha + (\sqrt{3}/2)J'_{YY}\{1-r[r(1+3\cos^2\alpha)/2 - R\cos\alpha]/(g^{YY})^2\}\sin^2\alpha,$$

$$E' = (\sqrt{3}/2)F_{YY}r^2(1-\cos\beta)\sin^2\alpha/q^2_{YY} + (\sqrt{3}/2)F'_{YY}[1-r^2(1-\cos\beta)/q^2_{YY}]\sin^2\alpha,$$

$$M = (3\sqrt{3}/4)H_{YXY}(r/R)\sin^3\alpha\cos\alpha/\sin^2\beta + (3\sqrt{3}/4)F_{YY}(r^3/R)\sin^3\alpha\cos\alpha/q^2_{YY} + (\sqrt{3}/2)J_{YY}(r^2/R)\sin^2\alpha(Rr\sin\alpha - (3/2)r^2\sin\alpha\cos\alpha)/(g^{YY})^2 + (\sqrt{3}/4)H'_{YXY}(r/R)\sin\alpha\cos\alpha(2\sin^2\beta - 3\cos\beta\sin^2\alpha)/\sin^3\beta + (\sqrt{3}/2) \times F'_{YY}(r/R)\sin\alpha\cos\alpha(1-3r^2\sin^2\alpha/2q^2_{YY}) + (\sqrt{3}/2)J'_{YY}(r/R)\sin\alpha[\cos\alpha - (Rr\sin\alpha - (1/2)r^2\sin\alpha\cos\alpha)\sin\alpha/(g^{YY})^2],$$

$$M' = (3\sqrt{3}/4)H_{YXY}(r/R)\sin^3\alpha\cos\alpha/\sin^2\beta + (3\sqrt{3}/4)F_{YY}(r^3/R)\sin^3\alpha\cos\alpha/q^2_{YY} + (\sqrt{3}/4)H'_{YXY}(r/R)\sin\alpha\cos\alpha(2\sin^2\beta - 3\cos\beta\sin^2\alpha)/\sin^3\beta + (\sqrt{3}/2)F'_{YY}(r/R)\sin\alpha\cos\alpha(1-3r^2\sin^2\alpha/2q^2_{YY})$$

Fig. 2. Notations used for the elements of the F-matrix.

$$A=\mu_1+\mu_2, \qquad B=\mu_1\cos\beta, \qquad C=\mu_1\cos\alpha,$$
$$C_0=2\mu_1, \qquad D=D''=-\mu_1\rho\sin\alpha,$$
$$D'=-\mu_1[(\rho-\cos\alpha)\cos\beta+(1-\rho\cos\alpha)\cos\alpha]/\sin\alpha,$$
$$D'''=(1/2)\mu_1\rho\sin\alpha, \qquad D_0=-\mu_1\sin\alpha,$$
$$L=\mu_1[2\rho^2-2\rho\cos\alpha+1]+\mu_2,$$
$$L'=\mu_1[(2\rho^2-2\rho\cos\alpha+\cos^2\alpha)\cos\beta-2(1-\rho\cos\alpha+\rho^2)\cos^2\alpha+1]/\sin^2\alpha$$
$$L''=2\mu_1\rho(\rho-\cos\alpha), \qquad L'''=-\mu_1\rho(\rho-\cos\alpha),$$
$$N=2\mu_1[1-3\rho\cos\alpha+3\rho^2\cos^2\alpha]/\sin^2\alpha+2\mu_2[5-9\cos^2\alpha-4\cos\beta]/3\sin^4\alpha,$$
$$N'=\mu_1[2(1-6\cos^2\alpha)-9\rho\cos\alpha(1-5\cos^2\alpha)+9\rho^2\cos^2\alpha(1-5\cos^2\alpha)+2(5-18\rho\cos\alpha+18\rho^2\cos^2\alpha)\cos\beta]/3\sin^4\alpha,$$
$$N''=\mu_1[2(4-9\cos^2\alpha)-36\rho\cos\alpha(1-2\cos^2\alpha)+36\rho^2\cos^2\alpha(1-2\cos^2\alpha)+2(5-18\rho\cos\alpha+18\rho^2\cos^2\alpha)\cos\beta]/3\sin^4\alpha,$$
$$N'''=\mu_1[1-6\cos^2\alpha+18\rho\cos^3\alpha-18\rho^2\cos^4\alpha+(5-18\rho\cos\alpha+18\rho^2\cos^2\alpha)\cos\beta]/3\sin^4\alpha+\mu_2(-1-3\cos^2\alpha+4\cos\beta)/3\sin^4\alpha,$$
$$E=-(\sqrt{3}/2)\mu_1\rho\cos\alpha,$$
$$E'=(1/\sqrt{3})(\mu_1/\sin^2\alpha)[(1-3\rho\cos\alpha)\cos\beta-(1-(3/2)\rho\cos\alpha-(3/2)\rho\cos^3\alpha)],$$
$$E''=(1/\sqrt{3})(\mu_1/\sin^2\alpha)[(1-3\rho\cos\alpha)\cos\beta+(2-3\cos^2\alpha)-3\rho\cos\alpha(1-2\cos^2\alpha)],$$
$$M=-(\sqrt{3}/2)(\mu_1\rho/\sin\alpha)(1+\cos^2\alpha-2\rho\cos\alpha),$$
$$M'=(1/\sqrt{3})(\mu_1/\sin^3\alpha)[(\cos\alpha-3\rho-3\rho\cos^2\alpha+6\rho^2\cos\alpha)\cos\beta+(-\cos\alpha+(3/2)\rho+3\rho\cos^2\alpha+(3/2)\rho\cos^4\alpha-3\rho^2\cos\alpha-3\rho^2\cos^3\alpha)],$$
$$M''=(1/\sqrt{3})(\mu_1/\sin^3\alpha)[(\cos\alpha-3\rho-3\rho\cos^2\alpha+6\rho^2\cos\alpha)\cos\beta+(2\cos\alpha-3\cos^3\alpha-3\rho+3\rho\cos^2\alpha+6\rho\cos^4\alpha+6\rho^2\cos\alpha-12\rho^2\cos^3\alpha)]$$

where

$$\mu_1=1/m_C, \quad \mu_2=1/m_{Cl}, \quad \rho=r/R.$$

Fig. 3. Notations used for the elements of the G-matrix.

$$G(A_{1g})=\begin{bmatrix} A+2B & & \\ \sqrt{6}\,C & C_0 & \\ D+2D'+D''+2D''' & \sqrt{6}\,D_0 & L+2L'+L''+2L''' \end{bmatrix} \tag{7a}$$

$$G(A_{1u})=[N+2N'-N''-2N'''] \tag{7b}$$

$$G(A_{2u})=\begin{bmatrix} A+2B & \\ D+2D'-D''-2D''' & L+2L'-L''-2L''' \end{bmatrix} \tag{7c}$$

$$G(E_g)=\begin{bmatrix} A-B & & \\ D-D'+D''-D''' & L-L'+L''-L''' & \\ E-2E'+E'' & M-2M'+M'' & N-N'+N''-N''' \end{bmatrix} \tag{7d}$$

$$G(E_u)=\begin{bmatrix} A-B & & \\ D-D'-D''+D''' & L-L'-L''+L''' & \\ \sqrt{3}\,(E-E'') & \sqrt{3}\,(M-M'') & N-N'-N''+N''' \end{bmatrix} \tag{7e}$$

where the notations A, B, and so on are given in Fig. 3. Using the **F**-matrices Eqs. 5 and the **G**-matrices Eqs. 7 the frequencies of normal modes can be calculated through the determinant[13]:

$$|\,\mathbf{GF}-\lambda\mathbf{E}\,|=0 \tag{8}$$

where **E** denotes the unit matrix.

A Numerical Example; Hexachloroethane

One of the molecules, to which the present treatment can adequately be applied, is hexachloroethane, for a rather large steric repulsion is expected for the large substituents, chlorine atoms, and seems to result in a high hindering potential barrier. In fact, according to an electron diffraction investigation by Morino and Iwasaki[14], the barrier height of 15 kcal/mole was reported, definitely higher than the level of thermal energy of about 600 cal/mole. Hence, the high barrier approximation is expected in this case.

By using Eqs. 5, 7, and 8 with appropriate force constants given in Table

13) E. Bright Wilson, Jr., ibid. **7**, 1047 (1939); **9**, 76 (1941).

14) Y. Morino and M. Iwasaki ibid. **17**, 216 (1949).

TABLE I

FORCE CONSTANTS USED FOR HEXACHLOROETHANE (in 10^5 dynes/cm).

$K_{CC}=2.15$, $F_{CCl}=0.55$, $F'_{CCl}=-0.04$, $H_{CCCl}=0.07$, $K_{CCl}=2.30$, $F_{ClCl}=0.70$, $F'_{ClCl}=-0.035$, $H_{ClCCl}=0.04$, $J_{ClCl}=0.090$, others assumed to be zero

TABLE II

CALCULATED AND OBSERVED FREQUENCIES OF NORMAL VIBRATIONS OF HEXACHLOROETHANE (in cm^{-1}).

		$\tilde{\nu}_{calc}$	$\tilde{\nu}_{obs}$	deviation (%)
A_{1g}	ν_1	969	974	− 0.6
	ν_2	469	431	+ 8.9
	ν_3	189	169	+12.0
A_{1u}	ν_4	62	—	—
A_{2u}	ν_5	671	675	− 0.6
	ν_6	354	—	—
E_g	ν_7	851	853	− 0.3
	ν_8	313	341	− 8.2
	ν_9	200	224	−10.6
E_u	ν_{10}	799	769	+ 3.9
	ν_{11}	249	—	—
	ν_{12}	143	—	—

TABLE III

CALCULATED AND OBSERVED ROOT MEAN SQUARE AMPLITUDES OF HEXACHLOROETHANE (in Å)

atom pair	calc.	obs.
C—C	0.055	—
C—Cl	0.051	0.06_6
C...Cl	0.071	0.06_9
Cl...Cl	0.070	0.06_4
*g*Cl...Cl	(0.136)	0.13_6
*t*Cl...Cl	0.069	0.10_9

I the frequencies of twelve normal vibrations were calculated; the results are summarized in Table II, where the observed data, if available, are given for comparison. It is seen that the discrepancy is somewhat large for ν_3 and ν_9; one is too high (+12.0%) and the other is too low (−10.6%). However, it was found difficult to make better the agreements of both frequencies simultaneously. Apart from this point, the set of force constants is satisfactory, though the low frequency vibrations active in the infrared have not yet been observed. (ν_6 of A_{2u} type and ν_{11} and ν_{12} of E_u type). Unfortunately all these bands are of low frequency and have large contributions to the root mean square amplitudes, so that the accuracies of the calculated root mean square amplitudes are limited.

The force constant J_{YY} was chosen to be $0.090 \cdot 10^5$ dynes/cm, which means the potential barrier of about 10 kcal/mole (see Eq. 6), and the frequency of the torsional mode was calculated to be 62 cm^{-1}. These values are chosen because they are consistent with the result of the recent electron diffraction experiment[11] (see the next section). Another force constant ϕ was simply set equal to zero, for the interaction between chlorine atoms was considered to be more important than the C—Cl bond interactions.

The **L**-matrices given by the relation $\mathbf{S}=\mathbf{LQ}$ are important not only for understanding the nature of the normal modes, but also for calculating the mean amplitudes. The following values were obtained for the elements of the **L**-matrices;

$$A_{1g}\begin{bmatrix}+0.179 & +0.154 & +0.011\\ -0.407 & +0.032 & -0.001\\ +0.469 & -0.048 & +0.167\end{bmatrix} \quad (9a)$$

$$A_{1u}\ [+0.356] \quad (9b)$$

$$A_{2u}\begin{bmatrix}+0.232 & -0.047\\ +0.399 & +0.301\end{bmatrix} \quad (9c)$$

$$E_g\begin{bmatrix}+0.369 & +0.054 & +0.018\\ -0.889 & +0.287 & +0.144\\ +1.090 & -0.432 & +0.186\end{bmatrix} \quad (9d)$$

$$E_u\begin{bmatrix}+0.373 & +0.003 & -0.013\\ -0.099 & +0.006 & +0.176\\ -0.335 & +0.239 & +0.054\end{bmatrix} \quad (9e)$$

where the unit is $(\text{a. m. u.})^{-1/2}$. It can be seen that the coupling between the bond stretching modes and the bond angle deformation vibrations is unusually large.

Mean Amplitudes and Determination of the Potential Barrier

The recent improvement in the electron diffraction technique, the sector-microphotometer method, gives us not only the equilibrium distances of atom pairs but also their mean square amplitudes $\langle \Delta r^2_{ij} \rangle_{Av}$[15]. Because Δr_{ij}, the small deviation from the equilibrium distance of atom pair (i, j), is one of the internal coordinates, it can be expressed in terms of the normal coordinates Q_k's:

$$\Delta \mathbf{r} = \mathbf{AULQ} \quad (10)$$

where **U** and **L** are the unitary and the **L**-matrices, as explained above, and **A** is a matrix which transforms the independent internal coordinates to a particular atom distance, for example between the two atom pair (i, j). Thus the mean amplitude $\langle \Delta r^2_{ij} \rangle_{Av}$ is given by

15) I. L. Karle and J. Karle, ibid. **17**, 1052 (1949).

$$\langle \Delta r^2_{ij} \rangle_{AV} = \mathbf{AUL} \langle \mathbf{Q}^2 \rangle_{AV} \mathbf{L}' \mathbf{U}' \mathbf{A}' \quad (11)$$

where $\langle \mathbf{Q}^2 \rangle_{AV}$ is the square of the normal coordinate averaged out over its vibrational states and is for the kth vibration given by

$$\langle Q^2_k \rangle_{AV} = (h/8\pi^2\nu_k)\coth(h\nu_k/2kT). \quad (12)$$

For hexachloroethane there are six atom pairs and their mean amplitudes have been observed except for the C—C atom pair which has too low scattering power to be measured accurately. Thus it is very interesting to compare these observed data with the calculated values based upon Eqs. 11 and 12. The agreement between them, though indirectly, indicates the validity of the force field we have applied. As shown in Table III, the agreement is very good when the experimental error and the approximation made for the force field are taken into consideration.

One atom pair, denoted as gCl—Cl in Table III, is particularly important for the determination of the potential barrier. The mean amplitude of the atom pair is also expressed by a sum of the mean square amplitudes of several normal vibrations, including that of the torsional oscillation, Q_4. If the classical approximation of Eq. (12) is applied for the torsional mode*, the mean amplitude of the gCl—Cl atom pair is given by

$$\langle r^2(g\text{Cl—Cl}) \rangle_{AV} = A + B/V_0, \quad (13)$$

where the first term A is the contribution from skeletal vibrations and the second term B/V_0 from the torsional mode, and the constant B is given by

$$B = (2/9)kT(r^4/(g^{ClCl})^2)\sin^4\alpha \sin^2\phi. \quad (14)$$

However, since the electron diffraction experiment gives us only this sum and cannot separate two parts, it is impossible to obtain the value of the potential barrier only by the observation. Now, since a good force field has become available for us, the unknown constant A can be calculated to be $11.53 \cdot 10^{-3}$ Å^2. Thus the observed mean amplitude $\langle r^2(g\text{Cl—Cl}) \rangle_{AV}$ determines the barrier height V_0. A remark must, however, be given to the value of A, which is indirectly a function of V_0, for the force constant J_{ClCl} determining V_0 enters also into the F-matrices of skeletal modes. The force constants given in Table I and the value of A shown above are all consistent with the final value of V_0 of about 10.8 kcal/mole. As described above, the force constants were able to reproduce the observed frequencies of normal vibrations with error of 10%, thus the uncertainties of the calculated mean square amplitudes are about 20% or less, and the height of potential barrier is also accurate in the same order of magnitude.

* The frequency of the torsion Q_4 is low, which allows us to treat it classically.

Discussion

The force field developed here is only of an approximate nature, hence the values of individual force constants given in Table I do not reflect exactly the interatomic interactions in molecules; other coupling constants omitted in the present investigation may influence strongly the values of force constants. It is, however, interesting to discuss the force constant J_{ClCl} introduced first in the present paper, for this constant determines the frequency of the torsional oscillation. The torsional mode is the only one belonging to the A_{1u} symmetry, hence the value of J_{ClCl} is relatively independent of the non-diagonal coupling constants in the F-matrices. In fact the constant J_{ClCl} plays the main role in the F-matrix of the A_{1u} symmetry [cf. Eq. 5b]. As stated above, its value can be determined by the recent electron diffraction experiment accurately enough to make it worth while to discuss further.

The origin of the hindrance of the internal rotation is very complicated; the diversity of the circumstances has already been noted in the Introduction. Lassettre and Dean[16] discussed the effect of the bond quadrupole interaction. In many instances this effect would be appreciable[17], but the steric repulsion is more important in the present example of hexachloroethane; if one considers the cis-configuration of this molecule the distance between the two eclipsed chlorine atoms becomes about 2.72 A, and the exchange force would be very large. Morino and Miyagawa[18] gave a semi-empirical expression for the repulsive potential between two chlorine atoms:

$$V = -1.515 \cdot 10^{-10} r^{-6} + 1.620 \cdot 10^{-7} r^{-12} \text{ erg/molecule}, \quad (15)$$

r being given in unit of Å. It is based

16) E. N. Lassettre and L. B. Dean, Jr., *J. Chem. Phys.* **17**, 317 (1949); L. J. Oosterhoff, *Discussions Faraday Soc.* **10**, 79 (1951).
17) H. S. Gutowsky and E. O. Stejskal, *J. Chem. Phys.* **22**, 937 (1954); D. R. Lide and D. K. Coles, *Phys. Rev.* **80**, 911 (1950) and so on; see also ref. 11.
18) Y. Morino and I. Miyagawa, *J. Chem. Soc. Japan, (Nippon Kagaku Zassi)* **68**, 62 (1947).

upon the potential obtained from the second virial coefficient of chlorine gas. The force constant J_{ClCl} corresponds to the second derivative of this potential at the equilibrium distance of gCl—Cl pair:

$$J_{ClCl}=(\partial^2 V/\partial r^2)_{r=g\mathrm{ClCl}}, \qquad (16)$$

which is calculated to be $0.17\cdot10^5$ dynes/cm, which is in the same order of magnitude with but about twice as large as that previously given in Table I.

The high barrier approximation was used through this paper, but the anharmonicity may be appreciable for the internal rotation. It is, however, of the order of magnitude of $(h\nu_4)^2/V_0$, which is very small, and can be neglected in the present discussion. If the barrier height becomes lower, each torsional level splits owing to the symmetry of the two CCl_3 groups; the three states $H^n{}_1$, $H^n{}_2$ and $H^n{}_3$ corresponding to the three minima and degenenerating in the high barrier case, must be replaced by the irreducible representation[3,5]:

$$\Psi^n{}_1=(1/3)^{1/2}\exp(-iK\phi/2)(H^n{}_1+H^n{}_2+H^n{}_3), \qquad (17a)$$

$$\Psi^n{}_2=(1/6)^{1/2}\exp(-iK\phi/2)(2H^n{}_1-H^n{}_2-H^n{}_3), \qquad (17b)$$

and $$\Psi^n{}_3=(1/2)^{1/2}\exp(-iK\phi/2)(H^n{}_2-H^n{}_3), \qquad (17c)$$

but this splitting due to the tunneling effect is also small and can be ignored in the present case.

The projected angle introduced here may be applied as one of the internal coordinates to other molecules of lower symmetries with the internal rotation of relatively high frequencies; the mathematical complexity involved is not very serious. If the internal rotation is included in this way in the treatment of the normal mode, its important coupling with other normal vibrations of low frequencies will be obtained, and also the more correct force constants for the latter modes.

The author wishes to express his appreciation to Professor Yonezo Morino, under whose guidiance this research was carried out.

Department of Chemistry
Faculty of Science
The University of Tokyo
Hongo, Tokyo

Spectrochemical Study of Microscopic Crystals. XVII[1]. *The Structure of Cupric Salts with Monocarboxylic Fatty Acids*[2]

By Shoichiro YAMADA, Hiroji NAKAMURA and Ryutaro TSUCHIDA

(Received December 18, 1957)

In 1953 van Niekerk and Schoening[3] showed with X-ray that copper acetate monohydrate in the crystalline state consisted of dimeric molecules with a formula of $Cu_2(CH_3COO)_4\cdot2H_2O$. It was concluded later from measurements of absorption spectra[1,4] that cupric propionate in organic solvents as well as in the crystalline state had dimeric molecules similar to those of cupric acetate monohydrate, involving a sort of interaction between the copper atoms. This was found to be in agreement with the conclusion derived from the unusual magnetic property of the compound in the crystalline state[5]. In these circumstances, it seemed to be of significance to examine whether cupric salts with higher homologues of monocarboxylic acids would involve the dimeric molecules, or not. About the structure of some of the cupric alkanoates, there have recently appeared a few reports[6,7], dealing mainly with magnetic properties. The present authors also have carried out

1) Part XVI of this series, S. Yamada, H. Nakamura and R. Tsuchida, This Bulletin, **30**, 953 (1957).
2) R. Tsuchida, S. Yamada and H. Nakamura, Presented in part before the Symposium on Co-ordination Compounds, Tokyo, October, 1956.
3) J. N. van Niekerk and F. R. L. Schoening, *Acta Cryst.*, **6**, 227 (1953).
4) R. Tsuchida and S. Yamada, *Nature*, **176**, 1171 (1957).
5) H. Abe, *Phys. Rev.*, **92**, 1572 (1953).
6) R. C. Herron and R. C. Pink, *J. Chem. Soc.*, **1956**, 3948.
7) R. L. Martin and H. Waterman, ibid., **1957**, 2545.

examinations about the structure of cupric butyrate, valerianate, capronate, caprylate, palmitate and stearate mostly on the basis of their polarized absorption spectra[2,8]. A brief report of this study was formerly presented as a communication[8], the detailed account of which is given below.

Experimental

Materials.—Cupric *n*-butyrate was prepared by the method of von Alth[9] from barium *n*-butyrate and cupric sulfate. Recrystallization of the product from water yielded the monohydrate in green crystals. Anhydrous cupric *n*-butyrate was obtained by repeated recrystallization from acetone or chloroform.

Cupric *iso*-butyrate was prepared in a similar way, and obtained in anhydrous crystals when recrystallized from water.

Cupric *n*-valerianate monohydrate was prepared by the same method as that for cupric butyrate[9]. Anhydrous cupric *n*-valerianate was obtained after dehydration of the monohydrate, followed by repeated recrystallization from chloroform.

Cupric *iso*-valerianate was prepared by the same method as in the case of the *n*-valerianate monohydrate. Recrystallization from water always yielded green crystals of the anhydrous *iso*-valerianate.

Cupric *n*-capronate was prepared according to the method of Freund[10] from cupric acetate and *n*-caproic acid. Recrystallization from ethanol gave green crystals of the anhydrous *n*-capronate.

Cupric *n*-caprylate was prepared according to the method of Zincke[11] from sodium *n*-caprylate and cupric sulfate. After recrystallization from ethanol, anhydrous *n*-caprylate was obtained in green crystals. The compound exists only in an anhydrous form.

The crystals of the above-described compounds all show a striking dichroism on their well-developed planes; that is, blue and green.

Cupric *n*-palmitate and *n*-stearate were prepared according to the method of Cady et al.[12] and Heintz[13]. Anhydrous forms of both the compounds were obtained in greenish-blue, powdery microcrystals. The crystals obtained were found to be too small for the dichroism measurement. Therefore, absorption spectra in the visible and the ultraviolet region of the compounds were determined only in solution.

Measurements.—Quantitative dichroism measurements in the visible and the ultraviolet region were carried out at room temperature by the same method as that in the previous papers of this series[14]. The measurements were made with respect to the directions of extinction on one of the well-developed planes which was shown in each figure. The notations refer to the directions shown in the figure.

Absorption spectra of the compounds in ethanol or carbon tetrachloride were determined at room temperature by a Beckman DU spectrophotometer. It was confirmed in every measurement that Beer's law was obeyed in the presence of the free aliphatic carboxylic acid in addition.

Infrared absorption spectra of the cupric compounds in Nujol mulls were determined in the rock salt region by a Hilger H-800 infrared spectrophotometer.

The notations in the present paper are the same as those used in the former papers of this series. Extinction coefficients, ε, are calculated, and referred to a formula weight instead of a molecular weight.

Results and Discussion

Polarized Absorption Spectra of the Cupric Alkanoates in the Crystalline State.—In the preceding paper[1], we have reported about the structure of cupric formate, acetate and propionate on the basis of their polarized absorption spectra. A similar treatment will be made here concerning the structure of cupric salts with higher homologues of monocarboxylic fatty acids. Since some of the results and discussions in the preceding paper are used in the present discussion, it would be appropriate to give a brief account of the conclusions obtained in the former paper.

Cupric acetate and propionate in the crystalline state and in organic solvents show in the visible and the near-ultraviolet region a band at about 80×10^{13}/sec. (band II) besides a band at about 43×10^{13}/sec. (band I), whereas most cupric compounds show in this wave-length region only one band which may be considered as corresponding to the band at 43×10^{13}/sec. For the band I, electric vector is more strongly absorbed along the complex plane than along the *z*-direction of the dimeric molecule. For the band II, electric vector is more strongly absorbed along the *z*-direction; the polarization for this band is the reverse of that for the band I. These facts were considered to show that the compounds involve along the *z*-direction a sort of copper-to-copper interaction characteristic of the dimeric molecule of the cupric carboxylates. The same result

8) R. Tsuchida, S. Yamada and H. Nakamura, *Nature*, **178**, 1192 (1956).
9) T. von Alth, *Ann.*, **91**, 170 (1854).
10) A. Freund, *J. prakt. Chem.*, (2) **3**, 233 (1871).
11) T. Zincke, *Ann.*, **152**, 11 (1869).
12) H. P. Cady and E. J. Baldwin, *J. Am. Chem. Soc.*, **43**, 648 (1921).
13) W. Heintz, *Ann.*, **84**, 239 (1852).

14) R. Tsuchida and M. Kobayashi, "The Colour and the Structure of Metallic Compounds," Zoshindo, Osaka, 1944, p. 180 (in Japanese).

was obtained with cupric propionate, hydrated or anhydrous. Thus the appearance of the band at about 80×10^{13}/sec., combined with the polarization property of the band, may be regarded as showing the existence of the dimeric molecule similar to that of cupric acetate or propionate involving the copper-to-copper interaction.

The results of the present measurements are shown in Figs. 1 to 8. As the components of the cupric compounds in the crystalline state may be under rather weak perturbation owing to the crystalline field, the polarized absorption spectra as determined on a suitable plane are regarded as representing the main features of the dichroism of the components. The exact arrangement of the components in the crystals is unknown for all the cupric compounds reported here. It is easy, however, to see the principal characteristics of the dichroism of the components themselves by comparing their absorption spectra with those of cupric acetate monohydrate whose crystal structure was accurately determined.

The present measurements indicate that cupric butyrate monohydrate in the crystalline state shows an absorption band at about 80×10^{13}/sec. in addition to a band at about 43×10^{13}/sec. Moreover, the polarization for the former band is found to be the reverse of the polarization for the latter (Fig. 1). This relationship, which closely resembles that encountered in the case of the acetate monohydrate, may suggest that cupric butyrate monohydrate in the crystalline state consists

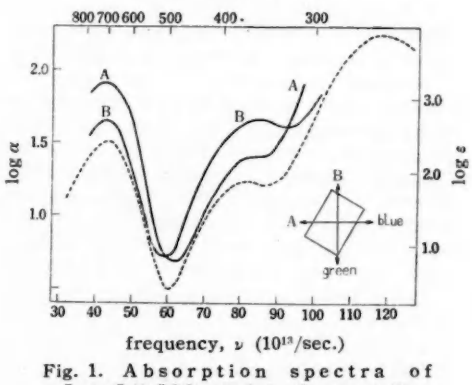

Fig. 1. Absorption spectra of $Cu(n\text{-}C_3H_7COO)_2\cdot H_2O$ in the crystalline state (——) and in ethanol (------).

of the binuclear molecules resembling those of copper acetate monohydrate. The crystal structure was formerly examined by Iball[15], who noted an unusual number of the molecules involved in a unit cell of the compound. This may presumably be related to the dimeric structure of the compound. It is certain that the A- and the B-absorption in Fig. 1 may represent the characteristics of the absorption along and perpendicular to the complex-plane, respectively.

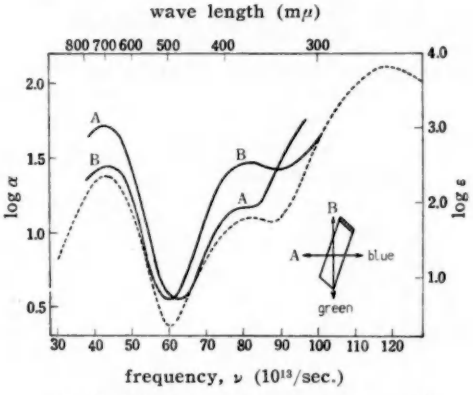

Fig. 2. Absorption spectra of $Cu(n\text{-}C_4H_9COO)_2\cdot H_2O$ in the crystalline state (——) and in ethanol (------).

Cupric valerianate monohydrate is found to show polarized absorption spectra, which are essentially similar to the acetate monohydrate[1], as shown in Fig. 2. Thus the appearance of the band at 80×10^{13}/sec. and the polarization of the band unanimously show, on the basis of the criteria mentioned in the earlier part of this discussion, that the valerianate monohydrate also consists of dimeric molecules.

Cupric *n*-butyrate and *n*-valerianate exist in either a monohydrated or an anhydrous form. Polarized absorption spectra of the anhydrous *n*-butyrate have also been determined in the present work (Fig. 3). It is seen that the anhydrous butyrate exhibits absorption bands at about 43 and 80×10^{13}/sec., the polarization for the latter band being the reverse of the polarization for the former. This relationship bears a close resemblance to that with cupric butyrate, indicating that the anhydrous butyrate contains the dimeric molecule which is fundamentally similar to that of the monohydrate. It may, therefore, be

15) J. Iball, *Nature*, **159**, 95 (1947).

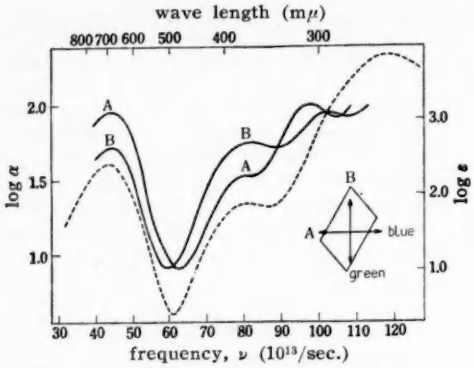

Fig. 3. Absorption spectra of $Cu(n\text{-}C_3H_7COO)_2$ in the crystalline state (——) and in ethanol (------).

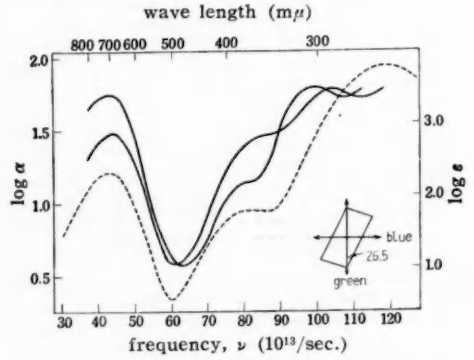

Fig. 4. Absorption spectra of $Cu(n\text{-}C_5H_{11}COO)_2$ in the crystalline state (——) and in ethanol (------).
(The angle 26.5 stands for 26.5°)

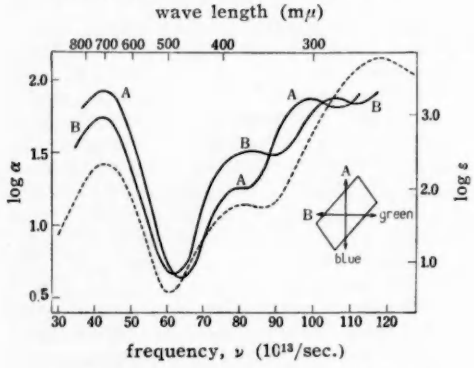

Fig. 5. Absorption spectra of $Cu(n\text{-}C_7H_{15}COO)_2$ in the crystalline state (——) and in ethanol (------).

concluded that both the monohydrated and the anhydrous form of cupric butyrate have the dimeric molecules with the possible interaction between the two copper atoms. Anhydrous cupric valerianate exhibits a similar color to that of the anhydrous butyrate. Although the dichroism has not been measured with the anhydrous valerianate, it may be certain that the anhydrous valerianate also shows polarized absorption spectra with the same characteristics as are observed with the butyrate, having the dimeric molecules of the same type. Note should be taken of the fact that the same relationships were obtained in the case of cupric propionate. It may be suggested that the linkage of the water molecule to the copper atom within the hydrated dimer is not strong.

Cupric capronate and caprylate exist only in an anhydrous form. Polarized absorption spectra of the two compounds have been determined in the crystalline state (Figs. 4 and 5). The crystal structure analysis has not been reported with either of them. It may be admitted, however, that the polarization property as well as the positions of the band maxima are the same as those of the compounds described above. It is most reasonable to assume that both the anhydrous compounds have the dimeric molecule with a general formula, $Cu_2(R\cdot COO)_4$.

In the above part, we have discussed about the cupric salts with normal carboxylic acids. Examination of the steric condition shows that the corresponding *iso*-alkanoates may be able to form the binuclear molecule, since the steric hindrance due to the branching alkyl-radical in the *iso*-series is not so great as to prohibit the formation of the binuclear molecules. Therefore, some of cupric

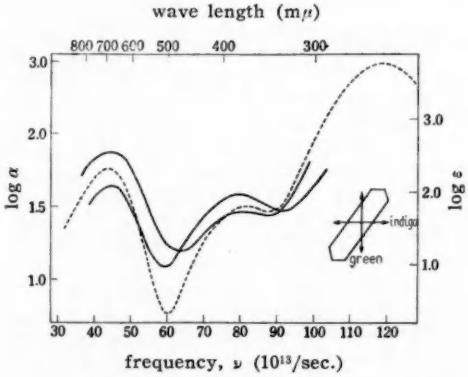

Fig. 6. Absorption spectra of $Cu(iso\text{-}C_3H_7COO)_2$ in the crystalline state (——) and in ethanol (------).

compounds with *iso*-carboxylic acids have been examined by the same method as that applied to the normal alkanoates. The polarized absorption spectra of anhydrous cupric *iso*-butyrate (Fig. 6) are found to be quite similar to those of cupric acetate monohydrate, showing the absorption band at about 80×10^{13}/sec. whose polarization is the reverse of that for the band at about 43×10^{13}/sec.

The same result has been obtained with cupric *iso*-valerianate (Fig. 7). These facts may readily be interpreted as showing, on the basis of the criteria as described above, that both cupric *iso*-butyrate

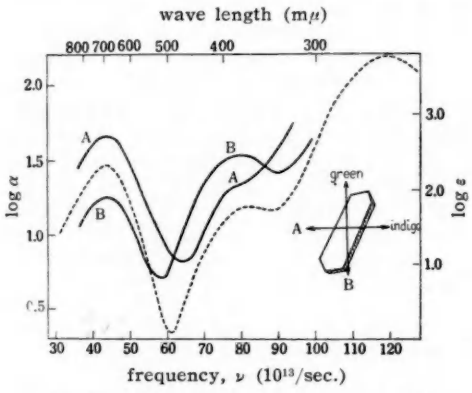

Fig. 7. Absorption spectra of $Cu(iso\text{-}C_4H_9COO)_2$ in the crystalline state (——) and in ethanol (------).

and *iso*-valerianate have the dimeric molecules with a formula of $Cu_2(iso\text{-}R\cdot COO)_4$. It may safely be assumed that the cupric *iso*-alkanoates in general consist of the binuclear molecules similar to the corresponding normal alkanoates.

Absorption Spectra of the Cupric Alkanoates in Solution.—Some of the cupric compounds examined in the present and preceding papers are soluble in water to dissociate into component ions to a great extent. Thus the absorption spectra of the alkanoates in water show the main characteristics of the aquated cupric ion, indicating a considerably great degree of dissociation of the compounds. Absorption spectra, therefore, were measured in organic solvents. When ethanol is used as solvent, it is supposed to form some amount of the ethyl alkanoate with a part of the free ligand which is added in excess. In all the present measurements, however, it was confirmed that Beer's law was obeyed on addition of the free ligand throughout the whole concentration range examined. Without the addition of the free ligand, the cupric alkanoate in solution was found to show deviation from Beer's law in the shorter wave-length region when the solution was much diluted.

It is seen from the measurements (Fig. 8) that all the above compounds in solution show absorption spectra which are closely similar to one another in both the wave-length and the molar extinction coefficients at their absorption maxima. Thus they show absorption bands with maxima at about 43 and 82×10^{13}/sec., and a much more intense absorption band in the shorter wave-length region. It seems to be of significance that the compounds

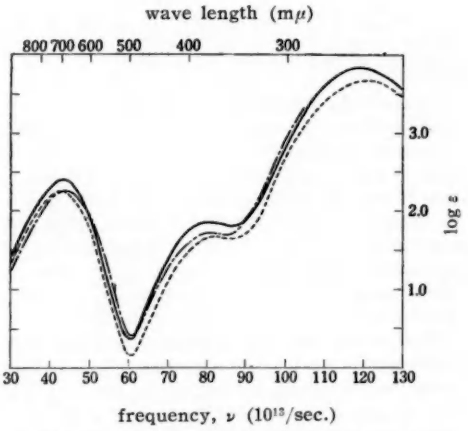

Fig. 8. Absorption spectra of cupric alkanoates: acetate (------) and butyrate (——) in ethyl alcohol, and palmitate (—·—·—) in acetic anhydride.

show an absorption band at 82×10^{13}/sec. even in solution. These facts indicate that the cupric alkanoates all have, in organic solvents, molecules of a similar type which may most probably be the binuclear molecule represented by a formula of $Cu_2(R\cdot COO)_4$. This molecule in solution may be solvated; then, this is represented by a molecular formula of $Cu_2(R\cdot COO)_4\cdot 2A$, A being a molecule of the solvent.

Absorption spectra of cupric *n*-palmitate (C 16) and *n*-stearate (C 18) were determined in acetic anhydride, since their solubility in other solvents is not sufficiently high. The absorption curves (Fig. 8 and Table I) are quite similar to those of the other alkanoates in ethanol. It is reasonable to conclude that cupric

TABLE I

VISIBLE AND ULTRAVIOLET ABSORPTION SPECTRA OF CUPRIC MONOCARBOXYLATES WITH AN EMPIRICAL FORMULA OF $Cu(RCOO)_2$*

R	band I		band II		band III	
	ν (10^{13}/sec.)	log ε	ν (10^{13}/sec.)	log ε	ν (10^{13}/sec.)	log ε
CH_3	42.8	2.25	82.0	1.65	120.1	3.68
C_2H_5	43.0	2.27	82.0	1.75	118.9	3.71
n-C_3H_7	43.1	2.42	81.4	1.87	118.4	3.90
iso-C_3H_7	43.4	2.22	81.6	1.71	117.6	3.67
n-C_4H_9	43.1	2.37	82.4	1.82	118.2	3.85
iso-C_4H_9	43.2	2.32	81.7	1.76	118.0	3.75
n-C_5H_{11}	43.0	2.33	81.1	1.80	118.1	3.80
n-C_7H_{15}	43.0	2.33	81.1	1.78	117.7	3.80
n-$C_{15}H_{31}$**	44.2	2.27	82.0	1.71		
n-$C_{17}H_{35}$**	44.2	2.26	82.4	1.72		

* Unless otherwise indicated, the used solvent is ethanol.

** Data in acetic anhydride.

n-palmitate and *n*-stearate in acetic anhydride consist of the dimeric molecules similar to the above described.

Infrared Absorption Spectra.—It is known that the carboxylate ion in general exhibits anti-symmetrical vibrations in the region between 1550 and 1700 cm^{-1}. Anti-symmetrical vibrations due primarily to the carboxylate-group have been examined with the cupric carboxylates in pressed potassium bromide discs and in Nujol mulls. Sodium acetate, which contains carboxylate ions in an ionized form, shows a broad and strong band around 1560 cm^{-1}, and cupric formate, which involves carboxylate-groups coordinated to copper ions in such a way that the dimeric molecule of the cupric salt is not formed, shows a broad and strong band over the region between 1560 and 1600 cm^{-1}. On the other hand, cupric acetate, propionate, butyrate, valerianate, caprylate, capronate, palmitate and stearate show the absorption at about 1595 to 1600 cm^{-1}, which is rather sharp and well-defined. The infrared spectra indicate that the state of the carboxylate ion in the latter group of the cupric compounds differs from that in cupric formate or sodium acetate, being in agreement with the afore-mentioned conclusion that the cupric compounds examined in the present study may involve the binuclear molecules similar to those of cupric acetate or anhydrous cupric propionate. Although such an evidence alone is not to be regarded as decisive, this, combined with other materials, may be confirmatory enough for us to reach the above conclusion of the binuclear structure.

General Discussion

Visible and Ultraviolet Absorption Spectra of the Compounds.—It is seen from the measurements that the cupric alkanoates show in the visible and the ultra violet region absorption bands at about 43 (band I) and 80×10^{13}/sec. (band II) besides a strong absorption band in the region of the shorter wave length. It is most probable that the band I may correspond to the band in the long wavelength region of cupric complexes of an ordinary type, which is usually ascribed to the copper ion under perturbation of the surrounding ligands. On the other hand, the band II is assumed to be closely related with the copper-to-copper interaction. This is borne out by the solvent effect upon these absorption bands. Thus when a solvent is alternated with a more polar one, the band I undergoes red-shift, while the band II shows blue shift. The solvent effect upon the former band agrees with that upon the band at the longer wave length of the cupric ethylenediamine and acetylacetonate complexes, showing that the two bands may be originated from similar electronic transitions. On the contrary, the band II differs in the origin from the absorption bands of the above type. The detailed discussion on the solvent effect will be reported elsewhere.

Although the crystal structure analyses have not been reported with most of the compounds in the present paper, we may make the following generalization about the dichroism of the above compounds.

The band I is polarized along the $Cu(O)_4$-plane, while the band II is polarized along the z-axis of the dimeric molecule, along

which the copper-to-copper interaction is expected to exist.

The relation for the band I is found to be the same as the dichroism for the absorption band at the longer wave length of cupric complexes, being in agreement with the assumption that these two bands correspond to each other.

Reviewing the absorption curves of the cupric alkanoates in organic solvents, we can obtain the following relationships which are valid for the cupric salts consisting of the dimeric molecules.

The compounds show absorption curves which are similar to one another. The wave length and the molar extinction coefficients at the corresponding band maxima are almost equal among the compounds. Moreover, the intensity ratio of the band I to the band II is equally three and a half for all the compounds examined in the present paper. This close similarity seems to be in agreement with the above conclusion that the compounds all have a similar structure, which involves the dimeric molecules.

The intensity of the band I is seen to be nearly ten times as great as that of the corresponding band exhibited by cupric complexes of an ordinary type with all the coordination positions occupied by oxygen atoms. This fact, which indicates a definite difference in the linkage between the present compounds and the compounds of an ordinary type, may be explained on the basis of the copper-to-copper linkage in the dimeric molecules of the cupric alkanoates.

Examination of the data (Table I) reveals that the intensity of the corresponding bands changes in the following order:

acet.<prop.<butyr.<valerian.
>capron.>capryl. (*n*-homologues).

Thus the intensity of the band increases as we go from the acetate to the valerianate, and then decreases as we go further down the series. Clear explanation for this tendency is not available at present.

Structure of the Cupric Alkanoates.— As described in the preceding part of the present paper, *cupric n- and iso-butyrate, n- and iso-valerianate, n-capronate, n-caprylate, n-palmitate and n-stearate, both in organic solvents and in the crystalline state, are considered to have the dimeric molecules with a kind of weak linkage between the two copper atoms.* Thus it is seen that the length or the shape of the alkyl-group causes no great effect upon the linkage of the carboxylate-group with the copper atom. It may be assumed further that cupric salts with higher homologues of *n*- or *iso*-carboxylic acids also contain the dimeric molecules, since increasing the length of the methylene chain or putting an alkyl-branch in the chain would give rise to no great change, sterically or electronically. This assumption is borne out by a recent study on the structure of cupric behenate (C 22) through magnetic measurements[7].

It is worth noting that cupric formate does not involve a dimeric molecule whereas the other cupric alkanoates consist of the dimeric molecules. This conspicuous difference may tentatively be explained from the standpoint of the electronic theory, when we take into account the effect caused upon the linkages around the copper atoms by increasing the number of the carbon atoms. As a radical neighboring the carboxylate-group is replaced by another, the electronic charge on the carbon atom in the carboxylate-group would change to a greater or lesser extent. Since the electronic theory of organic chemistry gives the following order with respect to the electron-attracting capacity: $H > CH_3 > C_2H_5 > C_3H_7 > \cdots\cdots$, the electronic charge on the carbon atom of the carboxylate-group may increase as we go from hydrogen down the series. The more the electronic density on the carbon atom of the carboxylate-group, the more negatively the oxygen atom would be charged, with the result that the electronic cloud on the copper atom would be withdrawn less strongly toward the oxygen atom. If we assume that the increase of the electronic density on the copper atom means increase of the electronic charge available for the additional linkage between the two copper atoms, the copper-to-copper linkage might become stronger as the electronic charge on the copper increases on going from the formate down the series of the homologous alkanoates. The above concept seems to be supported qualitatively by the decrease of acid strength on going from formic acid down the series of the homologous fatty acids.

Our measurements in the present and preceding papers show that a great difference in absorption maxima was not observed among the cupric alkanoates except cupric formate which involves

components of an exceptional sort. This may be interpreted as indicating that the electron-attracting capacity of the alkyl-groups changes only very slightly from one alkyl-group to another. In contrast to the other cupric alkanoates, cupric formate was not found to have a dimeric molecule. The electronic charge of the copper atom in cupric formate is assumed to be withdrawn toward the oxygen atom to such an extent that the linkage could not be formed between the two copper atoms. Thus the striking difference in the structure between cupric formate and acetate may be understandable on the assumption that the line of demarcation with respect to the electronic charge on the oxygen atom could be drawn somewhere between the formate and the acetate.

As was mentioned in the preceding part, cupric *n*-capronate and higher *n*-alkanoates exist only in an anhydrous form, whereas the lower *n*-alkanoates of copper, such as the acetate, propionate, *n*-butyrate and *n*-valerianate, have the dimeric molecules with water molecules bonded to the copper atom[16]. Thus crystals of anhydrous cupric capronate are precipitated on addition of water to an ethanolic solution of the compound. This critical difference between cupric valerianate and capronate may also be understood on the above described assumption. According to the above mentioned concept, we may assume that the positive charge on the copper atom, which seems to be necessary for the combination of a water molecule with the copper atom, should be greater than a threshold value in order that the copper atom may bind a water molecule. Since the positive charge on the copper atom decreases slightly as we go from the formate down the series, the linkage of the water to the copper atom may become weaker in that order. Thus there is good reason for us to suppose that the line of demarcation may be drawn between the valerianate and the capronate, beyond which the copper atom in the dimeric cupric alkanoates may not be able to bind the water molecule with ease. The inductive effect of the alkyl-group, on the basis of which the above discussion has been made, may not be the only factor. However, the explanation, as given above, seems to be qualitatively correct.

The effect of the water molecule upon the copper in the hydrated dimer of the cupric alkanoates is found to be comparatively small, since no great difference between them was observed in the absorption spectra. It is most probable that the linkage of the water to the copper atom is highly ionic.

A definite difference, however, was reported in the exchange interaction, which was estimated from magnetic measurements[17]. Thus the exchange energy between the two copper atoms was found to be greater in cupric stearate than in cupric acetate monohydrate. In this case, two effects may be regarded as responsible for the observed difference. One is the effect of replacing acetate by stearate groups, and the other is the effect of the water molecules. The two effects would compensate each other to a certain extent, but the above result may be assumed to show that the former overshadows the latter in this case.

Nature of the Copper-to-copper Linkage.—It is shown in the preceding part of the present paper that cupric acetate and higher alkanoates may have the dimeric molecules with a sort of linkage between the two copper atoms in a molecule. Although the nature of the copper-to-copper linkage is not completely clarified, the following two models for the extraordinary linkage may be regarded as most probable. One involves the d_z-d_z bonding. We assume in this model an extreme structure, in which the two copper atoms form octahedral d_2sp_3 hybridization orbitals. Two orbitals of them, each from one of the two copper atoms, over lap each other in the region above or below the complex-plane. It is interesting to note that the two copper atoms in this model have an electronic structure of a rare-gas type, the possible stability of which may be of some importance in this model.

In the second model, the overlap is assumed to take place between the two $3d_{x^2-y^2}$ orbitals, each from either of the two copper atoms in the molecule, since the copper atoms have non-bonding $3d_{x^2-y^2}$ orbitals which spread in the space above and below the complex-plane. This model was proposed by Martin et al.[7], who

16) We are here concerned with normal alkanoates only; cupric *iso*-butyrate and *iso*-valerianate are usually obtained as anhydrous compounds.

17) K. Kido and T. Watanabe, Presented at the Symposium on Co-ordination Compounds, Nagoya, November, 1957.

considered, mostly on grounds of energy, this type of interaction as more probable than the $d_\pi - d_\pi$ interaction. The present authors, however, are inclined to consider that the decision between the two models could not be made for the present.

Summary

In order to examine the structure of cupric alkanoates, the dichroism in the visible and the ultra violet region has been determined by the microscopic method with normal butyrate, valerianate, capronate and caprylate of copper(II). Visible and ultra-violet absorption spectra in organic solvents and infrared absorption spectra in Nujol mulls have been determined with the above compounds, along with cupric palmitate and stearate. *Iso*-alkanoates have also been examined in a similar way.

All these compounds in the crystalline state and in organic solvents are found to show similar absorption spectra having the dichroism with characteristics fundamentally similar to those of cupric acetate and propionate which had earlier been reported. From these results, it has been concluded that all the above compounds consist of the dimeric molecules.

The anhydrous forms of the compounds have been shown to consist of the dimeric molecules resembling those of the hydrated form.

All the above compounds show absorption bands at about 43 and 80×10^{13}/sec. The former is polarized along the $Cu(O)_4$-plane and the latter along the direction binding the two copper atoms in a molecule.

The present authors wish to thank the Ministry of Education for a grant.

Department of Chemistry, Faculty of Science, Osaka University, Kita-ku, Osaka

---

Studies on the Cobalt(III) Complexes Containing Only One Chelate Ring. II.[1] *Syntheses and Properties of Monoethylenediamine-tetrammine-cobalt(III) Complexes, [Co en $(NH_3)_4$]X_3*[2]

By Yoichi SHIMURA

(Received December 7, 1957)

No monoethylenediamine-tetrammine cobalt(III) complexes were hitherto known, while all the other members of ammine-ethylenediamine series of cobalt(III) complexes have thoroughly been studied. In the present paper, the syntheses of these missing luteo salts, [Co en $(NH_3)_4$]X_3, will be reported. And the absorption spectra of the cobalt(III) complexes which belong to the ammine-ethylenediamine series will be discussed.

Results and Discussion

Method of Syntheses.—For the syntheses of the monoethylenediamine-tetrammine complexes, after several preliminary attempts, the following scheme was adopted.

$$[\text{Co en } (NH_3)_2\ Cl_2^{(1)}_{(6)}]Cl \xrightarrow{\text{(i) KNCS}} [\text{Co en } (NH_3)_2\ (NCS)_2]^+ \xrightarrow{\text{(ii) } H_2O_2} [\text{Co en } (NH_3)_2\ (NH_3)_2]^{3+} \xrightarrow{\text{(iii) } H_2SO_4} [\text{Co en } (NH_3)_4]_2\ (SO_4)_3$$

The starting material, [Co en $(NH_3)_2$ $Cl_2^{(1)}_{(6)}$]Cl, was prepared from NH_4[Co en $(NH_3)_2(SO_3)_2]\cdot H_2O$ by Bailar and Pappard's method[3]. The possible three geometrical isomers of [Co en $(NH_3)_2$ $(NCS)_2]^+$ may result from the reaction i. The separation of these isomers, however, was not

1) Part I of this series: Y. Shimura, This Bulletin, **31**, 173 (1958).

2) Partly presented at the Symposium on Co-ordination Compounds, Tokyo, October 28, 1956.

3) J. C. Bailar, Jr. and D. F. Peppard, *J. Am. Chem. Soc.*, **62**, 105 (1940).

intended, because it was expected that all these isomers equally produce the desired complex by the reaction ii.

The reaction ii was carried out by a modification of the Werner's method[4], who prepared *trans*- and *cis*-$[Co\ en_2\ (NH_3)_2]X_3$ from the corresponding isothiocyanato-complexes by hydrolytic oxidation with chlorine or with hydrogen peroxide. These reactions leave the nitrogen atoms co-ordinated to the cobalt atom; the co-ordinated isothiocyanato-groups are transformed into co-ordinated ammonia molecules.

The crystals of the sulfate or the bromide of $[Co\ en\ (NH_3)_4]^{3+}$ are orange-colored and indistinguishable by the color from the other members of the ammine-ethylenediamine series. The monoethylenediamine-tetrammine complexes have rather high solubilities in water as compared with hexammine or trisethylenediamine complexes. For this reason, the purification of the chloride, $[Co\ en\ (NH_3)_4]Cl_3 \cdot xH_2O$, was not practical.

Unsuccessful Attempt on Optical Resolution.—Recently several X-ray[5,6] and infrared[7] studies have shown that the co-ordinated ethylenediamine molecule is not planar but takes so-called *gauche* form. This *gauche* configuration has a mirror image antipode. Therefore, it is very interesting to test the possibilities for the optical resolution of $[Co\ en\ (NH_3)_4]X_3$.

Firstly, the chemical resolution by *d*-tartrate was tried. By the double decomposition of $[Co\ en\ (NH_3)_4]Br_3 \cdot H_2O$ and silver *d*-tartrate(tart), an oily product was obtained, the composition of which is perhaps $[Co\ en\ (NH_3)_4]Br \cdot (d\text{-tart}) \cdot xH_2O$. The oily product was dissolved in water and fractionally treated with ethanol. But no evidences for the separation of diastereoisomers were obtained. Secondly, the method of asymmetric adsorption on optically-active quartz[8,9] was applied. But the result was also negative. These negative results, however, are not improbable, since the puckered five-membered ethylenediamine-cobalt ring may be easily inverted into its antipode.

The last method tested, though it was also unsuccessful, is an equilibrium method with the aid of rotatory dispersion measurements. Very recently, Kirschner[10] succeeded to demonstrate that $K_2[Cu\ (edta)]$ is optically active by showing that the mixed aqueous solution of *l*-quinone hydrobromide and the copper complex exhibits an anomalous rotatory dispersion in the vicinity of the absorption band of the complex. This fact indicated that there was a shift in the equilibrium, D-$[Cu(edta)]^{=} \rightleftarrows$ L-$[Cu(edta)]^{=}$, under the asymmetric influence of *l*-quinone hydrobromide.

Following the above method, the rotatory dispersion of the mixed aqueous solution of $[Co\ en\ (NH_3)_4]_2\ (SO_4)_3 \cdot 4H_2O$ and Rochelle salt was measured. In the region of 600~300 mμ, scarcely any anomalous rotatory dispersion was observed (Table I.).

TABLE I

OPTICAL ROTATION OF MIXED SOLUTION OF ROCHELLE SALT AND $[Co\ en(NH_3)_4]_2(SO_4)_3 \cdot 4H_2O$

λ(mμ)	ν(10¹³/sec.)	α_1	α_2	$\alpha_2-\alpha_1$
577	52.0	0.643°	0.640°	−0.003°
546	54.9	0.723	0.715	−0.008
492	61.0	0.890	0.878	−0.012
436	68.8	1.148	1.142	−0.006
405	74.1	1.328	1.323	−0.005
365	82.2	1.607	1.598	−0.009
312.6	96.0	1.972	1.967	−0.005

α_1: Optical rotation of 0.1 F aq. soln. of $NaKC_4H_4O_6 \cdot 4H_2O$ (1 dm, 28°C).

α_2: Optical rotation of mixed aq. soln. of 0.1F $NaKC_4H_4O_6 \cdot 4H_2O$ and 0.001 F $[Co\ en\ (NH_3)_4]\ (SO_4)_{1\frac{1}{2}} \cdot 2H_2O$ (1 dm, 28°C).

This result may be considered to indicate that little of the asymmetric shift of the equilibrium, D-$[Co\ en\ (NH_3)_4]^{3+} \rightleftarrows$ L-$[Co\ en\ (NH_3)_4]^{3+}$ occurred, or that the anomalous rotatory dispersion of this complex ion is very small. An alternative explanation is to postulate that the first and the second absorption band of this complex are optically inactive.

Absorption Spectra.—The absorption curves of the cobalt(III) complexes which belong to the ammine-ethylenediamine series are shown in Fig. 1. The numerical data of the first and the second absorption band are tabulated in Table II.

4) A. Werner, *Ann.*, **386**, 1 (1912); A. Werner, F. Bräunlich, E. Rogowina and C. Kreutzer, ibid., **351**, 65 (1907).

5) A. Nakahara, Y. Saito and H. Kuroya, This Bulletin, **25**, 331 (1952); K. Nakatsu, Y. Saito and H. Kuroya, ibid., **29**, 428 (1956) etc.

6) H. Kuroya, Y. Saito, A. Nakahara, Y. Komiyama and K. Nakatsu, *J. Inst. Polytech. Osaka City Univ.*, **5**, C, 1 (1956).

7) J. V. Quagliano and S. Mizushima, *J. Am. Chem. Soc.*, **75**, 6084 (1953); S. Mizushima, I. Ichishima, I. Nakagawa and J. V. Quagliano, *J. Phys. Chem.*, **59**, 293, (1955) etc.

8) R. Tsuchida, M. Kobayashi and A. Nakamura, *J. Chem. Soc. Japan, (Nippon Kagaku Zassi)*, **56**, 1339 (1935).

9) H. Kuroya, S. Aimi and R. Tsuchida, ibid. **64**, 995 (1943).

10) S. Kirschner, *J. Am. Chem. Soc.*, **78**, 2372 (1956).

TABLE II

ABSORPTION DATA OF [Co (en)x $(NH_3)_{6x-2x}]^{3+}$ SERIES

Complex Ion	First Absorption Band				Second Absorption Band				$\Delta(\nu_{max})$***	$\Delta(\log \varepsilon_{max})$****
	ν_{max} (10^{13}/sec.)	$\log \varepsilon_{max}$	l* (10^{13}/sec.)	δ** (10^{13}/sec.)	ν_{max} (10^{13}/sec.)	$\log \varepsilon_{max}$	l* (10^{13}/sec.)	δ** (10^{13}/sec.)		
$[Co(NH_3)_6]^{3+}$	62.9	1.68	10.3	0.45	88.3	1.60	12.5	0.35	25.4	−0.08
$[Co\ en(NH_3)_4]^{3+}$	63.6	1.83	10.7	0.55	88.4	1.76	13.1	0.55	24.8	−0.07
trans-$[Co\ en_2(NH_3)_2]^{3+}$	64.2	1.77	10.8	0.8	89.2	1.73	12.3	0.55	25.0	−0.04
cis-$[Co\ en_2(NH_3)_2]^{3+}$	64.4	1.79	10.7	0.65	89.4	1.74	12.6	0.5	25.0	−0.05
$[Co\ en_3]^{3+}$	63.9	1.94	10.4	0.55	88.4	1.90	12.0	0.4	24.5	−0.04

* l=half-value width. This corresponds to $\{\delta(+)+\delta(-)\}$ in Jørgensen's notation[13].

** δ=inclination parameter[14] or Inklination (in German)[15]. This parameter corresponds to $\frac{1}{2}\{\delta(+)-\delta(-)\}$ in Jørgensen's notation[13], and is defined by the equation $\delta=\frac{1}{2}\{\nu_k+\nu_l\}-\nu_{max}$, where ν_k and ν_l are the two frequencies where the formal extinction coefficients are equal to the half of ε_{max}.

*** Frequency difference between the maxima of the second and the first absorption band.

**** Difference between $\log \varepsilon_{max}$'s of the second and the first band.

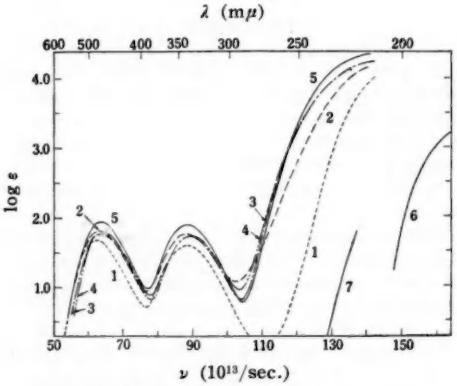

Fig. 1. Absorption curves of:
1, $[Co(NH_3)_6](ClO_4)_3$;
2, $[Co\ en(NH_3)_4](SO_4)_{1\frac{1}{2}}\cdot 2H_2O$;
3, *trans*-$[Co\ en_2(NH_3)_2](ClO_4)_3\cdot H_2O$;
4, *cis*-$[Co\ en_2(NH_3)_2](ClO_4)_3\cdot H_2O$;
5, $[Co\ en_3](ClO_4)_3$;
6, NH_3[11];
7, en[12].

From these data, the following conclusions are drawn.

i) Ethylenediamine has a higher position in the spectrochemical series [16,17] than that of ammonia.

ii) The successive substitution of ammonia molecules by ethylenediamine causes somewhat irregular shifts of band maxima. The change of the intensity by such a substitution is also irregular. Thus, for example, the first band of $[Co\ en(NH_3)_4]^{3+}$ is higher than that of *cis*- and *trans*-$[Co\ en_2(NH_3)_2]^{3+}$.

iii) The first or the second band of *cis*-$[Co\ en_2(NH_3)_2]^{3+}$ are at shorter wave lengths than those of the corresponding *trans* isomer. This fact coincides very well with the general rule which was reported previously by the present author[18].

iv) Generally speaking, the half-value width and the inclination parameter[14] are in the order of

$$trans\text{-}(NH_3)_2 > (NH_3)_4 > cis\text{-}(NH_3)_2 > en_3 > (NH_3)_6.$$

The larger half-value width and the larger inclination parameter of the first three members in the above series are possibly explained by the slight splitting of the bands owing to the lower symmetry of those ions.

v) For all the complexes studied, the intensity of the second band is lower than that of the first band.

vi) The mean value of the frequency difference between the maxima of the second and the first band, is 24.94×10^{13}/sec.

vii) The intense ultraviolet bands are perhaps due to the co-ordinated ammonia and ethylenediamine molecules. Roughly speaking, an additive nature can be seen in the intensities of these bands. But the quantitative curve analysis was abandoned since only a part of the long wave length side of the band is available.

11) H. Ley and B. Arends, *Z. physik. Chem.*, **B 17**, 177 (1932).
12) M. Linhard, *Z. Elektrochem.*, **50**, 224 (1944).
13) C. K. Jørgensen, *Acta. Chem. Scand.*, **8**, 1495 (1954).
14) Y. Shimura and R. Tsuchida, This Bulletin, **28**, 572 (1955).
15) H. Siebert and M. Linhard, *Z. physik. Chem.* N. F., **11**, 318 (1957).
16) R. Tsuchida, This Bulletin, **13**, 388, 436 (1938).
17) Y. Shimura and R. Tsuchida, This Bulletin, **29**, 311 (1956).
18) Y. Shimura, This Bulletin, **25**, 49 (1952).

Experimental

Ethylenediamine - tetrammine - cobalt(III) Sulfate Tetrahydrate, [Co en $(NH_3)_4]_2$ $(SO_4)_3 \cdot 4H_2O$—Ten grams of *trans*-[Co en $(NH_3)_2$ $Cl_2]Cl \cdot \frac{1}{2}H_2O$[8] is dissolved in 100 ml. of warm water and to this solution 10 g. of potassium thiocyanate in 20 ml. of water is added. The resulting green mixture is heated for 20 min. at 75~80°C on a water bath and for more 3 min. at 85°C. The dark red mixture is allowed to cool and acidified by a few drops of dilute sulfuric acid. Fifty milliliters of 30% hydrogen peroxide is next added drop by drop to the mixture. After being allowed to stand for several hours, the resulting dark orange solution is concentrated to about 75 ml. by evaporation, and cooled. Twenty five milliliters of dilute sulfuric acid and 150 ml. of ethanol is added to the solution. The crude complex separates in voluminous precipitates. The product is treated with a small amount of water and any less soluble materials are filtered off. Ethanol-water mixture is then added to the filtrate. The desired complex precipitates as orange-colored plates. The crystals were washed by ethanol and dried in air. For purification, the salt was recrystallized from ethanol-water mixture. The yield was 7 to 8 g. (about 50~60%). The crystals effloresced on exposure to the air. The crystals freshly dried were analyzed for water of crystallization. The analyses for the other components were performed by making use of the salts dehydrated at 100~110°C.

Anal. Found: H_2O, 9.93%. Calcd. for $[Co(C_2H_8N_2)(NH_3)_4]_2(SO_4)_3 \cdot 4H_2O$: H_2O 9.84%.

Found: Co, 17.7; C, 7.29; H, 6.16; SO_4^{--}, 43.83%. Calcd. for $[Co(C_2H_8N_2)(NH_3)_4]_2(SO_4)_3$: Co, 17.79; C, 7.25; H, 6.09; SO_4^{--}, 43.50%.

Ethylenediamine - tetrammine - cobalt(III) Bromide Monohydrate, [Co en $(NH_3)_4]Br_3 \cdot H_2O$—A solution of the above sulfate is treated with a solution of the equivalent amount of barium chloride and the resulting barium sulfate is filtered off. The filtrate is concentrated by evaporation. To this solution solid ammonium bromide is added. The desired bromide monohydrate separates as orange prismatic crystals. They are recrystallized from water containing a small amount of ethanol, washed with ethanol and dried in air.

Anal. Found: Br, 53.38; H_2O, 3.64%. Calcd. for $[Co(C_2H_8N_2)(NH_3)_4]Br \cdot H_2O$: Br, 53.88; H_2O, 4.05%.

The corresponding chloride, [Co en $(NH_3)_4]Cl_3 \cdot xH_2O$ was also prepared, but its purification was impractical because it is very soluble in water or in water-ethanol mixtures.

Absorption and Rotation Measurements.—The absorption measurements were made in aqueous solutions by a Beckman DU Spectrophotometer at room temperature. The concentration of the solutions varied from 1.0×10^{-2} to 1.0×10^{-4} gram complex-ion per liter. The measurements of optical rotation were made by a Rudolph photoelectric spectropolarimeter, Model 200S-80.

Summary

A new cobalt(III) luteo ion, [Co en $(NH_3)_4]^{3+}$, has been prepared by the hydrolytic oxidation of [Co en $(NH_3)_2$ $(NCS)_2]^+$. The sulfate and the bromide of the new complex ion have been isolated. Several attempts to resolve the ion were unsuccessful.

The visible and the ultraviolet absorption spectra of all the members of the cobalt(III) ammine-ethylenediamine series have been measured and discussed.

The author wishes to thank Professor R. Tsuchida for his kind guidance throughout this work.

Department of Chemistry, Faculty of Science, Osaka University, Kita-ku, Osaka

Studies on the Cobalt(III) Complexes Containing Only One Chelate Ring. III[1]. *Rotatory Dispersion of Tetrammine-l-leucinato-cobalt(III) Perchlorate,* $[Co(NH_3)_4(l\text{-}leuc)](ClO_4)_2$[2]

By Yoichi SHIMURA

(Received December 10, 1957)

It is well known that optically active complexes of cobalt(III) or chromium(III) exhibit very marked anomalous rotatory dispersion in the vicinity of their first absorption bands. In some cases, the curve of the anomalous rotatory dispersion is typical and has a point-symmetrical shape. In the present paper, such a point-symmetrical dispersion will be named as "inversive dispersion". In other cases, the rotatory dispersion is intricate and "anomalous" in the literal sense of the word. This "anomalous" rotatory dispersion, however, may be analyzed into two or more typical inversive dispersions as will be shown below.

The above results have been obtained mainly from the studies on the complexes of the $[M(AA)_3]$-[3] or $[M(AA)_2BC]$-type[4], in which the asymmetry is around the central metallic ion. As to the complexes, in which the asymmetric center is at the atom in the co-ordinated ligand, the studies of Lifschitz[5] and Pfeiffer et al.[6] have been reported. These authors stated that no anomalous rotatory dispersion occurred in the complexes having the asymmetric center far apart from the central metallic ion and that the anomalous rotatory dispersion might be produced by the so-called "vicinal effect" provided that the asymmetric center and the central metallic ion were so close to interact each other. The experimental evidences for the above claim, however, have scarcely ever been obtained.

In the present paper the rotatory dispersion of $[Co^{III}(NH_3)_4(l\text{-leuc})]^{2+}$* will be studied in the vicinity of its first and second absorption band. In this uni-chelate complex the asymmetric center is only on a carbon atom of the ligand leucinate ion. As a result of the measurements and the analyses of the rotatory dispersion curves, the existence of the "vicinal effect" between the central cobalt atom and the asymmetric carbon atom will be clarified.

Experimental

Tetrammine-*l*-leucinato-cobalt(III) Perchlorate, $[Co(NH_3)_4(l\text{-leuc})](ClO_4)_2$—This new compound was prepared by a modification of the method which was described in the part I of the present series for the syntheeses of the corresponding glycinato or alaninato complexes[7]. One gram of anhydrous sodium carbonate and 3.5 g. of *l*-leucine were dissolved in 60 ml. of hot water. To this solution were added 7.4 g. of $[Co(NH_3)_4(OH_2)Cl]SO_4$[8], 2 g. of decolorizing charcoal and 5 ml. of aqueous ammonia (30%). The resulting mixture was evaporated on a water bath almost to dryness. The residue was treated with about 50 ml. of warm water and insoluble materials** were filtered off by suction. After cooling, a large amount of 95% ethanol was fractionally added to the filtrate. First, about 2 g. of $[Co(NH_3)_6]SO_4 \cdot Cl \cdot 3H_2O$, and then the impure sulfate of the desired complex were precipitated. For purification the impure sulfate was converted into the perchlorate as follows. The impure sulfate was dissolved in a small quantity of water and was treated with an equivalent amount of barium chloride solution and the resulting barium sulfate was filtered off. To the filtrate, sodium perchlorate and ethanol were added and the solution was evaporated in vacuo over sulfuric acid. The desired perchlorate was separated as light red crystals. This was recrystallized from water-ethanol mixture by evaporation over sulfuric acid. The yield was very small (not exceed one g.).

Anal. Found: C, 15.90; H, 5.35; Cl, 15.40%. Calcd. for $C_6H_{24}O_{10}N_5Cl_2Co$: C, 15.80; H, 5.30; Cl, 15.55%.

1) Part II of This series: Y. Shimura, This Bulletin, **31**, 311 (1958).

2) Presented at the Symposium on Co-ordination Compounds, Nagoya, November 16, 1957.

3) J.-P. Mathieu, *J. chim. phys.*, **33**, 78 (1936).

4) J.-P. Mathieu, *Bull. soc. chim. France*, [5] **3**, 476 (1936).

5) I. Lifschitz, *Z. physik. Chem.*, **105**, 27 (1923); **114**, 485 (1925).

6) P. Pfeiffer, W. Christeleit, T. Hesse, H. Pfitzner and H. Thielert, *J. prakt. Chem.*, **150**, 261 (1938).

* The following abbreviations are used: gly, $NH_2CH_2CO_2^-$; alan, $NH_2CH(CH_3)CO_2^-$; leuc, $NH_2CH(CO_2^-)CH_2CH(CH_3)_2$.

7) Y. Shimura, This Bulletin, **31**, 173 (1958).

8) S. M. Jörgensen, *J. prakt. Chem.*, **42**, 211 (1890).

** This is a mixture of decolorizing charcoal and two geometrical isomers (pink and reddish violet) of $[Co^{III}(l\text{-leuc})_3]$.

TABLE
SUMMARY OF

Complexes	Inversive rotatory dispersion: Center of inversion[a]	Sign of Cotton effect	Degree of rotation[b]
$[Co(NH_3)_4$ (*l*-leuc)$]^{2+}$	Ia: 59.6	+	320°
	Ib: 65.6	−	650°
d-$[Co\ en_2\ (NH_3)Cl]^{2+}$	Ia: 54.6	+	580°
	Ib: 63.4	+	390°
d-$[Co\ en_2$ (*l*-leuc)$]^{2+}$	59.5	+	ca. 5000°
d-$[Co\ en_3]^{3+}$	61.2	+	ca. 4000°

a) These values are given by the unit of 10^{13}/sec.

d-$[Co\ en_2$ (*l*-leuc)$]Cl_2$—This was prepared and resolved by the method of Lifschitz[9] with reference to Mathieu's report[10].

d-$[Co\ en_2\ (NH_3)Cl]Br_2$—This was prepared and resolved by Werner and King's method[11].

d-$[Co\ en_3]Br_3 \cdot 2H_2O$—For the resolution Werner's method[12,13] was followed.

Measurements of Rotatory Dispersion and Absorption Spectra.—The rotatory dispersion measurements were made in aqueous solutions by a Rudolph photoelectric spectropolarimeter, Model 200S—80. The concentration of the solution was 1.0×10^{-3} gram complex-ion per liter. The absorption measurements were made by a Beckman DU spectrophotometer. All the measurements were made at room temperature.

Results and Discussion

The rotatory dispersion curve and the absorption curve of $[Co(NH_3)_4$ (*l*-leuc)$](ClO_4)_2$ are shown in Fig. 1. For comparison, similar measurements were also made for *d*-$[Co\ en_2$ (*l*-leuc)$]Cl_2$, *d*-$[Co\ en_2\ (NH_3)Cl]Br_2$ and *d*-$[Co\ en_3]Br_3 \cdot 2H_2O$ (Figs. 2—4). The numerical data for these measurements are summarized in Table I.

From the Figs. 1—4, it is seen that all the four complexes studied exhibit the remarkable change of rotation in the region of the first absorption bands. On the other hand, there have been found few indications of such anomalous rotatory dispersion in the region of their second absorption bands. This fact coincides with the observations reported heretofore by Mathieu[3], Kuhn and Bein[15], Tsuchida[16] and Kobayashi[17] for many cobalt(III) or chromium(III) complexes.

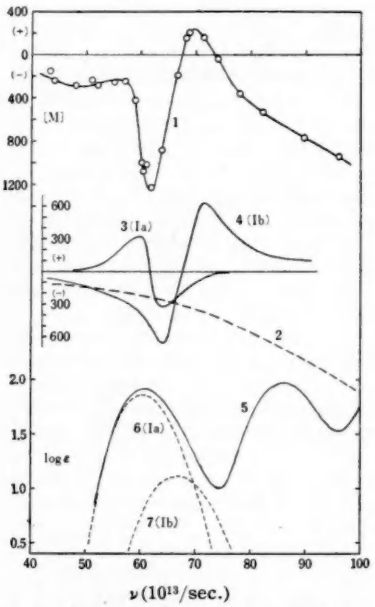

Fig. 1. Rotatory dispersion and absorption of $[Co(NH_3)_4$ (*l*-leuc)$](ClO_4)_2$:
1, rotatory dispersion curve; 2~4, curve analyses of the rotatory dispersion curve; 5, absorption curve; 6~7, curve analyses of the first absorption band.

The shape of the rotatory dispersion curve of $[Co(NH_3)_4$ (*l*-leuc)$]^{2+}$ in its first absorption band suggests that an overlapping of two inversive dispersions occurred. As a result of a tentative curve analysis, it was shown that the experimental dispersion curve (1) was well reproduced by

9) I. Lifschitz, *Rec. trav. chim.*, **58**, 785 (1939).
10) J.-P. Mathieu, *Bull. soc. chim. France*, [5] **6**, 873 (1939).
11) A. Werner and V. L. King, *Ber.*, **44**, 1887 (1911).
12) A. Werner, *Ber.*, **45**, 121 (1912).
13) D. H. Busch, *J. Am. Chem. Soc.*, **77**, 2747 (1955).
14) Y. Shimura and R. Tsuchida, This Bulletin, **28**, 572 (1955).
15) W. Kuhn and K. Bein, *Z. anorg. Chem.*, **216**, 321 (1934).
16) R. Tsuchida, *J. Chem. Soc. Japan (Nippon Kagaku Zassi)*, **58**, 621 (1937).
17) M. Kobayashi, ibid., **64**, 648 (1934).
18) J.-P. Mathieu, *Bull. soc. chim. France*, [5] **5**, 105 (1938).

I

MEASUREMENTS

	First absorption band				Second absorption band			
	ν_{max}[a)]	log ε_{max}	Half-value width[a)]	Inclination parameter[14),a)]	ν_{max}[a)]	log ε_{max}	Half-value width[a)]	Inclination parameter[14),a)]
	60.8	1.90	11.3	0.55	86.1	1.97	12.5	0.35
Ia:	57.0	1.85	10.2	0.5	82.7	1.90	12.4	0.3
Ib:	65.6	1.38	11.8	0.5				
	61.5	2.02	11.3	0.65	86.1	2.06	12.4	0.5
	63.9	1.94	10.4	0.55	88.4	1.90	12.0	0.4

b) The difference between the maximum and the minimum value of the partial inversive rotatory dispersion was halved.

TABLE II

ABSORPTION MAXIMUM AND THE CENTER OF INVERSIVE ROTATORY DISPERSION

Complex ion	ν_{rot}	ν_{abs}	$\nu_{abs}-\nu_{rot}$	Ref.
d-$[Co\,en_3]^{3+}$	61.2	63.9	+2.7	*
l-$[Co\,ox_3$**$]^{3-}$	48.8	50.2	+1.4	15
d-$[Co\,en_2\,ox]^{+}$	57.7	60.0	+2.3	4
d-$[Co\,en_2\,CO_3]^{+}$	57.0	59.0	+2.0	4
d-$[Co\,en_2\,(NH_3)_2^{(1)}_{(2)}]^{3+}$	60.4	64.4	+4.0	4
l-$[Co\,en_2\,gly]^{2+}$	58.8	61.4	+2.6	10
d-$[Co\,en_2\,(d\text{-alan})]^{2+}$	59.2	61.9	+2.7	10
l-$[Co\,en_2\,(l\text{-phenylalan})]^{2+}$	59.0	61.7	+2.7	10
d-$[Co\,en_2\,(d$-val***$)]^{2+}$	59.3	61.8	+2.5	10
d-$[Co\,en_2\,(l\text{-leuc})]^{2+}$	59.5	61.5	+2.0	*
d-$[Co\,en_2\,(NO_2)\,(OH_2)^{(1)}_{(2)}]^{2+}$	59.0	65.1	+6.1	4
l-$[en_2Co\langle^{NH_2}_{O_2}\rangle Co\,en_2]^{4+}$	60.9	64.3	+3.4	18
d-$[Co\,en_2\,(NH_3)\,Cl^{(1)}_{(2)}]^{2+}$ Ia:	54.6	57.0	+2.4	*
Ib:	63.4	65.6	+2.2	*
d-$[Cr\,en_3]^{3+}$	64.9	65.5	+0.6	3
d-$[Cr\,ox_3]^{3-}$	54.3	52.6	−1.7	3
d-$[Cr\,en_2\,ox]^{+}$	62.5	63.0	+0.5	4

ν_{rot}: Center of inversive rotatory dispersion (10^{13}/sec.).
ν_{abs}: Absorption maximum (10^{13}/sec.).
* New measurement by the present author. ** ox stands for oxalate ion.
*** val stands for valinate ion.

the overlap of the curves (2), (3) and (4). Thus it was concluded that the first absorption band of this complex showed two inversive dispersions, the one of which had positive Cotton effect and the other negative Cotton effect.

Since the complex ion, $[Co(NH_3)_4\,(l\text{-leuc})]^{2+}$, belongs to the type of $[CoN_5O]$, it is expected that its first absorption band splits into two components, Ia and Ib. Therefore, the two inversive dispersions above obtained probably correspond to the two components of the first absorption band.

A survey of the data for the cobalt(III) or chromium(III) complexes, which are found in literature as well as in the present author's measurements, revealed that the center of inversion of the rotatory dispersion was almost always in the longer wave-length region as compared with the position of the absorption maximum (Table II). Taking this fact into consideration, a tentative curve analysis was made to separate the two components of the first absorption band of $[Co(NH_3)_4\,(l\text{-leuc})]^{2+}$. In the analyses of the absorption curves, the experimental equation was used, which was recently developed by the present author[14]. The results are shown in Fig. 1. The similar curve analyses of the rotatory dispersion curve and the absorption curve were performed for *d*-$[Co\,en_2\,(NH_3)Cl^{(1)}_{(2)}]^{2+}$ (Fig. 2). In this case the two inversive dispersions

Ia and Ib have equally the positive sign of the Cotton effect. This coincides very well with the results of direct measurement of the Cotton effect (circular dichroism) by Mathieu[4].

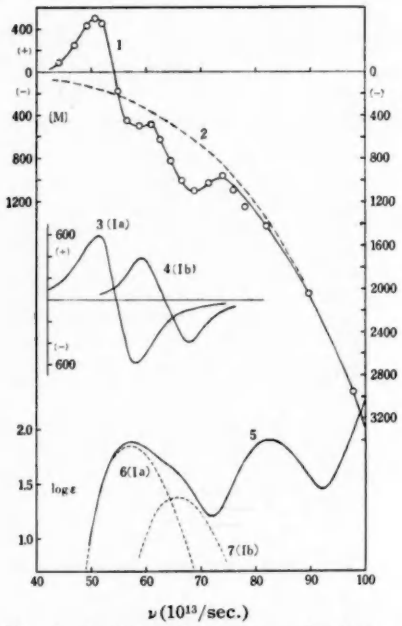

Fig. 2. Rotatory dispersion and absorption of *d*-[Co en$_2$ (NH_3)Cl]Br_2:
1, rotatory dispersion curve: 2∼4, curve analyses of the rotatory dispersion curve; 5, absorption curve; 6∼7, curve analyses of the first absorption band.

On the basis of the facts above discussed it is concluded that, so far as the first absorption band is concerned, the so-called "vicinal effect" exists between the cobalt atom and the asymmetric carbon atom C* in the structure of

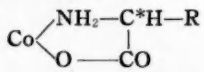

In contrast with $[Co(NH_3)_4$ (*l*-leuc)$]^{2+}$, no evidence was obtained for the overlap of two or more inversive dispersions in *d*-[Co en$_2$ (*l*-leuc)]Cl_2 (Fig. 3). The rotatory dispersion of the latter compound, as well as that of *d*-[Co en$_3$]$^{3+}$ (Fig. 4), has a typical shape of a single inversive dispersion. The reason for this difference between the *bis*-ethylenediamine complex and the tetrammine complex is unknown. It should be added, however, that the degree of rotation is extraordinarily greater in the *bis*-ethylenediamine complex than in the tetrammine complex. It is probable that the asymmetry around the central cobalt atom contributes more profoundly to the rotatory power of the region of the first absorption band than the asymmetric carbon atom in the co-ordinated ligand.

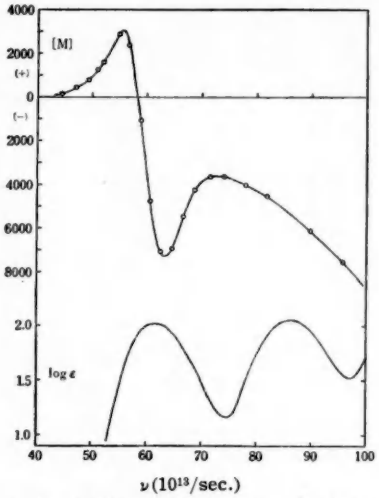

Fig. 3. Rotatory dispersion and absorption of *d*-[Co en$_2$ (*l*-leuc)]Cl_2.

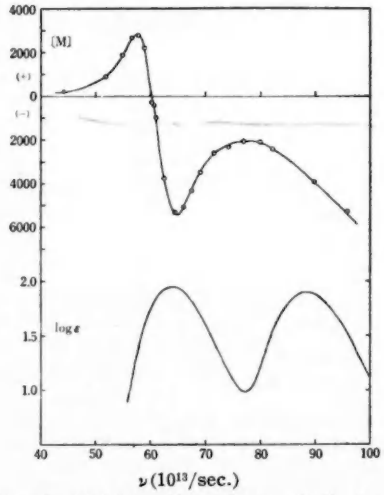

Fig. 4. Rotatory dispersion and absorption of *d*-[Co en$_3$]$Br_3 \cdot 2H_2O$.

Summary

A new complex compound, $[Co^{III}(NH_3)_4(l\text{-leuc})](ClO_4)_2$, has been prepared, in which the asymmetric center is only on a carbon atom of the ligand leucinate ion. From the measurements of the visible and the ultraviolet rotatory dispersion of this compound, it has been concluded that the so-called "vicinal effect" exists between the cobalt atom and the asymmetric carbon atom.

The rotatory dispersion measurements have also been made for *d*-$[Co\ en_2(l\text{-leuc})]Cl_2$, *d*-$[Co\ en_2(NH_3)Cl^{(1)}_{(2)}]Br_2$ and *d*-$[Co\ en_3]Br_3 \cdot 2H_2O$. On the basis of these data the relation of the splitting of the first absorption band with the so-called anomalous rotatory dispersion has been discussed. Thus it has been shown that the anomalous rotatory dispersion of $[Co(NH_3)_4(l\text{-leuc})]^{2+}$ or of $[Co\ en_2(NH_3)Cl]^{2+}$ is explicable by assuming the overlap of the two inversive dispersions, Ia and Ib, which correspond to the component bands, Ia and Ib, of the split first absorption band.

In agreement with the observations by several previous authors, it has been shown that all the complexes studied scarecely show the anomalous rotatory dispersion in the vicinity of their second absorption bands.

The author wishes to thank Professor R. Tsuchida for his kind guidance throughout this work.

Department of Chemistry, Faculty of Science, Osaka University
Kita-ku, Osaka

The Dielectric Properties of Thiacyclohexane

By Seiichi KONDO and Masaru MATSUMOTO

(Received November 28, 1957)

The thermodynamic properties of thiacyclohexane were studied by J.P. McCullough and others[1] and it was shown that the entropy of fusion of this material is 2.002 e.u. at 292.25°K. They also found three phase transitions at 240.02°K, 207°K and 201.4°K. One of the present writers studied the structure of high crystalline modification of this material by means of X-rays[2]. According to his result, this high modification is in a disordered state in respect to the molecular orientation on the lattice site, and it was suggested that the high thiacyclohexane belongs to the category of the plastic crystals. This material shows a similar thermodynamic behavior and crystal structure with those of high cyclohexane, in spite of the fact that thiacyclohexane has the lower molecular symmetry, C_s, than that of cyclohexane, D_{3d}, and also has the permanent dipole moment of about 1.7 D. The investigation of the dielectric properties of this material will be interesting and may give more information than the study of non-polar compounds can provide, for the purpose of clarifying further details of the structure of high thiacyclohexane and of obtaining the informations of some properties of other phases. From this point of view the authors carried out the dielectric measurement of this material and found some interesting results on the rotational mechanism of the molecule in the crystalline phases of this material.

Experimentals

The electric circuit for the dielectric measurement is an audio-frequency transformer bridge described elsewhere[3]. The frequencies used for the measurement range from 100 to 3×10^4 c.p.s. The electric condenser for the measurement of the sample consists of platinum electrodes sealed in a soft glass cell in order to keep the sample between the electrodes under low pressure without exposure to air, as illustrated in Fig. 1. This cell can keep about 0.5 cc. of the sample and its electric capacity is about 0.2 p.f. in vacuum. It is enclosed in a copper block with the drying agent such as silica gel and is dipped in liquid air or in an oil bath. The dielectric constant

1) J.P. McCullough, et al., *J. Am. Chem. Soc.*, **76**, 261 (1954).
2) S. Kondo, This Bulletin, **29**, 999 (1956).
3) S. Kondo and T. Oda, ibid., **27**, 567 (1954).

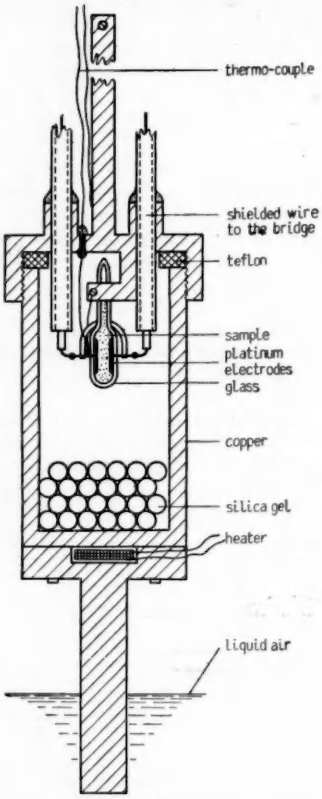

Fig. 1. The cell for the measurement of the dielectric constant of the sample.

of the sample can be determined by the comparison with those of purified benzene, carbon disulphide and ethyl ether. The sample was sent from the U.S. Bureau of Mines[4]. The purity of the sample thus received was stated to be 99.99 per cent. This sample was sublimed and sealed in the cell in Fig. 1. All these procedures were carried out without exposure to air or day light. The liquid in the cell is cooled very slowly at the freezing point, in order to avoid the formation of voids or cracks during the solidification of the sample. The temperature of the sample can be maintained constant within $\pm 0.1°$ for each set of observations with various frequencies. The dielectric constant of thiacyclohexane is shown in Fig. 2. There exist four condensed phases in this figure: liquid, solid phase III, solid phase II, and solid phase I according to the notation by McCullough and

4) This sample of thiacyclohexane was provided by the American Petroleum Institute Research Project 48 on "the production, isolation and purification of sulfur compounds and measurement of their properties" and were prepared and purified at the Petroleum and Oil Shale Experiment Station, U. S. Bureau of Mines, Laramie, Wyoming, U.S.A.

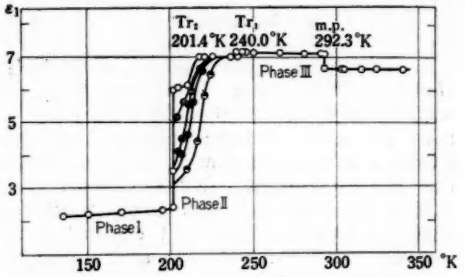

Fig. 2. The static dielectric constant of thiacyclohexane. The frequencies used for the measueement were 30 (◔), 10 (◉), 3 (●), 1 (◎), 0.1 (○) k.c.p.s.

others[1]. The dielectric interpretations of this curve as well as of the dielectric loss data will be made in the following sections.

Results and Discussion

Liquid and Solid Phase III.—The permanent electric dipole moment of thiacyclohexane in the liquid phase can be calculated by using the Onsager equation for pure polar liquid and is equal to 1.7 D. This value is equal to the dipole moment of this molecule estimated with the bond moment C—S, 1.4 D[5], and the valence angle C—S—C, 105°[1]. No dispersion phenomena were observed in the liquid phase.

In the solid phase III which is considered to be plastic, the dielectric constant measured may not include experimental errors which may arise from voids or cracks since the melt is solidified so carefully that repeated solidifications show the same value of the solid dielectric constant and no cracks or voids were assured visually. The dipole moment of thiacyclohexane in the plastic phase can be calculated by using the Onsager equation[6] and will give the same value as that in the liquid phase. This agreement seems to mean that the molecules in phase III behave in a manner roughly similar to those in the liquid phase except the fact that the molecules in the plastic phase are on the regular face-centered cubic lattice site. This dielectric interpretation is in good agreement with the result of thermodynamic[1] and X-ray[2] study of this material in the sense that these investigations revealed the very

5) G.C. Hampson, R.H. Farmer and L.E. Sutton, *Proc. Roy. Soc.* **A143** 147 (1933).

6) S. Kondo, *Memory of Osaka University of Liberal Arts and Education*, No. 6 (1957) (in press).

high disorder of molecular orientation in the phase III. In view of the existence of the relaxation phenomenon in phase II, there seems to be the molecular rotation with possibly smaller relaxation times and higher degree of rotational freedom, although in these two phases (the liquid phase and the phase III), there has been observed no relaxation phenomenon within the present frequency range. The value of dielectic loss, $\tan\delta$, is approximately equal to 3×10^{-4}.

Solid Phase II.—As seen in Fig. 2, The static dielectric constant of thiacyclohexane decreases by small amount from phase III to phase II at the transition point 240°K. The reason for this decrease could be either in the formation of many cracks during the phase transition which might decrease the apparent value of dielectric constant or in the intrinsic decrease of the dielectric constant in this phase II. Since no crystallographic or density data are available, it is impossible to decide which effect is more responsible for the decrease of the observed dielectric constant. However it may be supposed that the dipolar contribution still remains to some extent in this phase II, because the amout of change in the dielectric constant is comparatively small.

The low frequency dielectric dispersion was found in this phase. The Cole-Cole arcs are shown in Fig. 3 at 209.5° and

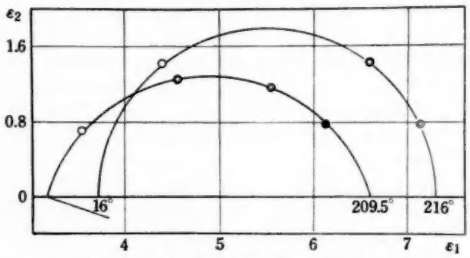

Fig. 3. The Cole-Cole plot of the dielectric relaxation of thiacyclohexane in the solid phase from 201.4°K to 200.02°K. The frequencies used are 30 (○), 10 (○), 3 (◎), and 1 (●) k.c.p.s.

216°K. At a higher temperature, the high frequency side more than 30 k.c.p.s. was not measured and the Cole-Cole arcs were drawn by the extrapolation. The relaxation times τ were obtained from these arcs at various temperatures and these values range from 3×10^{-6} to 6×10^{-5} sec. The $\ln\tau$ vs. reciprocal temperature curve is shown in Fig. 4. The activation energy of this relaxation phenomenon is calculated

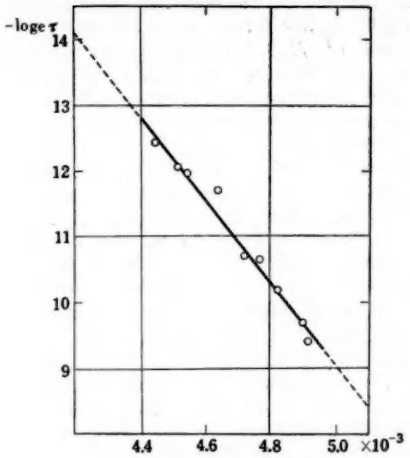

Fig. 4. The relaxation times vs. reciprocal temperature curve of thiacyclohexane.

from this curve to be 13.22 kcal. per mole and $\tau_0=5.75\times10^{-19}$ sec. This value of activation energy seems to be relatively greater than those which were found in such plastic crystals as *d*-camphor[7] and cyclohexane[8], determined by the dielectric and nuclear magnetic resonance experiments respectively, and which are considered to have the origin in the molecular rotations.

The radii of the Cole-Cole arcs seem to increase at higher temperatures. The Onsager equation for pure polar liquid can be modified to the following expression for the mixed case such as one consisting of a rotator component and a non-rotator component of the same one molecular species[9]. That is,

$$N_1=\frac{9kT}{4\pi\mu^2}\frac{(\varepsilon_s-\varepsilon_\infty)(2\varepsilon_s+\varepsilon_\infty)}{\varepsilon_s(\varepsilon_\infty+2)^2},$$

where μ and N_1 are the dipole moment and the number of the rotating molecules per c.c. respectively, k is the Boltzman constant and T is the absolute temperature. If it is assumed that the thiacyclohexane molecules began to rotate with some degree of rotational freedom with the activation energy 13.22 kcal. per mole, whose diople moment was constant, and if the density of this solid phase II were constant in

7) J.G. Powles, *J. Chem. Phys.*, **20**, 148 (1952).
8) E.R. Andrew and R.G. Eades, *Proc. Roy. Soc.*, **A216**, 398 (1953).
9) Refer, for instance, H. Fröhlich, "Theory of Dielectrics", Oxford (1949), p 36.

this dispersion region, the increase of the Cole-Cole arc radii might mean the increase of N_1. Therefore one may think that the number of rotating molecules would increase by temperature elevation and thus there would appear the order-disorder state during the process of the increase of N_1. This dielectric interpretation seems to be in good agreement with the thermal study by McCullough and others[1]. They found the λ type heat anomaly which will be the transition of higher order. The crystal structure analysis of this phase will make these discussions clearer.

Phase I.—The dielectric constant drops to a very small value at the transition point 201.4°K by cooling. There is no dielectric dispersion in the present frequency range in this phase I. The value of the dielectric constant in this phase lies in the range of the square of the optical refractive index and thus there seems to exist only the contribution of atomic and electronic polarizability to the dielectric constant. In other words, there seems to be no dipole rotation or disorder of dipolar orientation of molecules on the lattice sites in this phase.

Summary

1) The molecules are in the rotational states in the solid phases II, III and liquid phase, and not in the phase I.

2) There is an order-disorder transition in phase II which may have its origin in the molecular dipole rotation.

3) The dielectric behavior in phase III is similar to that of other polar plastic crystals.

The writers wish to express their thanks to Dr. John P. McCullough for his useful discussions and also for his kindness to supply pure thiacyclohexane.

Osaka University of Liberal Arts and Education, Tennoji-ku, Osaka

Bond Localization and the Hyperconjugative Effect in the Aromatic Carbonium Ions. I. Absorption Spectra of Benzenium-, Toluenium-, and Mesitylenium- Ions[1]

By Toshifumi MORITA

(Received December 14, 1956)

Reid's measurements of the absorption spectra of methylbenzenes in anhydrous hydrogen fluoride-boron trifluoride indicate that the bands of the longest wave length which Reid attributed to those of carbonium ions of methylbenzenes shift toward violet with the increasing number of methyl substituents[2]. To investigate this phenomenon theoretically seems to be of much interest. In performing the theoretical treatment on these carbonium ions, it should be taken into account, whether the hyperconjugation takes place or not between the aromatic ring and the H_2 group constructed by the attached proton together with the hydrogen atom already present at the position of proton attack in the ring. Under the assumption of localization of the H_2—C bond with respect to the conjugated part of molecules, Gold and Tye[3] have calculated the π-electron energies of the carbonium ions of many hydrocarbons and have suggested the order of base strengths of hydrocarbons[4]. Heilbronner and Simonetta[5] have also carried out similar computations on azulenium- and methyl azulenium- ions from the standpoint of the same hypothesis. In addition, it seems to be reasonable that these carbonium ions correspond to the transition state intermediates in the electrophilic substitution reactions from the fact that in methylbenzenes, a parallel relation exists between the equilibrium constants for the carbonium ion

1) As to the review on the experimental results, see, L. J. Andrews, *Chem. Revs.*, **54**, 713 (1954).
2) C. Reid, *J. Am. Chem. Soc.*, **76**, 3264 (1954).
3) V. Gold and F. L. Tye, *J. Chem. Soc.*, **1952**, 2184.
4) For polymethyl benzenes which are the objects of the present study, calculations have not been carried out.
5) E. Heilbronner and M. Simonetta, *Helv. Chim. Acta*, **35**, 1049 (1952).

formation and the rates of substitution in the electrophilic substitution reactions, with respect to the number of methyl substituents in the aromatics[6], and moreover the bond localization theory has gained much success in the interpretation of chemical reactivities[7-10], so that in the case of the aromatic carbonium ion also, the bond localization hypothesis will have much importance in the consideration of its behavior. On the other hand, Muller, Pickett, and Mulliken[11] have discussed the hyperconjugative effect of the H_2 group, and explained the absorption spectra of the benzenium ion. Generally speaking, it may be desirable to take the hyperconjugative effect of the H_2 quasi-atom into consideration. In the following, consequently, the experimental blue shifts are treated by the theoretical computation for benzenium-, toluenium- and mesitylenium- ions, using the semi-empirical LCAO MO method, from the point of the localization, on the one hand, and of the hyperconjugation, on the other, of the H_2—C bond.

Method of Calculation

Molecular Models. — The molecular models and the numbering in the present calculations are shown in Fig. 1 for the hyperconjugation and in Fig. 2 for the bond localization, in both cases (a), (b), and (c) being benzenium, toluenium, and mesitylenium ions, respectively. The attached proton at position 2 in the ring constructs the quasi-atom H_2 together with the hydrogen atom already present there, which takes part in hyperconjugation

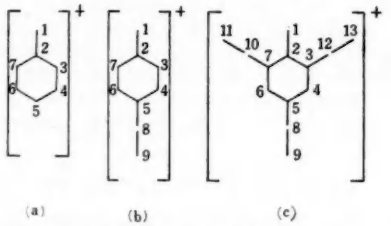

Fig. 1. Molecular models for the hyperconjugation.

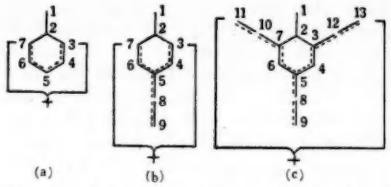

Fig. 2. Molecular models for the bond localization.

with the aromatic ring for the hyperconjugation model, but not for the bond localization one. The symmetry group to which these ions belong is C_{2v}. As for toluenium ion, there are other different models depending on the position at which proton attaches to the ring with respect to the methyl substituent, but only the C_{2v} type is adopted, because the selection rule is not applied to the molecules having attached proton at ortho- or meta-position with regard to the carbon atom linking to the methyl substituent, on account of lack of symmetry; furthermore it seems not bad to adopt the C_{2v} type from the analogy of the *p*- (and *o*-) orienting effect of the methyl substituent in the electrophilic substitution reaction of toluene.

Inclusion of Overlap.—Effects of neglect and inclusion of overlap on the various quantities, such as π-bond order, π-electron density, dipole moment, resonance energy, hyperconjugation energy, and absorption wave length, have been discussed in the numerous hydrocarbons and heteromolecules. As regards bond lengths, dipole moments and resonance energies there are little differences between their magnitudes calculated with and without overlap[12-16]. Mulliken et al.[17] have found that explicit inclusion of overlap improves the agreement of the calculations with the observed hyperconjugation shift in the ultraviolet absorption spectra, and with hyperconjugation energies, whereas for these empirical data the calculations without overlap gain less success[18]. Consequently in the present treatment also, overlap integrals between adjacent atoms are included.

Molecular Orbitals and Secular Equations.—Molecular orbitals used are of the

6) H. C. Brown, and J. D. Brady, *J. Am. Chem. Soc.*, **74**, 3570 (1952).
7) G. W. Wheland, ibid., **64**, 900 (1942).
8) M. J. S. Dewar, *J. Chem. Soc.*, **1949**, 463.
9) C. A. Coulson, *Research*, **4**, 307 (1951).
10) R. D. Brown, *Quart. Rev.*, **6**, 63 (1952).
11) N. Muller, L. W. Pickett and R. S. Mulliken, *J. Chem. Phys.*, **21**, 1400 (1953); *J. Am. Chem. Soc.*, **76**, 477 0 (1954).
12) D. W. Davies, *Trans. Faraday Soc.*, **51**, 449 (1955).
13) T. H. Goodwin and V. Vand, *J. Chem. Soc.*, **1955**, 1683.
14) T. H. Goodwin, ibid., **1955**, 4451.
15) R. H. Knipe, *J. Chem. Phys.*, **23**, 2089 (1955).
16) G. W. Wheland, *J. Am. Chem. Soc.*, **63**, 2025 (1941).
17) R. S. Mulliken and C. A. Rieke, ibid., **63**, 1770 (1941).
18) R. S. Mulliken, C. A. Rieke and W. G. Brown, ibid., **63**, 41 (1941).

LCAO (linear combination of atomic orbitals) type $\psi_j=\sum_\mu x_{j\mu}\phi_\mu$, where ψ_j is the j'th MO (molecular orbital), ϕ_μ the AO (atomic orbital) on the μ'th atom, $x_{j\mu}$ the coefficient of the μ'th AO in the j'th MO, ψ_j. The energies of the π-electron levels are given by the roots of the secular equation[10,19],

$$|\beta_{\mu\nu}+S_{\mu\nu}\lambda_{\mu\nu}|=0,$$

where

$$\beta_{\mu\nu}=\gamma_{\mu\nu}-(1/2)S_{\mu\nu}(\alpha_\mu+\alpha_\nu),$$

$$S_{\mu\nu}=\int\phi_\mu\phi_\nu d\tau,$$

$$\lambda_{\mu\nu}=(1/2)(\alpha_\mu+\alpha_\nu)-\varepsilon_j,$$

and

$$\gamma_{\mu\nu}=\int\phi_\mu H\phi_\nu d\tau, \quad \alpha_\mu=\int\phi_\mu H\phi_\mu d\tau,$$

$$\varepsilon_j=\int\psi_j H\psi_j d\tau.$$

The coefficient of each atomic orbital in the molecular orbital is computed by solving linear equations under the normalization condition of the molecular orbital with the knowledge of the energy of the latter.

Assumptions and Choice of Semi-empirical Parameters. — In the semi-empirical method, appropriate values of the resonance and the Coulomb integrals must be chosen. As for the resonance integrals several authors[6,20,21] have used the assumption of the proportionality of the parameter γ to the overlap integral S. However, in the present work the parameter β introduced for the first time by Mulliken[22] is assumed proportional to S[23]. Values of overlap integrals are obtained from Mulliken et al.[24], and those used in the present calculation are like those in Table I. For the value of the corrected term δ for the Coulomb integral of H_3 or H_2, several authors have used the empirical values of -0.2[4,6,25-28] or -0.5[10,20,21]. The value used in the present work is -0.3 obtained by I'haya[29] through the theoretical calculations.

TABLE I
VALUES OF OVERLAP INTEGRALS USED IN THE PRESENT CALCULATIONS

Bonds	Values of overlap integrals
C—H_2 or C—H_3	0.541[a]
C_{methyl}—C_{arom}[b]	0.203[c]
C—C[d]	0.247

a). See, ref. 21), footnote 27. b). The bond between the methyl carbon and the neighboring carbon atom in the ring. c). The value corresponding to the interatomic distance of 1.51 Å. d). The bond between the adjacent carbon atoms in the benzene ring.

The choice of the auxiliary inductive parameter, δ_{ind}, for the Coulomb integral of the carbon atom with which the H_3 or H_2 quasi-atom binds is considerably arbitrary and its decision is essentially empirical, although Goodman and Shull[30] have pointed out the possibility of finding the reasonable values from the experimental transition- and ionization-energy shifts due to this effect. Various values of this parameter have been used, such as $\delta_{ind}/\delta=1/4\sim1/10$[31], $1/2$[25], $1/5$[20], $1/8$[32,33] and $1/3\sim1/5$[34]. In the present treatment $\delta_{ind}/\delta=1/3$ is used in accordance with many investigators' arguments[35-37]. The use of this parameter is limited to the case of the bond localization calculations.

The Hyperconjugation Energy

The hyperconjugation energy, for example, of benzenium ion, is obtained as follows. (1) The π-electron energies of the hyperconjugation and of the bond localization model are calculated. (2) The vertical hyperconjugation energy is obtained by subtracting the ground state π-electron energy of the hyperconjugation model from that of the bond localization one. (3) The correction of the compressional energies[38] is carried out assuming that the bonds are distorted harmonically, taking the values of force constants,

19) L. Lofthus, ibid., **79**, 24 (1957).
20) C. A. Coulson and V. A. Crawford, *J. Chem. Soc.*, **1953**, 2052.
21) Y. I'haya, This Bulletin, **28**, 376 (1955).
22) R. S. Mulliken, *J. chim. phys.*, **46**, 497 (1949).
23) R. S. Mulliken, ibid., **46**, 675 (1949).
24) R. S. Mulliken, C. A. Rieke, D. Orloff and H. Orloff, *J. Chem. Phys.*, **17**, 1248 (1949).
25) B. Pullman, M. Mayot and G. Berthier, ibid., **18**, 257 (1950).
26) H. C. Longuet-Higgins and R. G. Sowden, *J. Chem. Soc.*, **1952**, 1404.
27) C. A. Coulson, *Proc. Phys. Soc.*, **45**, 933 (1952).
28) H. H. Jaffé, *J. Chem. Phys.*, **20**, 778 (1952).
29) Y. I'haya, ibid, **23**, 1165 (1955).
30) L. Goodman and H. Shull, *J. Chem. Phys.*, **23**, 33 (1955).
31) G. W. Wheland and L. Pauling, *J. Am. Chem. Soc.*, **57**, 2086 (1935).
32) P. O. Löwdin, *J. Chem. Phys.*, **19**, 1323 (1951).
33) H. H. Jaffé, *J. Am. Chem. Soc.*, **76**, 3527 (1954).
34) Y. I'haya, *J. Chem. Soc. Japan, Pure Chem. Sec. (Nippon Kagaku Zassi)*, **77**, 314 (1956).
35) G. E. K. Branch and M. Calvin, "The Theory of Organic Chemistry" Prentice-Hall, Inc., New York, 1941.
36) V. Gold, *Trans. Faraday Soc.*, **46**, 326 (1950).
37) H. H. Jaffé, *J. Chem. Phys.*, **20**, 279, 778, 1554 (1952); **21**, 415 (1953); *J. Am. Chem. Soc.*, **77**, 274 (1955).
38) Lennard-Jones, *Proc. Roy. Soc.*, A **158**. 280 (1937); D. F. Hornig, *J. Am. Chem. Soc.*, **72**, 5772 (1950); C. A. Coulson, and S. L. Altmann, *Trans. Faraday Soc.*, **48**, 293 (1952).

TABLE II

ELECTRIC STATES AND TRANSITION PROCESSES

Carbonium ions	Ground state	Lowest excited state	Transition	Polarization
Benzenium	$(1b_1)^2(2b_1)^2(1a_2)^2$	$(1b_1)^2(2b_1)^2(1a_2)^1(3b_1)^1$	$A_1 \rightarrow B_2$	y
Toluenium	$\cdots\cdots (3b_1)^2(1a_2)^2$	$\cdots\cdots (3b_1)^2(1a_2)^1(4b_1)^1$	$A_1 \rightarrow B_2$	y
Mesitylenium	$\cdots\cdots (4b_1)^2(2a_2)^2$	$\cdots\cdots (1a_2)^2(4b_1)^2(2a_2)^1(5b_1)^1$	$A_1 \rightarrow B_2$	y

TABLE III

THE FIRST TRANSITION ENERGIES CALCULATED FOR TWO MODELS AND EXPERIMENTAL VALUES

Carbonium ions	For hyperconjugation model (unit of $-\beta$)	For bond localization model (unit of $-\beta$)	Absorption wave length observed (A)	Oscillator strength observed
Benzenium	0.87083	0.80193	4170	0.15
Toluenium	0.87902	0.81574	4000	0.15
Mesitylenium	0.81801 0.81445	0.76018	3900	0.27

TABLE IV

THEORETICAL DATA FAITHFUL TO REID'S EXPERIMENTS

Carbonium ions	Model	Singlet-triplet separations assumed (eV)	Longest absorption wave length (A)	Oscillator strength
Benzenium	Bond localization	1.77	4168	0.31
Toluenium	Bond localization	1.95	3999	0.20
Mesitylenium	Hyperconjugation	2.10	3909	0.32

TABLE V

THE SECOND TRANSITIONS CALCULATED FOR TWO MODELS

Carbonium ions	Transition	Polarization	Transition energies for hyperconjugation (unit of $-\beta$)	Transition energies for bond localization (unit of $-\beta$)
Benzenium	$A_1 \rightarrow A_1$ $(2b_1 \rightarrow 3b_1)$	z	1.18005	1.21308
Toluenium	$A_1 \rightarrow A_1$ $(3b_1 \rightarrow 4b_1)$	z	1.09208	1.09131
Mesitylenium	$A_1 \rightarrow A_1$ $(4b_1 \rightarrow 5b_1)$	z	1.09661	0.93919

4.50×10^5, 9.57×10^5, and 4.80×10^5 dyne/cm. for C—C, C=C, and C—H bonds[39], respectively, and calculating π-bond orders by the following relations of Chirgwin and Coulson[40],

$$p_{\mu\nu} = (1/2)\sum_{j=1}^{m} n_j (x_{j\mu} y_{j\nu} + x_{j\nu} y_{j\mu}),$$

$$\nu, \mu = 1, 2, \cdots\cdots n, ; \nu \neq \mu,$$

$$y_{j\mu} = \sum_{\nu=1}^{n} S_{\mu\nu} x_{j\nu},$$

n_j: number of electrons occupying the j'th MO,

m: number of occupied molecular orbitals,

bond lengths being obtained by the correlation between the bond length and the total bond order[41]. Calculations show 10.28 kcal/mole[42] for the hyperconjugation energy.

It will be noticed here that this value is too large for the hyperconjugation energy itself, which is usually of the order of a few kcal./mole. Positive δ values indicate smaller hyperconjugation energies[10], but from the electronegativity consideration of the H_2 quasi-atom compared with the $2p\pi$ carbon negative values of δ will be accepted[10]. The value —0.3

39) G. Herzberg, "Infrared and Raman Spectra of Polyatomic Molecules", B. Van Nostrand, New York, N. Y. 1945, p. 193.

40) B. H. Chirgwin and C. A. Coulson, *Proc. Roy. Soc.*, A **201**, 196 (1950).

41) C. A. Coulson, ibid., A **169**, 413 (1939).

42) Energies are expressed by the unit of β, the resonance integral including overlap between the neighboring carbon atoms in benzene molecule, and in converting those into the unit of kcal. $\beta = -60$ kcal./mole is used. See, C. C. J. Roothaan and R. S. Mulliken, *J. Chem. Phys.*, **16**, 118 (1948).

for δ gives the smaller hyperconjugation energy than the value -0.5 does[10]. However, the difference between both cases is small and, in addition, $\delta=-0.5$ is adequate to account for the dipole moment and the spectral shift as well as the hyperconjugation energy of toluene[20,21]; consequently, it will not be of importance which value of these will have to be chosen. Matters will probably be otherwise; in fact the improved calculations by means of the self-consistent technique by Muller, Pickett, and Mulliken[10] show the smaller hyperconjugation energy, 5.9 kcal./mole. In relation to this, it will be very interesting to carry out the ASMO calculations.

The Spectra

Calculated results on the spectra and comparisons with experiments are indicated in Tables II, III, IV and V.

Table II shows the electronic states and transition processes for the first transitions. For these three aromatic carbonium ions, the manner in which electron transitions occur is the same, namely one electron elevates from the a_2 to the b_1 orbital, transition process being $A_1 \rightarrow B_2$, and polarization is in the y direction which is perpendicular to the molecular axis, z, and lies in the molecular plane.

Table III indicates the experimental values and the calculated transition energies for the first transitions. The experimental values of the absorption wave lengths in the fourth column are taken from the paper of Reid[11] and experimental oscillator strengths in the last column are determined roughly by the author on the basis of the experimental extinction curves by Reid through the following relation[43],

$$f=4.32\times10^{-9}\int\varepsilon_\nu d\nu,$$

where f is the oscillator strength, and ε_ν the extinction coefficient of the observed absorption of frequency ν. The calculated transition energies for the case of the bond localization model are those obtained using $\delta=-0.3$ as well as the auxiliary inductive parameter, $\delta_{\text{ind}}=-0.1$, while those for the hyperconjugation model correspond to the values obtained using only $\delta=-0.3$, except the second value of mesitylenium ion, the calculation of which includes $\delta_{\text{ind}}=-0.1$ also. All these are mean values of the transition energies to the singlet and the triplet excited states; consequently, in order to compare these calculated values with observed ones, an additional factor must be taken into account, e.g. the singlet-triplet separation in the excited state. Here, if it is assumed that the singlet-triplet splittings of these three molecules are not the same in general, but may not differ very much from each other, then it seems safe to let the calculated mean transition energies have the same tendency as the absorption shifts observed among these three substances. According to Table III, and from the view point just mentioned, the calculated mean transition energies for these three ions can explain the experimental "blue-shifts" in terms of neither the hyperconjugation nor the bond localization, although only the "blue-shift" of toluenium relative to benzenium ion is predicted by both models. At this point, if the bond localization rather than the hyperconjugation model is preferably chosen for benzenium and toluenium ion, while the hyperconjugation rather than the bond localization model, for mesitylenium ion, then there will be no contradiction between theories and experiments. However, this remains only to be an arrangement of the calculated results, so as to be faithful to Reid's measurements, and the critical discussion on this point will be performed in the following section.

The theoretical data arranged so as to be faithful to Reid's experiments are indicated in Table IV. When the values of siglet-triplet separations are assumed to be such as those shown in the third column and for the purpose of obtaining only the transition energies to the singlet excited states, a half of those values are added to the mean transition energies; the absorption wave lengths thus calculated may accord with the experimental values (compare the fourth column of Table IV with the fourth column of Table III). The theoretical oscillator strengths in the fifth column are computed by the relation[44],

$$f=1.085\times10^{11}\nu D,$$

$$D=\boldsymbol{Q}^2,$$

$$\vec{\boldsymbol{Q}}=\sqrt{2}\sum_\mu \boldsymbol{x}_{i\mu}\boldsymbol{x}_{j\mu}\vec{\boldsymbol{r}}_\mu,$$

43) J. R. Platt and H. B. Klevens, *Rev. Mod. Phys.*, **16**, 182 (1944).

44) R. S. Mulliken and C. A. Rieke, *Reports on Progress in Physics*, **8**, 231 (1941).

where, ν is the absorption frequency (in cm.$^{-1}$); D, the dipole strength; $x_{i\mu}$, $x_{j\mu}$, coefficients of μ'th atom in the molecular orbitals, i and j, respectively, which are concerned with the electron jump; $\vec{r}_\mu$, the position vector of the μ'th atom with respect to some convenient origin. Oscillator strengths calculated and observed agree satisfactorily with each other.

Calculated results for the second transitions are shown in Table V. One electron concerning this transition elevates from the b_1 to the b_1 molecular orbital, and the polarization is in the direction of the molecular axis, z.

Discussion

In the preceding section the bond localization model is assumed for benzenium- and toluenium- ions and the hyperconjugation one for mesitylenium ion. This assumption is, however, only having put a finger on one possibility of the π-electron structures of these ions, and must be verified also from other criterions, which, however, unfortunately are not available at present.

Our calculation is only very approximate. The more rigorous approximation[11] including the self-consistent technique can not either determine distinctly which of the bond localization and the hyperconjugation model is suitable to benzenium ion, and further complicated factors, besides those pointed out by Coulson and Dewar[45], will have to be taken into account, such as configuration interactions, which are useful in predicting the absorption spectra, and screening effects by the electron distributions enhanced through the existence of the methyl substituents in the aromatic nucleus; it is difficult to carry out calculations including the former factor in the simple LCAO MO treatments on these systems in question[46]; furthermore, reasonable computations including the latter factor are difficult in the present step. Because our calculation is only rough, jumping from one model (bond localization) to the other (hyperconjugation) may be probably open to suspicion. Generally speaking, whenever the H_2 or H_3 group exists in conjugated systems, it may be adequate to assume the presence of its hyperconjugation[47].

In order to avoid these difficulties mentioned above, we assume that the hyperconjugation always occurs but its extent is different in each case of these ions in question; then it may be said that benzenium as well as toluenium is less hyperconjugated than mesitylenium ion, if we admit the simple theory and Reid's experiments. If, as in the preliminary report[48], the eigenfunction Φ of these ions is written by the linear combination of the eigenfunctions Φ_{HCJ} of the perfect hyperconjugation and Φ_{BL} of the bond localization model, Φ is the so-called hybrid and has commonly the lower energy than both models, while now we assume that Φ has the intermediate energy between the two extreme models, namely bond localization and perfect hyperconjugation models. In this respect there have been some confusions in the preliminary report.

There will be an additional way of treating these intermediate systems; that is, the systems having intermediate energies between those of the perfect hyperconjugation and bond localization models. Namely, by attributing different values to the resonance integrals between atoms 2 and 3 (Fig. 1 or Fig. 2) in these three molecules in question, computations on the spectra may be carried out. However, in so far as the approximation made is rough, the calculated results here also remain only to point out one possibility of the π-electron structures of these aromatic carbonium ions.

Recently Kilpatrick and Hyman[49] have measured the absorption spectra of benzene, mesitylene, and hexamethylbenzene in the various acids including anhydrous hydrogen fluoride. They have indicated the loss of fine structure at 260 mμ band of benzene due to the effect of the acidic environment and have been unable to detect the presence of the protonated benzene. They entertain a doubt on the absorption band which Reid attributed to that of benzenium ion[50]. Further Kilpatrick and Hyman have shown that the bands of protonated hexamethylbenzene shifts towards red compared to those of

45) C. A. Coulson and M. J. S. Dewar, *Discussions Faraday Soc.*, **2**, 54 (1947).

46) As regards some alternant hydrocarbons, for example, polyacenes, inclusion of configuration interactions in the simple molecular orbital calculations, is possible. See, W. Moffitt, *J. Chem. Phys.*, **22**, 1820 (1954).

47) The author wishes to express his sincere thanks to Professor R. S. Mulliken (University of Chicago) for his critical advice on these points (private communication to the author).

48) T. Morita, *J. Chem. Phys.*, **25**, 1290 (1956).

49) Private communication to Dr. S. Nagakura.

protonated mesitylene. This fact may suggest that the band of mesitylenium ion shifts towards red compared to that of toluenium ion. If so, our calculations may predict this red shift in terms of both the bond localization and the hyperconjugation models. Unfortunately measurements on toluene in anhydrous hydrogen fluoride have not been shown. Probably protonated toluene (and/or benzene) will occur in the system of anhydrous hydrogen fluoride and toluene (and/or benzene), but on account of its small quantity the absorption band of this carbonium ion seems not to exhibit itself.

Because of these experiments contrary to Reid's and because of the ambiguity of the absorption bands of benzenium and toluenium ions, we reserve making any conclusion about the calculated results. At any rate, at present, experimental facts are scarce, and the performance of experiments from various view points may be desirable.

Summary

The semi-empirical LCAO MO treatment on the spectra of benzenium, toluenium, and mesitylenium ions have been carried out. Neither the localization nor the hyperconjugation of the H_2—C bond with respect to the aromatic ring can explain the blue-shifts of the experimental spectra by Reid with the increasing number of methyl substituents. If, however, benzenium and toluenium ions are assumed to be less hyperconjugated than mesitylenium ion, the spectroscopic behaviors of these aromatic carbonium ions are understandable. However, if the mesitylenium band is assumed to shift towards red compared with toluenium by the analogy of the case of protonated hexamethylbenzene and mesitylenium ion, whose absorption spectra have been measured by Kilpatrick and Hyman, our theoretical calculations will predict well the case of mesitylenium and toluenium ion in terms of both the bond localization and the hyperconjugation models. Unfortunately, however, the measurement on toluene in acid medium have not yet been made. Further the case of benzenium ion is yet open to question. Consequently we reserve making any distinct conclusions on these three aromatic carbonium ions.

The author wishes to thank Professor T. Titani (Tokyo Metropolitan University) for his interest and encouragement, Professor A. Kotera (Tokyo University of Education) for his intuitive guidance, Dr. S. Nagakura (University of Tokyo) for many valuable discussions, and Mr. Y. I'haya (Tokyo University of Education) for his helpful advice.

Department of Chemistry, Tokyo Metropolitan University
Setagaya-ku, Tokyo

50) Here see, H. Luther, and G. Pockels, *Z. Electrochem.*, **59**, 159 (1955). Luther and Pockels' measurements of the absorption spectra of the system, benzene-Al_2Br_6·HBr(or -Al_2Cl_6·HCl) and toluene-Al_2Br_6·HBr(or -Al_2Cl_6·HCl), indicate different absorption wave lengths from those of Reid, and the absorption wave lengths are time-dependent, but the tendency of the blue-shifts of the spectra through the presence of the methyl substituents exists. However, it is questionable whether $[ArH]^+$, where Ar is the aromatic molecule, is responsible for these spectra. See also the paper by E. L. Mackor [*Chem. Weekblad*, **52**, 240 (1956)], who suggested the presence of the more complicated complexes.

Formation and Aging of Precipitates. VI. Morphology of Crystals in Various Vanadium Pentoxide Sols by Electron Microscopy

By Kazuyoshi TAKIYAMA

(Received November 21, 1957)

Since the report of Biltz[1], the formation and aging of vanadium pentoxide sol has been investigated by many scholars. Recently, as the fibrous shape of the crystals contained in the sol which was confirmed distinctly with the electron microscope has attracted the attention of many investigators, morphological and crystallographic investigations have become popular. The crystals in Biltz sol were small fibrils at the outset and they grew like long fibers upon aging. Huber and Zbinden[2], watson, Heller and Wojtowicz[3] and Tamamushi[4] observed the growth of the crystals in Biltz sol with an electron microscope and they found that the fibrous crystals were nearly monodisperse at first, but they became polydisperse upon aging. The present author prepared vanadium pentoxide sols by Biltz', Müller's, and ion exchange method and studied the crystals in these sols by means of the electron microscopy to make a research on the aging process.

Experimental and Results

Formation of Sols.—*Biltz sol.* Two g. of ammonium metavanadate was mixed thoroughly with 6 ml. of 3 N hydrochloric acid in an agate mortar. The brownish red precipitate produced was washed in a glass filter and all the precipitate was dispersed completely in 200 ml. of water, giving a clear reddish brown sol.

Müller sol. Five g. of ammonium metavanadate was fused in a porcelain crucible for about half an hour and the melt was poured into 500 ml. of cold water. The sol formed in this way was dark reddish brown in color.

Ion exchange sol. Ammonium metavanadate solution (0.5%) was passed through a column of hydrogen ion exchange resin (Amberlite IR-120) and the yellow vanadic acid produced was decomposed in boiling water for about half an hour, and a reddish brown sol was formed.

Concentration of Sols and Quantity of Impurities.—The concentration of sols and the quantity of electrolytes in sols were determined as stated below.

Concentration of sols. The total quantity of vanadium pentoxide contained in the sols was determined as follows: a certain quantity of a sol was mixed with a small amount of 6 N sodium hydroxide solution, and the mixture was warmed until the vanadium pentoxide was completely dissolved. After the addition of sulfuric acid, the vanadic acid was titrated potentiometrically with 0.01 N standard ferrous ammonium sulfate.

Dissolved vanadium pentoxide in sols. A certain quantity of the sol was mixed with a suitable amount of potassium chloride solution to coagulate the disperse phase, and the coagulum was filtered and washed with potassium chloride solution. Vanadium pentoxide in the filtrate was determined as described above.

Ammonia in sols. The quantity of ammonia contained in the sol was determined by Kjeldahl's method.

Chloride in sols. The disperse phase of the sol was coagulated with potassium nitrate solution and the coagulum was filtered and washed. The filtrate was titrated with standard silver nitrate solution by potentiometry.

Results of the measurements. The results obtained by the above-mentioned methods are listed in Table I.

TABLE I
CONCENTRATION OF SOLS AND IMPURITIES

No.	Sol	Time of aging	Concn. of sol	Concn. of dissolved V_2O_5	Concn. of NH_3
			g./l.	g./l.	mg./l.
1	Biltz sol	0	7.083	1.052	—
2	〃	2 day	7.057	0.526	218.8
3	〃	6 months	7.120	0.281	—
4	〃	18 months	7.184	0.285	214.5
5	Müller sol	0	6.990	1.090	0.2
6	〃	10 days	6.420	0.325	—
7	Ion excange sol	0	6.094	0.400	0
8	〃	0	6.370	0.298	0

The concentration of every sol was about 7 g. V_2O_5 per liter. The amount of the dissolved vanadium pentoxide in Biltz and Müller sols was about 1 g. per liter (about 15% of the total vanadium pentoxide) in those fresh sols, but it decreased to about 0.28 g. per liter (about 4% of the total vanadium pentoxide) upon aging. In

1) W. Biltz, *Ber.*, **37**, 1095 (1904).
2) H. Huber and H. Zbinden, *Z. anorg. Chem.*, **258**, 188 (1949).
3) J. H. Watson, W. Heller and W. Wojtowicz, *Science*, **109**, 274 (1949).
4) B. Tamamushi, *J. Electron-Microscopy*, **1**, 35 (1950).

Fig. 1. Crystals in 2 days old Biltz sol. (Cr shadowing) × 20,000

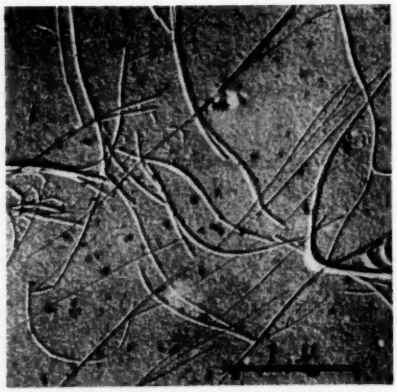

Fig. 2. Crystals in 2 weeks old Biltz sol. (Cr shadowing) × 20,000

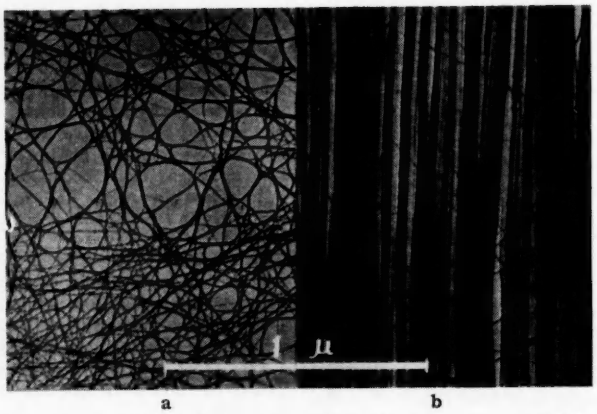

a b

Fig. 3. Crystals in 1 year old Biltz sol. × 40,000

the case of ion exchange sol the amount of the dissolved vanadium pentoxide was less than that in Biltz and Müller sols even in the incipient stage of standing. About 0.2 g. ammonia existed in one liter of Biltz sol, (about 0.013 mole NH_3/l.; $V_2O_5 : NH_3 = 3 : 1$), but only a trace of it was found in Müller sol, and it was not detected at all in the ion exchange sol. Chloride ion was not detected in any of the sols. pH of the sols was 2.5 to 3.0.

Morphology of Crystals in Sols by Electron Microscopy.—Morphological characteristics of crystals in the three kinds of sol described above were observed by means of electron microscopy.

Biltz sol. The crystals in Biltz sol were small fibrils, a few score mμ long and 14 mμ thick, at the outset as shown in Fig. 1, but they grew like long fibers on standing. They grew to about 1 μ in size after a week, about 2 μ after 2 weeks (Fig. 2) and over a few μ after a month, then fibrous crystals got intertwined with one another and their length could not be measured. But a few weeks old Biltz sol contained small fibrils also as seen in Fig. 2. The thickness was, however, about 14 mμ and almost constant. An electron micrograph obtained from a specimen of a year old sol mounted on a specimen holder without supporting film showed a network structure as in Fig. 3 a. The fibrous crystals of various lengths clung together, forming a network structure. Thin films of crystals were formed on the surface of the sol which was aged over a few months. They were floated on the water and were scooped up with specimen holders without supporting films. The electron micrographs of these specimens showed the orientation of fibrous crystals with their long axes parallel to one another as in Fig. 3 b. When a small amount of the old Biltz sol was allowed to flow on the surface of still water and was scooped up with a specimen holder, an electron micrograph similar to that described above was also obtained. This figure was formed by the orientation of fibrous crystals to the direction of the flow. The fibrous crystals in Biltz sol grew markedly extended along their long axes on standing, but the fibrils in the sol dialyzed

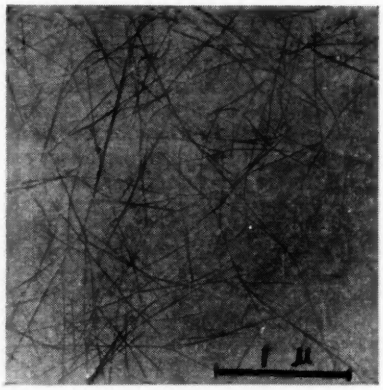

Fig. 4. Crystals in dialyzed Biltz sol. (1 year old sol) × 20,000

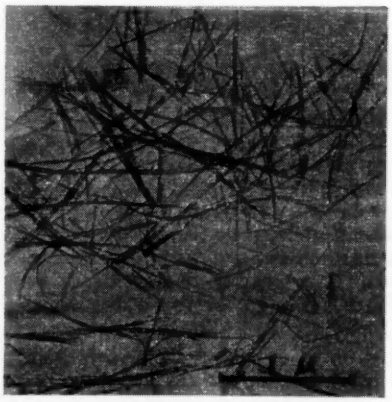

Fig. 5. Crystals in 1 year old Müller sol. × 20,000

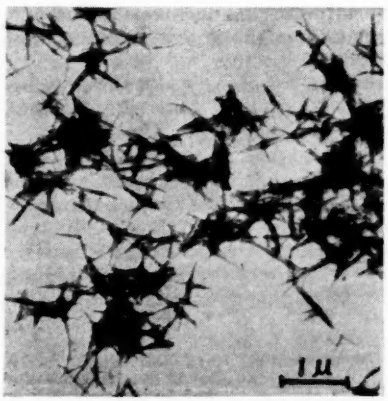

Fig. 6. Crystals in 2 months old ion exchange sol. × 10,000

immediately after preparation hardly grew at all as compared with the original Biltz sol, and an electron micrograph taken for one year old dialyzed sol showed needle crystals, a few μ long, as in Fig. 4.

Müller sol. The crystals in a freshly prepared Müller sol were small fibrils, about 50 mμ long and about 15 mμ thick, similar to those in Biltz sol. After standing for one year, their length was about 400 mμ and after 2 years it was about 1 μ as shown in Fig. 5. That is to say, the fibrous crystals more or less grew like fibers, but the rate of their growth was very small as compared with those of Biltz sol.

Ion exchange sol. The crystals in ion exchange sol were like needles, which were about 1.2 μ long and about 50 mμ thick, as shown in Fig. 6. Many needle crystals crossing at their center are observed in the micrograph. The shape and the size of the crystals are independent of the decomposition time and standing of the sol. A characteristic of the ion exchange sol is that the needle crystals in it do not grow on standing.

The crystals in these three kinds of sol described above were identified as vanadium pentoxide by electron diffraction method, which will de mentioned in the next paper.

Discussion of Results

There are two theories for the growth phenomena of the fibrous crystals in Biltz sol. One is the recrystallization theory and the other is the coagulation theory. Nemtsova[5] found the rapid growth of the crystals in Biltz sol when it was enclosed in a collodion bag and was dipped in saturated vanadium pentoxide solution. Tamamushi[6] reported that the aging of Biltz sol depended upon its adsorption of VO_3^- and H^+ ions on the fibrous crystals. These experiments suggested that the crystal growth in Biltz sol was attributed to the recrystallization. Lukjanovich[7] supported the coagulation theory by his studies of a phenomenon of the adsorption of colloidal silver on the ends of fibrous crystals in Biltz sol. Thiele and Kienast[8] also suggested the coagulation theory. The author will discuss the growth phenomenon by his experimental results as stated below.

The small fibrils in the freshly prepared

5) V. V. Nemtsova, *Doklady Akad. Nauk, USSR*, **79**, 297 (1951); *Chem. Abst.*, **45**, 6013 (1951).

6) B. Tamamushi, *Sci. Paper Coll. Gen. Ed. Univ. Tokyo*, **6**, 37 (1956); cf. H. Tanaka and K. Meguro, *J. Chem. Soc. Japan, Pure Chem. Soc. (Nippon Kagaku Zassi)*, **74**, 49 (1953).

7) A. V. Bromberg, V. M. Lukjanovich, V. V. Nemtsova, L. V. Radushkevich and K. C. Chemutov, *Doklady Akad. Nauk, USSR*, **79**, 281, 827 (1951); **80**, 615 (1952).

8) H. Thiele and G. Kienast, *Kolloid-Z.*, **127**, 134 (1952).

Biltz sol increase their length during the aging process, but the fibrils in the dialyzed Biltz sol, Müller sol, and ion exchange sol hardly grow at all on standing. As indicated in Table I, the concentrations of every sol are almost the same. The amount of the dissolved vanadium pentoxide in Biltz and Müller sols is somewhat greater than that in ion exchange sol at the outset of the standing, but it gradually decreased to a constant value, which is almost the same as the solubility of vanadium pentoside, 0.29 g. per liter[9]. The supersaturated vanadium pentoxide is deposited on the crystals during the aging, but this phenomenon seems not to be the origin of the growth of the fibrils to the very long fibrous crystals in Biltz sol, because the fibrils in Müller sol hardly grow at all on standing.

The main difference between the Biltz sol and the other sols is that of the amount of ammonia contained in the sols. Biltz sol contains about 219 mg. of ammonia per liter, but the Müller and the ion exchange sols contain little and no ammonia respectively. As the acidity of various sols is in the range of pH 2.5 to 3.0, it seems that the greater part of ammonia contained in Biltz sol combines with dissolved vanadium pentoxide (about 1 g. V_2O_5/l.) as ammonium vanadate at the initial stage of aging, and a part of ammonia is adsorbed by the crystals. The growth of the fibrous crystals in Biltz sol seems to be promoted by ammonium ion contained in the sol. Huber and Zbinden[2] prepared vanadium pentoxide sols from various alkali vanadates and indicated that alkali ions resulted from the preparation which promoted the growth of the fibrous crystals in sols and the effect increased with the increase of the atomic weight and the concentration of alkali ions. They also observed that the effect of the ammonium ion was almost the same as that of the potassium ion. It seemed that the vanadium pentoxide crystals in Biltz sol were apt to form ammonium vanadiate in the presence of ammonium ion and that the crystals of vanadium pentoxide were in equilibrium with dissolved ammonium vanadate and were liable to recrystallize.

By an electron microscopic observation, the small fibrils are found besides the long fibrous crystals in aged Biltz sol as shown in Fig. 2. The small fibrils were observed even in 2 months old Biltz sol and seemed to be formed by dissolution of small fibrous crystals.

The author considered that the growth of the fibrous crystals in Biltz sol was caused by Ostwald's ripening which was promoted by the increase of the solubility of the crystals owing to the presence of the ammonium ion in the sol.

9) M. Kerker, G. L. Jones, J. B. Reed, N. P. Yang and M. D. Schvenberg, *J. Phys. Chem.*, **58**, 1147 (1954).

Summary

Vanadium pentoxide sols were prepared by Biltz', Müller's and ion exchange method, and the crystals in the sols were observed with an electron microscope. The crystals in Biltz sol were small fibrils at first, but they grew into long fibrous crystals upon aging. The crystals in Müller and ion exchange sols were fibrils and needles respectively and hardly grew at all. The growth of the fibrous crystals in Biltz sol is likely to be due to the recrystallization of the fibrils.

The author acknowledges the guidance and discussion of Professor Eiji Suito of Kyoto University. He also particularly wishes to express his hearty thanks to Professor Masayoshi Ishibashi of Kyoto University for his discussions and encouragement throughout this investigation.

Institute for Chemical Research
Kyoto University, Takatsuki
Osaka

Studies on Sarkomycin—Preparation of Optically Active 2-Methylenecyclopentanone-3-carboxylic Acids

By Katsuyuki TOKI

(Received August 2, 1957)

Hooper et al.[1] reported in 1955 that the effective ingredient of the natural sarkomycin is 2-methylenecyclopentanone-3-carboxylic acid. Afterwards, the present author[2] synthesized *dl*-2-methylenecyclopentanone-3-carboxylic acid (I), starting from alkyl cyclopentanone-3-carboxylate. Tatsuoka et al.[3] showed that the naturally occurring sarkomycin is in the levoform.

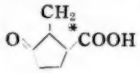

I

In the present paper, the preparation of optically active 2-methylenecyclopentanone-3-carboxylic acids is described.

Since 2-methylenecyclopentanone-3-carboxylic acid is a very unstable compound, and, moreover, is an α,β-unsaturated ketone liable to react with active amines, a direct resolution may be very difficult. As 2-methylenecyclopentanone-3-carboxylic acid has only one asymmetric carbon, preparation from an active intermediate is likely more convenient to obtain it in the optically active form. The use of active cyclopentanone-3-carboxylic acid being suggested, the present author resolved *dl*-cyclopentanone-3-carboxylic acid with brucine which was the best suited for this purpose.

When brucine was combined with *dl*-cyclopentanone-carboxylic acid in aqueous solution, 80% of the expected amount of brucine *d*-cyclopentanone-3-carboxylate was deposited, and the mother liquor gave the nearly pure brucine *l*-cyclopentanone-3-carboxylate on evaporation. Pure salts were obtained in theoretical yields by repeated recystallization from hot water. The active acid and the alkaloid were easily recovered by adding aqueous ammonia or a mineral acid.

When cinchonine was employed, separation of cinchonine *d*- and *l*-cyclopentanone-3-carboxylates required laborious recrystallization. The two optically active 2-methylenecyclopentanone-3-carboxylic acids were synthesized starting from the active cyclopeotanone-3-carboxylic acids by a four-stage process in the same manner as described for the racemic acid. Though ethyl 2-(piperidinomethyl)-cyclopentanone-3-carboxylate (II) from each active cyclopentanone-3-carboxylic acid, the final intermediate prepared by the Mannich reaction, was a mixture of two diastereoisomers, it was used without separation, because separation at this stage was unnecessary for the preparation of active 2-methylenecyclopentanone-3-carboxylic acid.

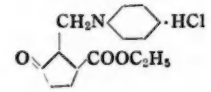

II

The infrared spectra of the synthetic optically active 2-methylene-cyclopentanone-3-carboxylic acids and natural sarkomycin Hooper[1] were essentially identical and exhibited a characteristic peak at 6.1 μ.

Details of the biological studies on the synthetic optically active 2-methylenecyclopentanone-3-carboxylic acid will be published elsewhere.

Experimental

Resolution of Cyclopentanone-3-carboxylic acid with Brucine.—A mixture of 112 g. (0.88 mol.) of racemic cyclopentanone-3-carboxylic acid and 400 g. of brucine-$4H_2O$ was warmed with 2000 ml. of water with stirring to a clear solution. When the solution was allowed to stand overnight in a refrigerator, 580 g. (wet) of silky needles of brucine *d*-cyclopentanone-3-carboxylate, m.p. 110~113°, precipitated. The crude product was recrystallized from hot water several times, m.p. 115~117°, $[\alpha]_D^{25}$ −28.4 (chloroform, C=1.6). Yield 205 g. Further 50 g. of the same substance was obtained on evaporation of the mother liquor and recrystallization. Total yield 255 g.

The combined mother liquor was evaporated to dryness and the residue was recrystallized

* Presented at the meeting of Japan Antibiotic Research Association, at the Institute of Infections Diseases, Tokyo, July 26, 1957.

1) I. R. Hooper et al., *Antibio. & Chem.*, **5**, 588 (1955).
2) K. Toki, This Bulletin, **30**, 450 (1957).
3) S. Tatsuoka et al., *J. Antibio., Ser. B*, **IX** 157 (1956).

from hot water several times to yield 250 g. of brucine *l*-cyclopentanone-3-carboxylate, m.p. 103 ~105°, $[\alpha]_D^{25}$ −38.5 (chloroform, C=1.3).

Brucine *d*-cyclopentanone-3-carboxylate (235 g.) was dissolved in 400 ml. of hot water and then an excess of concentrated aqueous ammonia was added to the solution.

After being cooled overnight in a refrigerator, 200 g. of silky needles of brucine was recovered by filtration. The filtrate was concentrated and acidified with hydrochloric acid. The condensed filtrate was saturated with ammonium sulfate, and extracted with ether. After removal of ether, *d*-cyclopentanone-3-carboxylic acid was distilled at 138~140°/0.2 mm. Yield 55 g. (98.2%), m.p. 66~67°, $[\alpha]_D^{21}$+22.1 (methanol, C=1.9).

Anal. Found: C, 56.20; H, 6.08. Calcd. for $C_6H_8O_3$: C, 56.25; H, 6.25%.

l-Cyclopentanone-3-carboxylate was obtained in the same manner as described above. Yield 53 g. (94.6%) from 250 g. of the brucine salt. b.p. 138~140°/0.2mm., m.p. 65~66°, $[\alpha]_D^{21}$−22.2 (methanol, C=2.0).

Anal. Found: C, 56.23; H, 6.21. Calcd. for $C_6H_8O_3$: C, 56.25; H, 6.25%.

Esterification of *d*- and *l*-Cyclopentanone-3-carboxylic Acids.—A mixture of 55 g. (0.43 mol.) of *d*-cyclopentanone-3-carboxylic acid, 50 g. of absolute ethanol, 80 g. of absolute benzene, and a small amout of *p*-toluenesulfonic acid, was heated on a water bath using a water separater for about eight hours. The reaction mixture was concentrated, poured into ice and aqueous sodium bicarbonate and extracted with ether. After drying over anhydrous sodium sulfate and evaporation, ethyl *d*-cyclopentanone-3-carboxylate was separated by fractional distillation. Yield 55.5 g. (83.7%), b.p. 116~118°/16 mm., n_D^{21} 1.4523, $[\alpha]_D^{21}$+20.0 (methanol, C=1.5).

Anal. Found: C, 61.73; H, 7.66. Calcd. for $C_8H_{12}O_3$: C, 61.54; H, 7.69%.

The 2,4-dinitrophenylhydrazone melted at 172 ~173°.

Anal. Found: C, 49.80; H, 4.93; N, 16.72. Calcd. for $C_{14}H_{16}O_6N_4$: C, 60.00; H, 4.76; N, 16.67%.

Unchanged *d*-cyclopentanone-3-carboxylic acid (6.4 g.) was recovered from the alkaline solution.

A mixture of 53 g. (0.41 mol.) of *l*-cyclopentanone-3-carboxylic acid, 50 g. of absolute ethyl alcohol, 80 g. of absolute benzene, and a small amount of *p*-toluenesulfonic acid, was treated similarly to obtain ethyl *l*-cyclopentanone-3-carboxylate. Yield 56.2 g. (87.80%), b.p. 117°/16 mm, n_D^{24} 1.4510, $[\alpha]_D^{21}$−21.9 (methanol, C=1.6).

Anal. Found: C, 61.49; H, 7.68. Calcd. for $C_8H_{12}O_3$: C, 61.54; H, 7.69%.

The 2,4-dinitrophenylhydrazone melted at 172 −173°.

Anal. Found: C, 49.89; H, 4.98; N, 16.62. Calcd. for $C_{14}H_{16}O_6N_4$: C, 50.00; H, 4.76; N, 16.67%.

Unchanged *l*-cyclopentanone-3-carboxylic acid (4.0 g.) was recovered from the alkaline solution.

Ethyl *d*- and *l*-2-Methylenecyclopentanone-3-carboxylates.—(*a*) *Ethyl d-2-methylenecyclopentanone-3-carboxylate.* A mixture of 10 g. (0.06 mol.) of ethyl *d*-cyclopentanone-3-carboxylate, 7.2 g. (0.06 mol.) of piperidine hydrochloride, and 4.3 g. of 37% formaline, was heated on a water bath at 75~80° with stirring for thirty minutes. After extracting the unchanged ethyl *d*-cyclopentanone-3-carboxylate with ether, the aqueous layer was concentrated to dryness under a reduced pressre. Ethyl 2-(piperidinomethyl)-*d*-cyclopentanone-3-carboxylate hydrochloride was produced in a semi-solid mass. The hydrochloride was purified by recrystallization from methanol for analysis. Yield 9.7 g., m.p. 156° (sinter), $[\alpha]_D^{25}$+37.5 (methanol C=1.6).

Anal. Found: C, 57.86; H, 8.22; N, 4.82. Calcd. for $C_{14}H_{24}O_3NCl$: C, 58.13; H, 8.30; N, 4.84%.

The 2,4-dinitrophenylhdrazone melted at 128 ~130°.

The residual oil separated from the crystals was considered to be a diastereo-isomer of ethyl 2-(piperidinomethyl)-*d*-cyclopentanone-3-carboxylate hydrochloride and could be also used for successing reaction.

The crystalline hydrochloride was disssolved in a amount of water and pH was adjusted to 9~10 with aqueous sodium bicarbonate. The mixture was extracted with ether and the ethereal solution was dried over anhydrous sodium sulfate and evaporated. The residue was distilled under a reduce pressure (90~100°/0.1 mm.).

The distillate was dissolved in ether and the solution was washed with diluted hydrochloric acid to remove piperidine. Thus ethyl *d*-2-methylenecyclopentanone-3-carboxylate was obtained. Yield 1.11 g. (11.0% from ethyl *d*-cyclopentanone-3-carboxylate), $[\alpha]_D^{26}$+15.8 (methanol, C=3.4).

The 2,4-dinitrophenylhydrazone melted at 179 ~180°

Anal. Found: C, 51.70; H, 4.52; N, 16.00. Calcd. for $C_{15}H_{16}O_6N_4$: C, 51.72; H, 4.60; N, 16.09%.

(*b*) *Ethyl l-2-methylenecyclopentanone-3-carboxylate.* A mixture of 10 g. (0.06 mol.) of ethyl *l*-cyclopentanone-3-carboxylate, 7.2 g. (0.06 mol.) of piperidine hydrochloride, and 4.3 g. of 37% formaline, was treated in the same manner as mentioned above. Ethyl 2-(piperidinomethyl)-*l*-cyclopentanone-3-carboxylate hydrochloride was obtained in this way. Yield 9.3 g., m.p. 155° (sinter), $[\alpha]_D^{23}$−37.3 (methanol, C=1.6).

The residual oil separated from the crystals was considered a diastereo-isomer of ethyl 2-(piperidinomethyl)-*l*-cyclopentanone-3-carboxylate hydrochloride and could be used for next reaction.

Anal. Found: C, 57.89; H, 8.19; N, 4.80. Calcd. for $C_{14}H_{24}O_3NCl$: C, 58.13; H, 8.30; N, 4.84%.

The 2,4-dinitrophenylhydrazone melted at 129 ~131°.

Ethyl *l*-2-methylenecyclopentanone-3-carboxylate was obtained by heat decomposition. Yield 0.89 g. (8.8% from ethyl *l*-cyclopentanone-3-carboxylate), $[\alpha]_D^{23}$−15.4 (methanol, C=1.3).

The 2,4-dinitrophenylhydrazone melted at 179 ~180°.

Anal. Found: C, 51.70; H, 4.48; N, 16.07. Calcd. for $C_{15}H_{16}O_6N_4$: C, 51.72; H, 4.60; N, 16.09%.

***d*- and *l*-2-Methylenecyclopentanone-3-carboxylic Acids.**—(*a*) *d-2-Methylenecyclopentanone-*

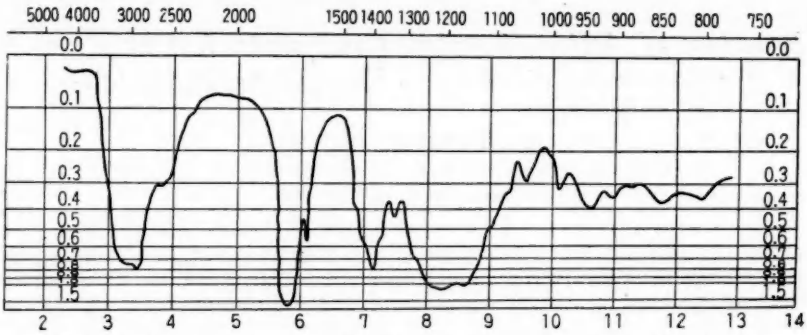

Fig. 1. Infrared spectrum of *d*-2-methylenecyclopentanone-3-carboxylic acid.

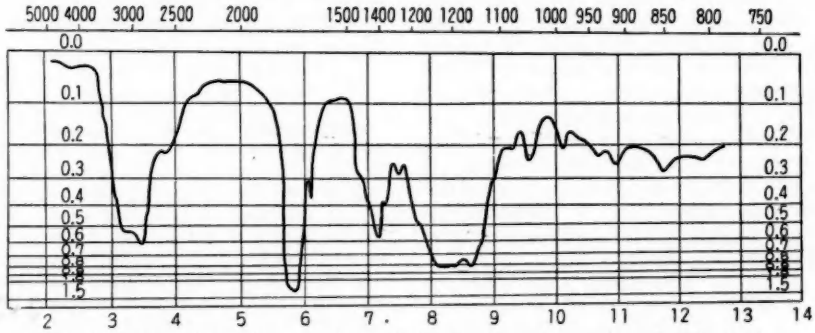

Fig. 2. Infrared spectrum of *l*-2-methylenecyclopentanone-3-carboxylic acid.

3-carboxylic acid. A mixture of 3.5 g. of ethyl *d*-2-methlenecyclopentanone-3-carboxylate and 35 ml. of a 5% acetone solution of the hydrochloride was allowed to stand at 20° for ten hours, and then an equivalent amount of aqueous sodium dicarbonate was added to the mixture with cooling. After removal of acetone under a reduced pressure, the aqueous layer was shaken with ether to recover the unchanged ester. The aqueous layer was then acidified with dilute hydrochloric acid with cooling, saturated with ammonium sulfate, and extracted with ethyl acetate. The ethyl acetate solution was concentrated under a reduced pressure. *d*-2-Methylenecyclentanone-3-carboxylic acid was obtained in a pale yellow oil in a yield of 0.85 g. (29.0%), $[\alpha]_D^{23}$ +28.9 ** (ethylacetate, C=1.6). The infrared spectrum is shown in Fig. 1.

Anal. Found: C, 59.81; H, 5.43. Calcd. for $C_7H_8O_3$: C, 60.00; H, 5·71%.

(*b*) *l-2-Methylenecyclopentanone-3-carboxylic acid.*—*l*-2-Methylenecyclopentanone-3-carboxylic acid (2.2 g.) was obtained in the same manner as mentioned above. Yield 0.39 g. (21.5% from 2.2 g. of the corresponding ethyl ester), $[\alpha]_D^{23}$ −28.4 **(ethyl acetate, C=1.6). Fig. 2. shows the infrared spectrum of the substance.

Anal. Found: C, 59.62; H, 5.31. Calcd. for $C_7H_8O_3$: C, 60.00; H, 5.71%.

** The values will be flexible becouse of the unstability of 2-methylenecyclopentanone-3-carboxylic acid.

Both *d*- and *l*-2-methylenecyclopentanone-3-carboxylic acid showed essentially identical infrared absorption as natural sarkomycin (Hooper[1]).

Summary

d- and *l*-2-Methylenecyclopentanone-3-carboxylic acid were synthesized starting from optically active cyclopentanone-3-carboxylic acid obtained by resolution of the racemic acid with brucine, and both *d*- and *l*-isomer, thus obtained, showed the same infrared absorption as natural sarkomycin (Hooper).

Thanks are due to Professor Shiro Akabori of Osaka University, Professor Hamao Umezawa of the National Institute of Health of Japan, and Professor Masanao Matsui of Tokyo University for their continous interest and encouragement through this investigation.

The author is also indebted to Mr. Naofumi Ohi and his associates for infrared analyses, to Mr. Noboru Nishimura and his associates for microanalyses, to Mr. Chiharu Saito for biological tests, and to Messrs. Hiroo Wada and Yoshio Suzuki for their helpful collaborations.

Sumitomo Chem. Co. Ltd.
Osaka Works

Reactions of Active Methylene Compounds. I. Alkylation of Cyclohexanone via Ethyl 2-Ketocyclohexylglyoxalate

By Yoshiyuki KAWASE

(Received February 19, 1957)

Alkylations of cyclohexanone derivatives are usually carried out by two methods, A and B shown in Chart I. The procedure of method A involves only one step employing sodium amide or potassium *t*-butoxide, and the ketone is alkylated at the α-carbon atom having less hydrogen according to the extended Saytzeff rule[1], but the product is contaminated with polyalkylated compounds. In the case of method B, the ketone is alkylated in the unsubstituted α-methylene group according to the Hofmann rule and the product is obtained in pure state, but the procedure involves many steps, namely, carbethoxylation (or formylation), alkylation, and hydrolytic decomposition.

A method of alkylation analogous to method B was reported by A. Kötz et al.[2] in 1912, in which substituted ethyl 2-ketocyclohexylglyoxalate was alkylated and the product was decomposed to alkylketone by alkaline hydrolysis. But this method has not often been used hitherto[1a,3].

Here, A. Kötz's method has been studied, and seems to be better than method B when the alkylation according to the Hofmann rule is desired. In this paper, some alkylations of cyclohexanone via ethyl 2-ketocyclohexylglyoxalate, which have not yet been reported, are described.

The sodio compound of ethyl 2-ketocyclohexylglyoxalate (I), prepared from cyclohexanone and ethyl oxalate in absolute ethanol without isolation, was refluxed with an alkylating reagent such as methyl iodide, benzyl bromide, ethyl bromoacetate, and 1-(diethylamino)-3-pentanone methyl iodide. (see Table).

As the alkylated product was obtained together with ethyl oxalate without hydrolysis, it seemed that the intermediate ethyl 1-alkyl-2-ketocyclohexylglyoxalate (II) was liable to cleave to alkylcyclohexanone and ethyl oxalate in ethanol. (see Chart II). In the case of methylation, 2-methylcyclohexanone (III) was purified by alkaline hydrolysis as it was contaminated by ethyl oxalate, and it seemed that the yield of ethyl 2-ketocyclohexylacetate (V) was lowered by secondary condensation of the product.

Experimental[4]

Preparation of 2-Methylcyclohexanone (III). (*a*) *From Cyclohexanone.*—A mixture of 19.6 g. of cyclohexanone and 29.2 g. of ethyl oxalate was slowly added with stirring below 10° to the sodium ethoxide solution (4.5 g. of sodium in 100 ml. of absolute ethanol) according to H.R. Snyder et al.'s method[5], and the mixture was allowed to stand overnight at room temperature. The was mixture heated at 70~80° for six hours with 40 g. of methyl iodide with stirring. After the solvent was evaporated, the cooled residue was diluted with water and extracted with ether. The ethereal solution was washed with water, fully dried on calcium chloride, and evaporated. By distillation of the residue, crude 2-methylcyclohexanone (III) was obtained in colorless oil boiling at 164~177° (mainly at 164~169°)[6]. Yield, 15 g. (68% of the theory from cyclohexanone). It was purified by hydrolysis with 30% aqueous sodium hydroxide, acidification, extraction with ether, drying on calcium chloride and distillation. From the aqueous mother solution of ether extraction, oxalic acid was obtained. The pure III was colorless oil boiling at 162~5°. Yield, 8.5 g. (40% of the theory from cyclohexanone), and gave semicarbazone, m.p. 189.5~190.5° (from ethanol).

Anal. of semicarbazone. Found: C, 56.87; H, 8.87; N, 24.82. Calcd. for $C_8H_{15}ON_3$: C, 56.87; H, 8.94; N, 24.83%.

The m.p. of semicarbazone showed no depression on admixture with an authentic sample, which was prepared in 30.5% yield from cyclohexanone by method B—a. Reported b.p. of III and m.p. of semicarbazone are 165° and 192° (prepared by method B—b)[7] respectively.

(*b*) *From Ethyl 2-Ketocyclohexylglyoxalate.*—

1) a) R. Cornubert et al., *Bull. soc. chim.*, (4) **49**, 1229 (1931); b) H. M. E. Cardwell, *J. Chem. Soc.*, **1951**, 2442.
2) A. Kötz et al., *Ber.*, **45**, 3702 (1912); *J. pr. Chem.*, (ii) **88**, 257 (1913); ibid., **90**, 382 (1914).
3) O. Wallach, *Ann.*, **397**, 197 (1913); ibid., **414**, 219 (1916).
4) Melting and boiling points are uncorrected.
5) H. R. Snyder, L. A. Brookes and S. H. Shapiro, "Org. Synth." Coll. Vol., **II**, 531 (1943).
6) Almost pure III was obtained in 70% yield by distillation under diminished pressure (b. p. 84°/50mm.).
7) H. K. Sen and K. Mondal, *J. Indian Chem. Soc.*, **5**, 621 (1928).

Chart I

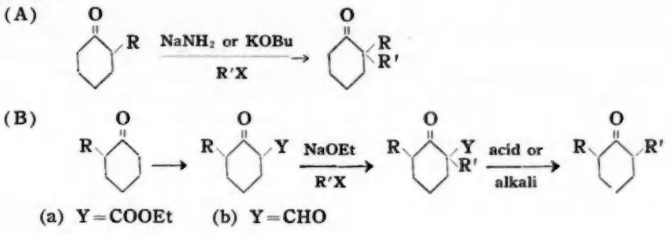

Chart II

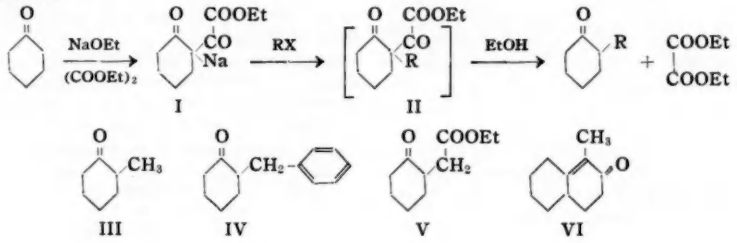

TABLE

Reagent	Reac. temp. (°C) & time (hr.)	Product	b.p. (°C/mm.)	m.p. (°C) of the deriv.[i]	Yield in %[ii]
MeI	70~80; 6	III	162~5	189.4~190.5 Se	40.
MeI	70~80; 6	III	159~161	189 Se	36.[iii]
MeI	method B—a	III	84/50	189 Se	30.5
$PhCH_2Br$	70~80; 7	IV	162~5/16[iv]	165~6 Se	60.
$PhCH_2Cl$	80~90; 8	IV	164~171/17	167~8 Se	37.2
$BrCH_2COOEt$	80~90; 6	V	131~142/17	194~5 Se	13.6
$BrCH_2COOEt$	method A	V	126~135/16	192~192.5 Se	43.
[v]	room tem.; 3 hr. then 80~90°; 2 hr.	VI	140~5/17	216 (dec.) Se 177 Dn	21.
[v]	method B—a	VI	136~140/15	213~4 (dec.) Se 175~7 Dn	16.8

i) Se and Dn mean semicarbazone and 2,4-dinitrophenylhydrazone, respectively.
ii) Yields were calculated from cyclohexanone.
iii) Ethyl 2-ketocyclohexylglyoxalate was isolated.
iv) M.p. was 28~31°.
v) 1-(diethylamino)-3-pentanone methyl iodide.

Ethyl 2-ketocyclohexylglyoxalate[5] (20 g.) was dropped into an absolute ethanol solution of sodium ethoxide (2.3 g. of sodium in 50 ml. of absolute ethanol) and the mixture was heated with 20 g. of methyl iodide at 70~80° for six hours, and treated as usual. Crude III distilled at 160~175° (mainly at 160~5°). Yield, 8.5 g. (75% of the theory). The pure III was obtained by purification in the same way as above, b.p. 159~161°. Yield, 6 g. (55%), and gave semicarbazone, m.p. 189° (from ethanol).

Preparation of 2-Benzylcyclohexanone (IV).—The sodio compound (I), prepared from 9.8 g. of cyclohexanone in the same way, was mixed with 17.1 g. of benzyl bromide, and the mixture was heated at 70~80° for seven hours. After the usual treatment, two fractions were obtained by vacuum distillation, that is fraction (i), b.p. 76~81°/17 mm. (10 g.), and fraction (ii), b.p. 162~177°/17 mm. (mainly 162~7°) (11.5 g.). As fraction i gave oxalic acid by alkaline hydrolysis, it seemed to consist mainly of diethyl oxalate, corresponding to about 60% of the amount initially used. By redistillation of fraction ii, 2-benzylcyclohexanone (IV) was obtained in colorless oil boiling at 162~5°/16 mm., and it crystallized afterwards, m.p. 28~31° (yield, 60% of the theory from cyclohexanone). It gave semicarbazone, m.p. 165~6° (from ethanol).

Anal. of semicarbazone. Found: C. 68.88; H. 7.84; N, 17.72. Calcd. for $C_{14}H_{19}ON_3$: C, 68.54; H, 7.81; N, 17.13%.

The m.p. of semicarbazone showed no depres-

sion on admixture with the authentic sample, prepared by method A[8]. Reported b.p. of IV and m.p. of semicarbazone are 165~6°/18 mm. and 166~7°[8] respectively. When the benzylation was carried out with benzyl chloride, instead of bromide, at 80~90° for eight hours, the yield was 37.2%.

Preparation of Ethyl 2-Ketocyclohexylacetate (V).—To the sodio compound (I) prepared from 9.8 g. of cyclohexanone, 16.7 g. of ethyl bromoacetate was added and the mixture was refluxed for six hours. After a similar treatment as described above, 10 g. (64% recovery) of ethyl oxalate, b.p. 81°/17 mm., and 2.5 g. (13.6% yield) of ethyl 2-ketocyclohexylacetate (V), b.p. 131~142°/17 mm. were obtained, and the latter gave semicarbazone, m.p. 194~5° (from ethanol).

Anal. of semicarbazone. Found: C, 54.83; H, 7.93; N, 17.44. Calcd. for $C_{11}H_{19}O_3N_3$: C, 54.75; H, 7.93; N, 17.41%.

The m.p. of semicarbazone showed no depression on admixture with the authentic sample, prepared by method A as follows: to the sodio compound of cyclohexanone, prepared from 10 g. of cyclohexanone and 4 g. of sodium amide in absolute ether, 17 g. of ethyl bromoacetate was added and the mixture was refluxed for six hours. By the usual treatment, ethyl 2-ketocyclohexylacetate (V) was obtained in colorless oil, boiling at 126~135°/16 mm. (yield, 8 g. or 43%), and gave semicarbazone, m.p. 192~192.5°.

Anal. of semicarbazone. Found: C, 54.85; H, 7.89; N, 17.50. Calcd. for $C_{11}H_{19}O_3N_3$: C, 54.75; H, 7.93; N, 17.41%.

Reported b.p. of V is 131~3°/9.8 mm. (25.4% yield from cyclohexanone by method B—a) and m.p. of semicarbazone is 191~3°[9].

Preparation of 2-Keto-1-methyl-2,3,4,5,6,-7,8,10-octahydronaphthalene (VI).—To the sodio compound (I) prepared from 9.8 g. of cyclohexanone, 1-(diethylamino)-3-pentanone methyl iodide (from 15.7 g. of amine and 14.2 g. of methyl iodide in 20 ml. of ethanol) was added and the mixture was allowed to stand at room temperature for three hours, and then refluxed for two hours. The solvent was evaporated, the residue was diluted with water, extracted with ether, the ethereal solution was washed with dilute hydrochloric acid and water, dried and evaporated. After the residue was refluxed with 50 ml. of 40% aqueous potassium hydroxide in 20 ml. of ethanol for fifteen hours, the resulting mixture was diluted with water, extracted with ether, the ethereal solution was washed with water, dried and evaporated. By the distillation of the residue, 3.4 g. (21% yield) of 2-keto-1-methyl-octahydronaphthalene (VI) was obtained in colorless oil boiling at 140~5°/17 mm. and gave 2,4-dinitrophenylhydrazone, m.p. 177° (from ethanol), and semicarbazone, m.p. 216° (decomp.) (from ethanol).

Anal. of 2,4-dinitrophenylhydrazone. Found: C, 59.37; H, 5.57; N, 15.39. Calcd. for $C_{17}H_{20}O_4N_4$: C, 59.29; H, 5.85; N, 16.29%. *Anal.* of semicarbazone. Found: C, 65.14; H, 8.38; N, 18.70. Calcd. for $C_{12}H_{19}ON_3$: C, 65.12; H, 8.65; N, 18.99%.

Their m.p. showed no depression on admixture with the authentic samples, prepared by method B—a according to the method of Robinson[10] as follows: to the sodio compound prepared from 7.4 g. of ethyl 2-ketocyclohexylcarboxylate and sodium ethoxide (from 2.3 g. of sodium) in absolute ethanol, 1-(diethylamino)-3-pentanone methyl iodide (from 6.8 g. of amine and 6.2 g. of methyl iodide) was added and the mixture was allowed to stand at room temperature for three hours and then refluxed for two hours. Then the product was cyclized and hydrolyzed into VI by refluxing with 40% aqueous potassium hydroxide in ethanol for fifteen hours. The product VI was colorless oil boiling at 136~140°/15 mm. (yield, 2 g. or 16.8% from cyclohexanone), and gave 2,4-dinitrophenylhydrazone, m.p. 175~7°, and semicarbazone, m.p. 213~4° (decomp.). Reported b.p. of VI is 125~7°/8 mm. (22% yield from cyclohexanone by the method described in footnote) and m.p. of semicarbazone is 212° (decomp.)[11].

The author wishes to express his hearty thanks to Professor K. Fukui for his helpful advice and encouragement, to Professor Y. Yukawa of Osaka University for his valuable discussion during the course of this work and to the members of Agricultural Department of Kyoto University for microanalyses.

Faculty of Literature and Science
Toyama University, Toyama

8) M. Tiffeneau and M. Porcher, *Bull. soc. chim.*, (4) **31**, 330 (1922).
9) Chang-Kong Chuang and Chi-Ming Ma, *Ber.*, **68B**, 871 (1935).
10) E. C. Du Feu, F. J. McQuillin, and R. Robinson, *J. Chem. Soc.*, **1937**, 53.
11) D. K. Banerjee, S. Chatterjee and S. P. Bhattacharaya, *J. Am. Chem. Soc.*, **77**, 408 (1955).

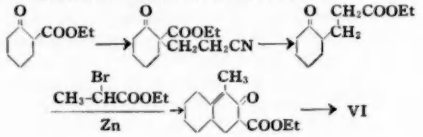

Partial Hydrogenation of 1, 4-Butynediol

By Tosao FUKUDA and Tokishige KUSAMA

(Received October 2, 1957)

For the partial catalytic hydrogenation of acetylenic compounds in the liquid phase, it is necessary to stop the hydrogenation purposely when one molecule of hydrogen has reacted. If we can, however, retard the hydrogenation of ethylenic compounds by some means other than that of acetylenic compounds, the preparation of ethylenic compounds will be simple.

Recently, O. Isler et al.[1] found that the palladium-charcoal catalyst was poisoned by quinoline hydrogenated acetylenic compounds to the corresponding ethylenic compounds, but not to the corresponding saturated compounds. H. Lindler[2] also observed similar phenomena in the hydrogenation of some acetylenic compounds with the palladium calcium-carbonate catalyst poisoned by lead acetate, with the addition of quinoline. W. Oroshnic et al.[3] and B. Elsner et al.[4] found that with the Raney nickel catalyst poisoned by zinc acetate and copper acetate, the hydrogenation of ethylenic compounds was selectively retarded by the addition of piperidine. Since then, some application of these methods have been developed[5].

It was shown that, when the palladium catalyst is poisoned, the hydrogenating activity for acetylenic compounds and that for ethylenic compounds are decreased at different rates[6]. It was also found that, in the case of nitrobenzyl chloride, the hydrogenation takes place selectively when quinoline is added[7]. However, the mechanism of the partial hydrogenation of acetylenic compounds has not clearly been explained.

The present paper describes the experimental results of the hydrogenation of 1, 4-butynediol carried out with the Pd-$CaCO_3$ catalyst poisoned by lead acetate and the poisons, and the partial hydrogenation achieved by using Pd-$CaCO_3$ catalyst with quinoline.

Experimental

Apparatus.—An about 300 cc. usual glass vessel shaken at a constant oscillation was employed.

Materials.—1, 4-Butynediol was recrystallized several times from ethyl acetate. Commercial hydrogen was used. Calcium carbonate was of a commercial extra pure grade (Koso Chemical Co., Tokyo).

Procedures.—Pd-$CaCO_3$ catalyst (Pd-content, 5% by wt.) was prepared from palladium chloride solution according to Lindler[1]. Its poisoning with lead acetate was carried out by adding various amounts of aqueous lead acetate (5g. of $(AcO)_2Pb \cdot 3H_2O$ in 100 cc. of water) to 2 g. of the catalyst. Aqueous 1, 4-butynediol was used. Catalytic hydrogenation was carried out at room temperature (12°~16°C) and at atmospheric pressure, with 250~300 turns oscillation.

Results.—The overall hydrogenation of 1, 4-butynediol proceeded in two distinct steps as shown in Fig. 1. When 30 g. (0.35 mol.) of 1, 4-butynediol in 150 cc. of water was hydrogenated on Pd-$CaCO_3$ catalyst, 8.5 l. (N. T. P.), or 0.38 mol., of hydrogen was absorbed, and the following products were obtained by the distillation of the reaction mixture.

Purified raw material		28 g.
Distillates	i~102°C/3 mmHg	2 g.
	102°~107°C/3 mmHg	19 g.
Decomposed product (found in the trap)		0.7 g.
Residue		5 g.

The product distilling at 102°~107°C/3 mmHg was proved to be a *cis*- and *trans*-1, 4-butenediol mixture by the infrared spectrographic analysis, and found to contain 0.0110 mol. double bond per one gram substance by bromine addition, the theoretical value for pure 1, 4-butenediol being 0.0116 mol.

Fig. 1 shows that the hydrogenation takes place mainly at 1, 4-butynediol in the first step, and then at 1, 4-butenediol. Hydrogenation was carried out with various concentrations of 1, 4-butynediol, 0.3 g. of Pd-$CaCO_3$ being used. The dependency of the initial velocity of the hydrogenation upon the concentration of 1, 4-butynediol is shown in Fig. 2.

1) O. Isler, et al.; *Helv. chim. Acta*, **30**, 1911 (1947).
2) H. Lindler; ibid., **35**, 446 (1952).
3) W. Oroshnik, G. Karmas and A. D. Mcbane; *J. Am. Chem. Soc.*, **74**, 295 (1952).
4) B. B. Elsner and P. F. M. Paul; *J. Chem. Soc.*, **1953**, 3156.
5) a) K. Hofmann and S. M. Sax, *J. Biol. Chem.*, **205**, 55 (1953): see also, L. Luzika and P. Muller, *Helv. chim. Acta*, **22**, 755 (1939); b) J. L. H. Allan, E. R. H. Jones and M. C. Whiting; *J. Chem. Soc.*, **1955**, 1862; c) W. Orcshnic, G. Karmas and A. D. Mcbane, *J. Am. Chem. Soc.*, **74**, 3807 (1952): P. Karrer and J. Kebele, *Helv. chim. Acta*, **35**, 2570 (1952).
6) K. Tamaru, This Bulletin. **23**, 180 (1950).
7) K. W. Rosenmond and F. Zetzsche, *Ber.*, **54**, 425 (1921).

The acivation energies of the hydrogenation were calculated to be 2.7 kcal./mol. for 1,4-butynediol and 5.2 kcal./mol. for 1,4-butenediol, from the hydrogenation experiments at 0°C and 30°C. The results of poisoning of Pd-$CaCO_3$ catalyst by lead acetate are schematically shown in Fig. 3 and Fig. 4. When 0.3 cc. of pyridine, piperidine, or quinoline was added to the reactant, the hydrogenation proceeded as shown in Fig. 5.

When 30 g. (0.35 mol.) of 1,4-butynediol in 150 cc. of water was hydrogenated with Pd-$CaCO_3$ catalyst in the presence of 0.3 cc. of quinoline, 8.2 l. (N. T. P.), or 0.37 mol. of hydrogen was absorbed, and then the reaction stopped. From the reaction mixture, the following products were obtained.

Puriefied raw material		29 g.
Distillates	i~102°C/3 mmHg	1 g.
	102°~107°C/3 mmHg	22 g.
Decomposed product (found in the trap)		1 g.
Residue		5 g.

The product distilling out at 102°~107°C/3 mmHg was proved to be a mixture of *cis*- and *trans*-1,4-butenediol by the infrared spectrographic analysis, and found to contain 0.0112 mol. double bond per one gram substance by bromine addition.

The Pd-$CaCO_3$ catalyst poisoned by lead acetate was used with 0.3 cc. of pyridine, piperidine or quinoline. The results are schematically shown in Figs. 6~8.

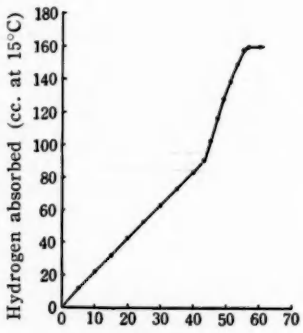

Fig. 1. The hydrogenation rate on Pd-$CaCO_3$ catalyst.

Pd-$CaCO_3$	0.30 g.
aqueous butynediol	20 cc. (butynediol, 0.34 g.)
experimental temp.	15°C

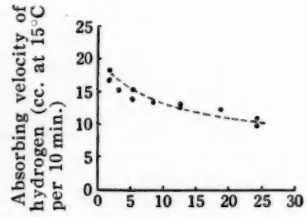

Fig. 2. The effect of the concn. of butynediol on the hydrogenation rate.

Pd-$CaCO_3$	0.30 g.
aqueous butynediol	20 cc.
experimental temp.	15°C

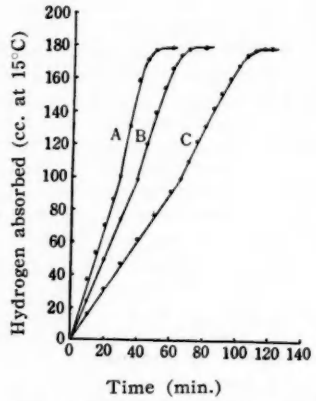

Fig. 3. The effect of lead acetate on the hydrogenating activity of Pd-$CaCO_3$ catalyst.

Pd-$CaCO_3$ poisoned by lead acetate 0.30 g.
aqueous butynediol 20 cc. (butynediol, 0.34 g.)
experimental temp. 15°C
A: the catalyst poisoned by 0.5 cc. of aqueous lead acetate
B: the catalyst poisoned by 2.0 cc. of aqueous lead acetate
C: the catalyst poisoned by 5.0 cc. of aqueous lead acetate

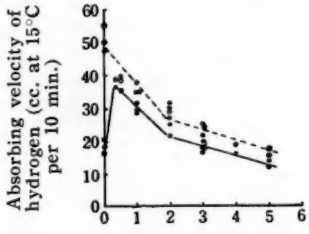

Fig. 4. The effect of lead acetate on the hydrogenating activity of Pd-$CaCO_3$ catalyst.

Pd-$CaCO_3$ poisoned by lead acetate 0.30 g.
aqueous butynediol 20 cc. (butynediol, 0.34 g.)
experimental temp. 15°C
●: the hydrogenation rate in the 1st step
○: the hydrogenation rate in the 2nd step

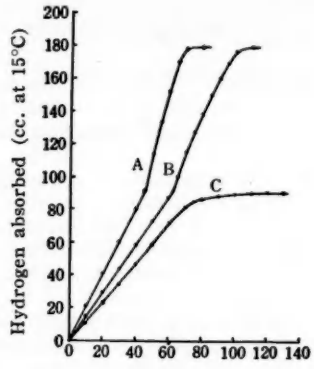

Fig. 5. The effect of poisons on the hydrogenating activity of Pd-$CaCO_3$ catalyst.
Pd-$CaCO_3$ 0.30 g.
aqueous butynediol 20 cc.
(butynediol, 0.34 g.)
experimental temp. 15°C
A: 0.3 cc. of pyridine was added
B: 0.3 cc. of piperidine was added
C: 0.3 cc. of quinoline was added

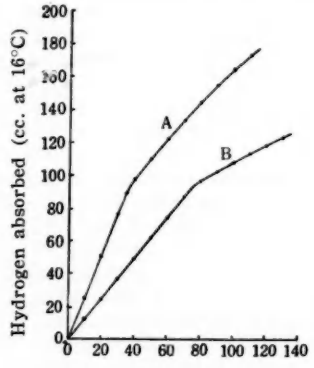

Fig. 6. The effect of pyridine on the hydrogenating activity of the Pd-$CaCO_3$ catalyst poisoned by lead acetate.
Pd-$CaCO_3$ poisoned by lead acetate 0.30 g.
aqueous butynediol 20 cc.
(butynediol, 0.34 g.)
pyridine 0.3 cc.
experimental temp. 16°C
A: the catalyst poisoned by 1.0 cc. of aqueous lead acetate
B: the catalyst poisoned by 5.0 cc. of aqueous lead acetate

Discussion

The hydrogenation of 1,4-butynediol with Pd-$CaCO_3$ catalyst at room temperatures takes place in two distinct steps; the first step is the hydrogenation to 1,4-butenediol, and the second step is its hydrogenation to 1,4-butanediol. The effect of lead acetate and the poisons were

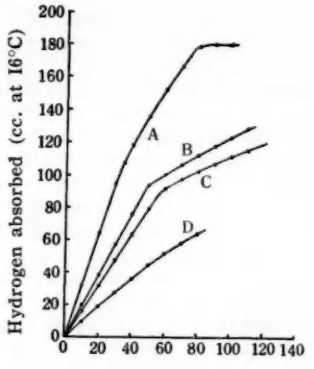

Fig. 7. The effect of piperidine on the hydrogenating activity of the Pd-$CaCO_3$ catalyst poisoned by lead acetate.
Pd-$CaCO_3$ poisoned by lead acetate 0.30 g.
aqueous butynediol 20 cc.
(butynediol, 0.34 g.)
piperidine 0.3 cc.
experimental temp. 16°C
A: the catalyst poisoned by 0.5 cc. of aqueous lead acetate
B: the catalyst poisoned by 0.7 cc. of aqueous lead acetate
C: the catalyst poisoned by 0.9 cc. of aqueous lead acetate
D: the catalyst poisoned by 1.5 cc. of aqueous lead acetate

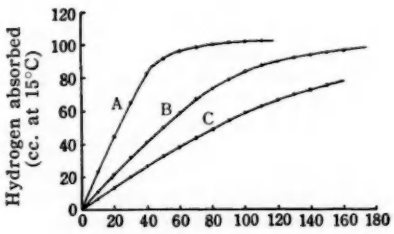

Fig. 8. The effect of quinoline on the hydrogenating activity of the Pd-$CaCO_3$ catalyst poisoned by lead acetate.
Pd-$CaCO_3$ poisoned by lead acetate 0.30 g.
aqueous butynediol 20 cc.
(butynediol, 0.34 g.)
quinoline 0.3 cc.
experimental temp. 15°C
A: the catalyst poisoned by 0.2 cc. of aqueous lead acetate
B: the catalyst poisoned by 0.7 cc. of aqueous lead acetate
C: the catalyst poisoned by 1.0 cc. of aqueous lead acetate

found to be very interesting. When Pd-$CaCO_3$ catalyst is poisoned by increasing amount of lead acetate, the activity for the hydrogenation of 1,4-butynediol increases at first, and then gradually decreases as the poisoning proceeds. On the other hand, that for the hydrogenation of 1,4-butenediol simply decreases with increasing amount of lead acetate. The hydrogenation of 1,4-butynediol is slightly retarded by quinoline, but not by pyridine or piperidine. On the other hand, the hydrogenation of 1,4-butenediol is retarded to some extent by pyridine, more markedly by piperidine and stopped almost completely by quinoline. The effect of these bases is almost the same when they are applied to the Pd-$CaCO_3$ catalyst poisoned by lead acetate. Accordingly, the partial hydrogenation of 1,4-butynediol can be achieved by the use of quinoline.

The reaction velocity in the first step of the hydrogenation is approximated by the following equation, which indicates the retardation of the hydrogenation by 1,4-butynediol,

$$-\frac{dV}{dt}=\frac{k}{1+bC}$$

where V denotes the volume of hydrogen absorbed, t, the time, C, the concentration of 1,4-butynediol, and k and b stand for constants. The retardation may result from the strong adsorption of 1,4-butynediol on the catalyst surface. This theory may be supported by the fact that 1,4-butynediol is adsorbed on the catalyst surface prior to 1,4-butenediol, and the latter is unable to be adsorbed while the former is present. Thus, the hydrogenation may take place in two distinct steps.

The phenomena found on the Pd-$CaCO_3$ catalyst poisoned by lead acetate indicate that the properties of the catalyst are changed by the adsorption of lead acetate. It may be stated that, when pyridine, piperidine, or quinoline is added, these substances are adsorbed on the catalyst surface, even when 1,4-butynediol (or lead acetate and 1,4-butynediol) has been adsorbed previously. The properties of the catalyst surface may also be affected by the adsorption of these bases. Their effect on the palladium catalyst might be different from that of lead acetate. Consequently, the selective hydrogenation may take place as observed.

Summary

1. The effect of lead acetate and the poisons on the Pd-$CaCO_3$ catalyst was studied with the hydrogenation of 1,4-butynediol.

2. The hydrogenation of 1,4-butynediol with the Pd-$CaCO_3$ catalyst at room temperatures takes place in two distinct steps; the first step is the hydrogenation to 1,4-butenediol, and the second is its hydrogenation to 1,4-butanediol.

3. When Pd-$CaCO_3$ catalyst is poisoned by increasing amount of lead acetate, the activity for the hydrogenation of 1,4-butynediol increases at first, and then gradually decreases as the poisoning proceeds. On the other hand, that for the hydrogenation of 1,4-butenediol simply decreases with increasing amount of lead acetate.

4. The hydrogenation of 1,4-butynediol with Pd-$CaCO_3$ catalyst is slightly retarded by quinoline, but not by pyridine or piperidine. On the other hand, the hydrogenation of 1,4-butenediol is retarded to some extent by pyridine, more markedly by piperidine, and stopped almost completely by quinoline. The effect of these bases is almost the same when they are applied to the Pd-$CaCO_3$ catalyst poisoned by lead acetate.

5. The partial hydrogenation of 1,4-butynediol can be achieved by using quinoline, but not by using pyridine or piperidine.

6. The selective hydrogenation may result from the strong adsorption of 1,4-butynediol on the catalyst surface. When the catalyst adsorbs the poisons, the properties of the catalyst surface may be changed. As a result, the selectivity of the catalyst may become very characteristic. Consequently, the selective hydrogenation may take place as observed.

This study was carried out in the Institute of Carbide Chemistry, Yokohama National University, and the cost was defrayed from the Institute. The assistance of Industrial Research Institute of Kanagawa Prefecture, in the infrared spectrographic analysis is gratefully acknowledged. The authors are also indebted to Professor K. Tamaru, for his valuable advice on this study.

Faculty of Engineering
Yokohama National University
Minami-ku, Yokohama

Partial Hydrogenation of 1, 4-Butynediol. II. On the Role of Calcium Carbonate as a Carrier of the Palladium Catalyst

By Tosao FUKUDA

(Received January 20, 1958)

As previously reported[1], when palladium-calcium carbonate catalyst was poisoned by lead acetate, the activity for the hydrogenation of 1,4-butenediol decreased with increasing amount of lead acetate, but was not suppressed completely. When it was poisoned by quinoline, the activity for the hydrogenation of 1,4-butenediol disappeared almost completely, while that for the hydrogenation of 1,4-butynediol decreased only slightly. On the other hand, when Pd-$CaCO_3$ catalyst was poisoned by pyridine or piperidine, the activity for the hydrogenation of 1,4-butenediol decreased only to some extent and did not disappear. When the Pd-$CaCO_3$ catalyst poisoned by lead acetate was poisoned furthermore by quinoline, similar results were obtained. Consequently, it has been shown that the partial hydrogenation of 1,4-butynediol can be achieved by using the Pd-$CaCO_3$ catalyst with quinoline.

However, it is well-known that the properties of a catalyst occasionally depend upon the kind of the carrier on which it is deposited[2]. Accordingly, the selectivity of the catalyst would also be associated with the kind of the carrier. Therefore, the effect of calcium carbonate as a carrier was studied in the hydrogenation of 1,4-butynediol. This paper describes the experimental results and the consideration on the role of calcium carbonate as a carrier of Pd-$CaCO_3$ catalyst.

Experimental

The same apparatus as previously described was employed[1].

1,4-Butynediol was recrystallized several times from ethyl acetate. Commercial hydrogen was used. Calcium carbonate, active charcoal, alumina, silica gel, and Kieselguhr were all obtained from the commercial products. Barium carbonate and barium sulfate were prepared from barium chloride and sodium carbonate and sulfuric acid, respectively.

Various catalysts were prepared from aqueous solutions of palladium (II) chloride by H. Lindler's method[3].

Twenty cc. of an aqueus solution of 0.34 g. of 1,4-butynediol was used. The hydrogenation experiments were carried out at 25°C and at about the atmospheric pressure, with 200 turns oscillation, using 0.3—0.6 g. of the catalyst.

Results and Discussion

With various catalysts the whole hydrogenation of 1,4-butynediol took place in two distinct steps at room temperature. The first step is the hydrogenation of 1,4-butynediol to 1,4-butenediol and the second is that of the latter to 1,4-butanediol, as shown in the previous paper[1].

The absorbing velocity of hydrogen depended upon the kind of the carrier

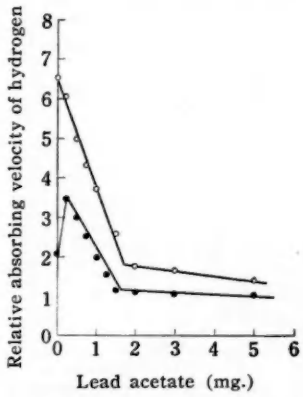

Fig. 1. The poisoning effect of lead acetate on the activities of Pd-$CaCO_3$ catalyst, at 25°C.
Pd-$CaCO_3$ catalyst (Pd, 5%) 0.3 g.
1,4-butynediol solution 20 (1,4-butynediol, 0.34 g.)
●: the effect on the hydrogenation of 1,4-butynediol
○: the effect on the hydrogenation of 1,4-butenediol

1) T. Fukuda and T. Kusama, This Bulletin **31**, 339 (1958).

2) N. D. Zelinsky and A. A. Balandin, *Z. Phys. Chem.*, **126**, 267 (1927); T. Sabalitschka and K. Moses, *Ber.*, B. **60**, 786 (1927); J. T. McCartney, W. K. Hall and L. T. E. Hofer, *Ind. Eng. Chem.*, **39**, 1618 (1947); A. Wheeler, "Catalysis", Vol. 2, p 110 (1950).

3) H. Lindler, *Helv. chim. Acta*, **35**, 446 (1952).

used, as shown in Table I. The activity of Pd-$CaCO_3$ catalyst was not the highest.

When 1.0 cc. each of aqueous solutions of lead acetate, containing various amounts of lead acetate, was added to the reactant prior to hydrogenation, the activity of Pd-$CaCO_3$, Pd-$BaCO_3$, Pd-alumina, and Pd-$BaSO_4$ catalyst decreased with increasing amount of lead acetate, as shown in Figs. 1~4. That is, when Pd-$CaCO_3$ and Pd-$BaCO_3$ catalyst were poisoned by increasing amount of lead acetate, the activity for the hydrogenation of 1,4-butynediol increased at first, and then decreased as the poisoning proceeded. On the other hand, that for 1,4-butenediol monotonously

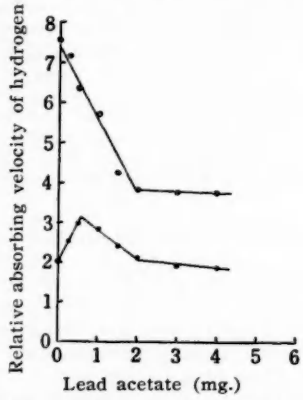

Fig. 2. The poisoning effect of lead acetate on the activities of Pd-$BaCO_3$ catalyst, at 25°C.
Pd-$BaCO_3$ catalyst (Pd, 3%) 0.3 g.
1,4-butynediol solution 20 cc. (1,4-butynediol, 0.34 g.)
●: the effect on the hydrogenation of 1,4-butynediol
○: the effect on the hydrogenation of 1,4-batenediol

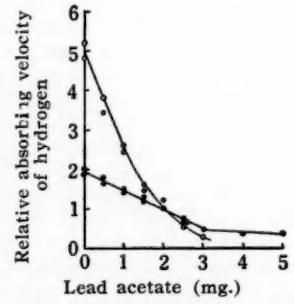

Fig. 3. The poisoning effect of lead acetate on the activities of Pd-alumina catalyst, at 25°C.
Pd-alumina catalyst (Pd, 5%) 0.3 g.
1,4-butynediol solution 20 cc. (1,4-butynediol, 0.34 g.)
●: the effect on the hydrogenation of 1,4-butynediol
○: the effect on the hydrogenation of 1,4-butenediol

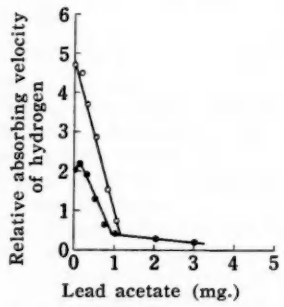

Fig. 4. The poisoning effect of lead acetate on the activities of Pd-$BaSO_4$ catalyst, at 25°C.
Pd-$BaSO_4$ catalyst (Pd, 5%) 0.3 g.
1,4-butynediol solution 20 cc. (1,4-butynediol, 0.34 g.)
●: the effect on the hydrogenation of 1,4-butynediol
○: the effect on the hydrogenation of 1,4-butenediol

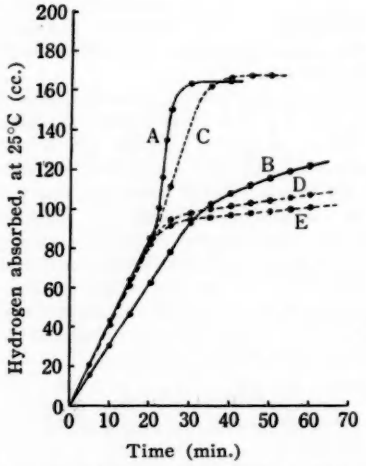

Fig. 5. The poisoning effect of quinoline on the activity of Pd-$BaCO_3$ catalyst, at 25°C.
Pd-$BaCO_3$ catalyst (Pd, 3.5%)
1,4-butynediol solution
A: no poison was added
B: quinoline (0.3 cc.) was added
C: lead acetate (3 mg.) was added
D: lead acetate (3 mg.) and quinoline (0.3 cc.) was added
E: lead acetate (5 mg.) and quinoline (0.3 cc.) was added

TABLE I

THE ABSORBING VELOCITY OF HYDROGEN, AT 25°, IN THE HYDROGENATION OF 1,4-BUTYNEDIOL ON THE VARIOUS CATALYSTS

Catalysts	Pd-content (% by wt.)	Used amt. (g.)	Absorbing velocity of hydrogen, per 10 min. (at 25°C) 1st step (cc., N.T.P.)	2nd step (cc., N.T.P.)
Pd-$CaCO_3$	5	0.3	18～20	46～ 59
〃	2	0.6	17～19	75～ 91
Pd-$BaCO_3$	3.5	0.3	36～37	163～174
〃	2	0.6	32～34	156～169
Pd-Alumina	5	0.3	16～20	35～ 46
〃	2	0.6	12～14	27～ 31
Pd-Charcoal	5	0.3	26～28	92～101
Pd-Kieselguhr	5	0.6	14～16	38～ 39
Pd-$BaSO_4$	5	〃	18～20	38～ 40
〃	3.5	〃	15～16	33～ 35
Pd-Silica-gel	3.5	〃	17～18	35～ 37

TABLE II

THE VOLUME OF HYDROGEN ABSORBED IN THE HYDROGENATION OF 1,4-BUTYNEDIOL ON THE VARIOUS CATALYSTS

Catalysts*	(Pd-content)	Poisons	(amt.)	Absorbing volume of hydrogen per 0.3 g. of 1,4-butynediol, at 25°C 1st step (cc., N.T.P.)	2nd step (cc., N.T.P.)	total volume (cc., N.T.P.)	%**
Pd-$CaCO_3$	(5%)	none	—	83	68	151	85.4
〃	〃	lead-acetate	(1 mg.)	85	83	168	95.0
〃	〃	〃	(5 〃)	〃	〃	〃	〃
〃	〃	piperidine	(0.3 cc.)	〃	〃	〃	〃
〃	〃	quinoline	〃	87	—	—	49.6
Pd-$BaCO_3$	(3.5%)	none	—	84	67	151	85.4
〃	〃	lead-acetate	(1 mg.)	85	69	154	87.0
〃	〃	〃	(5 〃)	〃	〃	〃	〃
〃	〃	piperidine	(0.3 cc.)	87	72	159	89.9
Pd-Charcoal	(5%)	none	—	76	69	145	82.0
〃	〃	lead-acetate	(1 mg.)	78	67	〃	83.1
〃	〃	piperidine	(0.3 cc.)	70	88	158	89.3
Pd-Alumina	(5%)	none	—	82	74	156	88.2
〃	〃	lead-acetate	(1 mg.)	〃	〃	〃	〃
〃	〃	piperidine	(0.3 cc.)	78	90	168	95.0
Pd-$BaSO_4$	(5%)	none	—	84	79	163	92.1
〃	〃	lead-acetate	(1 mg.)	88	82	170	96.0
Pd-Kieselguhr	(5%)	none	—	85	73	158	89.3

* 0.3 g. of the catalyst was used in all the experiments.
** Calculated adsorption (177 cc., N.T.P.) was taken as 100%.

decreased with increasing amount of lead acetate. When Pd-alumina catalyst was poisoned by lead acetate, its catalytic activity for both steps of the hydrogenation decreased monotonously. Pd-charcoal catalyst (Pd, 1～5% by weight) was not affected by lead acetate in the experimental range (1～5 mg. of lead acetate to 0.3 g. of the catalyst).

When 0.3 cc. of piperidine or quinoline was added to the reactant, the hydrogenation proceeded as shown in Figs. 5～7 with Pd-$BaCO_3$, Pd-charcoal, and Pd-alumina catalyst, respectively. The activity of Pd-$CaCO_3$ catalyst was diminished by quinoline, but the effect of quinoline was small for the hydrogenation of 1,4-butynediol and relatively great for that

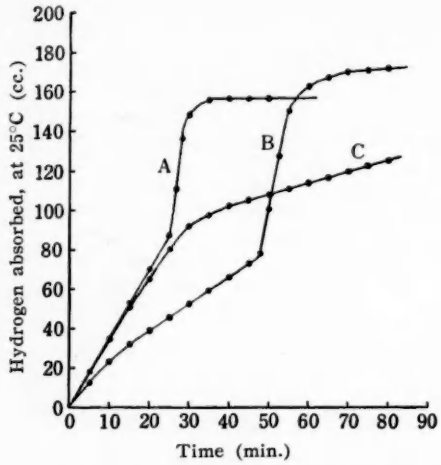

Fig. 6. The poisoning effect of piperidine and quinoline on the activity of Pd-charcoal catalyst, at 25°C.

Pd-charcoal catalyst (Pd, 5%) 0.3 g.
1,4-butynediol solution 20 cc. (1,4-butynediol, 0.34 g.)
A: no poison was added
B: piperidine (0.3 cc.) was added
C: quinoline (0.3 cc.) was added

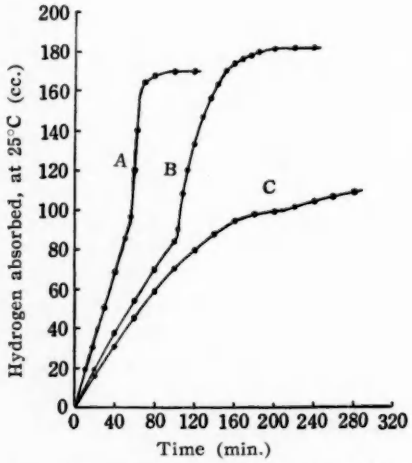

Fig. 7. The poisoning effect of piperidine and quinoline on the activity of Pd-alumina catalyst, at 25°C.

Pd-alumina catalyst (Pd, 5%) 0.3 g.
1,4-butynediol solution 20 cc. (1,4-butynediol, 0.34 g.)
A: no poison was added
B: piperidine (0.3 cc.) was added
C: quinoline (0.3 cc.) was added

of 1,4-butenediol. On the other hand, the activity of Pd-$BaCO_3$ catalyst was not diminished by piperidine. The activity of Pd-alumina catalyst for the hydrogenation of 1,4-butynediol was more markedly diminished by piperidine and by quinoline, and that for the hydrogenation of 1,4-butenediol was markedly diminished, especially by quinoline. When Pd-charcoal catalyst was poisoned by piperidine, the activity for the hydrogenation of 1,4-butynediol markedly decreased, and that for the hydrogenation of 1,4-butenediol remained almost unchanged. When it was poisoned by quinoline, however, the former was not changed much on the contrary, while the latter decreased markedly.

When Pd-$BaCO_3$ catalyst was used with lead acetate and quinoline, the hydrogenation proceeded as shown by dotted lines in Fig. 2. Its activity for the hydrogenation of 1,4-butenediol was suppressed much remarkably than when quinoline alone was used, while that for the hydrogenation of 1,4-butynediol did not change substantially.

As the properties of the catalyst depend upon the kind of the carrier, it is considered that the effect of the poisons varies complicatedly with the kind of the carrier. But it should be noticed that the partial hydrogenation of 1,4-butynediol might also be achieved by using the Pd-$BaCO_3$ catalyst poisoned by both lead acetate and quinoline, though it would not be in the same manner as in the case of Pd-$CaCO_3$ catalyst.

The volume of hydrogen absorbed during the hydrogenation depended upon the kind of the carrier and the poison added to the catalyst. The results are shown in Table II. The volume absorbed was relatively large in the case of the poisoned Pd-$CaCO_3$ catalyst.

According to the previous research, the catalytic hydrogenation of acetylene always causes the acetylene polymerization as its side reaction.[4] The polymerization may be depressed if the catalyst is poisoned[5]. The polymerization may be accompanied with the decrease of the absorbing volume of hydrogen. It is thus considered that 1,4-butynediol also polymerizes during the hydrogenation. Accordingly, the variation of the absorbed volume of hydrogen as observed may be

4) K. Tamaru, This Bulletin, **23**, 64, 180, 184 (1950).
5) M. Sato and N. Ota, *Catalyst*, **12**, 45 (1955); T. Yamanaka; *J. Scientific Research Institute*, **29**, 319 (1948).

attributed to 1,4-butynediol polymerization. It seems that the role of calcium carbonate as a carrier consists in suppressing the polymerization with the poisons, but not in increasing the hydrogenating activity, nor in giving the selectivity for the hydrogenation.

Summary

1. The role of calcium carbonate as carrier of the palladium catalyst was studied in the hydrogenation of 1,4-butynediol.

2. The hydrogenation velocity on Pd-$CaCO_3$ catalyst was not the highest among various palladium catalysts. And the partial hydrogenation of 1,4-butynediol might also be achieved by using the Pd-$BaCO_3$ catalyst poisoned by both lead acetate and quinoline. On the poisoned Pd-$CaCO_3$ catalyst, however, the 1,4-butynediol polimerization, a side reaction of the hydrogenation, was suppressed largely.

3. Consequently, it seems that the role of calcium carbonate as a carrier is to decrease the polymerization as a side reaction of the hydrogenation, but not to increase the activity for the hydrogenation, nor to give the selectivity for the hydrogenation.

This study was carried out in the Institute of Carbide Chemistry, Faculty of Engineering, Yokohama National University, and the cost of this study was defrayed by the Institute. The author is indebted to Professor T. Kusama and Professor K. Tamaru for their valuable advice. The author is also indebted to Mr. H. Kawakami for assistance.

Faculty of Engineering, Yokohama National University, Minami-ku Yokohama

---

Steroids. XXI[1]*. The Oxidation and Hypobromous Acid Addition of Steroids by Means of Isocyanur Bromide*

By Ken-ichi MORITA

(Received January 9, 1958)

Recently it was shown that isocyanur chloride[2-5] is an effective reagent for oxidation[6] and hypochlorous acid addition[7,8] of steroids. The present investigation aims at elucidating the characteristics of isocyanur bromide, which has not yet been obtained in a pure state, towards oxidation, hypobromous acid addition and allylic bromination of steroids.

The synthesis of isocyanur bromide was attempted by Chattaway and Wadmore[2] about half a century ago. Adding bromine to a solution of cyanuric acid in a cold 5% solution of caustic potash, they obtained a pale yellow substance which rapidly decomposed on exposure to air, evolving bromine. They posturated that the substance was a bromine addition product of a bromoimino derivative of cyanuric acid, in which all the imino-hydrogen atoms of the cyanuric acid were not substituted. The present author added bromine to an alkaline solution of cyanuric acid in the cold with swirling with hand, and obtained a similar substance, while, when bromine was carefully added with vigorous stirring at 0~3°C, a somewhat stable substance was obtained. A better result was obtained when the order of addition was reversed, namely, when the alkaline cyanuric acid solution was added to bromine[9]. It was necessary to remove

1) Part XX: K. Morita, *J. Chem. Soc. Japan, Pure Chem. Sec.* (*Nippon Kagaku Zassi*), **78**, 1705 (1957).

2) F. D. Chattaway and J. M. Wadmore, *J. Chem. Soc.*, **1902**, 191.

3) C. H. G. Hands, F. R. White and J. W. C. Phillips, *J. Soc. Chem. Ind.*, **61**, 66 (1948); Brit. Pat., 634, 801; *Chem. Abst.*, **44**, 7356e (1950).

4) T. Ishii, S. Kanai and T. Ueda, *J. Soc. Org. Synth. Chem. Japan* (*Yuki Gosei Kagaku Kyokaishi*), **15**, 241 (1957).

5) Isocyanur chloride is also a bleaching and sterilizing agent. Cf. *Chem. Trade J.*, **140**, 884 (1957).

6) F. Mukawa, *J. Chem. Soc. Japan, Pure Chem. Sec.* (*Nippon Kagaku Zassi*), **78**, 450 (1957).

7) Idem., ibid., **78**, 452 (1957).

8) S. Mori, K. Morita and F. Mukawa, *Proc. Japan Acad.*, **23**, 535 (1956).

9) Y. Yukawa and U. Suzuki (*Mem. Inst. Sci. Ind. Des. Osaka Univ.*, **10**, 190, (1952) stated that the addition of alkaline succinimide to a mixture of bromine and water was preferable for preparation of *N*-bromosuccinimide.

the moisture in the cake after filtration as fast as possible. The moisture lingering in the product markedly decreased the purity. The percentage of bromine in the product was determined by micro Carius method and by iodometry[4] with well coincident results. The purity of the product was 80~92%. In some cases the isocyanur bromide contained bromine in a percentage as low as 50% (cf. experimental part), but it should be noted that for oxidation and hypobromous acid addition, 50~70% isocyanur bromide was usable as well.

Isocyanur bromide is a white or slightly yellow crystalline powder. It has an odour resembling that of hypobromous acid. It does not melt below 300°C, but decomposes when heated by direct flame. It dissolves to some extent in water and in glacial acetic acid with hydrolysis. When it is added to hydrobromic acid, bromine is liberated. It liberates iodine from hydroiodic acid and from an aqueous solution of potassium iodide. When added to aqueous ammonia, a violent decomposition takes place.

Mukawa[6] reported that the reaction of cholestane-3 β,5 α,6 β-triol (II) with isocyanur chlorid and pyridine in warm benzene furnished cholestane-3 β,5 α-diol-6-one (III) in 80% yield. Under similar conditions the starting material was recovered when isocyanur bromide was used instead of isocyanur chloride, while the oxidation took place smoothly to produce cholestane-3 β,5 α-diol-6-one (III) when *tert*-butanol was used as the solvent. Fieser et al.[10] reported that the oxidation of cholesterol (I) with *N*-bromosuccinimide and acetic acid in aqueous acetone produced cholestane-3 β,5 α-diol-6-one (III) and choleterol dibromide. Under nearly the same conditions except that isocyanur bromide was used in place of *N*-bromosuccinimide cholestane-3 β,5 α,6 β-triol (II) and cholesterol dibromide were obtained but cholestane-3 β,5 α-diol-6-one (III) was not detected. A similar result was reported by Ueno[11], who found that oxidation of cholesterol with *N*,*N*-dibromobenzenesulfonamide gave cholestane-3 β,5 α,6 β-triol (II). It is concluded that isocyanur bromide is an oxidizing agent milder than *N*-bromosuccinimide or isocyanur chloride.

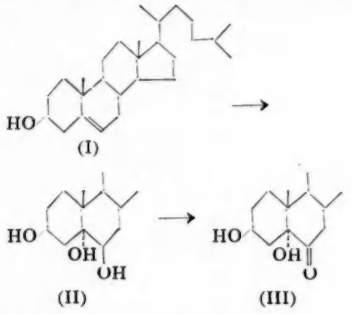

Hypochlorous acid addition of 5-ene-steroids by means of isocyanur chloride and acetic acid in aqueous acetone is known to produce corresponding chlorohydrins in good yields[7,8]. Hypobromous acid addition of cholesteryl acetate (IV) by means of isocyanur bromide and acetic acide in the same solvent furnished 5 α-bromocholestane-3 β,6 β-diol 3-monoacetate (V) and cholesteryl acetate dibromide (VII) only in low yields. Fried and Sado[13] demonstrated that hypobromous acid addition of 4,9(11)-pregnadiene-17 α,21-diol-3,20-dione 21-acetate with *N*-bromoacetamide in dioxane containing dilute sulfuric acid gave 9 α-bromohydrocortisone acetate in only 48% yield, while in dioxane containing dilute perchloric acid, 9 α-bromohydrocortisone acetate was obtained in 80~90% yield[14]. Mori[15] reported that the reaction of cholesteryl acetate (IV) with *N*-bromoacetamide in ether containing dilute sulfuric acid gave no hypobromous acid addition product V, but gave cholesteryl acetate dibromide (VII). The present author obtained the bromohydrin (V) from cholesteryl acetate (IV) in 61% yield with *N*-bromoacetamide and dilute perchloric acid in dioxane and in 49% yield with isocyanur bromide and dilute perchloric acid in the same solvent. Ueno[12] reported

10) L. F. Fieser and S. Rajagopalan, *J. Am. Chem. Soc.*, **71**, 3938 (1949).
11) Y. Ueno, *J. Pham. Soc. Japan* (*Yakugaku Zasshi*), **72**, 1626 (1952).
12) Idem., ibid., **72**, 1622 (1952).
13) J. Fried and E. F. Sabo, *J. Am. Chem. Soc.*, **79**, 1136 (1957).
14) Perchloric acid has been employed on hydroxybromination of 9(11)-ene-steroids (H. B. Henbest et al., *J. Chem. Soc.*, **1955**, 2477; R. H. Lenhars and S. Bernstein, *J. Am. Chem. Soc.*, **77**, 6665 (1955)), of 11-ene-steroids (J. E. Herzig et al., ibid., **78**, 2017 (1956)), and of 5-ene-steroids (B. Ellis and V. Petrow, *J. Chem. Soc.*, **1956**, 4417). Cf. B. Loenken et al., *J. Am. Chem. Soc.*, **78**, 1738 (1956).
15) S. Mori, *J. Chem. Soc. Japan, Pure Chem. Sec.* (*Nippon Kagaku Zassi*), **73**, 505 (1952).

the same hydroxy-bromination reaction with *N*-bromosuccinimide and with *N,N*-dibromobenzenesulfonamide and acetic acid in aqueous acetone, obtaining compound V in 15 and 37% yields, respectively[16]. Proof for the bromohydrin structure was obtained from its coversion into cholesteryl acetate β-oxide (VI) by a reaction with potassium acetate and into 5α-bromocholestan-3β-ol-6-one acetate by oxidation with chromic acid in acetic acid.

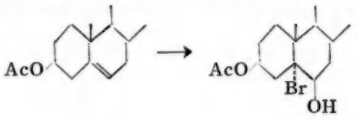

(IV) (V)

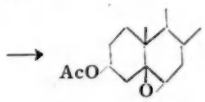

(VI)

It seemed to be of interest to study the allylic bromination with isocyanur bromide, since Ziegler and his coleagues[17] described the allylic chlorination of cyclohexene with isocyanur chloride. Reaction of cholesteryl acetate (IV), 4-cholesten-3-one and testosterone benzoate with isocyanur bromide in boiling carbon tetrachloride under a strong illumination, however, failed to produce brominated compounds but resulted in the recovery of the starting materials, except only in special case (See experimental part).

Experimental[18]

Isocyanur Bromide.—Ten grams of bromine and 60 ml. of distilled water were mixed and cooled in an ice-salt bath to 0°C. A solution of 2 g. of cyanuric acid (purity 92.5%[4]) and 3 g. of potassium hydroxide in 60 ml. of distilled water was added dropwise to the well-stirred mixture at 0~3°C, caution being taken not to cool down below 0°C. After the addition, the mixture was stirred for further twenty minutes. The solid was collected, washed thoroughly with ice water to neutral reaction, with purified acetone several times and twice with ether, (in order to remove the moisture quickly and stored in a sulfuric acid desiccator. Yield 5.3 g. or 75% of the theoretical.

Anal. Found: Br, 60.38% (micro Carius method; 92.2% of the theoretical); Br, 60.02% (Iodometry[4]); 91.8% of the theoretical). Calcd. for $C_3O_3N_3Br_3$: Br, 65.54%.

The purity was practically unchanged after stored in a sulfuric acid desiccator for three months in the dark. In other runs the percentage of bromine in the product ranged from 80% to 92%, doubtlessly owing to slight changes of washing procedures. When the precipitate was washed with dioxane and then with ether, nearly the same results were obtained. It took about ten days to dry the product completely over sulfuric acid and the purity became about 40~50%. When dried over phosphorous pentoxide under a reduced pressure (5 mmHg) overnight the purity also decreased to 55~60%.

Similar results were obtained when the reaction was carried out under illumination.

Cholestane-3β,5α,6β-triol (II).—A suspension of 4.5 g. of cholesterol (I) in 200 ml. of acetone and 25 ml. of water was mixed with 3.3 g. (1.25 equiv.) of 55.1% isocyanur bromide and 2.5 ml. of acetic acid and the mixture was shaken occasionally at room temperature. Soon the mixture became yellow in color. In about one hour the whole solid went into solution and in 2.5 hours from the beginning a new solid appeared. After being kept over night, the suspension was filtered off and extracted with ether, and the extract was washed with water and alkali, dried and concentrated until crystals began to separate. After cooling with ice, the crystalline material was collected. Recrystallization from chloroform gave colorless needles melting at 237~238°C. Yield 1.0 g.

The identity was established by conversion into the diacetate[19], m.p. and mixed m.p. 165~166°C. The product did not produce a phenylhydrazone.

The ethereal mother liquor was evaporated under a reduced pressure and triturated with methanol to give 1.2 g. of a solid with m.p. 107~118°C*. Recrystallization from ethanol gave colorless needles, m.p. 121~122°C, which was identified as cholesterol dibromide by a mixed m.p. determination.

Cholestane-3β,5β-diol-6-one (III).—To a solution of 251 mg. of compound II in 25 ml. of *tert*-butyl alcohol 0.5 ml. of pyridine, 0.5 ml. of water and 99.5 mg. of 83.8% isocyanur bromide were added successively. The mixture was warmed at 65~70°C for 30 minutes. After filtration the filtrate was diluted with ether, washed with a 10% bisulfite solution, aqueous alkali and water, and dried over anhydrous sodium sulfate. The solution was concentrated under a reduced pressure. Careful dilution with water gave needles, m.p. 230~233°C (decomp.), which was not depressed when admixed with an authentic sample[10]. Yield 228 mg.

The substance was further characterized by

16) Ueno obtained a small anount of 6β-bromocholestane-3β, 5α-diol 3-acetate from the mother liquor, but the present author did not attempt to isolate it.

17) K. Ziegler, A. Spath, E. Schauf, W. Schumann and E. Winklman, *Ann.*, **551**, 80 (1942).

18) All melting points are uncorrected. All rotations are measured in chloroform solution. Concentrations (*c*) are expressed in g. per 100 ml. of solution. The author is indebted to Mr. T. Iwama for microanalyses and to Mr. F. Mukawa for the supply of cyanuric acid.

19) V. A. Petrow, *J. Chem. Soc.*, **1937**, 1077.

* All of brominated steroids described in this paper melted with decomposition.

coversion into the phenylhydrazone[20], m.p. 163～164°C and into 3-monoacetate[10], m.p. 232～233°C.

Attempted Oxidation of Cholestane-3β, 5α, 6β-triol (II) with Isocyanur Bromide and Pyridine in Benzene.—A mixture of 0.25 g. of compound II, 20 ml. of benzene, 0.12 g. of 91.8% isocyanur bromide and 0.3 ml. of pyridine was heated under reflux for 15 minutes and treated as described above. The strating material, m.p. 215～225°C, was recovered. (0.19 g.) Recrystallized material melted at 236～238°C.

The identity was established by conversion into the diacetate[19], m.p. and mixed m.p. 165～166°C,

Hypobromous Acid Addition of Cholesteryl Acetate (IV).—(*a*) *Perchloric Acid-Isocyanur Bromide Method.* A solution of 1 g. of compound IV in 50 ml. of dioxane and 7 ml. of water was mixed with 0.6 g. of 84.5% isocyanur bromide and 0.3 ml. of 60% perchloric acid and the mixture was shaken occasionally at room temperature (19°C). After two hours the suspension was diluted with 25 ml. of a 10% sodium bisulfite solution and left to stand in a refrigerater (5°C) for one hour, and the solid was collected by filtration. The material was dried and extracted with a small volume of hot chloroform and the chloroform solution was diluted with petroleum ether. Crystals were collected. Needles, m.p. 160～165°C (0.68 g.). Recrystallization from chloroform-petroleum ether gave fine needles, m.p. 174～175°C, $[\alpha]_D^{21.5}$ −35 (c, 0.998). Yield 0.6 g. or 49% of the theoretical. The melting point was not depressed on admixture with authentic 5α-bromocholestane-3β, 6β-diol 3-monoacetate[15]. (Found: Br, 15.42%, Calcd. for $C_{29}H_{49}O_3Br$; Br 15.24%) Reported m.p. 177°C, $[\alpha]_D$ −37[21]; m.p. 175°C, $[\alpha]_D$ −33.8[12]; m.p. 177～178°C[15].

(*b*) *Perchloric Acid-N-Bromoacetamide Method.* A mixture of 1 g. of compound IV, 50 ml. of dioxane, 7 ml. of water, 0.45 g. of *N*-bromoacetamide and 0.3 ml. of 60% perchloric acid were treated in the same way as described above. Recrystallization from chloroform-petroleum ether gave needles, m.p. 158～161°C (0.9 g.). Further recrystallization yielded the pure substance, m.p. 174～175°C, $[\alpha]_D^{21}$ −38 (c, 1.02). Yield 0.75 g. or 61% of the theoretical. The melting point was not depressed on admixture with a specimen from method *a*.

(*c*) *Acetic Acid-Isocyanur Bromide Method.* A mixture of 2.5 g. of compound IV, 1.3 g. of 83.8% isocyanur bromide, 150 ml. of acetone, 10 ml. of water and 4 ml. of acetic acid was refluxed for ten minutes, poured into an excess of water, and extracted with ether. The extract was washed with water, dried over anhydrous sodium sulfate, and evaporated. The oily residue was dissolved in ethyl acetate and methanol was added to produce faint turbidity. Then a small volume of ether was added and the mixture was left to stand in a refrigerator (5°C) for 5 days. Crystals (m.p. 100～158°C) were collected and recrystallized from ether-methanol to produce long needles with m.p. 112～115°C (0.3 g.). The melting point was not depressed on admixture with authentic cholesteryl acetate dibromide.

The mother liquor from the above experiment was concentrated to produce crystals, which were mainly cholesteryl acetate dibromide (0.2 g.). The mother liquor from the above concentrate was again concentrated to produce crystals, which were collected and recrystallized from chloroform-petroleum ether to give needles, m.p. 174～175°C (0.2 g.). This substance did not depress the melting point of 5α-bromocholestane-3β, 6β-diol 3-monoacetate (V).

A solution of the mixture (0.75 g.) of the products from methods *a*, *b* and *c* in acetic acid (26 ml.) and water (7 drops) was oxidized with chromic acid (0.35 g.) to give 5α-bromocholestan-3β-ol-6-one acetate (0.6 g.), m. p. 165～166°C. (Found: Br, 15.18%. Calcd. for $C_{29}H_{47}O_3Br$: Br, 15.26%). Reported m.p. 164～166°C[12], 164～165°C[15], 163°C[22].

Cholesteryl Acetate β-Oxide (VI).—To a suspension of 212 mg. of compound V in 7 ml. of ethanol was added 0.4 g. of sodium acetate (crystalline) and the mixture was refluxed for 1.5 hours. Soon the solid went wholly into solution and a new solid appeared. After cooling, water was added and the solid was collected by filtration. The crystals, after recrystallized from aqueous methanol, gave a negative Beilsterin test, and melted at 111～112°C. Needles (189 mg.). The melting point was not depressed when admixed with authentic cholesteryl acetatate β-oxide[24] (VI). Reported m.p. 111～113°C; $[\alpha]_D$ −1[23], 113°C[24].

The product (21.2 mg.) in chloroform (0.5 ml.) was treated with 4 N hydrogen bromide in acetic acid (0.5 ml.) for 10 minutes at room temperature to give needles with m.p. 172～174°C when recrystallized from chloroform-petroleum ether. The melting point was not depressed on admixture with 5α-bromocholestane-3β, 6β-diol 3-monoacetate (V).

Attempted Allylic Bromination of Testosterone Benzoate.—(*a*) *With Isocyanur Bromide washed with Acetone as Described Above.* A mixture of 0.5 g. of testosterone benzonate and 0.25 g. of 91.8% isocyanur bromide in 10 ml. of carbon tetrachloride was refluxed for 30 minutes with exposure to strong light. The starting material was recovered in nearly quantitative yield. Under nearly the same conditions, 4-cholesten-3-one and cholesteryl acetate could not be brominated.

(*b*) *With Isocyanur Bromide not washed with Acetone but left to stand in a Sulfuric Acid Desiccator Overnight.* To a solution of 1 g. of testosterone benzoate in 20 ml. of carbon tetrachloride was added 1.2 g. of the isocyanur bro-

20) R. H. Pickard and J. Yates, ibid., **93**. 1678 (1908).
21) D. R. Jones and C. W. Shoppee, ibid., **1954**, 4224.
22) I. M. Heilbron, E. R. H. Jones and F. S. Spring, ibid., **1937**, 801.
23) P. A. Plattner et al., *Helv. chim. Acta*, **27**, 513 (1944).
24) S. Mori, *J. Chem. Soc. Japan, Pure Chem. Sec. (Nippon Kagaku Zassi)*, **64**, 981 (1943).

mide and the mixture was refluxed for 30 minutes with exposure to strong light. The solid was removed by filtration and the solution was evaporated to dryness. Recrystallization from acetone-methanol gave needles with m.p. 150~152°C (0.55 g.). After recrystallization from ethyl acetate-methanol, the analytical sample showed m.p. 178°C, $[\alpha]_D^{19}$+86 (c, 0.370), λ_{max} 232 mμ (ε 23,800).

Anal. Found: Br, 17.29%. Calcd. for $C_{26}H_{31}O_3Br$: Br, 16.96%.

Ruzicka et al.[25] reported m.p. 176~177°C for 6ξ-bromotestosterone benzoate. The product may be 6ζ-bromotestosterone benzoate, since the same substance was obtained when testoserone benzoate was brominated with *N*-bromosuccinimide as described below and it is known that reactions of 4-ene-3-ketosteroids and *N*-bromosuccinimide give corresponding 6ξ-bromo-4-ene-3-ketosteroids[26]. But the abnormal shift of the ultraviolet absorption maximum to the shorter wavelength can not be explained[27].

(*c*) *With N-Bromosuccinimide.* One half gram of testosterone benzoate was treated with 0.25 g. of *N*-bromosuccinimide in refluxing 10 ml. of carbon tetrachloride for 30 minutes under the ordinary light. After evaporation under a reduced pressure, the residue was triturated with *n*-hexane to give a colorless solid (0.45 g.), m.p. 143~144°C. The melting point was raised to 177~177.5°C when recrystallized from ethyl acetate-methanol and was not dedressed on admixture with the sample obtained above.

The author is indebted to Professor S. Mori of Tokyo Metropolitan University for his encouragement throughout this work. The author's thanks are also due to Dr. M. Nakamura and Mr. R. Mamine of this Institute for their interest in this investigation.

Sugiyama Chemical Research Institute
Mure, Mitaka, Tokyo

25) R. Ruzicka et al., *Helv. chim. Acta*, **20**, 328 (1937).
26) C. Djerassi et al., *J. Am. Chem. Soc.*, **72**, 4534 (1950); F. Sondheimer et al., ibid., **75**, 4712, 5932 (1953); B. Camerino et al., *Gazz. chim. ital.*, **84**, 301 (1954); *Chem. Abst.*, **49**, 14787b (1955); V. R. Mattox et al., *J. Biol. Chem.*, **197**, 261 (1952).
27) Cf. K. Morita, *J. Chem. Soc. Japan, Pure Chem. Sec.* (*Nippon Kagaku Zassi*), **78**, 1581 (1957).

Benzylation of Acetylene. II. On the Structure and Oxidation of 3-Benzyl-3,4-diphenyl-1-Butyne

By Teisuke Ando and Niichiro Tokura

(Received July 24, 1957)

We reported the formation of 3,4-diphenyl-1-butyne (I) and its isomer, 3,4-diphenyl-1,2-butadiene (II), by the reaction of benzyl chloride and sodium or lithium acetylide in liquid ammonia[1], whereas formation of benzylacetylene had been expected[2]. In the present paper, we report the formation and the structure of 3-benzyl-3,4-diphenyl-1-butyne (III).

It is particularly interesting that III was produced in addition to I and II in the reaction using an equimolar ratio of benzyl chloride to a metallic acetylide and that III resisted oxidation.

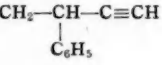

I

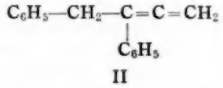

II

III was obtained as a fraction distilling at 207°C (4.5 mmHg) and following the fraction of I and II from the reaction mixture. III was a yellowish, viscous liquid and formed complex salts with silver nitrate and with alkaline mercuric iodide[3,4], showing the presence of an ethynyl group —C≡CH. The presence of the terminal acetylenic bond was reassured by a strong absorption maximum at 3320 cm.$^{-1}$ due to stretching vibration of the bond and a weak one at 2120 cm.$^{-1}$ for a monosubstituted acetylene[5]. The

1) T. Ando and N. Tokura, This Bulletin, **30**, 259 (1957).
2) T. H. Vaughn, G. F. Hennion, R. R. Vogt and J. A. Nieuwland, *J. Org. Chem.*, **2**, 1 (1938).
3) J. R. Johnson and W. L. McEwen, *J. Am. Chem. Soc.*, **48**, 469 (1926).
4) B. B. Elsner and P. F. M. Paul, *J. Chem. Soc.*, **1951**, 893.
5) L. J. Bellamy, "The Infra-red Spectra of Complex Molecules", John Wiley and Sons, Inc., New York (1954), p 49.

ethynyl group of III resisted strongly against oxidizing agents, as compared with a double bond between ordinary aliphatic carbon atoms[6]. Namely, (1) by passing air into a solution of III for many hours at room temperature, III was not oxidized and was completely recovered. (2) When an alkaline aqueous solution of III (a part was dissolved but most part remained as a suspension) was agitated with 30% aqueous hydrogen peroxide and the solution was left to stand for one night, the substance was not oxidized. Even when the alkaline solution was mixed with an excess of hydrogen peroxide and the solution was heated on a water bath, it remained without being oxidized. (3) When 5% ozone was introduced into a solution of III in ethyl acetate for 30 minutes at −10°C, a minute amount of benzoic acid was produced, but the main part remained without being oxidized. The above results well coincided with the experiment of Criegee and Lederer[7] on an ethynyl compound. III was oxidized with potassium permanganate either in neutral, alkaline or acidic solution at room temperature. The oxidation in an acidic medium gave a white crystalline substance (A), m.p. 139~140°C, in a low yield, but the yield was increased to 92% in a neutral solution. The aqueous solution of A was acidic. When a piece of A was dropped into concentrated sulfuric acid, instant vesication was observed, showing A was an α-keto acid. An absorption of carboxyl ion $-COO^-$[8] was observed at 1370 cm.$^{-1}$ in infrared spectrum of A. Absorptions at 1711 cm.$^{-1}$ and 1722 cm.$^{-1}$ showed that the substance was a derivative of pyruvic acid, according to Icherweed[9] and Jones[10]. In addition to the above I.R. spectra, elementary analysis of A corresponded to $C_{23}H_{20}O_3$. This acid (A) is therefore considered to be phenyldibenzylpyruvic acid (IV).

By either decarbonylation by heat or oxidation with hydrogen peroxide or potassium permanganate, IV always gave a white crystalline substance (B), melting at 122~123°C. When III was reduced with hydrogen and palladium carbon, a colorless, slightly viscous oil (C), b.p. 192~194°C (3 mmHg), was produced through absorption of one mole of hydrogen. In C, the absorptions of the ethynyl group (3320 cm.$^{-1}$) disappeared, but stretching vibration of C=C (non-conjugate)[11] newly appeared at 1668 cm^{-1}. Absorption maxima at 1430 cm.$^{-1}$ and 912 cm.$^{-1}$ showed the presence of a vinyl group ($-CH=CH_2$). C was therefore assumed to be 3-benzyl-3,4-diphenyl-1-butene (V).

Oxidation of V with potassium permanganate gave an acid, m.p. 139~140°C, and no lowering of the melting point of a mixture of this acid and IV was observed. It was supposed that, when gently oxidized with potassium permanganate, III and V gave the same keto-acid owing to the degradation of ethynyl and vinyl group, respectively. When oxidized with ozone, V gave an acid, m.p. 122~123°C, which was identified as B by the mixed melting point.

Treatment of III with sulfuric acid in the presence of mercuric sulfate gave a crystalline substance (VI) in a yield of 78%, b.p. 230~240°C (6 mmHg), m.p. 84~84.5°C. I.R. spectrum of VI showed carbonyl stretching vibration in open chain ketones[11] at 1700 cm.$^{-1}$ and methyl deformation of methyl ketone[12] at 1354 cm.$^{-1}$. From the above I.R. spectral analyses and a positive iodoform reaction, it should have a methyl ketone group, but it has not yet yielded oxime, hydrazone nor semicarbazone. We suppose that this ketone is difficult to react with the carbonyl reagents on account of the steric hindrance by the three phenyl groups.

Furthermore, an attempt to reduce VI by Clemmensen's method failed. When oxidized with hypobromite[13], VI gave an acid of m.p. 122~123°C, which was identified as B by the mixed melting point.

When B was allowed to stand about two months at room temperature, the melting point was raised to 153~154°C from 122~123°C, but I.R. and U.V. spectra did not change. We call the higher melting substance α-form and the lower melting one β-form tentatively.

Hauser and Brasen[14], and Baker[15] reported the benzylation of benzyl cyanide in liquid ammonia. We carried out the same reaction and prepared 2-benzyl-2,3-diphenylpropionitrile (VII). Hydrolysis

6) F. Bohlmann and J. Sinn, *Ber.* **88**, 1869 (1955).
7) R. Criegee and M. Lederer, *Ann.* **583**, 29 (1953).
8) M. st. C. Flett, *J. Chem. Soc.*, **1951**, 962.
9) F. A. Icherweed, *Nature*, **195**, 419 (1955).
10) R. L. Jones, ibid., **173**, 121 (1954).
11) R.B. Barmes, R.C. Gore, U. Lidded and V.Z. Williams, "Infra-red Spectroscopy", Reinhold Publishing Co. (1944).
12) J.A. Anderson and W.D. Seybried, *Anal. Chem.*, **20**, 998 (1948).
13) W. S. Johnson, C. D. Gustsche and R. D. Offenhauer, *J. Am. Chem. Soc.*, **68**, 1648 (1946).
14) C. R. Hauser and W. R. Brasen, ibid., **78**, 494 (1956).
15) R. H. Baker, ibid., **70**, 3857 (1948).

of this nitrile to an acid amide (VIII) by refluxing for four days with sulfuric acid in glacial acetic acid, followed by treatment with sodium nitrite, gave 2-benzyl-2,3-diphenylpropionic acid (IX), m.p. 153~154.5°C, which on admixture with the β-form (m.p. 153~154.5°C) showed no depression of the melting point.

It is also of interest that Hauser's[14] acid, obtained by the same procedure as above, showed the same melting point 124~125°C, as our α-form.

When we compared melting points of nitrile VII, amide VIII and acid IX to those of Hauser's[14] and Baker's[15] substance, respectively (Table I), we found that our values resembled Baker's closely except acid IX.

TABLE I

	Author	Hauser et al.[14]	Baker[15]
Nitrile VII	81~83°C	92~92.5°C	82°C
amide VIII	112.7~114°C	—	111~112°C
acid IX	α 122~123°C	124~125°C	131~132°C
	β 153~154.5°C		

It was observed that nitrile VII affords two forms, m.p. 92°C and 82°C. We concluded the α-form and the β-form are polymorphs of 2-benzyl-2,3-diphenylpropionic acid (IX). Such cases often occur in sterically hindered systems[16].

It appears likely that Baker's acid was a mixture of the α- and the β-form. Table II shows a series of compounds derived from III was described above. Since the structure of IX has been thus decided, the structure of III, IV, V and VI are established, as already assumed, as 3-benzyl-3,4-diphenyl-1-butyne, phenyldibenzylpyruvic acid, 3-benzyl-3,4-diphenyl-1-butene and 3-benzyl-3,4-diphenyl-2-butanone, respectively.

A similar benzylation of allylbenzene in liquid ammonia has given 3-benzyl-3,4-diphenyl-1-butene (V) in a good yield, as will be reported later.

Experimental[17]

3-Benzyl-3,4-diphenyl-1-butyne (III).— Metallic sodium was dissolved in liquid ammonia and to this solution acetylene gas was introduced to form sodium acetylide, and the product was added to an equimolar amount of benzyl chloride in liquid ammonia, for the mixture to be treated as reported in the preceding paper[1]. Following the fraction of I and II, 3-benzyl-3,4-diphenyl-1-butyne (III) distilled at 207°C (4.5 mmHg), a pale yellow oil; yield, 15.3% or 30 g. from 252 g. of benzyl chloride.

Anal. Found: C, 93.48; H, 6.64. Calcd. for $C_{23}H_{20}$: C, 93.20; H, 6.80%. I.R. ν max: 3320 and 2120 cm.$^{-1}$ Mol. wt.: Found, 296; Calcd. for $C_{23}H_{20}$: 296.

A mercuric complex[3] was given as white fine needles from petroleum ether (b.p. 40~60°C), m.p. 159~159.5°C.

Mercury determination of the complex salt: 4.093 mg. of the substance gave 1.0379 mg. or 25.36% of Hg. Calcd. for $C_{46}H_{38}Hg$: Hg, 25.36%.

Oxidation of III with Potassium Permanganate. Phenyldibenzylpyruvic Acid (IV).— (*a*). *Oxidation in a neutral medium.* A three necked flask of two litre capacity equipped with an air-tight agitator and a reflux condenser are used as the reaction vessel. III (4.2 g.) was dissolved in 400 cc. of acetone and to the solution 8 g. of potassium permaganate dissolved in 400 cc. of water was added and the mixture was agitated for 48 hours at room temperature. After distilling off acetone, sulfur dioxide gas cooled with ice

TABLE II

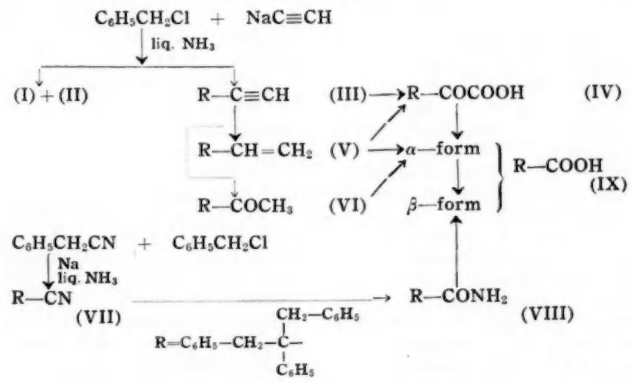

16) W. V. Miller and G. Rohde, *Ber.*, **25**, 2017 (1892).

17) Melting points were not corrected.

was introduced into the residue and then the solution was made basic with dilute aqueous sodium hydroxide. Unchanged neutral part was extracted with ether and the remaining alkaline layer was acidified with hydrochloric acid and extracted with ether. After removal of ether, 4.5 g. of crystals melting at 139.51~40°C were obtained in a yield of 92%.

Anal. Found: C, 80.68; H, 5.92. Calcd. for $C_{23}H_{20}O_3$: C, 80.21; H, 5.85%. I.R. ν max: 1722, 1711, and 1370 cm.$^{-1}$

In other experiments oxidation was carried out for 100 hours at room temperature and 8 hours at boiling water bath temperature, the yields of IV being depressed to 17.2 and 21%, respectively, when the precipitate of manganese dioxide was not decomposed with sulfur dioxide.

(*b*) *Oxidation in an alkaline medium.* One gram of III was vigorously agitated and emulsified with 150 cc. of water and 20 cc. of 2N potassium hydroxide solution. To the emulsion 200 cc. of 1% aqueous potassium permanganate was added and then agitation was continued for 150 hours at room temperature. Then the solution was treated as stated above yielding 0.1 g. (8.6%) of crystals (IV), m.p. 139.5~140°C.

(*c*) *Oxidation in an acidic medium.* Two grams of III was dissolved in 500 cc. of glacial acetic acid, and 300 cc. of 1% aqueous potassium permanganate was added to the solution. By 3 hours agitation, reddish violet color disappeared. When the solution was treated as described above, only a minute amount of an acidic part was obtained.

Partial Hydrogenation, 3-Benzyl-3,4-diphenyl-1-butene (V).—Two grams of III was dissolved in 100 cc. of metanol in a reducing flask. In a Willstätter reducing apparatus III was reduced at 15°C in the presence of 0.5 g. of 5% palladium carbon. In 25 minutes, 160 cc. of hydrogen was absorbed. Then the reaction was discontinued and the solvent was distilled off. The residue was distilled under a reduced pressure, and 1.8 g. of V was obtained, b.p. 192~194°C (3 mmHg).

Anal. Found: C, 92.17; H, 7.61. Calcd. for $C_{23}H_{22}$: C, 92.57; H, 7.43%. I.R. ν max: 1668, 1430, 1002 and 912 cm.$^{-1}$

Oxidation of V with Potassium Permanganate.—Two grams of V was dissolved in 500 cc. of acetone in a three-necked flask of 1 liter capacity and to the solution 100 cc. of a 4.2% potassium permanganate solution was added. The mixture was agitated for 48 hours at room temperature, and then for 15 hours at 45°C. After removal of the solvent, sulfur dioxide gas was introduced under cooling with ice. The residue was made basic with dilute caustic alkali and extracted with ether. The aqueous layer was acidified and extracted with ether. After removal of the solvent from the ethereal solution, 0.5 g. (21%) of white globular crystals were obtained; m.p. 138~140°C. It was confirmed that they were identical with IV by a melting point determination of the mixed crystals after recrystallization.

Hydration of III. 3-Benzyl-3,4-diphenyl-2-butanone (VI).—Ten grams of III was dissolved in 200 cc. of methanol in a three-necked flask equipped with a mechanical agitator and a reflux tube. To the solution a mixture of 1.5 g. of mercuric sulfate, 3 cc. of concentrated sulfuric acid and 10 cc. of water was added and agitated under reflux. After 6 days, the reaction was terminated, the insoluble substances were filtered off and the solvent was distilled off from the filtrate. Then the residue was distilled under a reduced pressure. A reddish brown viscous oil was obtained; b.p. 230~240°C (6 mm Hg). On addition of a small amount of ethanol to the oil, white heavy plates were crystallized, m.p. 84~84.5°C; yield, 8.3 g. (78%).

Anal. Found: C, 87.79; H, 7.13. Calcd. for $C_{23}H_{22}O$: C, 87.86; H, 7.05%. I.R. ν max: 1700, 1354, 1152, 1078 and 1031 cm^{-1}.

The α-Form of 2-Benzyl-2,3-diphenylpropionic Acid (IX).—(*a*) *Heat decarbonylation of IV.* IV (0.5 g.) was taken in a small test tube and gradually heated on a sulfuric acid bath. On elevation of the temperature of the bath above the melting point of IV, 140°C, the evolution of a gas from the substance was observed. When the temperature of the bath reached to 220°C, splitting of carbon monoxide occurred very quickly. While the temperature of the bath was elevated to 260°C for 1 hour, the gas evolution was completed. The colorless fused substance changed orange and then to reddish orange in color. After cooling, the product was crystallized form ligroin (b.p. 80~100°C), yielding white crystals, m.p. 122~122.5°C (α-form); yield, 0.1 g. (21.7%).

(*b*) *Reaction of IV with hydrogen peroxide.*—In a beaker of 200 cc. capacity, 1.5 g. of IV was mixed with 20 cc. of 10% sodium hydroxide solution and 30 cc. of 10% hydrogen peroxide, and the mixture was allowed to stand for one night in an ice box. Then another 10 cc. portion of hydrogen peroxide (10%) was added to the mixture with stirring. After 8 hours, the mixture was acidified and extracted with ether. When the ethereal solution was dried and evaporated, fine scales were afforded, m.p. 115~120°C; yield, 0.4 g. (87%). When recrystallized from ligroin (b.p. 80~100°C), 0.28 g. of white scales were obtained, m.p. 122~123°C (α-form).

(*c*) *Oxidation of IV with potassium permanganate.* IV (0.5 g.) was dissolved in 100 cc. of 2% aqueous sodium hydroxide in a round flask of 300 cc. capacity, and to the solution 50 cc. of 1% aqueous potassium permanganate was added. The mixture was agitated for 8 hours and left to stand for one night. The mixture was neutralized with dilute sulfuric acid, treated with sulfur dioxide gas to dissolve manganese dioxide, and then extracted with ether. When the ether was distilled off, white crystals remained. On recrystallization from ligroin (b.p. 80~100°C), 0.2 g. (43.5%) of white scales were obtained, m.p. 121~122°C (α-form).

(*d*) *Oxidation of V with ozone.* Two grams of V was dissolved in 100 cc. of ethyl acetate,

cooled at −60°C and ozone (0.01 mole/hour) was passed for 50 minutes. The solvent in the reaction mixture was distilled off under a reduced pressure. After decomposition of the ozonide in the residue with ice, 10 cc. of 10% aqueous sodium hydroxide and 5 cc. of 10% hydrogen peroxide were added; the mixture was left to stand for one night, and extracted with ether to remove the neutral part. The residual solution gave 1.5 g. (71%) of an acid, m.p. 119~121°C, on acidification. When the product was recrystallized from ligroin (b.p. 80~100°C), crystals (1.2 g.) m.p. 122~123°C (α-form), were obtained.

(*e*) ***Oxidation of VI with sodium hypobromite.*** To 50 cc. of 1,4-dioxane containing 5 g. of VI, a sodium hypobromite solution (5 cc. of bromine in 50 cc. of ice-cooled alkali solution containing 15 g. of the alkali hydroxide) was added with vigorous agitation and the mixture was left to stand for two days at room temperature. The dioxane layer was separated and concentrated to a greyish white semisolid, which was dissolved in ether and washed with water. From the ether layer 1.6 g. (yield, 32%) of crystals were obtained, m.p. 118~120°C. On recrystallization from petroleum ether, white plates were obtained m.p. 122~123°C (α-form).

Anal. Found: C, 83.51; H, 6.45. Calcd. for $C_{22}H_{20}O_2$: C, 83.51; H, 6.37%. I.R. ν max: 3500, 2200 and 1700 cm.$^{-1}$ U.V. λ max: 258 mμ (log ε: 2.67) and 265 mμ (log ε: 2.56).

The specimens obtained by the above five reactions were confirmed to be the same acid by the melting point determination of mixed crystals.

On standing about two months at room temperature, the melting point of the crystals (IX, α-form) rose to 153~154°C (β-form) from 122 ~123°C (α-form). In I.R. and U.V. spectra of these two forms, no difference was observed.

Benzylation of Benzylcyanide. 2-Benzyl-2,3-diphenylpropionitrile (VII), 2-Benzyl-2,3-diphenylpropioamide (VIII), and the β-Form of 2-Benzyl-2,3-diphenylpropionic Acid (IX).—We carried out the benzylation reaction, as reported by Hauser et al.[14] and Baker[15] to get VII in a fair yield.

The product, 2-benzyl-2,3-diphenylpropionitrile, (VII), m.p. 81~83°C, b.p. 204~205°C (2 mm Hg). was mixed with 70% sulfuric acid in glacial acetic acid and the mixture was refluxed for 4 days to afford 2-benzyl-2,3-diphenylpropioamide (VIII), m.p. 122.7~114°C (Baker[15] reported m.p. 111~ 112°C).

Anal. Found: N, 4.20, Calcd. for $C_{22}H_{21}ON$: N, 4.44%.

When amide VIII was treated with sodium nitrite, 2-benzyl-2,3-diphenylpropionic acid (IX) (β-form) was given, m.p. and mixed m.p. with an authentic specimen of β-form, 153~154.5°C.

Anal. Found: C, 83.51; H, 6.45. Calcd. for $C_{22}H_{20}O_2$: C, 83.51; H, 6.37%. I.R. ν max: 5300, 2200 and 1700 cm^{-1}. U.V. λ max: 258 mμ (log ε: 2.67) and 265 mμ (log ε: 2.56).

Summary

The equimolar reaction between benzyl chloride and sodium acetylide in liquid ammonia resulted in the formation of 3-benzyl-3,4-diphenyl-1-butyne in addition to 3,4-diphenyl-1-butyne and 3,4-diphenyl-1,2-butadiene. This compound resisted various oxidative reagents except potassium permanganate. 2-Benzyl-2,3-diphenylpropionic acid was obtained in two polymorphs.

Infrared absorption sepectra were measured by Professor Kinumaki and his associates of this Institute and the elementary analyses were performed in the Laboratory of Shionogi Drug Manufg. Co., Ltd., to whom the writers are deeply indebted.

Chemical Research Institute of Non-aqueous Solutions, Tohoku University
Katahira-cho, Sendai

Polarographic Investigations of Vitamin C. I. On the Oxidation Waves of L-Ascorbic Acid and the Reduction Wave of Dehydro-L-ascorbic Acid

By Sôzaburo ONO, Masanosuke TAKAGI and Tamotsu WASA

(Received September 24, 1957)

Although the physiological importance of vitamin C (V. C) has been well known since its discovery, there still remain many problems unsolved concerning this vitamin. Namely, very little knowledge has been obtained even for the mechanism of its antiscorbutic processes[1]. The vitamin has been also discussed on its role as a member of the oxidation-reduction systems in both vegetable and animal bodies, and the measurements of the oxidation-reduction potentials of the system have been exhaustively carried out by several investigators[2~4]. In spite of their efforts, the previous knowledge may not seem to be sufficient to interpret the specificity of V. C. There are considerably many related substances of V. C which also possess close oxidation-reduction potentials to those of V. C and still do not show any physiological similitude[5~7].

On the other hand, as to the polarographic investigations of V. C hitherto reported, L-ascorbic acid (A. A.) has been known to be readily oxidizable at the dropping mercury electrode and the half-wave potential of the first wave (at pH= 0) is about 200 mV. more positive than the corresponding standard oxidation-reduction potential measured potentiometrically, while its oxidized form dehydro-L-ascorbic acid (D. A. A.) has been believed to show no reduction wave under the ordinary polarographic conditions[8~12].

In order to interpret these phenomena, many experimental and theoretical studies have been made by several investigators[13~16]. Indeed, the analysis of these disagreements between the polarographic and the potentiometric results would be expected to offer some clue to obtain real knowledge on the specificity of V. C.

It is, however, important to realize that the previous discussions have not been developed on the basis of the sufficient experimental results of both A. A. and D. A. A., and therefore the problem may not be said to have been solved even qualitatively.

In the present experiments, first the reinvestigations of the already known facts on the oxidation waves of A. A. were made and followed by the more careful and detailed experiments in alkaline region than previously known, and further a reduction wave of D. A. A. was obtained.

Although some of the observations concerning this reduction wave of D. A. A. have been already reported by the present authors[17], more detailed results are presented in this paper and discussions are made on the mechanism of the electrode reactions of both A. A. and D. A. A.

Experimental

Materials:—A. A. was a product of Takeda Pharmaceutical Ind. which was used without further purification.

D. A. A. was first prepared by using Pecherer's method[18], but later A. A. in aqueous solution was oxidized to D. A. A. with equimolar amount of iodine or bimolar amount of silver nitrate.

1) A. Szent-Györgyi, "Bioenergetics", Academic New York Press, (1957) p. 49.
2) H. Borsook and G. Keighly, *Proc. Nat. Acad. Sci.*, **19**, 875 (1933).
3) R. Wurmser and J. A. De Loureiro, *J. chim. phys.*, **31**, 419 (1934).
4) E. G. Ball, *J. Biol. Chem.*, **118**, 219 (1937).
5) G. M. Richardson and R. K. Cannan, *Biochem. J.*, **23**, 68 (1929).
6) N. Mayer, *J. chim. phys.*, **34**, 107 (1937).
7) R. Wurmser, N. Mayer and O. Crepy, ibid., **33**, 101 (1936).
8) E. Kodicek and K. Wenig, *Nature*, **142**, 35 (1937).
9) C. Cattaneo and G. Sartori, *Gazz. chim. ital.*, **72**, 351 (1942).
10) Y. Okada, *J. Agr. Chem. Soc. Japan*, (*Nippon Nogei Kagaku Kaishi*), **19**, 749, 955 (1943).
11) D. Nomura, Thesis for the graduation, Kyoto Univ. (1942).
12) C. Go, *J. Ferment. Technol. Japan*, **28**, 165 (1945).
13) Z. Vavrin, *Coll. Czech. Chem. Communs.*, **14**, 367 (1949).
14) R. Brdicka and P. Zuman, ibid., **15**, 766 (1950).
15) D. H. M. Kern, *J. Am. Chem. Soc.*, **76**, 4234 (1954).
16) J. Koutecky, *Coll. Czech. Chem. Communs.*, **20**, 116 (1955).
17) S. Ono, M. Takagi and T. Wasa, *J. Am. Chem. Soc.*, **75**, 4369 (1953).
18) B. Pecherer, ibid., **73**, 3827 (1951).

In order to obtain D. A. A. solutions of relatively high concentrations as purely as possible, the latter method was used preferably. In the case of the oxidation with iodine, iodine was used in an aqueous solution containing about twice mole of potassium iodide, and after the oxidation in a volumetric flask, the resulting solution was partly neutralized with sodium hydroxide or sodium acetate and then filled up to the mark. The solution was used without removing iodide ions. Silver nitrate as an oxidizing reagent was also used in an aqueous solution. After the oxidation of A. A. in a volumetric flask, some amounts of sodium hydroxide or sodium acetate which had been taken to adjust the pH of the solution to the desired value. The solution was filled up to the mark and then the silver precipitate was filtered off. The filtrate was used as D. A. A. solution.

The aqueous solution of D. A. A. was prepared each time freshly, since D. A. A. is fairly unstable even in acidic solution.

Buffer Solutions:—For the acidic range, McIlvaine's buffer solutions (pH 2.2~8.0) and acetate buffer solutions (pH 3.6~5.6) were used. For the alkaline range Kolthoff's buffer solutions (pH 8.0~12.0) and 0.1N sodium hydroxide (pH 13) were used. In the course of experiments, it was sometimes necessary to avoid the use of borate in the electrolytic solutions as will be seen later and in such cases, pH's were adjusted with sodium hydroxide and disodium hydrogen phosphate.

The water for preparing stock solutions of the sample and the buffer solutions was redistilled 3 or 4 times with a glass apparatus, since even the presence of trace of the copper ion is still unfavorable for the stability of A. A.

As maximum suppressor, aqueous solution of gelatin was used whose concentration was about 0.005% in the final electrolytic solution.

Apparatus and Procedure:—A Yanagimoto Polarograph with photographic recorder was used. The maximum sensitivity of the galvanometer was 5.5×10^{-9} A. The characteristics of the capillary used were $m=1.323$ mg./sec. and $t=2.7$ sec./drop in 0.1N potassium chloride solution at open circuit when the height of the mercury reservoir was 60 cm. A normal calomel electrode (N.C.E.) was used as a reference electrode. For the experiments of the oxidation waves of A. A. and D. A. A., the height of the mercury reservoir was usually 60 cm. The electrolytic cells were the most simple and common ones. Although no thermostat was used, the room temperature was roughly controlled at 15°±1°C during the experiments. For the experiments in acidic range, polarograms were taken from +0.3 V. (vs. N. C. E.).

As it is well known, A. A. in aqueous solution is readily oxidized by the atmospheric oxygen, especially in an alkaline medium, even the stock solution, whose pH was usually adjusted to less than 4 with buffer solution or meta phosphoric acid, was freed from oxygen by bubbling nitrogen gas, while a known volume of buffer solution (usually less than 7 ml.) was taken into an electrolytic cell and it was also bubbled with nitrogen gas for twenty minutes. Thereafter, a knwon volume of the stock solution (usually about 1 ml.) was pipetted out and added into the electrolytic cell, bubbling of nitrogen gas being still continued through the buffer solution. The bubbling was stopped after a few minutes and the polarogram was taken immediately. The concentration of the sample was usually 10^{-4} to 10^{-3} mol./l.

For obtaining the reduction wave of D. A. A. experiments were carried out under the following conditions.

Concentration range of D. A. A.:
0.025~0.1 mol./l.
pH range: 2~5
Temperature range:
10~50°C at 5°C intervals.

For the temperature control, the electrolytic cell fitted with a jacket was used, through which water of a constant temperature was circulated. The accuracy of the temperature control was ±0.05°C. Nitrogen was used for the removal of oxygen from the electrolytic solution.

Controlled Potential Electrolysis:—In order to know whether the electroreduction product of D. A. A. is A. A. or not, a manually controlled potential electrolysis, modifying Lingane's method[19], was employed. To omit the procedure to take up some portion of the electrolytic solution each time after the electro-reduction at the mercury pool, the electrolytic cell as shown in Fig. 1 was used; after the electrolysis for a given time at a fixed potential (a), the capillary is dipped into the same cell and polarograms are taken, using a calomel electrode as the outer reference electrode (b). For the salt bridge potassium nitrate was used in stead of potassium

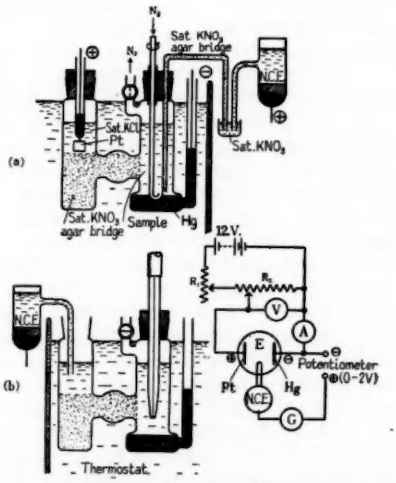

Fig. 1. Controlled potential electrolysis.
V—Voltometer A—Ammeter
E—Electrolytic cell G—Galvanometer

19) J. J. Lingane, *Discussions Faraday Soc.*, **1**, 203(1947).

chloride, since the anodic wave of A. A. is masked by that of the chloride ion. The preparation of D. A. A. by oxidation with iodine was not used for this electrolysis, since the presence of the iodide ion is not favorable in the same meaning as above.

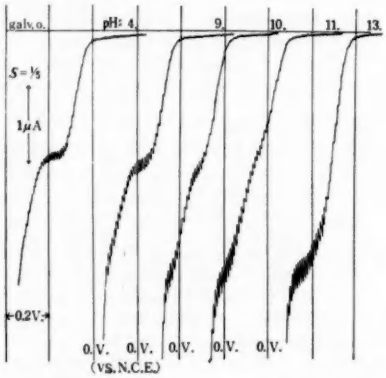

Fig. 2. Polarograms of A. A. in various pH. concn. of A. A. = 2.3×10^{-4} mol./l.

Results and Discussion

Oxidation Waves of A. A.—As is seen in Fig. 2, A. A. shows one oxidation wave at pH less than 8 and two at pH more than 8. Both the first and the second waves have almcst an equal height. Since two-electron transfer has been known with the first wave[8~16] the second wave should also involve another two-electron transfer. This total four-electron transfer for the oxidation of A. A. in alkaline range coincides with the observation by Euler and Hasselquist[20,21] who studied the oxidation of A. A. by means of the titration with 2, 6-dichlorophenol indophenol. Concerning the presence of the second wave, Müller and Phillips[22] have already stated it briefly, but they did not present its polarograms and, since then, there has been no other report which confirms even the presence of the wave. The second wave should not be overlooked, since there is certain possibility that it might be confused with the first one.

The relation between the half-wave potential of the first wave and pH was not so much different from those reported by other authors[9~14], but it was remarked that above pH 12 the measurement of the potential becomes difficult because of the superimposing of the first wave with the second.

The instability of A. A. should be also taken into consideration to obtain reliable data with A. A., especially in alkaline range. Fig. 3 shows an example of the change of the waves with time. The rate of the decrease of the wave height strongly depends on pH.

In Fig. 3 the first wave seems to decrease more quickly than the second. Considering only this phenomenon, it was first

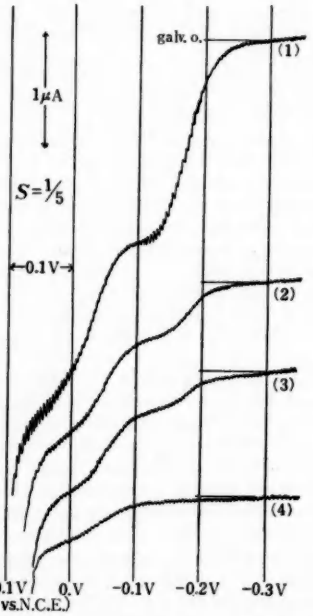

Fig. 3. Decrease of wave heights of A. A. due to the air-oxidation. pH=10.27, borate-NaOH buffer solution.
(1) concn. of A. A.=2.3×10^{-4} mol./l. without airation. (2) after 20 min. airation. (3) after 30 min. airation. (4) after standing for 24 hr. without airation.

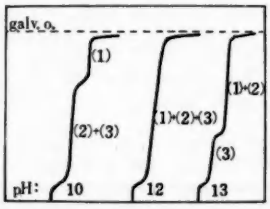

Fig. 4. Schematic polarograms of A. A. containing its decomposition product in alkaline buffer solution. (1) 1st wave (2) 2nd wave (3) 3rd wave

20) H. v. Euler and H. Hasselquist, *Arkiv Kemi*, **4**, 169 (1952).
21) H. Hasselquist, ibid., **4**, 370 (1952).
22) O. H. Müller and R. A Phillips, *Am. J. Physiol.*, **129**, 426 (1940).

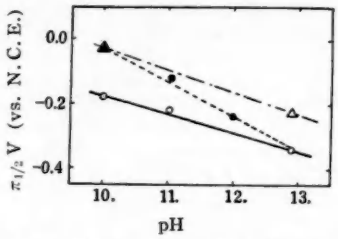

Fig. 5. pH dependence of the three waves of A. A.
○ 1st wave ●, 2nd wave, △ 3rd wave; $\pi_{1/2}$ of the large drawn wave at pH 12 was taken as the value of the 2nd wave at the pH.

supposed that the first oxidation product of A. A. in bulk alkaline solution would be identical with the electro-oxidation product corresponding to the first wave. But it was soon revealed that the above supposition was not adequate; it is readily seen when the same kind of experiment as shown in Fig. 3 is carried out at higher pH's. Fig. 4 schematically shows three different waves in alkaline range after partial oxidation of A. A. Here A. A. was first partially oxidized in alkaline solution and reacidified by metaphosphoric acid to pH 4 and used as stock solution. The experimental values of the half-wave potential of the three waves are presented in Fig. 5. From Figs. 4 and 5, it is apparent that the third wave which appeared after oxidation should be distinguished from the other two which have been initially present. At present it is, however, still difficult to predict to which stage of the oxidation processes of A. A. this third wave corresponds.

D. A. A. was also examined, in order to know its behavior in alkaline solution, in comparison with the above described three waves of A. A.; D. A. A. does not show any oxidation wave in the buffer solutions which contain more or less borate, though the three waves of A. A. were observed in the same buffer solutions. D. A. A. or 2, 3-diketogulonic acid (D. G. A.) seems to combine with the borate ion to a product which may be no more oxidizable at the dropping mercury electrode. This coincides with Militzer's observation[23] that the oxidation of D. A. A. or D. G. A. with methylene blue or the copper ion was completely hindered by the borate ion in alkaline solution. The present results may be also referred to Pasternak's report[24] that the disappearance of the polarographic reduction wave of benzil was caused by the reaction of its carbonyl group with the borate ion.

However, when buffer solutions were prepared only with sodium hydroxide and disodium hydrogen phosphate, D. A. A. showed very unstable and complicated oxidation waves. They were much less

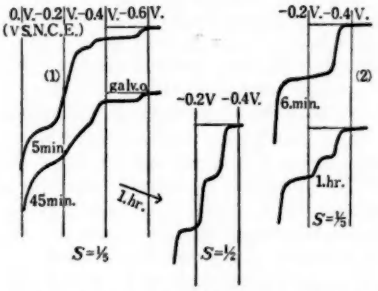

Fig. 6. Change of oxidation waves of A. A. and D. A. A. in alkaline solution (pH=12.9). (1) started with D. A. A. of 4.3×10^{-4} mol./l. (2) started with A. A. of 7.5×10^{-5} mol./l.

stable than those of A. A. and under the present experimental conditions they decreased quickly with time, even if the electrolytic solutions were kept from oxygen as free as possible. Fig. 6 shows an example of the change of the waves with time; starting with D. A. A. the waves were first considerably different from those of A. A., but after a certain time they seemed to show quite a similar character to each other. Above all, when the solution was reacidified, the polarogram of the former showed a wave which had the same $\pi_{1/2}$ as that of A. A. at the given pH. From these observations, though the possibility of reduction of D. A. A. to A. A. in alkaline solutions seems not to be denied, it may be more reasonable to consider the formation of some endiol compound which has a similar $\pi_{1/2}$ to that of A. A., e. g., triose-reductone[14].

The fact that D. A. A. or its decomposition products showed complicated oxidation waves may indicate that there must be several alkaline decomposition products of D. A. A., each of which has an endiol group or some other functional group as readily oxidizable as an endiol, as Petuely and Künssberg[25] have widely investigated with many of the related substances.

23) W. E. Militzer, *J. Biol. Chem.*, **158**, 247 (1945).

24) R. Pasternak, *Helv. Chim. Acta*, **30**, 1984 (1947).

25) F. Petuely and U. Künssberg, *Monatsh.*, **83**, 80 (1952).

Also the fact that some endiol compounds are formed during the decomposition process of D. A. A. in alkaline solution has been known by Euler and Hasselquist[26]. On the other hand, Trnka[27] found three different anodic waves during the decomposition process of glucose in alkaline solution from which he predicted three kinds of endiol compound. Taking into account the possibility of some common processes between the decomposition of glucose and that of A. A., it would be expected to find some common endiols, and further investigations of this kind may seem to be interesting to continue. For that purpose, however, not only polarography but some other more direct methods should be used. At present, therefore, no further discussion is made.

In consideration of the present results together with the previous knowledge on endiol compounds obtained by Euler et al.[28,29] and Petuely et al.[25], the stepwise electrode reactions of A. A. in alkaline solution may be expressed in one way as follows.

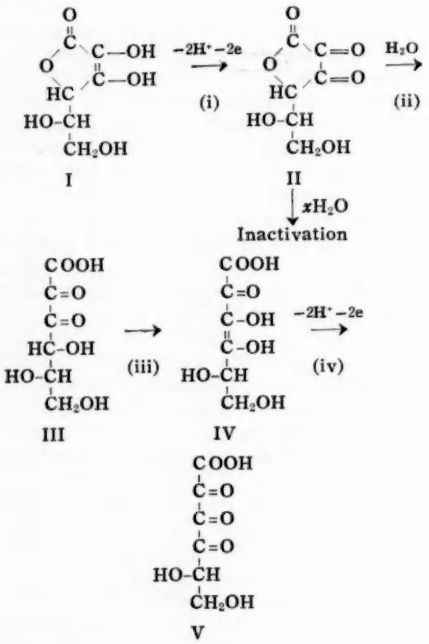

In the above diagram, i) is the reaction corresponding to the first wave of A. A. and iv) to the second. Here it is supposed that D. A. A. which has been produced by the reaction i) opens its lactone ring (ii) and further it is converted into an endiol by the rearrangement iii). The endiol is further oxidized at the dropping mercury electrode (iv). In this case the rate of reaction of both ii) and iii) must be by all means enough rapid, compared with the diffusion process. Since it has been found that D. A. A. or D. G. A. reacts with the borate ion to an electroinactive substance, the rate of both ii) and iii) must be also sufficiently rapid than that of the above inactivation reaction. Further it may be supposed that the substances IV and V can be decomposed in the bulk solution. Above all, the fact that though D. A. A. or D. G. A. reacts with the borate ion to produce an inactive substance, A. A. showed an oxidation wave of its decomposition product after standing of the solution even in the presence of the borate ion, may suggest the possibility of the direct opening of the lactone ring.

Reduction Wave of D. A. A.—D. A. A. shows a small reduction wave at the potential between −0.3 and −0.5 V. (vs. N. C. E.) in pH 2~5, when polarograms are taken at room temperature with D. A. A. of relatively high concentrations (0.025 ~0.1 mol./l.).

The reduction wave of D. A. A. at 25°C corresponds to about 1/1000 of its expected diffusion current which can be approximately estimated from the oxidation wave of A. A. The shape of the wave of D. A. A. and its inclination differ considerably from those of A. A. Also the reduction wave of D. A. A. shows all the typical characteristics of a kinetic current: constancy of the wave height, independency of the height of the mercury reservoir (Fig. 7) and its great temperature coefficient, which was 7~8%/degree (Fig. 8).

At a given temperature, the wave height

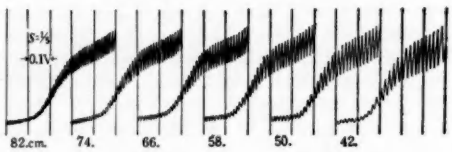

Fig. 7. Constancy of the wave height of D. A. A., independent of the height of the mercury reservoir. Concn. of D. A. A.=0.1 mol./l. in McIlvaine buffer, pH 2.8, 25°C.

26) H. v. Euler and H. Hasselquist, *Arkiv Kemi*, **8**, 67 (1955).
27) J. Trnka, *Proc. I. Intern. Polarogr. Congr. Prag* **III**, 518 (1951).
28) H. v. Euler and H. Hasselquist, "Die Reduktone", Stuttgart, Enke (1950).
29) H. v. Euler and H. Hasselquist, *Arkiv Kemi*, **5**, 49 (1952).

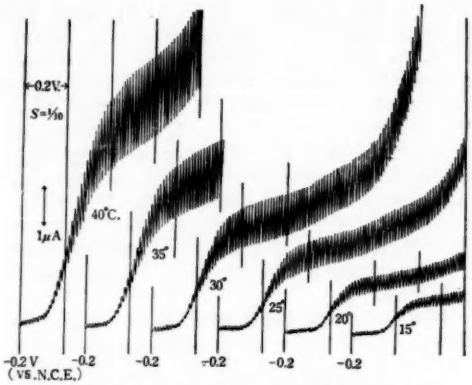

Fig. 8. Increase of wave height of D. A. A. with increasing temperature. Concn. of D. A. A.=0.1 mol./l. in McIlvaine buffer solution, pH 2.8.

of D. A. A. was roughly proportional to its concentration and was not appreciably changed with pH and it was also the case even in the neighborhood of pH 0.

TABLE I
HALF-WAVE POTENTIALS OF D. A. A. IN McILVAINE BUFFER SOLUTION AT 25°C.
Conc. of D. A. A.=0.025 mol./l.

pH	2.20	2.66	2.96	3.48
$\pi_{1/2}$(vs. N.C.E.)	−0.350	−0.372	−0.392	−0.410
pH	3.80	4.22	4.63	5.04
$\pi_{1/2}$(vs. N.C.E.)	−0.432	−0.450	−0.462	−0.480

The half-wave potential of the reduction wave is presented in Table I. Whether the half-wave potential, the wave height or the shape of the wave can be influenced by the components of the buffer or the manner of preparation of D. A. A. was examined and no appreciable change has been observed except for the D. A. A. prepared by the oxidation with iodine in aqueous solution, in which the presence of the iodide ion caused the shift of the half-wave potential of D. A. A. toward a little more negative value.

On plot of the logarithms of the wave heights of D. A. A. against reciprocal absolute temperature, a linear relationship has been obtained and its inclination was found to be independent of pH and the concentration of D. A. A. as seen in Fig. 9.

Above pH 5 the rate of decomposition of D. A. A. increases abruptly and besides the reduction wave of D. A. A., another reduction wave begins to grow up which may be due to one of the decomposition products of D. A. A. whose $\pi_{1/2}$ is slightly more negative than that of D. A. A. Consequently it becomes difficult to take reproducible polarograms of D. A. A. and in the present studies further experiments in pH more than 5 have not been made.

As stated in the experimental part, gelatin, an ordinary maximum suppressor, was not used for obtaining well defined polarograms, since gelatin markedly influenced the shape of the reduction wave of D. A. A. Fig. 10 shows the effect of gelatin on the reduction wave of D. A. A. On addition of only 1 drop of 0.5% gelatin

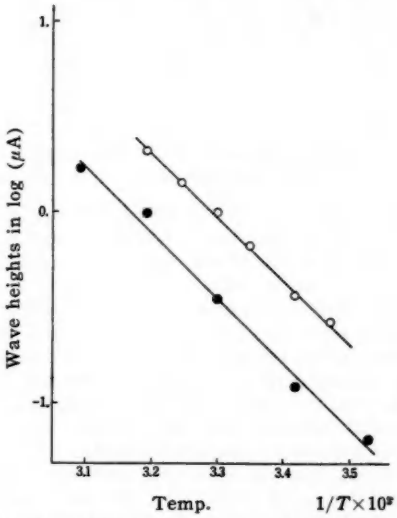

Fig. 9. Relationship between the logarithm of the height of the reduction wave of D. A. A. and reciprocal absolute temperature.
○ Concn. of D.A.A.=0.1 mol./l. at pH 2.8
● Concn. of D.A.A.=0.05 mol./l. at pH 2.7

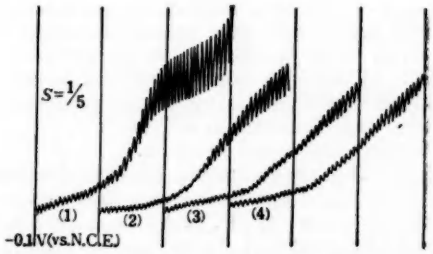

Fig. 10. Influence of gelatin on the reduction wave of D. A. A. Concn. of D. A. A.=0.1 mol./l., pH 2.8, 30°C.
(1) without gelatin
(2) 1 drop of 0.5% gelatin to 10 ml. of the soln. (1)
(3) 2 drops of 0.5% gelatin
(4) 3 drops of 0.5% gelatin

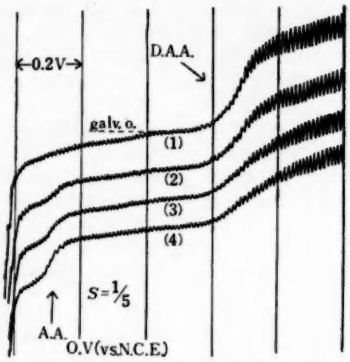

Fig. 11. Controlled potential electrolysis of D. A. A. at −0.7 V. (vs. N. C. E.), Concn. of D. A. A. = 0.1 mol./l., pH 3.5, 25°C
(1) before electrolysis (2) after 20 min. (3) 40 min. (4) 60 min.

aqueous solution into 10 ml. of the electrolytic solution, the wave was strongly deformed; with three drops of the same gelatin solution, the wave became completely drawn out. Though no further experiments have been carried out concerning this problem, the above phenomena may indicate that a reaction which proceeds before the electrode reaction is retarded by the presence of the surface active substance such as gelatin.

Fig. 11 shows that the growth of the anodic wave of A. A. can be observed as the electrolysis proceeds. In this case, it may be easily understood that the anodic wave of A. A. increases with increasing time, while the cathodic wave of D. A. A. remains almost unchanged, since the former has the character of a normal diffusion current and the latter that of a typical kinetic one. During the electrolysis it was found that the reduction wave of D. A. A. was gradually deformed with time. It may be considered to owe to a surface active property of the agar-agar which was dissolved from the salt bridge into the electrolytic solution.

From the above series of experiments on D. A. A., it has been seen that the reduction wave of D. A. A. is a typical kinetic current and its reduction product is A. A. Then, the attention should be turned to the inactive form of D. A. A. in the follow ingsystem in which the inactiavtion reaction of D. A. A. must be reversible.

$$\text{Inactive form of D. A. A.} \rightleftharpoons \text{D. A. A.} \underset{-2H^+-2e}{\overset{+2H^++2e}{\rightleftharpoons}} \text{A. A.} \quad (1)$$

The inactive form of D. A. A. may be most probably its hydrated form. What D. A. A. may react with water to produce a hydrated product, has long since been suggested by Herbert et al.[30], and also Vavrin[13] supposed the hydration when he interpreted the discrepancy between the $\pi_{1/2}$ of the anodic wave of A. A. and its potentiometrically obtained π_0. However, any detail of the hydration itself has not been discussed. It may be partly because no reduction wave of D. A. A. has been obtained.

The hydrated form of D. A. A. which is proposed as the most probable one by the present authors, is II′ of the following two configurations.

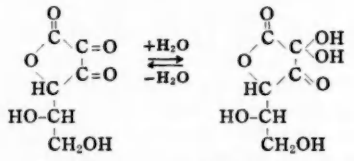

D. A. A. II — Hydrated D. A. A. II′

The high reducibility of D. A. A. (II) at the dropping mercury electrode is readily understood since three carbonyl groups are conjugated, while the hydrate (II′) seems difficult to be reduced since the conjugation of II is here completely hindered by the hydration at the central carbonyl group of the three. The most feasible hydration at the central carbonyl group among the three may be inferred from the electronic effect caused with two other carbonyl groups on the central.

As for the similar type of hydration of carbonyl group, it is seen in the investigations of some aldehydes, especially of formaldehyde[31~34] and acetaldehyde[35~37].

On the other hand, there must be certain possibility of hydration not only at the central carbonyl group but also at either one of the other two or both. Let us, however, assume, for convenience'

30) R. W. Herbert, E. L. Hirst, E. G. V. Parcival, R., J. W. Reynolds and F. Smith, *J. Chem. Soc.*, **1933**, 1270.
31) K. Vesely and R. Brdicka, *Coll. Czech. Chem. Communs.*, **12**, 313 (1947).
32) R. Bieber and G. Trümpler, *Helv. Chim. Acta*, **30**, 706 (1947).
33) R. Brdicka, *Coll. Czech. Chem. Communs.*, **20**, 387 (1955).
34) J. Koutecky, ibid., **21**, 652 (1956).
35) R. Bieber and G. Trümpler, *Helv. Chim. Acta*, **30**, 2000 (1947).
36) R. P. Bell and J. C. Clunie, *Trans. Faraday Soc.*, **48**, 439 (1952).
37) R. P. Bell and J. C. Clunie, *Proc. Roy. Soc.*, (*London*), **212A**, 33 (1952).

sake, only one hydrated form of D. A. A., namely II'. Since the reduction wave of D. A. A. is much smaller than its expected diffusion current and possesses all the typical characteristics of the kinetic current, the equation derived by Koutecky[16,38,39] may be applied to the present problem.

$$\text{Hydrated D. A. A.} \underset{k_2}{\overset{k_1}{\rightleftarrows}} \text{D. A. A.} \underset{\text{Electrode reaction}}{\rightleftarrows} \text{A. A.} \qquad (1')$$

$$k_1 = [i_k/(i_d - i_k)]^2 1.31 K_h/t \qquad (2)$$

where k_1 and k_2 are the rate constants of the dehydration and hydration, respectively, and i_d and i_k are the expected diffusion current and actual kinetic current, respectively. K_h is the hydration constant and equal to k_2/k_1 and t, the drop time. If the diffusion constant of D. A. A. is assumed to be approximately equal to that of A. A., i_d may be calculated with the latter which is readily known from the anodic diffusion current of A. A. However, in order to obtain k_1 and k_2 from the kinetic current of D. A. A. by using the above equation, the hydration constant K_h should be known. It seems scarcely possible to obtain its reliable value even by the spectrophotometric method as it was applied by Bieber and Trümpler[32] to measure the hydration constant of formaldehyde, since the equilibrium between D. A. A. and its hydrated form seems much shifted toward the hydrated form and also D. A. A. is unstable in an aqueous solution.

Reversibility of the A. A. and D. A. A. System:— Aside from the question how the problem is related to the biological meaning, it must have some value to consider the reversibility of the system from the electrochemical standpoint.

Compared with the fact that an impression as if the reduction wave of D. A. A. were in any way unobtainable has been hitherto maintained among polarographists, the results of the present investigations may be said to have ascertained at least that D. A. A. can be reduced to A. A. at the dropping mercury electrode at a relatively positive potential. But it does not mean that the present data would directly give an evidence of the reversibility of the system in the sense of thermodynamics.

In order to consider the reversibility of the system, both the reduction wave of D. A. A. and the oxidation wave of A. A. should be studied not only with their limiting current but also with the whole current-voltage curve of the system.

Concerning the problem of this kind, after the previous paper[17] had been published by the present authors, Koutecky[16] reported his mathematically rigorous studies on the system which may coincide with the present one (1) in the case where the latter electrode reaction itself is reversible. He also discussed the character of both the reduction wave of D. A. A. and the oxidation wave of A. A. as an application of his theory.

According to Koutecky, if his theory is valid for the case of the A. A. and D. A. A. system, the height of the reduction wave should take the value to satisfy the relation

$$i_0/i_\infty = 10^{-6.9} \qquad (3)$$

where i_0 and i_∞ correspond to the limiting currents of D. A. A. and A. A. of the same concentration, respectively. The above relation may be derived by substituting the experimentally obtained potential shift of the $\pi_{1/2}$ of the oxidation wave from the π_0 of the system, into his equation; the potential shift is usually observed to be about 200 mV. Also the half-wave potential of the reduction wave should be identical with that of the oxidation wave.

In spite of his above conclusion, the discrepancies between the present experimental results and the above theoretically deduced value are quite large; the actual reduction wave is greater by the order of 10^4 and its half-wave potential is about 0.5 V. more negative than that theoretically expected.

Therefore Koutecky's theory may not be said to be applicable to the present problem as he already pointed out. Nevertheless, it seems also interesting to consider the causes from which the above disagreements should arise. In this respect, the assumption of the reversibility of the electrode reaction should be first reconsidered.

If the electrode reaction itself is more or less irreversible, the above phenomena will be more readily understood, though their quantitative analysis may hardly be possible. Also the fact that many investigators remarked the slow establishment of the equilibrium potential of the A. A.

38) J. Koutecky and R. Brdicka, *Coll. Czech. Chem. Communs.*, **12**, 337 (1947).
39) J. Koutecky, ibid., **18**, 597 (1953).

and D. A. A. system[40], when they investigated it potentiometrically, may remind us of the possibility of the polarographically irreversible electrode reaction.

Consequently the reversible character of the oxidation wave should be reinvestigated. Even the experimental results of the half-wave potential dependence on drop time of mercury obtained by Kern[15] do not seem to be in good agreement with his own theory in which he also derived an equation for the oxidation wave which differs from Koutecky's only in the numerical factors.

Summary

L-Ascorbic acid (A. A.) shows an oxidation wave at pH less than 8 and two in a more alkaline range. After standing of A. A. in alkaline solution, the third oxidation wave has been observed.

Dehydro-L-ascorbic acid (D. A. A.) has been also tested in alkaline solution. The mechanism of the electrode oxidation of A. A. and its decomposition in alkaline solution are discussed. The reduction wave of D. A. A. has been obtained at pH 2 to 5, in which the half-wave potential is about −0.3 to −0.5 V. (vs. N. C. E.).

The wave height is about 1/1000 of its expected diffusion current at room temperature. The wave has all the typical characteristics of the kinetic current. The wave height is roughly proportional to the concentration and is not appreciably influenced by pH and the components of the buffer solution, but the shape of the wave is strongly deformed by adding small amounts of surface active substance such as gelatin.

The reduction product of D. A. A. at the dropping mercury electrode has been polarographically proved to be A. A.

Discussions are made on the configuration of the inactive form of D. A. A. and the reversibility of the A. A. and D. A. A. system.

The authors wish to express their thanks to Professor Isamu Tachi of Kyoto University and Assistant Professor Shinji Koide of Mukogawa Women's University for their kind advice and encouragement.

Laboratory of Biophysical Chemistry
College of Agriculture
University of Osaka Prefecture, Sakai

40) See for example E. G. Ball's report[41].

Polarographic Investigations of Vitamin C. II. On the Reduction Waves of Some Conjugated Tricarbonyl Compounds as Related Compounds of Dehydro-L-ascorbic Acid

By Sôzaburo ONO, Masanosuke TAKAGI and Tamotsu WASA

(Received September 24, 1957)

In the previous papers[1,2], it has been reported that dehydro-L-ascorbic acid (D.A.A.) shows a reduction wave which has the character as a kinetic current and the reduction product at the dropping mercury electrode is L-ascorbic acid(A.A.), and discussions were made on the inactive form of D.A.A. in aqueous solution and the hydration of carbonyl group was considered.

Since the possibility of the hydration in D.A.A. was proposed to be due to its conjugated three carbonyl groups, there must be seen also the same kind of kinetic current in other conjugated tricarbonyl compounds and it seems also interesting to study their behavior as kinetic current, in relation to their molecular configuration.

In the present investigations, following three conjugated tricarbonyl compounds were thus taken up.

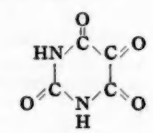

Alloxan
(I)

1) S. Ono, M. Takagi and T. Wasa, *J. Am. Chem. Soc.*, **75**, 4369 (1953).
2) S. Ono, M. Takagi and T. Wasa, This Bulletin, **31**, 356 (1958).

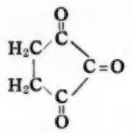

Dehyro-reductic acid
(II)

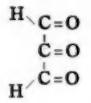

Mesoxalaldehyde
(III)

Of these three substances, the reduction wave of alloxan was already studied by Sartori and Liberti[3], but they do not seem to have paid any attention on its behavior as a kinetic current. Concerning other two substances, though their reduced forms i.e. reductic acid[4] and triose-reductone[5] have been polarographically studied, the reduction waves of dehydro-reductic acid and mesoxalaldehyde have not been hitherto believed to be available.

In the present paper, it will be therefore emphasized that each of the above three substances shows a reduction wave which has a similar behavior to that of D.A.A. and discussions will be developed on some correlations between the characteristics of the waves of these four substances including D.A.A. and their oxidation-reduction potentials.

Experimental

Materials.—L-Ascorbic acid was the same specimen as used in the previous works[1,2]. Triose-reductone was kindly given to us by Professor Hans von Euler of Stockholm University and later it was also prepared in our laboratory according to his method[6].

Reductic acid was prepared by Reichstein and Oppennauer's method[7].

Alloxan monohydrate was a product from Eastman Kodak Co.

Of the above four substances, alloxan could be directly used in aqueous solution for the purpose of the present experiments, while other three substances needed to be oxidized, in order to obtain their dehydro-forms. For that, various oxidizing reagents e.g. iodine, silver acetate and quinone were tried, since it would not be interesting if the polarograms should be unfavorably influenced by the oxidizing reagent used. The oxidation method finally used was as follows.

Each of the above substances, whose amount is weighed to produce 10 or 25 ml. of 0.1 mol./l. solution, is taken in a 10 or 25 ml. volumetric flask and dissolved with a small amount of the four times redistilled water (usually 2 or 5 ml.). Silver nitrate in aqueous solution, whose amount is so weighed as to be bimolar of the sample, is added into the same volumetric flask. After the oxidation has been completed, sodium acetate is added and then the whole solution is filled up with distilled water. The amount of the sodium acetate is taken according to the components of the acetate buffer so that the pH of the resulting solution is to be about 3.5. The solution is then filtered and the filtrate is immediately used as polarographic solution, in which the dehydro-form of 0.1 mol./l., sodium nitrate of 0.2 mol./l. and the components of the acetate buffer are included. In order to prepare the solutions of the dehydro-form whose concentrations are less than 0.1 mol./l., sodium nitrate and components of the acetate buffer are added into the preparation before filling up so that the resulting solutions contain the same concentrations of sodium nitrate and buffer components as above.

Alloxan was directly dissolved into the acetate buffer with sodium nitrate.

The final pH of the polarographic solutions was checked with a glass electrode. McIlvaine's buffer solutions were sometimes used instead of the distilled water to fill up the solutions of samples, and pH's were randomly changed in a limited range between 2.2 and 4.0.

Procedure and Apparatus.—The polarograph was the same one as used in the previous work[1,2]. The maximum galvanometer sensitivity was 1.72×10^{-9} A. The characteristics of the capillary used were $m=0.908$ mg./sec. and $t=4.21$ sec./drop in the buffer solution (pH 3.4) when the height of the mercury reservoir was 60 cm. and the applied potential was -0.4 V. (vs. N.C.E.) at 25°C. For the temperature control, the same cell fitted with a jacket as used in the previous work, was employed. Polarograms were taken from 10°C to 50°C at 5°C intervals. The accuracy of the temperature control was ±0.05°C. As the reference electrode, a normal calomel electrode was used.

Controlled Potential Electrolysis.—The controlled potential electrolysis of alloxan was carried out by means of the same apparatus as described in the previous paper[2].

Results and Discussion

The polarograms of alloxan, dehydro-reductic acid and mesoxalaldehyde are presented in Figs. 1, 2 and 3, respectively. As immediately seen from the above figures, the temperature coefficient of the wave height of each substance is so great as in the case of D.A.A. The wave height was also found to be independent of the height of the mercury reservoir. Therefore it may be said that all the three substances show the character as kinetic currents which are similar to that of D.A.A.

The relationship between the wave height of each substance and the temperature

3) G. Sartori and A. Liberti, *Ricerca sci.*, **16**, 313 (1946).
4) F. Santavy and B. Bitter, *Coll. Czech. Chem. Communs.*, **15**, 112 (1950).
5) R. Brdicka and P. Zuman, ibid., **15**, 766 (1950).
6) H. v. Euler and H. Hasselquist, "Reduktone", Stuttgart, Enke (1950).
7) T. Reichstein and R. Oppennauer, *Helv. Chim. Acta*, **16**, 988 (1933).

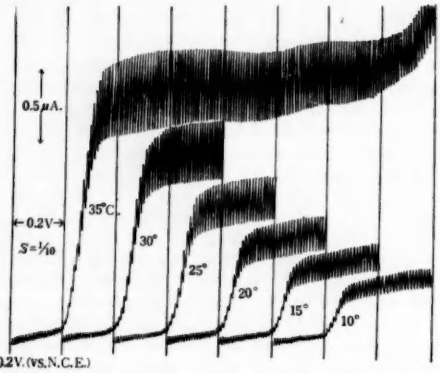

Fig. 1. Temperature dependence of the wave height of alloxan. Concn. of Alloxan = 5×10^{-3} mol./l., pH 3.6, Hg 60 cm.

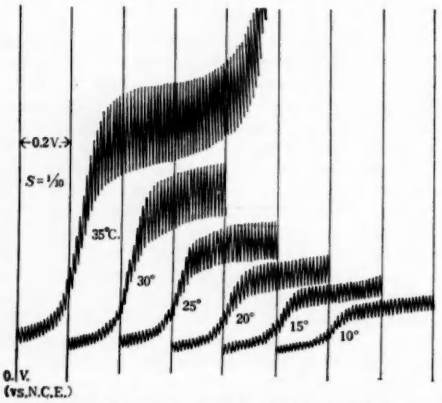

Fig. 2. Temperature dependence of the wave height of Dehydro-reductic acid. Concn. of dehydro-reductic acid = 0.05 mol./l., pH 2.8, Hg 60 cm.

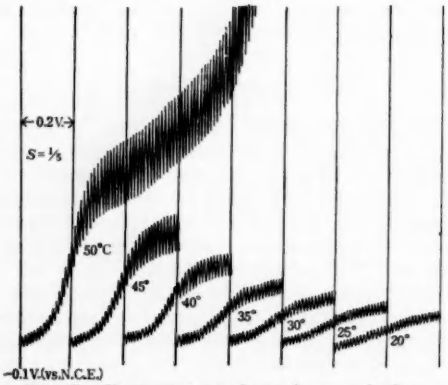

Fig. 3. Temperature dependence of the wave height of Mesoxalaldehyde. Concn. of mesoxalaldehyde = 0.1 mol./l., pH ≒3.0, Hg 60 cm.

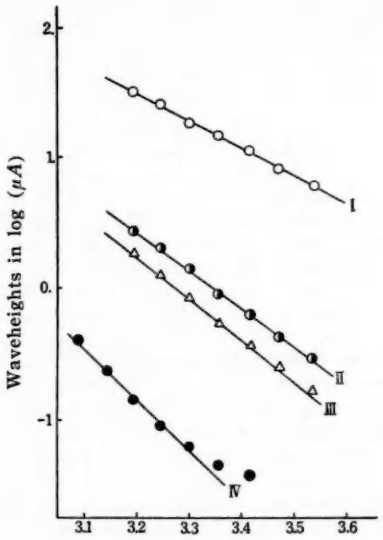

Fig. 4. Plot of logarithm of the reduction wave height against reciprocal absolute temperature.
I Alloxan
II Dehydro-reductic acid
III Dehydroascorbic acid
IV Mesoxalaldehyde
Concn. of each substance = 0.1 mol./l., pH 3.5, Hg 60 cm.

is shown in Fig. 4, where the logarithm of the wave height is plotted against the reciprocal absolute temperature. Since the wave height of each substance, including D.A.A., was found to be roughly proportional to its concentration at a given temperature, the wave heights of the substances of 0.1 mol./l. were in some cases recalculated from the experimental values obtained with more dilute concentrations. Although it was not strictly examined whether the relationship presented in Fig. 4 is valid for a wider pH range, no appreciable change in the wave height has been observed, in a range between pH 2.2 and 4.0.

Since all the substances are not stable enough in aqueous solution, the experiments with changing pH were not made in the outer range other than above mentioned. The half-wave potentials of these substances in pH 3.5 are listed in Table I.

It seems to be difficult to find any correlation between the wave height and the half-wave potential from Fig. 4 and Table I, while it may be of interest to consider

TABLE I

$\pi_{1/2}$ in pH 3.5	Alloxan	Dehydro-reductic acid	Dehydroascorbic acid	Mesoxalaldehyde
V(vs. N.C.E.)	−0.05	−0.27	−0.42	−0.35

TABLE II

$\pi_0-\pi_{1/2}$ of the reduced form	Dialuric[8] acid, Alloxan	<	Reductic acid,[9] Dehydro-reductic acid	<	Ascorbic acid,[10] Dehydro-ascorbic acid	< Triose-reductone,[11] Mesoxalaldehyde
Height of the reduction wave	Alloxan	>	Dehydro-reductic acid	>	Dehydro-ascorbic acid	> Mesoxalaldehyde
Temp. coeff. of the reduction wave	Alloxan	<	Dehydro-reductic acid	<	Dehydro-ascorbic acid	< Mesoxalaldehyde

the present results in connection with the standard oxidation-reduction potential π_0 of the corresponding system and the half-wave potential $\pi_{1/2}$ of the anodic wave of the reduced form.

As Brdicka and Zuman pointed out[5], each of the reduced forms of the above substances (i.e. dialuric acid, reductic acid, triose-reductone and D.A.A.), shows a considerable shift of the $\pi_{1/2}$ of the anodic wave from its corresponding π_0 to a more positive potential. Therefore, they described this fact as a characteristic of endiol group. In their paper, however, no further considerations on these potential shifts were made.

In Table II, these four substances are arranged in the order of magnitude of the above stated potential shift, the reduction wave height and its temperature coefficient, respectively. It may be said, of these four oxidation-reduction systems, that the smaller the height of the reduction wave, the larger both the shift of $\pi_{1/2}$ of the anodic wave from the corresponding π_0 and the temperature coefficient of the reduction wave height.

In the previous paper[2], discussions were made on the problem of the reversibility of the A.A. and D.A.A. system, on the basis of the experimental results, referring to the theoretical studies made by Koutecky[12]. Considerable disagreements between the experimental values and Koutecky's theoretical ones were found when the electrode reaction of the system was assumed to be reversible. Then, as a cause of these disagreements, the irreversible electrode reaction was assumed by the present authors. However, the correlation between the height of the reduction wave and $\pi_0-\pi_{1/2}$ of the anodic wave, presented in Table II, may suggest that although the electrode reaction itself is not reversible, the inactivation of the oxidized form in aqueous solution must be one of the most important factors which may cause both the potential shift and the kinetic current. The inactivation may be due to the hydration at the central carbonyl group among the conjugated three, as it was in the case of D.A.A.

As for the effort to interpret the above disagreements from different standpoint, though Zuman suggested the possibility of the opening of the lactone ring in the case of D.A.A.[13], such may not be taken into consideration, since the above three substances other than D. A. A. have different configurations and still show quite similar behavior of the kinetic current to that of D.A.A. Despite of that, there remains another kind of possibility, that the reducible form which causes the kinetic current is not the completely dehydrated one as shown in I, II and III, but the one in which hydration is still maintained at either one of the two carbonyl groups except the central.

Let us now consider again the reversibility of the above four oxidation-reduction systems. It is obviously seen that the $\pi_{1/2}$ of the reduction waves of D.A.A., dehydro-reductic acid and mesoxalaldehyde do not coincide with those of the corresponding oxidation waves, but in contrast with them, alloxan was expected to give the coincidence of the potentials in this respect, since the $\pi_{1/2}$ of alloxan is considerably more positive than those of the other three; also Sartori and Liberti[3] reported the reversible character of the dialuric acid and alloxan system.

8) G. M. Richardson and R. K. Cannan, *Biochem. J.*, **23**, 68 (1929).
9) N. Mayer, *J. chim. phys.*, **34**, 107 (1937).
10) G. Ball, *J. Biol. Chem.*, **118**, 219 (1937).
11) R. Wurmser, N. Mayer and O. Crepy, *J. chim. phys.*, **33**, 101 (1936).
12) J. Koutecky, *Coll. Czech. Chem. Communs.*, **20**, 116 (1955).
13) P. Zuman, A private communication to the authors. See also M. Brezina and P. Zuman, "Die Polarographie in der Medizin, Biochemie und Pharmazie" Akademische Verlagsgesellschaft, Leipzig, (1956), p. 423.

though they do not seem to have paid any attention on the characteristics of alloxan as a kinetic current.

As seen in Fig. 5, a practically perfect coincidence of the $\pi_{1/2}$ of the reduction wave with that of the oxidation wave, which is due to dialuric acid formed by

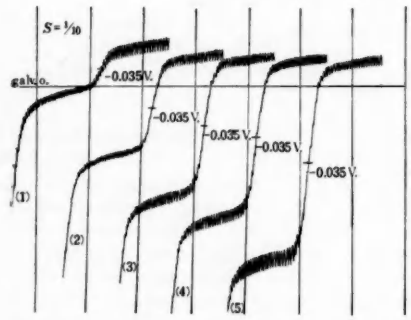

Fig. 5. Controlled potential electrolysis of alloxan at −0.2 V. (vs. N.C.E.). Polarograms were taken at 45 min. intervals. Conc. of alloxan $=1\times10^{-3}$ mol./l., pH 3.09, temp. 35°C, Hg 60 cm.

the electrolysis, has been observed. It may be readily understood that the height of the oxidation wave becomes larger than that of the initial reduction wave as the electrolysis proceeds, since the former is a diffusion current, while the latter a kinetic one.

From these observations, it may be said that the theory derived by Koutecky is at least applicable to the case of alloxan.

In order to solve the question why the electrode reaction is reversible only with the dialuric acid and alloxan system and irreversible with the other three systems, the investigations will be further developed.

Summary

Alloxan, dehydro-reductic acid and mesoxalaldehyde show reduction waves which are similar to that of dehydro-L-ascorbic acid. The half-wave potentials of alloxan, dehydro-reductic acid, dehydro-L-ascorbic acid and mesoxalaldehyde in pH 3.5 are −0.05, −0.27, −0.42 and −0.35 V. (vs. N.C.E.), respectively.

Of these four substances, the lower the height of the reduction wave, the greater both the shift of the half-wave potential of the anodic wave of the corresponding reduced form from the standard oxidation-reduction potential of the system and the temperature coefficient of the height of the reduction wave.

Inactive forms of these substances at the electrode reaction may be the hydrated ones as proposed in the case of dehydro-L-ascorbic acid.

Alloxan has been proved to be polarographically reversible by the controlled potential electrolysis and the half-wave potential of the reduction wave coincides with that of the oxidation wave of dialuric acid, while no such observations have been made with the other three.

The authors would like to express their sincere thanks to Professor Hans von Euler and his coworkers for their kindness that they have given them a specimen of pure triose-reductone.

Laboratory of Biophysical Chemistry
College of Agriculture, University
of Osaka Prefecture, Sakai

Determination of Small Quantities of Acetone in Methyl Methacrylate Monomer

By Yuzi TAKAYAMA* and Fumikazu TOKIWA**

(Received May 24, 1957)

At the present time for the determination of acetone in methyl methacrylate monomer (simply M-MM), hydroxylamine hydrochloride method has been used, but the method is common to both ketones and aldehydes, so that it can not determine acetone only.

Many studies on the determination of acetone are reported and each of them has its own characteristics. Especially, salicylaldehyde method generally is not applicable to the determination of acetone in M-MM on account of coloration of M-MM itself. One of the best is J. Messinger's[1] iodo titration method by iodoform reaction and some of the reported modifications of Messinger's[1] technique indicate the widespread utility of this procedure. But iodometry has generally too low an accuracy for the determination of small quantities of acetone. Absorption method in the ultraviolet region has been well studied including the work of Barthauer[2], Nogare[3], Stolyarov[4], Andreev[5], Etienner[6] and Shchukarev[7]. Nogare's method may be considered as surpassing the others in easiness of obtaining the reagents, and in relative simplicity of the method; it seems also to be comparatively sensitive, but its application is, limited in determination of acetone in either aqueous solution or non-aqueous solvent which is miscible with water. In this report the application of Nogare's method was investigated for determination of small quantities of acetone in a medium which is immiscible with water to establish a method superior to those previously used.

Iodoform has a strong absorption in the ultraviolet region from 400 to 250 mμ. This is characterized by three defined maxima occurring at 274, 307 and 347 mμ, in chloroform as shown in Fig. 1. Therefore, acetone in sample M-MM is caused to react in an alkaline solution with sodium hypoiodite by vigorous shaking. The absorbancy of resulting iodoform is measured at 347 mμ.

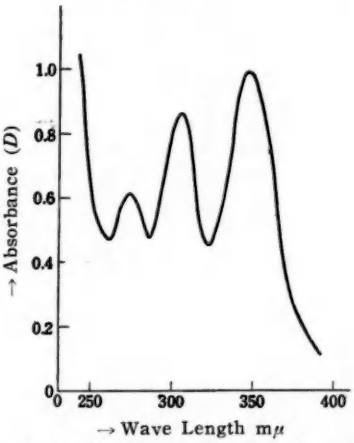

Fig. 1. Iodoform absorption spectrum.

Experimental

Apparatus.—Shimadzu's photoelectric spectrophotometer with glass cells of 10 mm. thickness and a tungsten lamp was used for absorbancy measurement.

Reagents.—Sodium hydroxide solution: 25% aqueous solution.

Iodine solution: 4 g. of potassium iodide and 20 g. of iodine in 80 ml. of water.

Sodium thiosulfate solution: 5% aqueous solution.

Anhydrous sodium sulfate: First grade reagent.

Chloroform: First grade reagent.

Procedure.—Place 7 ml. of 20% iodine solution in a 100 ml. separatory funnel and add 2 ml. of 25% sodium hydroxide solution. Mix by swirling. When the resulting solution is not distinctly orange-yellow, add iodine solution drop by drop. To this hypoiodite solution add 1 ml. of the sample containing no more than 400 γ acetone, and mix immediately. Shake for 5 minutes at

* Mitsubishi Rayon Co., Ltd., Kyobashi, Tokyo.
** Tokyo Scientific College, Shinjuku-ku, Tokyo.

1) J. Messinger, *Ber.*, **21**, 3366 (1888).
2) G. L. Barthauer, F. V. Jones and A. V. Metler, *Ind. Eng. Chem., Anal. Ed.*, **18**, 354 (1946).
3) S. D. Nogare, T. O. Narris and J. Mitchell, *Anal. Chem.*, **23**, 1473 (1951).
4) K. P. Stolyarov and I. A. Stolyarova, *Zhur. Anal. Khim.*, **8**, 33 (1953).
5) S. N. Andreev and R. I. Gindina, *Zhur. Priklad. Khim.*, **26**, 104 (1953).
6) H. Etienne, *Ind. Chem. Belge.*, **17**, 455 (1952).
7) S. A. Shchukarev, S. N. Andreev and O. V. Sapozhnikava, *Zhur. Anal. Khim.*, **9**, 193 (1954).

room temperature continuously to keep the mixture apparently homogeneous. When the orange-yellow color gradually fades, add more iodine solution dropwise until the color is restored.

After reaction, discharge the iodine color with a few drops of 5% sodium thiosulfate. Add 14 ml. of chloroform from a burette and extract the produced iodoform by shaking. Let stand until the phases are separated and transfer the chloroform layer to another 100 mm. separatory funnel containing approximately an equal volume of water. Shake vigorously, and transfer the chloroform layer to a 10 ml. glass cell, through a funnel containing a thin bed of anhydrous sodium sulfate supported on a glass wool as shown in Fig. 2. Measure the absorbancy of this chloroform extract against water in a 10 mm. glass cell. Calculate the amount of acetone using the calibration curve, shown in Fig. 3, obtained by the following procedure.

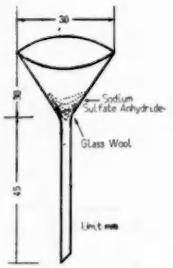

Fig. 2. Drying funnel

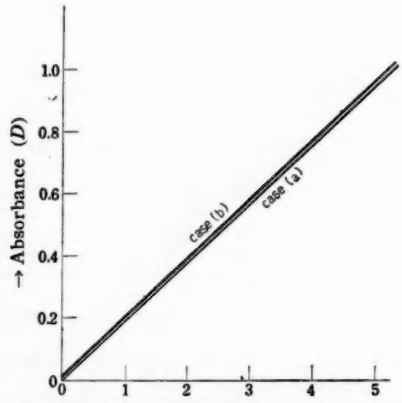

Fig. 3. Working curve for acetone.

Preparation of the calibration curve. Prepare the sodium hypoiodite solution similarly, to which less than 5 ml. of standard solution containing 79.6 γ of acetone in 1 ml. of water is added. Treat this similarly and extract the iodoform with 15 ml. of chloroform; wash the chloroform extract with water. The calibration curve obtained with pure acetone is shown in Fig. 3.

Discussion

(i) *On the calibration curve*:—On drawing the calibration curve employing 1 ml. of M-MM, the iodoform is extracted with 14 ml. of chloroform, as M-MM transfers to chloroform layer. When the M-MM is refined as shown in the following a), the calibration curve is in good agreement with that in Fig. 3; in the case of following b), it deviates higher than in the case of Fig. 3 by 0.1 in the absorbancy scale. This is due to the very small quantity of impurities, the presence of M-MM not affecting this analytical procedue.

(a) After washing M-MM with 10% sodium hydroxide, wash it with water five times, remove the water with calcium chloride, and collect the middle fraction 46°C, 100 mmHg, by vacuum distillation with cuprous chloride as stabilizer. Repeat this operation.

(b) After washing M-MM with 10% sodium hydroxide, wash it twice with water, remove the water with calcium chloride, and then collect the middle fraction similarly.

(ii) *Reaction conditions*:—The critical studies made by Hatcher and Mueller[8] and Nogare[3] showed that both the concentration and the order of addition of reagents determined the yield of the iodoform obtained. It was confirmed that the highest conversion from acetone into iodoform is effected by adding in the order iodine solution, sodium hydroxide solution, on the sample. Concerning the concentration of the reagents, the optimum condition is indicated by the orange-yellow color of the solution obtained by mixing 20% iodine solution and 25% sodium hydroxide. This experiment also exhibits that an insufficient or an excessive iodine relative to sodium hydroxide results in lower conversion into iodoform. Namely it is important to make the sample react in an orange-yellow solution and to maintain this orange-yellow by dropwise addition of iodine solution, when this color is discharged during reaction.

The effect of time on iodoform reaction under the optimum conditions is shown in Table I. Five minutes suffice; no marked change was observed with increasing reaction time up to 7 minutes. No significant difference was observed with the reaction temperature in this experiment but a low-temperature is desirable in order to avoid evaporation of M-MM. After reaction, the excess of iodine in the hypoiodite mixture can also be removed with sodium

8) W. H. Hatcher and W. H. Mueller, *Trans. Roy. Soc. Can.*, **23**, Sect. 3, 35 (1929).

TABLE I

EFFECT OF TIME ON IODOFORM REACTION

Sample	Acetone, mg.	Reaction time, min.	Absorbancy
A	0.232	2	0.465
	0.232	3	0.505
	0.232	4	0.540
	0.232	5	0.550
	0.232	6	0.550
	0.232	7	0.550
B	0.256	2	0.530
	0.256	3	0.590
	0.256	4	0.605
	0.256	5	0.610
	0.256	6	0.610
	0.256	7	0.610

sulfite or additional sodium hydroxide without sodium thiosulfate.

(iii) *On the volume of the sample*:—When more than one ml. of the sample is taken, the absorbancy becomes lower than that calculated or the results are not reproducible, as shown in Table II. The

TABLE II

RELATION BETWEEN THE VOLUME OF THE SAMPLE M-MM AND ABSORBANCY

Sample	Volume		
	1 ml.	2 ml.	3 ml.
D	0.095	0.169 obs. 0.190 calcd.	0.210 obs. 0.285 calcd.
E	0.286	0.535 obs. 0.572 calcd.	0.810 obs. 0.845 calcd.
F	0.317	0.555 obs. 0.630 calcd.	0.835 obs. 0.940 calcd.

calcd.: Absorbance at sampling volume 1 ml. × sampling volume.

reason may be considered as follows. The M-MM layer and the aqueous layer should be mixed well by shaking and acetone in the M-MM layer should be transfered to the aqueous layer, since acetone reacts with sodium hypoiodite in the aqueous layer. On taking more than 1 ml. of the sample, the M-MM and the aqueous layer do not mix perfectly, as M-MM is very easily separated from water.

(iv) *On iodoform*:—The intensity of the absorption in chloroform-M-MM layer was not affected by temperature from 15°C to 30°C. It was observed that iodoform slowly decomposed to liberate iodine in chloroform to decrease the absorbancy; it did not decompose, however when M-MM was present in the chloroform and maintained the absorbancy unchanged for more than one hour.

Ultraviolet absorption spectrum of the chloroform extract, using commercial M-MM as a sample showed complete agreement with that by the use of a mixture of aqueous acetone solution and refined M-MM. It can be ascertained that the product of the reaction is iodoform.

(v) *Effect of coexisting substance*:—Interference will be encountered from compounds which give iodoform by reaction with sodium hypoiodite. Possible interfering compounds are acetaldehyde, ethanol and methyl ethyl ketone, but in this method conversion of acetaldehyde and ethanol into iodoform is, respectively, 58 and 0.3%[3]. In many cases carbonyl compounds which interfere with the absorption at 347 mμ can be washed away from the chloroform extract with aqueous hydroxylamine hydrochloride.

Effect of methanol, formaldehyde, hydroquinone and peroxides which possibly coexist with M-MM is shown in Table III. Small quantities of methanol and formaldehyde do not affect this method.

TABLE III

EFFECT OF COEXISTING SUBSTANCE

Acetone mg.	Coexisting substance		Absorbancy
		(%)	
0.256	M-M only		0.610
0.256	Methanol*	(0.5)	0.615
	〃	(0.2)	0.610
0.256	Formaldehyde	(0.1)	0.610
	〃	(0.05)	0.610
0.256	Hydroquinone	(0.04)	0.520
	〃	(0.02)	
0.256	Hydrogen Peroxide	(0.06)	0.505
	〃	(0.04)	0.610

* Large quantities of methanol cause white precipitate.

(vi) *Example of analysis*:—A commercial M-MM (90 ml.) was used as the sample of unknown concentration of acetone; this was submitted to single distillation and 5 ml. fractions were collected from forerun fraction in order. These fractions were, respectively named sample No. A_1,

TABLE IV

EXAMPLE OF ANALYSIS OF ACETONE IN M-MM FRACTION

Sample No.	Acetone content mg./ml.
A_1*	0.656
A_2*	0.608
A_3*	0.504
A_4	0.364
A_5	0.268

* Measured after twice dilution.

A_2,……, A_5 and the acetone in these fraction determined by the procedure mentioned above. Table IV shows an example of the results.

Summary

The method described here is based on the utilization of the iodoform reaction. The essential point of this method consists in the complete shaking of the methyl methacrylate monomer with sodium hypoiodate solution. The methyl methacrylate monomer is water-insoluble and iodoform reaction proceeds in an aqueous medium. As a result, it was confirmed that methyl methacrylate monomer does not affect this reaction substantially and one ml. sample makes it possible to determine small quantities (0.001%) of acetone in the sample monomer. This method is more sensitive than the hydroxylamine hydrochloride method previously used.

Institute of Techno-Analytical Chemistry
Faculty of Engineering, Tokyo
University, Hongo, Tokyo

Ion-Exchange Separation of Fission Products[*1]

By Eiiti MINAMI, Masatake HONDA and Yukiyoshi SASAKI

(Received May 27, 1957)

Ion-exchange methods were studied for fission product separation in order to find a suitable separation procedure to prepare pure carrier-free radioactive isotopes and for radiochemical assay purpose. In this field we can refer to the prominent works which were performed during the War by American scientists. Their method, published in 1947[1] and 1948[2], consisted of the application of a cation-exchange chromatography. They used oxalic acid as the eluent for zirconium and niobium, and alkaline earths. Ruthenium, iodine and tellurium were grouped in the filtrate of sample solutions passed through hydrogen-form (HR) cation exchanger. The extension of this method, however, has not much been reported, in spite of recent considerable development of ion-exchange separation techniques[3].

The purpose of our studies was to find a systematic separation method for the fission product mixture, taking into account the minor constituents which are distributed in so-called "trough" region on the curve of the fission yield vs. mass number. For this purpose, both cation- and anion-exchange experiments were carried out using individual radioactive isotopes of these elements. Our interest was especially directed to the change of the exchange behavior caused by the formation of different oxidation states or of different ionic species.

The preliminary experiments showed that an anion-exchange method is not practical for the extraction of the transition elements, antimony and tellurium in the form of chloride complexes from the mixture. It owed to the complex behavior of ruthenium which is usually one of the main constituents in gross fission products. Then in this study a cation exchange was applied to the first step of group separation and various eluents were tested for fractional elution of cesium, rare earths and alkaline earths. However, characteristic behavior of antimony, tellurium and some transition elements to anion exchanger was found to be useful for their mutual isolation.

Measurement of Radioactivity

In this work the behavior of the elements was observed in their carrier-free state whenever possible. The counting device was G-M counter with ordinary scaler or with a self-recording rate meter. The effluents from the ion-exchange column were either collected and evaporated on a glass plate for counting, or led directly under

[*1] This communication was presented at the XVth Congress of International Union of Pure and Applied Chemistry held on 13th of September, 1956 at Lisbon.

1) E. R. Tompkins, J. X. Khym and W. E. Cohn, *J. Am. Chem. Soc.*, **69**, 2769 (1947).

2) W. E. Cohn, G. W. Parker and E. R. Tompkins, *Nucleonics*, **3**, No. 5, 22 (1948).

3) K. A. Kraus and F. Nelson, Report presented at the International Conference on the Peaceful Uses of Atomic Energy (Genève, 1955), A/CONF 8/P/837.

the mica end-window of the counting tube through a spiraled vinyl tube.

Ion-exchange Behavior of Individual Element

Ruthenium:—The solution chemistry of ruthenium is fairly complex. We have performed some experiments with carrier-free ruthenium using a cation exchanger, Dowex 50, and several kinds of anion exchanger, Dowex 1, Dowex 3, Amberlite IRA-400, Amberlite IRA-411 and Amberlite IR-4B. The gross fission products[*2] were imported from the United States, Atomic Energy Commission (US, AEC).

Ruthenium-106 was presented in the stock solution (4 M nitric acid solution) and was found to be fractionated into the following three groups according to the behavior towards the ion exchangers (Table I).

TABLE I

BEHAVIOR OF CARRIER-FREE RUTHENIUM ON ION-EXCHANGE RESINS

Species	Content	Ion-exchange behavior
Neutral part	26%	Passed through a mixed bed of anion- and cation-exchangers (RCl+HR).
Anionic part	20%	Adsorbed on anion exchanger (RCl or RNO_3).
Cationic part	54% (by difference)	Adsorbed on HR from dilute acid solution.

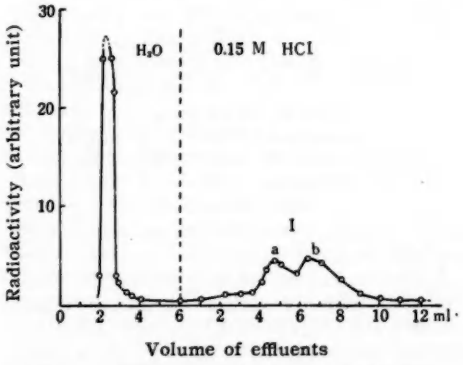

Fig. 1. Elution curve of cationic ruthenium.
Column: Dowex 50-X10, 3 ml. (HR form)

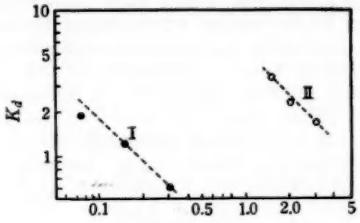

Fig. 2. Cation exchange of cationic ruthenium in $HClO_4$ solutions.
I: weakly retained species.
II: strongly retained species.
K_d's (ml./g.) were calculated from column experiment by
$$K_d = (V - I)/M$$
where V: volume of effluents flowed until the elution of the peak,
I: void volume of the column,
M: weight of dry resin (g.).

The major part of the cationic ruthenium, adsorbed on a cation exchanger, was easily eluted with hydrochloric acid solution stronger than 0.1 M. The elution curve showed two reproducible peaks (Fig. 1). But a small percentage of cationic ruthenium was adsorbed rather strongly, and a more concentrated mineral acid was needed for its rapid elution.

The affinites, distribution coefficients (K_d), of these two cationic species to a cation exchanger are shown with reference to hydrogen-ion concentration (Fig. 2). The inclination of two linear curve suggests that both species are probably univalent cations.

When the stock solution of fission products was treated with concentrated hydrochloric acid, evaporated to dryness and then dissolved in dilute hydrochloric acid solution, all the ruthenium was converted into an anionic species which passes through the column of cation exchanger. After being kept standing more than one week, however, two cationic species were found again from this solution.

This phenomenon might be attributed to the hydrolysis of the anionic chloro-complex formed by the treatment with concentrated hydrochloric acid. In this case, two peaks which could be refered to weakly retained cationic ruthenium were not resolved into separate peaks. This fact is in contrast to the experiments (Fig. 1) using original stock solution of the gross fission products.

The anionic part of ruthenium was

[*2] The sample used in this experiment was sufficiently aged, so that its composition was rather simple, i. e. it consisted of chiefly rare earths, strontium-90, cesium-137, ruthenium-106 and their daughters. Antimony-125 was found in the filtrate of the cation exchanger through which the sample solution had passed. The activity was ca. 0.1% of total. The data as far as obtained suggest the sample being cooled for 3~4 years[4].

4) M. Honda, Y. Sasaki and H. Natsume, *Japan Analyst, (Bunseki Kagaku)*, **4**, 240 (1955).

strongly adsorbed from acid solution on strongly basic anion exchangers such as Dowex 1, Dowex 2, Amberlite IRA-400 and Amberlite IRA-411. It was eluted out with 12 M hydrochloric acid in two broad peaks. On the other hand, it was noticed that the weakly basic anion exchangers, Dowex 3 and Amberlite IR-4B, react irreversibly with ruthenium in hydrochloric acid solutions.

Detection of rhodium-106, the short lived daughter of ruthenium-106, was easily performed from this anionic part of ruthenium. Rhodium was found in the effluents of 6~12 M hydrochloric acid passed through with a high flow rate. The decay curve of the activities of rhodium was drawn

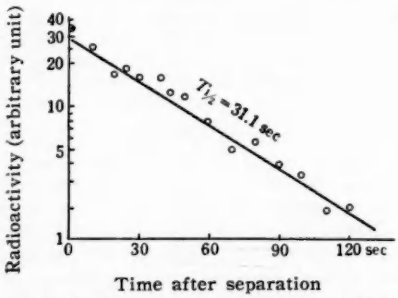

Fig. 3. Decay curve of rhodium-106 isolated by anion exchange.

with an automatic recording rate-meter and it showed $T_{1/2} = 31.1$ seconds (Fig. 3).

Antimony:—The tracer used was antimony-124 imported from the U.S., AEC. It contained 20 microgram Sb/ml. as a carrier, and was stocked in 6 M hydrochloric acid. Appreciable volatility of the activity was noticed during the evaporation of the solution. Then, if necessary, a few milligrams of antimony, Sb(V), were added and the activity was precipitated as antimony(III) sulfide.

Cation exchange. Antimony(V) was passed quantitatively through a cation exchanger in dilute acid solution. On the other hand, antimony(III) which was obtained by reduction with sulfur dioxide was adsorbed completely.

The adsorbability of antimony(III) by cation exchanger indicated the presence of univalent cation, possiblity SbO^+. That is, the plot of log K_d vs. log (HCl) has the slope of about one in the range of 0.05~0.3 M HCl (Fig. 4). These two species of antimony, Sb(V) and Sb(III), were separated from each other by a simple procedure (Fig. 5). Antimony(III) was also

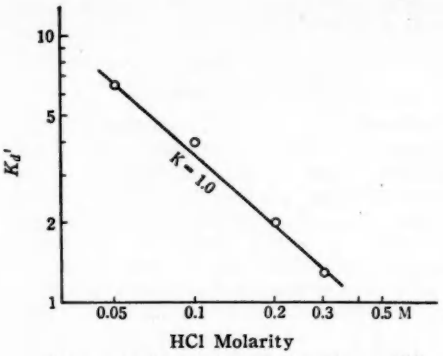

Fig. 4. Cation exchange of antimony(III) in HCl soln.
Exchanger: Dowex 50-X1
K_d': volume distribution coefficient corrected for swelling and measured by column method (Fig. 2).
(adsorption amount/ml. resin)/(concn. in soln.).
K: selectivity coefficient,
{SbOR/(SbO)}/HR/(H)}.

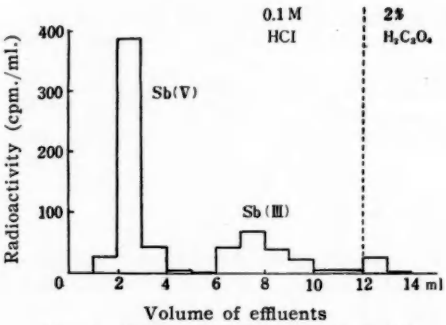

Fig. 5. Separation of Sb(V) and Sb(III).
Column: Dowex 50-X1, 5.5 ml. (capacity 2.10 meq.).

easily eluted out with dilute solution of oxalic acid from cation exchangers.

Anion exchange. High reproducibility was obtained by anion exchange using antimony(V) in hydrochloric acid solution, whereas antimony(III) showed quite complicated behavior. Reproducible results with anion exchangers who obtained by a preliminary treatment with hydrochloric acid solution containing free bromine. This treatment was necessary and effective to eliminate any irreversible reactions in the column. Bromine was retained in the resin phase as Br_3^- or Br_2Cl^-, and kept the proper oxidation state of antimony throughout the procedure. Elution constants are tabulated in Table II.

TABLE II
ELUTION CONSTANTS AND HCl CONCENTRATION IN ANION EXCHANGE[5]
Exchanger: Dowex 1-X4

	Concentration of HCl (M)					
	0.1	1	2	3	4	6
Sn(IV)	1.3*	<0.1	<0.1	<0.1	<0.1	<0.1
Te(IV)		1.3	0.1	<0.1	<0.1	<0.1
Sb(V)		1.3	1.3	1.0	0.3	<0.1
In(III)	1.3	0.5	—	0.3	—	0.3

* Maximum value of elution constant, 1.3, corresponds to no adsorption to anion exchanger. Elution constant $= v/(I+M\cdot K_d)$, v: column volume (see Fig. 2).

Tellurium:—The carrier-free tellurium-127 was obtained from the gross fission products, which were cooled for about three months, according to the processes described later. If necessary, a few milligrams of inactive tellurium were added in the form of chloride, and the activity was isolated in metallic tellurium precipitated with sulfur dioxide.

Cation exchange[6,7]. Tellurium(IV) was adsorbed by a cation exchanger and eluted out with dilute mineral acid. It behaves as a univalent cation such as $Te(OH)_3^+$ or $TeOOH^+$ in dilute perchloric acid solution. On the other hand telluium(VI) has no affinity towards cation exchangers.

Anion exchange[5,8]. The anion-exchange properties of tellurium(IV) in hydrochloric acid solution were studied using a few milligrams of tellurium tagged with tellurium-127. The results are tabulated in Table II. It was confirmed by some preliminary experiments that the carrier-free behavior was the same as the weighable amount of tellurium(IV) in both cation- and anion-exchange. The affinity of tellurium(VI) to anion exchanger is also negligibly small in acid solution.

Other minor constituents:—Some preliminary experiments were performed using the radioactive isotopes of cadmium, indium and tin (Fig. 6; Table II).

By cation exchange, using 0.5~1 M hydrochloric acid solution as an eluent, one can separate these elements, Cd, Sn(IV), Sb(III) and Te(IV), in one group from the gross fission products. By the following treatment with anion exchanger, cadmium and tin would be separated from antimony and from tellurium.

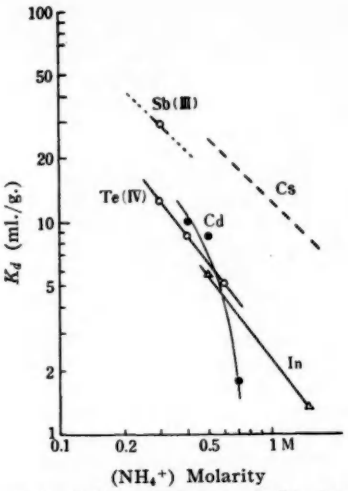

Fig. 6. Cation exchange of Cd, In and Te(IV) in HCl soln.
Exchanger: Dowex 50-X8.

Cesium, rare earths and alkaline earths:—The cation-exchange properties of cesium, rare earths and alkaline earths are rather well known. Some considerations, however, might be needed for the selection of the eluent for the separation of these elements which are adsorbed on the top of HR-form cation-exchange column.

In general, complexing reagent is most effective to remove rare earths from cation exchangers. But every complexing reagent, as far as the solution of its ammonium salt is used, elutes not only rare earths but also cesium from a column of HR-form cation-exchange resin with slightly different rates (Figs. 7 and 8). Therefore in this experiment cesium was eluted beforehand with ca. 1 M hydrochloric acid or 0.5 M ammonium salt of a mineral acid. The identification of the nuclide is possible from the position of the peak in the elution curves.

Detection of barium-137m, the daughter of cesium-137, was performed by cation-exchange separation. Cesium fraction was adsorbed again on the top of a cation-exchange column (NH_4R form), and barium activity was eluted out with ammoniacal 0.01 M EDTA solution. The effluents were directly led under the mica window of a counter tube through a vinyl tube, and the half-life of 2.60 min. was measured repeatedly with the same sample.

Acetate and EDTA were applied for the elution of rare earths and alkaline earths

5) Y. Sasaki, This Bulletin, **28**, 615 (1955).
6) F. Aoki, ibid., **26**, 480 (1953).
7) Y. Sasaki, *Japan Analyst* (*Bunseki Kagaku*), **4**, 637 (1955).
8) Y. Sasaki, This Bulletin, **28**, 89 (1955).

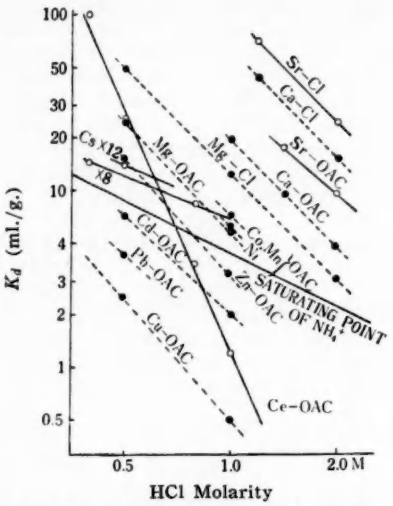

Fig. 7. Cation exchange of several elements in ammonium salt solutions.
Cs and Me—Cl: in NH_4Cl solutions.
OAc: NH_4OAc+HOAc (pH 4.6).
Exchangers: Colloidal Dowex 50 (for alkaline earths); Dowex 50-X8 (for others).

from the cation-exchange column. Ammonium acetate has been used as a fractionating eluent by changing the concentration for the group of rare earths, some transition elements[9] and alkaline earths[10,11]. This eluent has an advantage over any other organic reagent in that it can easily be removed by simple evaporation. Therefore this eluent is not only useful for the titrimetric determination of carrier metals by complexometric method which enables us to compare the elution curves of carriers and activities, but also convenient for the counting of carrier-free nuclides without the difficulty arising from self-absorption.

EDTA is a valuable reagent for the separation of rare earths and alkaline earths, especially for the separation into individual elements by the careful control of the pH. The smaller solubility of the free acid, however, prevents the direct use of HR-form column. For the elution of alkaline earths the mixture containing 0.01 M EDTA and 0.1 M ammonium acetate could be used at the pH between 7 and 9 to separate each member successively.

9) M. Honda. *Japan Analyst (Bunseki Kagaku)*, **4**, 384 (1955).
10) M. Honda, ibid., **3**, 132 (1954).
11) K. Kimura, E. Minami, M. Honda and others, ibid., **3**, 335 (1954).

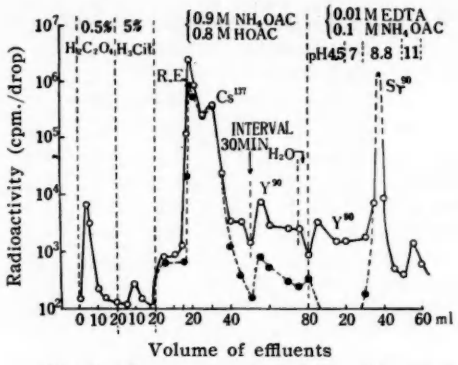

Fig. 8. Group separation with cation exchanger[4].
Sample: the fission products (Batch No. 19) (Oak Ridge Natl. Lab.) ca. 4 mc. in 4 M HNO_3 solution.
-o-o- measured just after the elution.
-•-•- measured after 2 months.
Column: Dowex 50-X8, 5 ml.

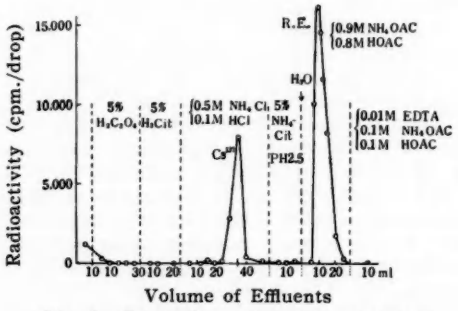

Fig. 9. Separation of cesium and rare earths[4]. (See Fig. 8)
Sample: 10~30 ml. fraction of NH_4OAc effluents in Fig. 8.
Column: Dowex 50-X8, 5 ml.

Systematic Separation Process

The properties of the elements described above could be applied to the systematic ion-exchange separation process for fission-product mixture. The possible scheme of such a process is outlined in Fig. 10. The sample of gross fission products free from heavy metals, is treated with concentrated hydrochloric acid, evaporated to dryness, and dissolved in a few milliliters of 0.1~0.2 M hydrochloric acid solution which contains free bromine. By these procedures, ruthenium is converted into anionic complexes, and bromine will oxidize antimony to its quinquevalent state. This solution is slowly passed through a small cation-exchange column (HR form),

and the column is washed with water. All ruthenium and antimony will be found in the effluents. The latter is treated with sulfur dioxide and passed through another cation-exchange column, which will take up antimony reduced to tervalent state. Oxalic acid (1%) or dilute hydrochloric acid (1 M) could be used for the elution of this element.

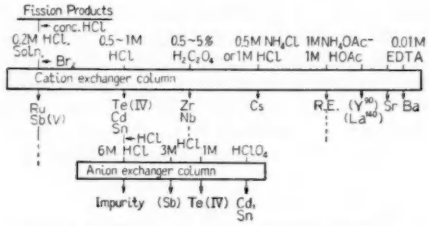

Fig. 10. Method of systematic separation of fission product mixture.

Tellurium(IV), cadmium and tin(IV) are eluted rapidly with 0.5~1 M hydrochloric acid from the former column. To the effluents, concentrated hydrochloric acid is added and the concentration of the acid is adjusted to 6 M. The impurities will be removed from this fraction by passing it through an anion-exchange column, Dowex 1-X4 (pretreated with 6 M HCl), and washing it with 6 M hydrochloric acid. Then carrier-free tellurium is eluted with 1 M hydrochloric acid. Finally, minor constituents, cadmium and tin, would be eluted out with perchloric acid or nitric acid.

After the elution of tellurium and others, zirconium and niobium will be eluted with 0.5~5% oxalic acid from the cation-exchange column. Cesium, rare earths and alkaline earths are then treated as illustrated in Figs. 8 and 9. If the addition of ammonium chloride is not favorable, the use of NH_4R-form cation exchanger and ca. 1 M ammonium acetate solution which is buffered with acetic acid can be recommended to separate rare earths from cesium. In this case, rare earths appear in the effluent with the added eluent and can be separated from cesium which has the elution peak at the same position as in the case in which HR-form resin is used.

In Figs. 8 and 9, citrate and oxalate were used to remove possible heavy-metal impurities.

Department of Chemistry
Faculty of Science
The University of Tokyo
Hongo, Tokyo

SHORT COMMUNICATIONS

New Colorimetric Method for the Determination of Uranium with Neo-thorone

By Shozo Shibata and Teiichi Matsumae

(Received February 10, 1958)

In order to determine a microgram amount of uranium, a new colorimetric method has been developed that is based upon the stable blue colored uranium complex of Neo-thorone[1] (*o*-arsonophenylazo-chromothropic acid[2]) in an aqueous solution.

Absorption spectra of the reagent and of the complex with uranium are respectively presented in Fig. 1a and 1b. These curves were measured in a buffered solution of pH 6.0. The blue colored complex of uranium was formed by adding several micrograms of uranium (as $UO_2(NO_3)_2$) and 1.0 ml. of 0.1% reagent solution to a 25 ml. volumetric flask and diluting to the mark with a buffered solution. Color was developed for five minutes and its stability was found to be quite adequate for the determination of uranium, the absorbance being proportional to uranium concentration in the range from 1 μg. to at least 40 μg. At 600 mμ, the molar extinction coefficient is about 25,000. or 0.0095 μg. U/cm^2 corresponding to $\log I_0/I=0.001$. Thus this

1) M. Ishibashi and S. Higashi, *Japan Analyst (Bunseki Kagaku)*, **4**, 14 (1955); **5**, 135 (1956).
2) V. I. Kuznetsov, *Compt. rend. acad. sci. U.S.S.R.*, **31**, 898 (1941).

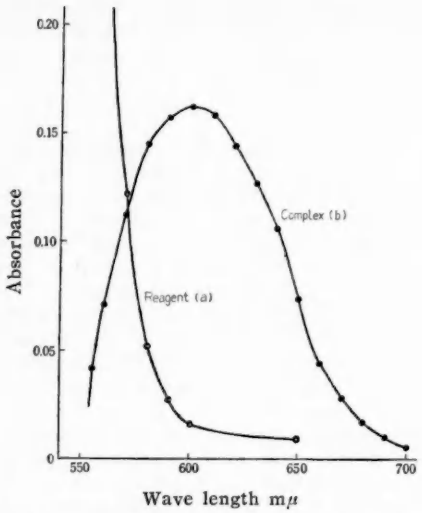

Fig. 1. Absorption spectra of reagent and its complex.

method appears to offer a good basis for the colorimetric determination of a microgram amount of uranium.

Details of the study will be published later.

Government Industrial Research Institute
Nagoya, Kita-ku, Nagoya

Triboluminescence of Zinc Sulfide Phosphors

By Kiyotake NARAOKA
and Yoshihide KOTERA

(Received November 27, 1957)

It has been known that cubic-ZnS : Mn displays remarkable triboluminescence when lightly ground or agitated in a hard container*.

In the present paper, we will report that almost all zinc sulfide phosphors embeded in the resin produce triboluminescence. The phosphor powder is dispersed in the benzene solution of polymethylmetacrylate, and this viscous and suspended mixture is painted on a plate. When the dry phosphor-resin layer is rubbed with hard materials such as a knife-edge and a needle, triboluminescence is recognized. The experimental results are:

1) The color of triboluminescence of ZuS : Mn is orange and is the same as that of the photoluminescence, and we can detect it in the daytime.

2) The phosphors activated with manganese, such as (Zn : Cd) S : Mn, ZnS : Cu : Mn and ZnS : Pb : Mn, are found to emit orange triboluminescence. ZnS : Cu : Mn emits yellow photoluminescence, which consists of both green copper band and orange manganese band, but they emit orange luminescence when they are rubbed mechanically, because the green copper emission is negligibly weak in triboluminescence. ZnS : Pb : Mn is similar to ZnS : Cu : Mn.

3) Triboluminescence of ZnS : Cu or ZnS : Pb is green and the same color as the photoluminescence; the brightness of the triboluminescence is very weak compared with that of manganese-activated sulfides, so we can detect it only in a dark room.

TABLE I

Sample:	Tribo.		Photo.	
Zn:S:Mn	orange	s	orange	fired at 950°C
ZnS:Mn	orange	s	orange	fired at 1200°C
(Zn:Cd)S:Mn	orange	s	orange	
ZnS:Cu:Mn	orange	s	yellow	
ZnS:Pb:Mn	orange	s	yellow	
ZnS:Cu	green	w	green	
ZnS:Pb	green	w	green	
ZnS:Ag	——	f	blue	
(Zn:Cd)S:Ag	green	w	green	medium persistance
(Zn:Cd)S:Ag	——	f	yellow	

s, strong; w, weak; f, feeble.

4) ZnS : Ag emits feeble triboluminescence but we can not detect the color.

The characteristics of some phosphors are shown in Table I.

As seen in these results, the zinc sulfide phosphors with manganese activator display remarkable triboluminescence, but the other sulfides produce very weak triboluminescence. The influence of polymethylmetacrylate on triboluminescence has not been studied, but it seems that there is no important mutual action between the phosphor and the resin, for the manganese-activated sulfides are found to emit triboluminescence by the previous grind-method.

Government Chemical Industrial Research Institute, Yoyogi P.O., Tokyo

* H. W. Leverenz, "An Introduction to Luminescence of Solids" John Wiley & Sons, New York, (1950) p. 171.

The Relationship between the Conformation of Epimeric 6-Substituted 4-ene-3-Ketosteroids and their Ultraviolet and Infrared Absorption Spectra

By Ken-ichi MORITA

(Received January 25, 1958)

In the previous paper[1] an empirical rule has been presented for the absorption spectra of C_6-substituted 4-ene-3-keto-steroids. Namely, 6β-isomers have lower K-band intensities in the ultraviolet absorption spectra than the corresponding 6α-isomers. The effect was ascribed to the greater steric hindrance involved in 6β-isomers in which 6β-substituents have 1:3-X:C_{10}Me and 1:3-X:C_8H interactions[2].

Both α and β substituents in the system cause only the small wavelength displacements ($\pm\Delta\lambda\simeq 5$ mμ) accompanied by decreases in ε. Hence, the type of spectral effects arising from the steric hindrance in the system may be associated with transitions between non-planar ground states and planar or near-planar excited states[3]. Thus the angles θ between the C_3 carbonyl groups and 4,5-unsaturated linkages in the ground state may be calculated from an equation $\cos^2\theta=\varepsilon/\varepsilon_0$, presented by Braude and Sondheimer[3], where ε_0 is the value for the unhindered compound in which $\theta=0$, if it is assumed that the 4-ene-3-keto system of 4-cholesten-3-one has uniplanar conformation. The values of θ derived in this way are given in Table I.

TABLE I

ULTRAVIOLET SPECTRA OF EPIMERIC 6-SUBSTITUTED 4-CHOLESTEN-3-ONE[4]

Compound	λ_{max}^{alc} (mμ)	ε	$\varepsilon/\varepsilon_0$	θ°
4-cholesten-3-one	241	18,000[5]	1.	0
6α-hydroxy-	240	17,080	0.95	13
6β-hydroxy-	237	14,500	0.80	27
6α-acetoxy-	238	15,800	0.88	20
6β-acetoxy-	237	13,200	0.73	31
6α-chloro-	239	17,500	0.97	10
6β-chloro-	241	15,100	0.84	23
6α-bromo-	238	15,800	0.88	20
6β-bromo-	246	13,500	0.75	30
6α-methyl-	241	16,650	0.92	16
6β-methyl-	241	15,100	0.84	23

1) K. Morita, *J. Chem. Soc. Japan, Pure Chem. Sec.* (*Nippon Kagaku Zassi*), **78**, 1581 (1957).
2) D. H. R. Barton, *J. Chem. Soc.*, **1953**, 1027; D. H. R. Barton and R. C. Cookson, *Quart. Rev.*, **10**, 44 (1956).
3) E. A. Braude and F. Sondheimer, *J. Chem. Soc.*, **1955**, 3754.
4) See Table I of ref. 1 and literatures cited there.

The greater values in the interplanar angles for the 6β-substituted 4-ene-3-keto-steroids, deduced from the difference in ultraviolet absorption, may be reflected in the infrared spectra. Unfortunately, only a limited number of the infrared spectra of these compounds have been reported[6,7,8]. In the infrared spectra of epimeric 6-acetoxy-4-cholesten-3-one[6] the location of the carbonyl band for 6β-isomer approaches that of saturated ketone more than that for 6α-isomer. A rough linear relationship[9] appears to exist between the interplanar angle θ deduced from difference in ultraviolet and $\Delta\nu/\Delta\nu_0$ where $\Delta\nu$ refers to the shift with respect to an unconjugated ketone (taken as 1713 cm.$^{-1}$) and $\Delta\nu_0$ refers to the shift in the 4-cholesten-3-one (Table II).

TABLE II

INFRARED SPECTRA OF EPIMERIC 6-ACETOXY-4-CHOLESTEN-3-ONE IN CAREON DISULFIDE[4]

Compound	$\nu_{C=O}$(cm.$^{-1}$)	$\Delta\nu/\Delta\nu_0$	$\nu_{C=C}$(cm.$^{-1}$)
4-cholesten-3-one	1684	1.	1626
6α-acetoxy-	1692	0.72	1631
6β-acetoxy-	1698	0.52	—

Sugiyama Chemical Research Institute
Mure, Mitaka, Tokyo

5) L. Dorfman, *Chem. Rev.*, **53**, 47 (1953). cf. D. H. R. Barton and E. R. H. Jones, *J. Chem. Soc.*, **1943**, 602.
6) L. F. Fieser, *J. Am. Chem. Soc.*, **75**, 4377 (1953).
7) K. Dobriner, E. R. Katzenellenbogen and R. N. Jones, "Infrared Absorption Spectra of Steroids", Chart 203, (1953).
8) R. N. Jones and F. Herling, *J. Org. Chem.*, **19**, 1252 (1954).
9) E. A. Braude and C. J. Timmons, *J. Chem. Soc.*, **1955**, 3766.

Photodesorption and Photoadsorption of Oxygen on Zinc Oxide

By Yuzaburo FUJITA
and Takao KWAN

(Received December 26, 1957)

Photodesorption of oxygen was first observed by Terenin[1] with oxygen-zinc oxide when irradiated by iron spark. The phenomenon was re-investigated by us with lights having wavelengths near fundamental absorption of the adsorbent on both degassed and oxidized zinc oxide samples. It was found that while Terenin's finding was confirmed at room temperature and below on the degassed sample, the photoresponse turned out to be

1) A. N. Terenin, *Problems of Kinetics and Catalysis*, **8**, 17 (1955) USSR; *Chem. Abst.*, **50**, 1452 (1956).

an irreversible adsorption on the oxidized sample. In this communication we show such a reversal of the photoresponse and suggest that weakly chemisorbed oxygen molecules play a role in this phenomenon.

A 0.28 g. portion of zinc oxide sample with a surface of 6.2 m^2 per g.[2], placed in a Pyrex vessel of *ca.* 40 cm^3 volume, was degassed at 300°C for several hr. A small amount of oxygen was then admitted to the oxide kept at a desired temperature, equilibrium pressure being kept always below 10^{-3} mm Hg. Irradiation was made by a Matsuda mercury lamp SHL-100, passed through a Matsuda solid filter and a quartz cell containing cupric sulfate solution to remove light of long wavelengths. The pressure change of oxygen due to irradiation was recorded by a Pirani gauge having a sensitivity 5×10^{-7} mm Hg/div. for O_2. The oxidized zinc oxide was prepared by heating in 0.1 mm Hg oxygen at 300°C for about one hour, cooling down to room temperature and being degassed for about thirty minutes. The photoeffect with this sample was investigated similarly as above.

As shown in Fig. 1a and 1b, photoexcited desorption of oxygen took place with the degassed sample at room temperature in a reversible fashion, whereas an irreversible photoadsorption was found to occur on the oxidized sample. Photoeffect of this kind was most effective by the irradiation of light at wavelengths less than 4500 Å. With rise of temperature of the adsorption vessel, the photoeffect became faint and disappeared above 200°C. At −195°C photodesorption occurred with the degassed sample but this may partly be ascribed to thermal[3] or non-electronic response since nitrogen was likewise able to desorb upon irradiation.

The oxygen-zinc oxide system has been the subject of many investigations. Therefore it would be relevant to review some results relating to the interaction of oxygen with zinc oxide. i) Let us quote first the p-T relation of the oxygen-degassed zinc oxide system obtained when the temperature of the adsorption vessel was raised from room temperature to 300°C at a constant rate. Maximum appeared in the plot of p against T at 150—200°C. At first sight this might indicate that the adsorption of oxygen is *physical* below 150°C or that the photodesorption has actually taken place in the *molecular* layer. ii) Exchange reaction of oxygen, $^{18}O_2+{}^{16}O_2=2{}^{18}O^{16}O$, was investigated by Winter et al.[4] over a zinc oxide sample at temperatures where the exchange of oxygen with the surface is negligible. Accordingly the exchange reaction is not perceptible below 119°C. This finding provides the view that oxygen adsorption may occur without dissociation at least around room temperature. iii) The shape of the conductivity-temperature curve[5] due to Stöckmann with zinc oxide kept in an atmospheric air much resembles

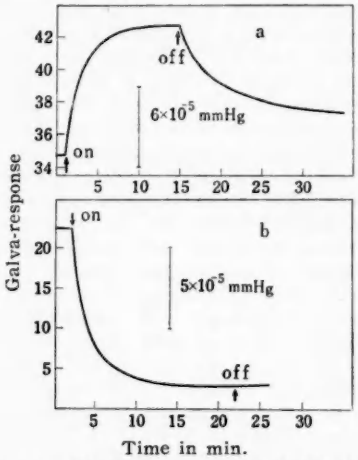

Fig. 1. Typical example for the photodesorption of oxygen (a) with a degassed zinc oxide sample and the photoadsorption (b) on an oxidized zinc oxide at room temperature.

our p-T relation; it deviates from the generally accepted linearity of $\log\sigma$ against $1/T$ of zinc oxide alone apparently near 200°C. On the other hand, according to Melnick[6] the photoconductivity of zinc oxide is entirely due to the desorption of chemically adsorbed oxygen *atoms*.

These facts now point toward the indication that weakly chemisorbed oxygen molecules are present having a kind of electronic interaction with the surface of zinc oxide. Probably molecular oxygen ion, O_2^-, is best fitted for such an adsorbed oxygen intermediate, and photodesorption or -adsorption may occur by combining with positive hole or electron of zinc oxide created upon irradiation.

Research Institute for Catalysis and Chemistry Department, Hokkaido University, Sapporo

2) T. Kwan, T. Kinuyama and Y. Fujita, *J. Res. Inst. Catalysis*, **3**, 28 (1953).
3) A. J. Rosenberg and C. S. Martel, Jr., *J. Phys. Chem.*, **61**, 512 (1957).
4) E. R. S. Winter, *J. Chem. Soc.*, **1934**, 1522.
5) F. Stöckmann, *Z. Physik*, **127**, 563 (1950).
6) A. D. Melnick, *J. Chem. Phys.*, **26**, 1136 (1957).